Summary of the Bulletin of the International Seismological Centre

2019

January – June

Volume 56 Issue I

www.isc.ac.uk

ISSN 2309-236X

2021

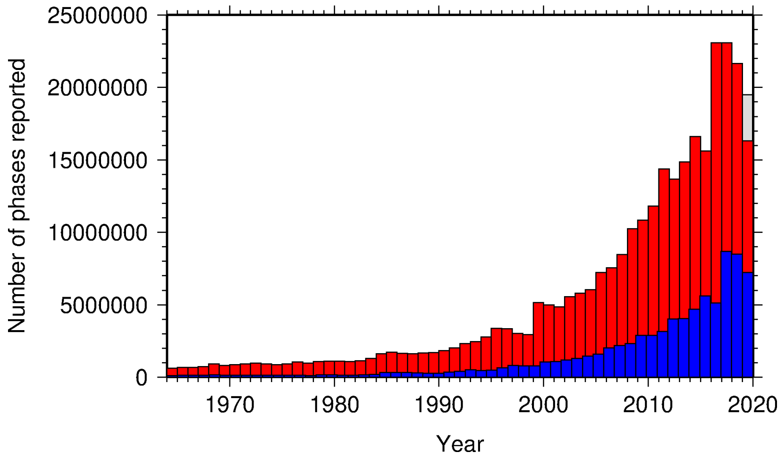

The number of phases (red) and number of amplitudes (blue) collected by the ISC for events each year since 1964. The data in grey covers the current period where data are still being collected before the ISC review takes place and are accurate at the time of publication. See Section 7.3.

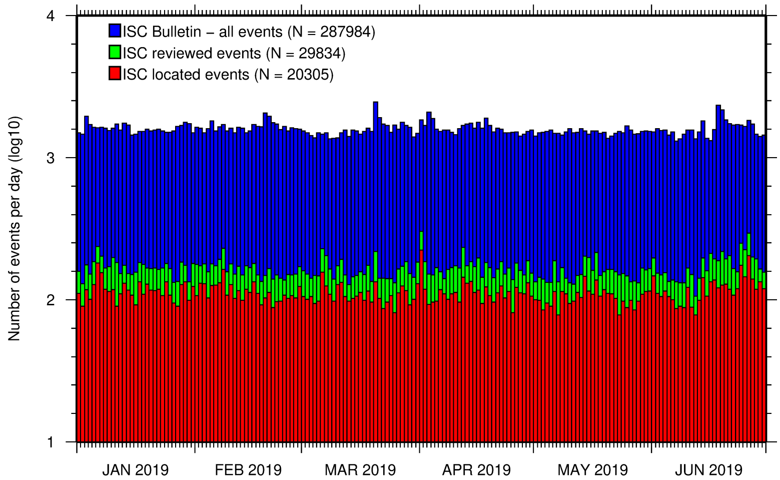

The number of events within the Bulletin for the current summary period. The vertical scale is logarithmic. See Section 8.1.

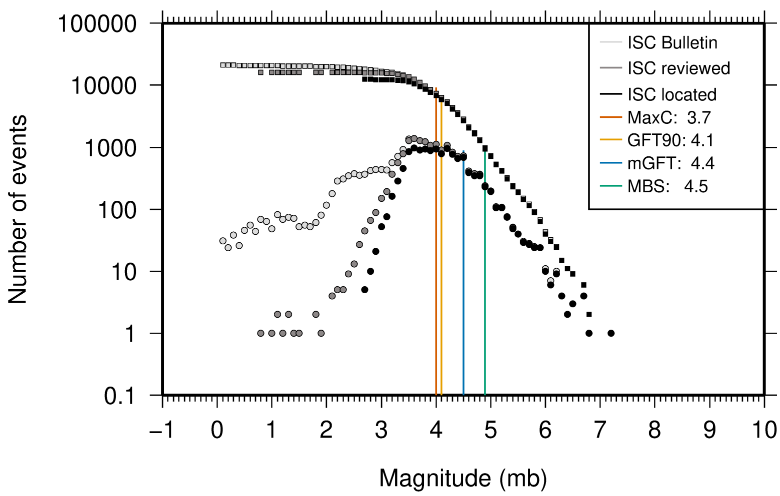

Frequency and cumulative frequency magnitude distribution for all events in the ISC Bulletin, ISC reviewed events and events located by the ISC. The magnitude of completeness (M_C) is shown for the ISC Bulletin. Note: only events with values of m_b are represented in the figure. See Section 8.4.

Summary of the Bulletin of the International Seismological Centre

2019

January - June

Volume 56 Issue I

Produced and edited by:
Kathrin Lieser, James Harris and Dmitry Storchak

Published by
International Seismological Centre

The International Seismological Centre (ISC) is a Charitable Incorporated Organization (CIO) registered with The Charity Commission for England and Wales. Registered charity number: 1188971.

ISC Data Products

http://www.isc.ac.uk/products/

ISC Bulletin:

http://www.isc.ac.uk/iscbulletin/search

ISC Bulletin and Catalogue monthly files, to the last reviewed month in FFB or ISF1 format:

ftp://www.isc.ac.uk/pub/[isf|ffb]/bulletin/*yyyy*/*yyyymm*.gz

ftp://www.isc.ac.uk/pub/[isf|ffb]/catalogue/*yyyy*/*yyyymm*.gz

Datafiles for the ISC data before the rebuild:

ftp://www.isc.ac.uk/pub/prerebuild/[isf|ffb]/bulletin/*yyyy*/*yyyymm*.gz

ftp://www.isc.ac.uk/pub/prerebuild/[isf|ffb]/catalogue/*yyyy*/*yyyymm*.gz

ISC-EHB Bulletin:

http://www.isc.ac.uk/isc-ehb/search/

IASPEI Reference Event List (GT bulletin):

http://www.isc.ac.uk/gtevents/search/

ISC-GEM Global Instrumental Earthquake Catalogue:

http://http://www.isc.ac.uk/iscgem/download.php

ISC Event Bibliography:

http://www.isc.ac.uk/event_bibliography/bibsearch.php

International Seismograph Station Registry:

http://www.isc.ac.uk/registries/search/

Seismological Contacts:

http://www.isc.ac.uk/projects/seismocontacts/

International Seismological Centre
Pipers Lane
Thatcham
RG19 4NS
United Kingdom
www.isc.ac.uk

The International Seismological Centre (ISC) is a Charitable Incorporated Organization (CIO) registered with The Charity Commission for England and Wales. Registered charity number: 1188971.

ISSN 2309-236X

Printed and bound in Wales by Cambrian Printers.

Contents

1

Preface

Dear Colleague,

This is the first 2019 issue of the Summary of the ISC Bulletin, which remains the most fundamental reason for continued operations at the ISC. This issue covers earthquakes and other seismic events that occurred during the period from January to June 2019. Users can search the ISC Bulletin on the ISC website. The monthly Bulletin files are available from the ISC ftp site. For instructions, please see www.isc.ac.uk/iscbulletin/.

This publication contains information on the ISC, its staff, Members, Sponsors and Data providers. It offers analysis of the data contributed to the ISC by many seismological agencies worldwide as well as analysis of the data in the ISC Bulletin itself. This issue also includes seismological standards and procedures used by the ISC in its operations.

I would like to reiterate here that all ISC hypocenter solutions (1964-present) are now based on the ak135 velocity model and all ISC magnitudes (1964-present) are based on the latest robust procedures.

We usually publish invited articles on notable seismic earthquakes as well as those describing the history, status and operational procedures at networks that contribute data to the ISC. This time, the topic of an invited article from the University of Bergen is somewhat different – describing their experience of using the ISC data.

We hope that you find this publication useful in your work. If your home-institution or company is unable, for one reason or another, to support the long-term international operations of the ISC in full by becoming a Member or a Sponsor, then, please, consider subscribing to this publication by contacting us at admin@isc.ac.uk.

With kind regards to our Data Contributors, Members, Sponsors and users,

Dr Dmitry A. Storchak
Director
International Seismological Centre (ISC)

2

The International Seismological Centre

2.1 The ISC Mandate

The International Seismological Centre (ISC) was set up in 1964 with the assistance of UNESCO as a successor to the International Seismological Summary (ISS) to carry forward the pioneering work of Prof. John Milne, Sir Harold Jeffreys and other British scientists in collecting, archiving and processing seismic station and network bulletins and preparing and distributing the definitive summary of world seismicity.

Under the umbrella of the International Association of Seismology and Physics of the Earth Interior (IASPEI/IUGG), the ISC has played an important role in setting international standards such as the International Seismic Bulletin Format (ISF), the IASPEI Standard Seismic Phase List (SSPL) and both the old and New IASPEI Manual of the Seismological Observatory Practice (NMSOP-2) (www.iaspei.org/projects/NMSOP.html).

The ISC has contributed to scientific research and prominent scientists such as John Hodgson, Eugine Herrin, Hal Thirlaway, Jack Oliver, Anton Hales, Ola Dahlman, Shigeji Suehiro, Nadia Kondorskaya, Vit Karnik, Stephan Müller, David Denham, Bob Engdahl, Adam Dziewonski, John Woodhouse and Guy Masters all considered it an important duty to serve on the ISC Executive Committee and the Governing Council.

The current mission of the ISC is to maintain:

- the **ISC Bulletin** – the longest continuous definitive summary of World seismicity (in collaboration with ∼150 seismic networks and data centres in ∼100 countries)
- the **International Seismographic Station Registry** (IR)
- the **IASPEI Reference Event List** (Ground Truth, GT, jointly with IASPEI)
- the **ISC-EHB dataset** - a groomed subset of the ISC Bulletin, where teleseismically well-constrained events are selected and relocated using the EHB algorithm to minimise errors in location (particularly depth) due to assumed 3D Earth structure
- the **ISC-GEM catalogue** – the catalogue of large earthquakes with homogeneous hypocentre and magnitude determinations and their uncertainties that cover the entire period of instrumental observations from 1904 till present
- the **Event Bibliography** – a search for references to scientific publications linked to both natural and anthropogenic events that have occurred in a geographical region of interest

- the **Dataset Repository** – a supplementary ISC service that allows individual researchers or groups to submit seismological datasets that they wish to be openly available to scientific community for a long period of time
- the **Seismological Contacts** – contact details of seismologists and seismological agencies around the world

These are fundamentally important tasks. Bulletin data produced, archived and distributed by the ISC for over 55 years are the definitive source of such information and are used by thousands of seismologists worldwide for seismic hazard estimation, for tectonic studies and for regional and global imaging of the Earth's structure. Key information in global tomographic imaging is derived from the analysis of ISC data. The ISC Bulletin served as a major source of data for such well known products as the ak135 global 1-D velocity model and the EHB (Engdahl et al., 1998) and Centennial (Engdahl and Villaseñor, 2002) catalogues. It presents an important quality-control benchmark for the Comprehensive Nuclear-Test-Ban Treaty Organization (CTBTO). Hypocentre parameters from the ISC Bulletin are used by the Data Management Center of the Incorporated Research Institutions for Seismology (IRIS DMC) to serve event-oriented user-requests for waveform data. The ISC-GEM catalogue is a cornerstone dataset used by the Global Earthquake risk Model Foundation (GEM).

The ISC Bulletin contains over 9 million seismic events: earthquakes, chemical and nuclear explosions, mine blasts and mining induced events. Over 2 million of them are regional and teleseismically recorded events that have been reviewed by the ISC analysts. The ISC Bulletin contains approximately 255 million individual seismic station readings of arrival times, amplitudes, periods, SNR, slowness and azimuth, reported by over 19,000 seismic stations currently registered in the IR. Over 10,000 stations have contributed to the ISC Bulletin in recent years. This number includes the numerous sites of the USArray. The IASPEI GT List currently contains ∼11,500 events for which latitude, longitude and depth of origin are known with high confidence (to 5 km or better) and seismic signals were recorded at regional and/or teleseismic distances.

2.2 Brief History of the ISC

Earthquake effects have been noted and documented from the earliest times, but it is only since the development of earthquake recording instruments in the latter half of the 19th century that a proper study of their occurrence has been possible. After the first teleseismic observation of an earthquake in 1889, the need for international exchange of readings was recognised in 1895 by Prof. John Milne and by Ernst von Rebeur Paschwitz together with Georg Gerland, resulting in the publication of the first international seismic bulletins. Milne's "Shide Circulars" were issued under the auspices of the Seismological Committee of the British Association for the Advancement of Science (BAAS), while co-workers of Gerland at the Central Bureau of the International Association of Seismology worked independently in Strasbourg (BCIS).

Following Milne's death in 1913, Seismological Bulletins of the BAAS were continued under Prof. H.H. Turner, later based at Oxford University. Upon formal post-war dissolution of the International Association of Seismology in 1922 the newly founded Seismological Section of the International Union of

Geodesy and Geophysics (IUGG) set up the International Seismological Summary (ISS) to continue at Oxford under Turner, to produce the definitive global catalogues from the 1918 data-year onwards, under the auspices of IUGG and with the support of the BAAS.

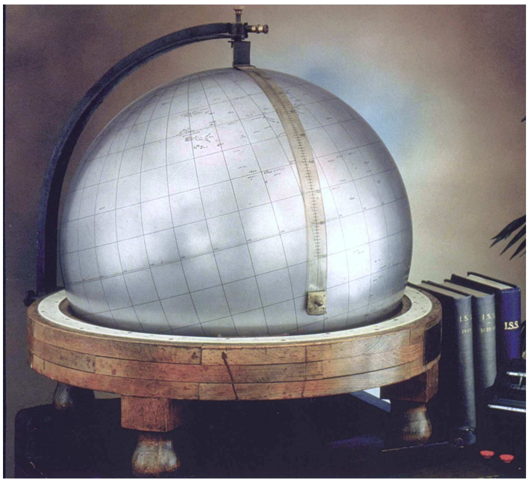

Figure 2.1: *The steel globe bearing positions of early seismic stations was used for locating positions of earthquakes for the International Seismological Summaries.*

ISS production, led by several professors at Oxford University, and Sir Harold Jeffreys at Cambridge University, continued until it was superseded by the ISC Bulletin, after the ISC was formed in Edinburgh in 1964 with Dr P.L. Willmore as its first director.

During the period 1964 to 1970, with the help of UNESCO and other international scientific bodies, the ISC was reconstituted as an international non-governmental body, funded by interested institutions from various countries. Initially there were supporting members from seven countries, now there are almost 60, and member institutions include national academies, research foundations, government departments and research institutes, national observatories and universities. Each member, contributing a minimum unit of subscription or more, appoints a representative to the ISC's Governing Council, which meets every two years to decide the ISC's policy and operational programme. Representatives from the International Association of Seismology and Physics of the Earth's Interior also attend these meetings. The Governing Council appoints the Director and a small Executive Committee to oversee the ISC's operations.

Figure 2.2: *ISC building in Thatcham, Berkshire, UK.*

In 1975, the ISC moved to Newbury in southern England to make use of better computing facilities there. The ISC subsequently acquired its own computer and in 1986 moved to its own building at Pipers Lane, Thatcham, near Newbury. The internal layout of the new premises was designed for the ISC and includes not only office space but provision for the storage of extensive stocks of ISS and ISC publications and a library of seismological observatory bulletins, journals and books collected over many tens of years.

In 1997 the first set of the ISC Bulletin CD-ROMs was produced (not counting an earlier effort at USGS). The first ISC website appeared in 1998 and the first ISC database was put in day-to-day operations from 2001.

Throughout 2009-2011 a major internal reconstruction of the ISC building was undertaken to allow for more members of staff working in mainstream ISC operations as well as major development projects such as the CTBTO Link, ISC-GEM Catalogue and the ISC Bulletin Rebuild.

2.3 Former Directors of the ISC and its U.K. Predecessors

John Milne
Publisher of the Shide Cicular Reports on Earthquakes
1899-1913

Herbert Hall Turner

Seismological Bulletins of the BAAS

1913-1922
Director of the ISS
1922-1930

Harry Hemley Plaskett
Director of the ISS
1931-1946

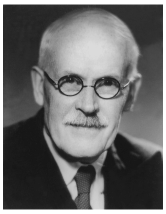

Harold Jeffreys
Director of the ISS
1946-1957

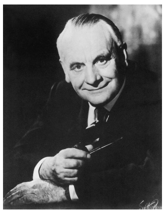

Robert Stoneley
Director of the ISS
1957-1963

P.L. (Pat) Willmore
Director of the ISS
1963-1970
Director of the ISC
1964-1970

Edouard P. Arnold
Director of the ISC
1970-1977

Anthony A. Hughes
Director of the ISC
1977-1997

Raymond J. Willemann
Director of the ISC
1998-2003

Avi Shapira
Director of the ISC
2004-2007

2.4 Member Institutions of the ISC

Article IV(a-b) of the ISC Working Statutes stipulates that any national academy, agency, scientific institution or other non-profit organisation may become a Member of the ISC on payment to the ISC of a sum equal to at least one unit of subscription and the nomination of a voting representative to serve on the ISC's governing body. Membership shall be effective for one year from the date of receipt at the ISC of the annual contribution of the Member and is thereafter renewable for periods of one year.

The ISC is currently supported with funding from its 62 Member Institutions and a four-year Grant Award EAR-1417970 from the US National Science Foundation.

Figures 2.3 and 2.4 show major sectors to which the ISC Member Institutions belong and proportional financial contributions that each of these sectors make towards the ISC's annual budget.

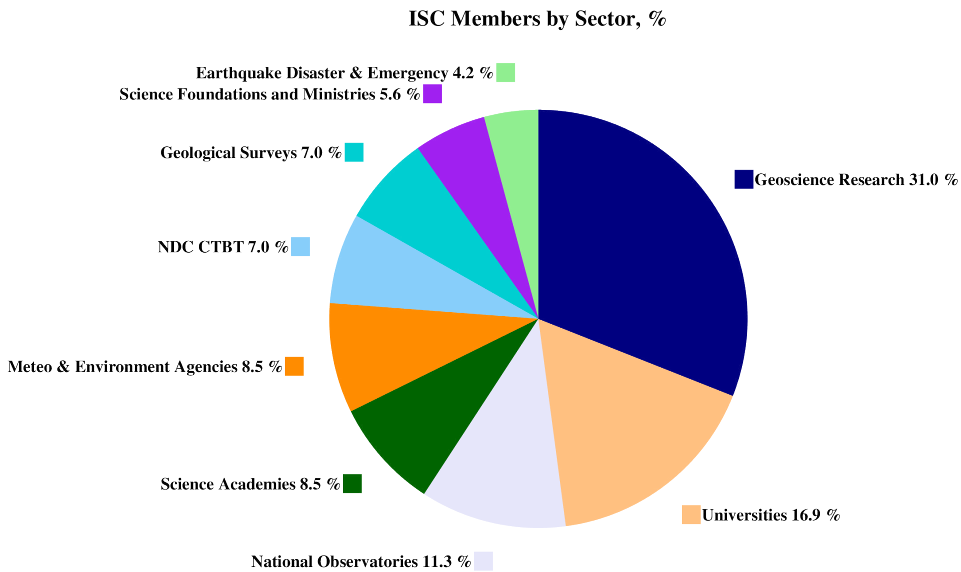

Figure 2.3: *Distribution of the ISC Member Institutions by sector in year 2013 as a percentage of total number of Members.*

There follows a list of all current Member Institutions with a category (1 through 9) assigned according to the ISC Working Statutes. Each category relates to the number of membership units contributed.

Centre de Recherche en Astronomie, Astrophysique et Géophysique (CRAAG)
Algeria
www.craag.dz
Category: 1

Geoscience Australia
Australia
www.ga.gov.au
Category: 4

Federal Ministry for Education, Science and Research
Austria

Category: 2

Centre of Geophysical Monitoring (CGM) of the National Academy of Sciences of Belarus
Belarus
www.cgm.org.by
Category: 1

Belgian Science Policy Office (BELSPO)
Belgium

Category: 1

Seismological Observatory, Institute of Geosciences, University of Brasilia
Brazil
www.obsis.unb.br
Category: 1

Observatorio Nacional
Brazil
www.on.br
Category: 1

Universidade de São Paulo, Centro de Sismologia
Brazil
www.sismo.iag.usp.br
Category: 1

National Institute of Geophysics, Geodesy and Geography (NIGGG), Bulgarian Academy of Sciences
Bulgaria
www.niggg.bas.bg
Category: 1

The Geological Survey of Canada
Canada
gsc.nrcan.gc.ca
Category: 4

Centro Sismologico Nacional, Universidad de Chile
Chile

Category: 1

China Earthquake Administration
China
www.cea.gov.cn
Category: 4

Institute of Earth Sciences, Academia Sinica
Chinese Taipei
www.earth.sinica.edu.tw
Category: 1

Geological Survey Department
Cyprus
www.moa.gov.cy
Category: 1

Institute of Geophysics, Czech Academy of Sciences
Czech Republic

Category: 1

Geological Survey of Denmark and Greenland (GEUS)
Denmark
www.geus.dk
Category: 2

National Research Institute for Astronomy and Geophysics (NRIAG), Cairo
Egypt
www.nriag.sci.eg
Category: 1

The University of Helsinki
Finland
www.helsinki.fi
Category: 2

Institute National des Sciences de l'Univers
France
www.insu.cnrs.fr
Category: 4

Laboratoire de Détection et de Géophysique/CEA
France
www-dase.cea.fr
Category: 2

Institute of Radiological and Nuclear Safety (IRSN), joint authority of the Ministries of Defense, the Environment, Industry, Research, and Health
France

Category: 1

Bundesanstalt für Geowissenschaften und Rohstoffe
Germany
www.bgr.bund.de
Category: 4

GeoForschungsZentrum Potsdam
Germany
www.gfz-potsdam.de
Category: 2

The Seismological Institute, National Observatory of Athens
Greece
www.noa.gr
Category: 1

Institute of Earth Physics and Space Science (EPSS), Hungarian Research Network (ELKH)
Hungary

Category: 1

The Icelandic Meteorological Office
Iceland
www.vedur.is
Category: 1

National Geophysical Research Institute (NGRI), Council of Scientific and Industrial Research (CSIR)
India

Category: 2

National Centre for Seismology, Ministry of Earth Sciences of India
India
www.moes.gov.in
Category: 4

Iraqi Meteorological Organization and Seismology
Iraq
www.imos-tm.com
Category: 1

Dublin Institute for Advanced Studies
Ireland
www.dias.ie
Category: 1

Geological Survey of Israel
Israel

Category: 1

Soreq Nuclear Research Centre (SNRC)
Israel
www.soreq.gov.il
Category: 1

Istituto Nazionale di Geofisica e Vulcanologia
Italy
www.ingv.it
Category: 3

Istituto Nazionale di Oceanografia e di Geofisica Sperimentale
Italy
www.ogs.trieste.it
Category: 1

University of the West Indies at Mona
Jamaica
www.mona.uwi.edu
Category: 1

Japan Agency for Marine-Earth Science and Technology (JAMSTEC)
Japan
www.jamstec.go.jp
Category: 2

National Institute of Polar Research (NIPR)
Japan
www.nipr.ac.jp
Category: 1

The Japan Meteorological Agency (JMA)
Japan
www.jma.go.jp
Category: 5

Earthquake Research Institute, University of Tokyo
Japan
www.eri.u-tokyo.ac.jp
Category: 3

Centro de Investigación Científica y de Educación Superior de Ensenada (CICESE)
Mexico
resnom.cicese.mx
Category: 1

Institute of Geophysics, National University of Mexico
Mexico
www.igeofcu.unam.mx
Category: 1

The Royal Netherlands Meteorological Institute (KNMI)
Netherlands
www.knmi.nl
Category: 2

GNS Science
New Zealand
www.gns.cri.nz
Category: 3

The University of Bergen
Norway
www.uib.no
Category: 2

Stiftelsen NORSAR
Norway
www.norsar.no
Category: 2

The Centre for Earth Evolution and Dynamics (CEED), the University of Oslo
Norway

Category: 1

Institute of Geophysics, Polish Academy of Sciences
Poland
www.igf.edu.pl
Category: 1

Instituto Português do Mar e da Atmosfera
Portugal
www.ipma.pt
Category: 2

Red Sísmica de Puerto Rico
Puerto Rico
redsismica.uprm.edu
Category: 1

Korean Meterological Administration
Republic of Korea
www.kma.go.kr
Category: 1

National Institute for Earth Physics
Romania
www.infp.ro
Category: 1

Russian Academy of Sciences
Russia
www.ras.ru
Category: 5

Earth Observatory of Singapore (EOS), an autonomous Institute of Nanyang Technological University
Singapore
www.earthobservatory.sg
Category: 1

Environmental Agency of Slovenia
Slovenia
www.arso.gov.si
Category: 1

Council for Geoscience
South Africa
www.geoscience.org.za
Category: 1

Institut Cartogràfic i Geològic de Catalunya (ICGC)
Spain
www.icgc.cat
Category: 1

Institute of Marine Sciences (ICM-CSIC)
Spain

Category: 1

National Defence Research Establishment (FOI)
Sweden
www.foi.se
Category: 1

Uppsala Universitet
Sweden
www.uu.se
Category: 2

The Swiss Academy of Sciences
Switzerland
www.scnat.ch
Category: 2

Disaster and Emergency Management Authority (AFAD)
Turkey
www.deprem.gov.tr
Category: 2

Kandilli Observatory and Earthquake Research Institute
Turkey
www.koeri.boun.edu.tr
Category: 1

The Royal Society
United Kingdom
www.royalsociety.org
Category: 6

British Geological Survey
United Kingdom
www.bgs.ac.uk
Category: 2

AWE Blacknest
United Kingdom
www.blacknest.gov.uk
Category: 1

Texas Seismological Network (TexNet), Bureau of Economic Geology, J.A. and K.G. Jackson School of Geosciences, University of Texas at Austin
U.S.A.
www.beg.utexas.edu
Category: 1

University of Utah Seismograph Stations (UUSS)
U.S.A.

Category: 1

The National Science Foundation of the United States. (Grant No. EAR-1811737)
U.S.A.
www.nsf.gov
Category: 9

Alaska Earthquake Center (AEC), University of Alaska Fairbanks
U.S.A.

Category: 1

National Earthquake Information Center, U.S. Geological Survey
U.S.A.
www.neic.usgs.gov
Category: 1

Incorporated Research Institutions for Seismology
U.S.A.
www.iris.edu
Category: 1

In addition the ISC is currently in receipt of grants from the International Data Centre (IDC) of the Preparatory Commission of the Comprehensive Nuclear-Test-Ban Treaty Organization (CTBTO), FM Global, Lighthill risk Network, USGS (Award G18AP00035) and BGR.

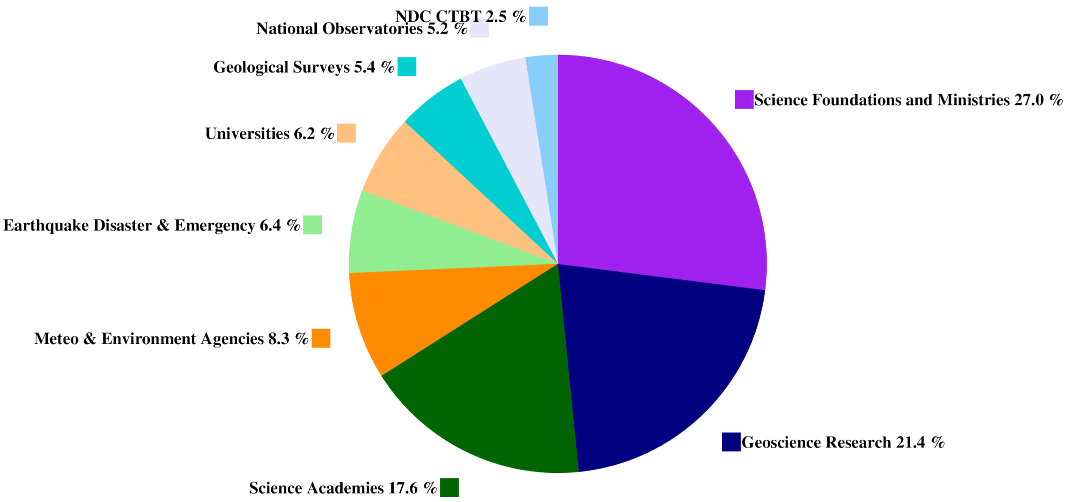

Figure 2.4: *Distribution of Member's financial contributions to the ISC by sector in year 2013 as a percentage of total annual Member contributions.*

2.5 Sponsoring Organisations

Article IV(c) of the ISC Working Statutes stipulates any commercial organisation with an interest in the objectives and/or output of the ISC may become an Associate Member of the ISC on payment of an Associate membership fee, but without entitlement to representation with a vote on the ISC's governing body.

REF TEK SYSTEMS INC. www.reftek.com

REF TEK designs and manufactures application specific, high-performance, battery-operated, field-portable geophysical data acquisition devices for the global market. With over 35 years of experience, REF TEK provides customers with complete turnkey solutions that include high resolution recorders, broadband sensors, state-of-the-art communications (V-SAT, GPRS, etc), installation, training, and continued customer support. Over 7,000 REF TEK instruments are currently being used globally for multiple applications. From portable earthquake monitoring to telemetry earthquake monitoring, earthquake aftershock recording to structural monitoring and more, REF TEK equipment is suitable for a wide variety of application needs.

GeoSIG swiss made to measure http://www.geosig.com/

GeoSIG provides earthquake, seismic, structural, dynamic and static monitoring and measuring solutions As an ISO Certified company, GeoSIG is a world leader in design and manufacture of a diverse range of high quality, precision instruments for vibration and earthquake monitoring. GeoSIG instruments are at work today in more than 100 countries around the world with well-known projects such as the NetQuakes installation with USGS and Oresund Bridge in Denmark. GeoSIG offers off-the-shelf solutions as well as highly customised solutions to fulfil the challenging requirements in many vertical markets including the following:

- Earthquake Early Warning and Rapid Response (EEWRR)
- Seismic and Earthquake Monitoring and Measuring
- Industrial Facility Seismic Monitoring and Shutdown
- Structural Analysis and Ambient Vibration Testing
- Induced Vibration Monitoring
- Research and Scientific Applications

泰德 TAIDE http://www.tai-de.com/en/

Zhuhai Taide Enterprise Co., Ltd. (Taide), a China based seismograph manufacturer, was set up in 1992. It is located in the city of Zhuhai, Guangdong Province, south-east China. The main products of Taide include data loggers, digitizers, all-band seismometers and accelerometers, intensity meters, magnetometers, strain meters, and software for earthquake related analysis. Over 80 professional engineers are employed at Taide, responsible for R&D, assembling and updating the hardware and software, and a team of 10 are engaged in stringent quality control and marketing.

In 2016, in collaboration with the Institute of Geophysics (China Earthquake Administration), Taide set up an Engineering Research Center for Earthquake Monitoring Techniques, aiming to improve the quality of earthquake observations. Taide-made instruments have been widely adapted by earthquake observation and monitoring networks, early warning systems, marine geophysical observation projects and deep borehole projects in China, as well as by seismograph networks in Indonesia, Nepal, Cuba, Pakistan and Kenya.

güralp http://www.guralp.com/

Güralp has been developing revolutionary force-feedback broadband seismic instrumentation for more than thirty years. Our sensors record seismic signals of all kinds, from teleseismic events occurring on the other side of the planet, to microseisms induced by unconventional hydrocarbon extraction. Our sophisticated digitisers record these signals with the highest resolution and accurate timing.

We supply individual instruments or complete seismic systems. Our services include field support such as installation and maintenance, to complete network and data management.

We design our instruments to meet increasingly complex requirements for deployment in the most challenging circumstances. As a result, you will find Güralp instruments gathering seismic data in the harshest of environments, from the Antarctic ice sheet; to boreholes 100s of metres deep; to the world's most active volcanoes and deepest ocean trenches.

SEISMOLOGY RESEARCH CENTRE http://src.com.au/

The Seismology Research Centre is an Australian earthquake observatory that began developing their own seismic recorders and data processing software in the late 1970s when digital recorders were uncommon. The Gecko is the SRC's 7th generation of seismic recorder, now available with a variety of integrated sensors to meet every monitoring requirement, including:

- Strong Motion Accelerographs
- 2Hz and 4.5Hz Blast Vibration Monitors
- Short Period 1Hz Seismographs
- Broadband 200s-1500Hz Optical Seismographs

Visit src.com.au/downloads/waves to grab a free copy of the SRC's MiniSEED waveform viewing and analysis software application, Waves.

MS&AD
MS&AD InterRisk Research & Consulting http://www.irric.co.jp/en/corporate/

MS&AD InterRisk Research & Consulting, Inc. is responsible for the core of risk-related service businesses in the MS&AD group. We provide services which meet various expectations of the clients, including consulting, research and investigation, seminars and publications for risk management in addition to the think-tank functions.

sara electronic instruments http://www.sara.pg.it

SARA designs and manufactures seismometers, accelerometers and portable multichannel seismographs for both seismology and applied geophysics. Since 2002 we provided over 5000 seismic units, 15000 acceleration transducers and 15000 geophysical exploration channels to thousands of professionals and researchers which are using our equipment with success. Providing low-cost instrumentation for developing countries is our main goal. We provided instruments from remote areas with radio telemetry to the Earth's depth such as a seismic array down to 285 meters in a borehole. Engineers use our systems to monitor historical monuments in Italy and in the middle east. Earthquake Early warning Systems in Italy and Turkey use our accelerometers and accelerographs. Our passion brings us to run our own seismic network including a small aperture seismic array in central Italy. We developed our seismological software SEISMOWIN which provides full support for all international file formats and communication standards like miniSEED, GSE, SeedLink and a number of tools for earthquake location and site assessment. The GEOEXPLORER software suite offers a number of modules for geological surveys. Visit our web site and download the free tools available at: www.sara.pg.it.

2.6 Data Contributing Agencies

In addition to its Members and Sponsors, the ISC owes its existence and successful long-term operations to its 149 seismic bulletin data contributors. These include government agencies responsible for national seismic networks, geoscience research institutions, geological surveys, meteorological agencies, universities, national data centres for monitoring the CTBT and individual observatories. There would be no ISC Bulletin available without the regular stream of data that are unselfishly and generously contributed to the ISC on a free basis.

The Institute of Seismology, Academy of Sciences of Albania
Albania
TIR

Centre de Recherche en Astronomie, Astrophysique et Géophysique
Algeria
CRAAG

Instituto Nacional de Prevención Sísmica
Argentina
SJA

Universidad Nacional de La Plata
Argentina
LPA

National Survey of Seismic Protection
Armenia
NSSP

Curtin University
Australia
CUPWA

Geoscience Australia
Australia
AUST

Zentralanstalt für Meteorologie und Geodynamik (ZAMG)
Austria
VIE

International Data Centre, CTBTO
Austria
IDC

Republican Seismic Survey Center of Azerbaijan National Academy of Sciences
Azerbaijan
AZER

Royal Observatory of Belgium
Belgium
UCC

Observatorio San Calixto
Bolivia
SCB

Republic Hydrometeorological Service, Seismological Observatory, Banja Luka
Bosnia and Herzegovina
RHSSO

Botswana Geoscience Institute
Botswana
BGSI

Instituto Astronomico e Geofísico
Brazil
VAO

Observatory Seismological of the University of Brasilia
Brazil
OSUNB

National Institute of Geophysics, Geology and Geography
Bulgaria
SOF

Canadian Hazards Information Service, Natural Resources Canada
Canada
OTT

Centro Sismológico Nacional, Universidad de Chile
Chile
GUC

China Earthquake Networks Center
China
BJI

Institute of Earth Sciences, Academia Sinica
Chinese Taipei
ASIES

Central Weather Bureau (CWB)
Chinese Taipei
TAP

Red Sismológica Nacional de Colombia
Colombia
RSNC

Sección de Sismología, Vulcanología y Exploración Geofísica
Costa Rica
UCR

Seismological Survey of the Republic of Croatia
Croatia
ZAG

Servicio Sismológico Nacional Cubano
Cuba
SSNC

Cyprus Geological Survey Department
Cyprus
NIC

Institute of Geophysics, Czech Academy of Sciences
Czech Republic
WBNET

The Institute of Physics of the Earth (IPEC)
Czech Republic
IPEC

Institute of Geophysics, Czech Academy of Sciences
Czech Republic
PRU

Korea Earthquake Administration
Democratic People's Republic of Korea
KEA

Geological Survey of Denmark and Greenland
Denmark
DNK

Universidad Autonoma de Santo Domingo
Dominican Republic
SDD

Observatorio Sismologico Politecnico Loyola
Dominican Republic
OSPL

Servicio Nacional de Sismología y Vulcanología
Ecuador
IGQ

National Research Institute of Astronomy and Geophysics
Egypt
HLW

Servicio Nacional de Estudios Territoriales
El Salvador
SNET

Institute of Seismology, University of Helsinki
Finland
HEL

Laboratoire de Détection et de Géophysique/CEA
France
LDG

Institut de Physique du Globe de Paris
France
IPGP

EOST / RéNaSS
France
STR

Laboratoire de Géophysique/CEA
French Polynesia
PPT

Institute of Earth Sciences/ National Seismic Monitoring Center
Georgia
TIF

Alfred Wegener Institute for Polar and Marine Research
Germany
AWI

Bundesanstalt für Geowissenschaften und Rohstoffe
Germany
BGR

Seismological Observatory Berggießhübel, TU Bergakademie Freiberg
Germany
BRG

Geophysikalisches Observatorium Collm
Germany
CLL

National Observatory of Athens
Greece
ATH

Department of Geophysics, Aristotle University of Thessaloniki
Greece
THE

University of Patras, Department of Geology
Greece
UPSL

INSIVUMEH
Guatemala
GCG

Hong Kong Observatory
Hong Kong
HKC

Geodetic and Geophysical Reasearch Institute, Hungarian Academy of Sciences
Hungary
KRSZO

Icelandic Meteorological Office
Iceland
REY

National Centre for Seismology of the Ministry of Earth Sciences of India
India
NDI

National Geophysical Research Institute
India
HYB

Badan Meteorologi, Klimatologi dan Geofisika
Indonesia
DJA

International Institute of Earthquake Engineering and Seismology (IIEES)
Iran
THR

Tehran University
Iran
TEH

Iraqi Meteorological and Seismology Organisation
Iraq
ISN

Dublin Institute for Advanced Studies
Ireland
DIAS

The Geophysical Institute of Israel
Israel
GII

MedNet Regional Centroid - Moment Tensors
Italy
MED_RCMT

Dipartimento per lo Studio del Territorio e delle sue Risorse (RSNI)
Italy
GEN

Laboratory of Research on Experimental and Computational Seimology
Italy
RISSC

Istituto Nazionale di Oceanografia e di Geofisica Sperimentale (OGS)
Italy
TRI

Istituto Nazionale di Geofisica e Vulcanologia
Italy
ROM

Jamaica Seismic Network
Jamaica
JSN

Japan Meteorological Agency
Japan
JMA

National Institute of Polar Research
Japan
SYO

National Research Institute for Earth Science and Disaster Resilience
Japan
NIED

Jordan Seismological Observatory
Jordan
JSO

National Nuclear Center
Kazakhstan
NNC

Seismological Experimental Methodological Expedition
Kazakhstan
SOME

Kyrgyz Seismic Network
Kyrgyzstan
KNET

Institute of Seismology, Academy of Sciences of Kyrgyz Republic
Kyrgyzstan
KRNET

Latvian Seismic Network
Latvia
LVSN

National Council for Scientific Research
Lebanon
GRAL

Geological Survey of Lithuania
Lithuania
LIT

Macao Meteorological and Geophysical Bureau
Macao, China
MCO

Antananarivo
Madagascar
TAN

Geological Survey Department Malawi
Malawi
GSDM

Instituto de Geofísica de la UNAM
Mexico
MEX

Centro de Investigación Científica y de Educación Superior de Ensenada
Mexico
ECX

Institute of Geophysics and Geology
Moldova
MOLD

Seismological Institute of Montenegro
Montenegro
PDG

Centre National de Recherche
Morocco
CNRM

The Geological Survey of Namibia
Namibia
NAM

National Seismological Centre, Nepal
Nepal
DMN

IRD Centre de Nouméa
New Caledonia
NOU

Institute of Geological and Nuclear Sciences
New Zealand
WEL

Central American Tsunami Advisory Center
Nicaragua
CATAC

Seismological Observatory Skopje
North Macedonia
SKO

Stiftelsen NORSAR
Norway
NAO

University of Bergen
Norway
BER

Sultan Qaboos University
Oman
OMAN

Universidad de Panama
Panama
UPA

Manila Observatory
Philippines
QCP

Philippine Institute of Volcanology and Seismology
Philippines
MAN

Private Observatory of Pawel Jacek Wiejacz, D.Sc.
Poland
PJWWP

Institute of Geophysics, Polish Academy of Sciences
Poland
WAR

Sistema de Vigilância Sismológica dos Açores
Portugal
SVSA

Instituto Português do Mar e da Atmosfera, I.P.
Portugal
INMG

Instituto Dom Luiz, University of Lisbon
Portugal
IGIL

Centre of Geophysical Monitoring of the National Academy of Sciences of Belarus
Republic of Belarus
BELR

Inst. of Seismology and Geodynamics, V.I. Vernadsky Crimean Federal University
Republic of Crimea
CFUSG

Korea Meteorological Administration
Republic of Korea
KMA

National Institute for Earth Physics
Romania
BUC

Altai-Sayan Seismological Centre, GS SB RAS
Russia
ASRS

Geophysical Survey of Russian Academy of Sciences
Russia
MOS

Mining Institute of the Ural Branch of the Russian Academy of Sciences
Russia
MIRAS

Kamchatka Branch of the Geophyisical Survey of the RAS
Russia
KRSC

Kola Regional Seismic Centre, GS RAS
Russia
KOLA

Sakhalin Experimental and Methodological Seismological Expedition, GS RAS
Russia
SKHL

Federal Center for Integrated Arctic Research
Russia
FCIAR

Yakutiya Regional Seismological Center, GS SB RAS
Russia
YARS

Baykal Regional Seismological Centre, GS SB RAS
Russia
BYKL

North Eastern Regional Seismological Centre, GS RAS
Russia
NERS

Saudi Geological Survey
Saudi Arabia
SGS

Seismological Survey of Serbia
Serbia
BEO

Geophysical Institute, Slovak Academy of Sciences
Slovakia
BRA

Slovenian Environment Agency
Slovenia
LJU

Council for Geoscience
South Africa
PRE

Institut Cartogràfic i Geològic de Catalunya
Spain
MRB

Instituto Geográfico Nacional
Spain
MDD

Real Instituto y Observatorio de la Armada
Spain
SFS

University of Uppsala
Sweden
UPP

Swiss Seismological Service (SED)
Switzerland
ZUR

Thai Meteorological Department
Thailand
BKK

The Seismic Research Centre
Trinidad and Tobago
TRN

Institut National de la Météorologie
Tunisia
TUN

Disaster and Emergency Management Presidency
Turkey
AFAD

Kandilli Observatory and Research Institute
Turkey
ISK

IRIS Data Management Center
U.S.A.
IRIS

Red Sísmica de Puerto Rico
U.S.A.
RSPR

Texas Seismological Network, University of Texas at Austin
U.S.A.
TXNET

Pacific Northwest Seismic Network
U.S.A.
PNSN

National Earthquake Information Center
U.S.A.
NEIC

The Global CMT Project
U.S.A.
GCMT

Subbotin Institute of Geophysics, National Academy of Sciences
Ukraine
SIGU

Main Centre for Special Monitoring
Ukraine
MCSM

Dubai Seismic Network
United Arab Emirates
DSN

International Seismological Centre Probabilistic Point Source Model
United Kingdom
ISC-PPSM

International Seismological Centre
United Kingdom
ISC

British Geological Survey
United Kingdom
BGS

Institute of Seismology, Academy of Sciences, Republic of Uzbekistan
Uzbekistan
ISU

Fundación Venezolana de Investigaciones Sismológicas
Venezuela
FUNV

Institute of Geophysics, Viet Nam Academy of Science and Technology
Viet Nam
PLV

Goetz Observatory
Zimbabwe
BUL

2.7 ISC Staff

Listed below are the staff (and their country of origin) who were employed at the ISC during the time period when the ISC worked on the data covered by this issue of the Summary.

- Dmitry Storchak
- Director
- Russia / United Kingdom

- Lynn Elms
- Administration Officer
- United Kingdom

- James Harris
- Senior System and Database Administrator
- United Kingdom

- Oliver Rea
- System Administrator
- United Kingdom

- Gary Job
- Data Collection Officer
- United Kingdom

- Domenico Di Giacomo
- Senior Seismologist
- Italy/UK

- Tom Garth
- Seismologist / Senior Developer
- United Kingdom

- Ryan Gallacher
- Seismologist / Developer
- United Kingdom

- Natalia Poiata
- Seismologist / Developer
- Moldova

- Rosemary Hulin
- Analyst
- United Kingdom

- Blessing Shumba
- Seismologist / Senior Analyst
- Zimbabwe

- Rebecca Verney
- Analyst
- United Kingdom

- Elizabeth Ayres
- Analyst / Historical Data Officer
- United Kingdom

- Kathrin Lieser
- Analyst Administrator / Summary Editor / Seismologist
- Germany

- Peter Franek
- Seismologist / Analyst
- Slovakia

- Burak Sakarya
- Seismologist / Analyst
- Turkey

- Daniela Olaru
- Historical and Bibliographical Data Officer
- Romania/UK

3

Availability of the ISC Bulletin

The ISC Bulletin is available from the following sources:

- Web searches
  The entire ISC Bulletin is available directly from the ISC website via tailored searches.
  (www.isc.ac.uk/iscbulletin/search)
  (isc-mirror.iris.washington.edu/iscbulletin/search)
  - Bulletin search - provides the most verbose output of the ISC Bulletin in ISF or QuakeML.
  - Event catalogue - only outputs the prime hypocentre for each event, producing a simple list of events, locations and magnitudes.
  - Arrivals - search for arrivals in the ISC Bulletin. Users can search for specific phases for selected stations and events.
- CD-ROMs/DVD-ROMs

  CDs/DVDs can be ordered from the ISC for any published volume (one per year), or for all back issues of the Bulletin (not including the latest volume). The data discs contain the Bulletin as a PDF, in IASPEI Seismic Format (ISF), and in Fixed Format Bulletin (FFB) format. An event catalogue is also included, together with the International Registry of seismic station codes.
- FTP site

  The ISC Bulletin is also available to download from the ISC ftp site, which contains the Bulletin in PDF, ISF and FFB formats. (ftp://www.isc.ac.uk)
  (ftp://isc-mirror.iris.washington.edu)

Mirror service

A mirror of the ISC database, website and ftp site is available at IRIS DMC (isc-mirror.iris.washington.edu), which benefits from their high-speed internet connection, providing an alternative method of accessing the ISC Bulletin.

4

Citing the International Seismological Centre

Data from the ISC should always be cited. This includes use by academic or commercial organisations, as well as individuals. A citation should show how the data were retrieved and may be in one of these suggested forms:

4.1 The ISC Bulletin

International Seismological Centre (2021), On-line Bulletin, `https://doi.org/10.31905/D808B830`

The procedures used for producing the ISC Bulletin have been described in a number of scientific articles. Depending on the use of the Bulletin, users are encouraged to follow the citation suggestions below:

a) For current ISC location procedure:

Bondár, I. and D.A. Storchak (2011). Improved location procedures at the International Seismological Centre, *Geophys. J. Int.*, *186*, 1220-1244, `https://doi.org/10.1111/j.1365-246X.2011.05107.x`

b) For Rebuilt ISC Bulletin (currently: 1964-1990):

Storchak, D.A., Harris, J., Brown, L., Lieser, K., Shumba, B., Verney, R., Di Giacomo, D., Korger, E. I. M. (2017). Rebuild of the Bulletin of the International Seismological Centre (ISC), part 1: 1964–1979. *Geosci. Lett.* (2017) 4: 32. `https://doi.org/10.1186/s40562-017-0098-z`

c) For principles of the ISC data collection process:

R J Willemann, D A Storchak (2001). Data Collection at the International Seismological Centre, *Seis. Res. Lett.*, *72*, 440-453, `https://doi.org/10.1785/gssrl.72.4.440`

d) For interpretation of magnitudes:

Di Giacomo, D., and D.A. Storchak (2016). A scheme to set preferred magnitudes in the ISC Bulletin, *J. Seism.*, *20(2)*, 555-567, `https://doi.org/10.1007/s10950-015-9543-7`

e) For use of source mechanisms:

Lentas, K., Di Giacomo, D., Harris, J., and Storchak, D. A. (2020). The ISC Bulletin as a comprehensive source of earthquake source mechanisms, *Earth Syst. Sci. Data*, *11*, 565-578,`https://doi.org/10.5194/essd-11-565-2020`

Lentas, K. (2018). Towards routine determination of focal mechanisms obtained from first motion P-wave arrivals, *Geophys. J. Int.*, *212(3)*, 1665–1686.`https://doi.org/10.1093/gji/ggx503`

f) For use of the original (pre-Rebuild) ISC Bulletin as a historical perspective:

Adams, R.D., Hughes, A.A., and McGregor, D.M. (1982). Analysis procedures at the International Seismological Centre. *Phys. Earth Planet. Inter. 30:* 85-93,https://doi.org/10.1016/0031-9201(82)90093-0

4.2 The Summary of the Bulletin of the ISC

International Seismological Centre (2021), Summary of the Bulletin of the International Seismological Centre, January - June 2019, *56(I)*,https://doi.org/10.31905/M8L1R7WI

4.3 The historical printed ISC Bulletin (1964-2009)

International Seismological Centre, Bull. Internatl. Seismol. Cent., 46(9-12), Thatcham, United Kingdom, 2009.

4.4 The IASPEI Reference Event List

International Seismological Centre (2021), IASPEI Reference Event (GT) List, https://doi.org/10.31905/32NSJF7V

Bondár, I. and K.L. McLaughlin (2009). A New Ground Truth Data Set For Seismic Studies, *Seismol. Res. Lett.*, *80*, 465-472, https://doi.org/10.1785/gssrl.80.3.465

Bondár, E. Engdahl, X. Yang, H. Ghalib, A. Hofstetter, V. Kirichenko, R. Wagner, I. Gupta, G. Ekström, E. Bergman, H. Israelsson, and K. McLaughlin (2004). Collection of a reference event set for regional and teleseismic location calibration, *Bull. Seismol. Soc. Am.*, *94*, 1528-1545, https://doi.org/10.1785/012003128

Bondár, E. Bergman, E. Engdahl, B. Kohl, Y.-L. Kung, and K. McLaughlin (2008). A hybrid multiple event location technique to obtain ground truth event locations, *Geophys. J. Int.*, *175*, https://doi.org/10.1111/j.1365-246X.2011.05011.x

4.5 The ISC-GEM Catalogue

International Seismological Centre (2021), ISC-GEM Earthquake Catalogue, https://doi.org/10.31905/d808b825, 2021.

Depending on the use of the Catalogue, to quote the appropriate scientific articles, as suggested below.

a) For a general use of the catalogue, please quote the following three papers (Storchak et al., 2013; 2015; Di Giacomo et al., 2018):

Storchak, D.A., D. Di Giacomo, I. Bondár, E.R. Engdahl, J. Harris, W.H.K. Lee, A. Villaseñor and P. Bormann (2013). Public Release of the ISC-GEM Global Instrumental Earthquake Catalogue (1900-2009). *Seism. Res. Lett.*, *84*, 5, 810-815, https://doi.org/10.1785/0220130034

Storchak, D.A., D. Di Giacomo, E.R. Engdahl, J. Harris, I. Bondár, W.H.K. Lee, P. Bormann and A. Villaseñor (2015). The ISC-GEM Global Instrumental Earthquake Catalogue (1900-2009): Introduction, *Phys. Earth Planet. Int.*, *239*, 48-63, https://doi.org/10.1016/j.pepi.2014.06.009

Di Giacomo, D., E.R. Engdahl and D.A. Storchak (2018). The ISC-GEM Earthquake Catalogue (1904–2014): status after the Extension Project, *Earth Syst. Sci. Data*, *10*, 1877-1899, https://doi.org/10.5194/essd-10-1877-2018

b) For use of location parameters, please quote (Bondár et al., 2015):

Bondár, I., E.R. Engdahl, A. Villaseñor, J. Harris and D.A. Storchak, 2015. ISC-GEM: Global Instrumental Earthquake Catalogue (1900-2009): II. Location and seismicity patterns, *Phys. Earth Planet. Int.*, *239*, 2-13, https://doi.org/10.1016/j.pepi.2014.06.002

c) For use of magnitude parameters, please quote (Di Giacomo et al., 2015a; 2018):

Di Giacomo, D., I. Bondár, D.A. Storchak, E.R. Engdahl, P. Bormann and J. Harris (2015a). ISC-GEM: Global Instrumental Earthquake Catalogue (1900-2009): III. Re-computed MS and mb, proxy MW, final magnitude composition and completeness assessment, *Phys. Earth Planet. Int.*, *239*, 33-47, https://doi.org/10.1016/j.pepi.2014.06.005

Di Giacomo, D., E.R. Engdahl and D.A. Storchak (2018). The ISC-GEM Earthquake Catalogue (1904–2014): status after the Extension Project, *Earth Syst. Sci. Data*, *10*, 1877-1899, https://doi.org/10.5194/essd-10-1877-2018

d) For use of station data from historical bulletins, please quote (Di Giacomo et al., 2015b; 2018):

Di Giacomo, D., J. Harris, A. Villaseñor, D.A. Storchak, E.R. Engdahl, W.H.K. Lee and the Data Entry Team (2015b). ISC-GEM: Global Instrumental Earthquake Catalogue (1900-2009), I. Data collection from early instrumental seismological bulletins, *Phys. Earth Planet. Int.*, *239*, 14-24, https://doi.org/10.1016/j.pepi.2014.06.005

Di Giacomo, D., E.R. Engdahl and D.A. Storchak (2018). The ISC-GEM Earthquake Catalogue (1904–2014): status after the Extension Project, *Earth Syst. Sci. Data*, *10*, 1877-1899, https://doi.org/10.5194/essd-10-1877-2018

e) For use of direct values of M0 from the literature, please quote (Lee and Engdahl, 2015):

Lee, W.H.K. and E.R. Engdahl (2015). Bibliographical search for reliable seismic moments of large earthquakes during 1900-1979 to compute MW in the ISC-GEM Global Instrumental Reference Earthquake Catalogue (1900-2009), *Phys. Earth Planet. Int.*, *239*, 25-32, https://doi.org/10.1016/j.pepi.2014.06.004

4.6 The ISC-EHB Dataset

International Seismological Centre (2021), ISC-EHB Dataset, https://doi.org/10.31905/PY08W6S3

Engdahl, E.R., R. van der Hilst, and R. Buland (1998). Global teleseismic earthquake relocation with improved travel times and procedures for depth determination, *Bull. Seism. Soc. Am.*, *88*, 3, 722-743.

http://www.bssaonline.org/content/88/3/722.abstract

Weston, J., Engdahl, E.R., Harris, J., Di Giacomo, D. and Storchack, D.A. (2018). ISC-EHB: Reconstruction of a robust earthquake dataset, *Geophys. J. Int.*, *214*, 1, 474-484, https://doi.org/10.1093/gji/ggy155

4.7 The ISC Event Bibliography

International Seismological Centre (2021), On-line Event Bibliography, https://doi.org/10.31905/EJ3B5LV6

Also, please reference the following SRL article that describes the details of this service:

Di Giacomo, D., Storchak, D.A., Safronova, N., Ozgo, P., Harris, J., Verney, R. and Bondár, I., 2014. A New ISC Service: The Bibliography of Seismic Events, *Seismol. Res. Lett.*, *85*, 2, 354-360, https://doi.org/10.1785/0220130143

4.8 International Registry of Seismograph Stations

International Seismological Centre (2021), International Seismograph Station Registry (IR), https://doi.org/10.31905/EL3FQQ40

4.9 Seismological Dataset Repository

International Seismological Centre (2021), Seismological Dataset Repository, https://doi.org/10.31905/6TJZECEY

4.10 Data transcribed from ISC CD-ROMs/DVD-ROMs

International Seismological Centre, Bulletin Disks 1-29 [CD-ROM], Internatl. Seismol. Cent., Thatcham, United Kingdom, 2021.

The ISC is named as a valid data centre for citations within American Geophysical Union (AGU) publications. As such, please follow the AGU guidelines when referencing ISC data in one of their journals. The ISC may be cited as both the institutional author of the Bulletin and the source from which the data were retrieved.

5

Notes from ISC Data Users

5.1 Using ISC Data

Jens Havskov[1] and Kathrin Lieser[2]

(1) University of Bergen, Department of Earth Science, Bergen, Norway

(2) International Seismological Centre, Thatcham, UK

Jens Havskov

Kathrin Lieser

It is well known the ISC has the most complete database of seismic event parameter data available anywhere and it also has the most complete catalogue of epicenters. The ISC will receive and store any data that is submitted so the ISC can also function as a useful backup for individual agencies. All that data is available online. Currently there are more than 27000 stations registered in the International Seismograph Station Registry and there has been a large increase in data received by ISC since it was founded in 1964 (see Figs. 7.3 and 7.7). To review all data available today would be too time-consuming and therefore, currently only events larger than magnitude 3.5 and a few others smaller than 3.5 under specific conditions (see Chapter 10.1 ISC Operational Procedures in Appendix, p. 110) are reviewed and/or relocated and magnitudes recalculated. For unreviewed events, only the hypocentres and magnitudes from the submitting agencies are given while for reviewed events ISC magnitudes and hypocentres are given in addition, if available. This of course is mostly the case for distant events. In addition, not all data is used in the reprocessing such as some amplitudes and back azimuths. While the hypocentres and magnitudes calculated by the ISC are very uniform, some associated data is less so (e.g., amplitudes that are reported by different agencies with different standards). Therefore, extracting a data set comprised of reviewed and unreviewed events will result in a non uniform data set and reprocessing it to make it uniform requires some filtering. In this note we will give some guidelines on how this can be done and give some examples.

The user can take out data from the ISC Bulletin in two formats: ISF (see Example 1) (`http://www.isc.ac.uk/standards/isf/`) and QuakeMl (`https://quake.ethz.ch/quakeml/`). The extracted ISC data will be illustrated using the most used ISF format. Some of the converted data is tested with SEISAN (*Havskov et al.*, 2020) which has software to convert ISF format to SEISAN (`http://seisan.info`).

5.1.1 Hypocentres

How the ISC is processing: The ISC reviews all events above M3.5 and certain events between 2.5 and 3.5 dependent on azimuthal gap, number of reported phases and number of reporting agencies. However, during review, tiny local events can also become reviewed events, e.g., when it is needed to move phases out into larger events. But not all reviewed events have an ISC hypocentre. At least two different agencies must report phases and an azimuthal gap of less than 315 degrees is required for an event to qualify for an ISC solution. If the event does not meet the criteria for an ISC solution the event is fixed to an agency hypocentre, i.e. residuals are calculated with the ak135 velocity model (*Kennett et al.*, 1995) where the hypocentre parameter of an agency are used (origin time, RMS, latitude, longitude, depth etc.) and the phase names are changed according to ak135. If several hypocentres are available one will be designated the prime hypocentre. If an ISC solution is available this will usually be the prime hypocentre (see Example 1), except for some rare cases where the IASPEI solution for reference events was set as prime for nuclear explosions. If there is no ISC solution the prime is found by a score based on the network coverage. Should this not be available it is essentially random.

There are some exceptions to these rules regarding IDC (International Data Center of CTBTO). All events reported by IDC are reviewed and unless IDC is the only hypocentre author with less than six associated seismic phases in an event, the ISC will try to calculate an ISC hypocentre.

In short: every ISC solution is reviewed but not all reviewed events have an ISC solution. Reviewed events will show residuals according to ak135 while unreviewed events are not relocated and will not show residuals even if the reporting agency has reported any residuals. For more details see ISC Operational Procedures (Appendix).

If, for a particular area, the user takes out a mixture of reviewed and unreviewed events, the data set will not be uniform since different programs and earth models might have been used by the several reporting agencies. To create a uniform data set it must be relocated as not all reported hypocentres have been calculated with ak135 and unreviewed events do not show any residuals. That can lead to problems with phase names, see next section. Note that when searching the ISC Bulletin for a particular area and an event has several hypocentres, the event will be selected if any of the hypocentres are within the selected area. Similarly, if any of the magnitudes are within the given range, the event will be selected. However, there is an option to only take magnitudes determined by a specific author into account.

Recommendation: Use the prime solution. However be aware that the prime hypocentre in an unreviewed event with several reporting agencies might not always be the best fitting solution and the quality can only be judged by reviewing it after relocation. It should also be mentioned that not all agencies send all of their station data to the ISC and an agency's hypocentre might have been calculated with more stations available to the local agency than is shown in the ISC Bulletin.

5.1.2 Seismic Phases

The IASPEI Commission on Seismological Observation and Interpretation (*Storchak et al.*, 2003, `http://www.isc.ac.uk/standards/phases/`) has given a recommended list of official phases that should be used in reporting. The identification of phases varies a great deal between the currently 150 reporting agencies. The ISC location program, ISCloc (*Bondar and Storchak*, 2011) will reinterpret the phase type so it best fits the ak135 model used for location which will make the phase identification more uniform for reviewed events. The original phase names provided by the agencies are stored and the user can get them by extracting data in QuakeMl format but not in the ISF format. The original data files submitted to the ISC can be found online on the agency web pages of the ISC web site: `http://www.isc.ac.uk/iscbulletin/agencies/`.

The ISC uses a relative weighting scheme to ensure that arrivals picked less reliably or prone to phase identification errors are down-weighted in the location algorithm (see *Bondar and Storchak*, 2011; ISCloc manual (`http://www.isc.ac.uk/iscbulletin/iscloc/`) and ISC Operational Procedures (Appendix)). Reported weights and weights calculated by ISCloc are not provided and the only indication on a high or low weight is if the phase is flagged as time defining or not. Note that phase weights reported by the agencies are not used.

ISCloc is allowed to re-interpret phases in every distance range, e.g., P phases can become Pn, Pb, Pg, PP, PnPn, PKiKP, Pdif, PcP, PKP(ab/bc/df) etc as well as depth phases, with a similar set up for S phases. There are certain rules to that, e.g., depth phases cannot be set as first arrivals by ISCloc or P phases cannot be renamed as S phases. An analyst can fix a phase to every available phase name manually though. Some agencies report their phases as just P, even if they are actually a PP, PKPbc or PKiKP phase and thus ISCloc needs to be flexible. Obviously, this can go wrong and will be fixed during review by an analyst. Only P and S type phases are used for location and phases like Lg and T are not used. If residuals are larger than 60 s the phase is treated as unidentified. For more details see ISCloc manual (`http://www.isc.ac.uk/iscbulletin/iscloc/`). ISCloc will take all IASPEI phases into account but not all phases necessarily become time defining. This depends on the weighting algorithm in ISCloc, e.g., very large residuals are rejected. Phases not contributing (meaning weighted out) will not have a time defining flag but the residuals will be calculated. Example 1 shows an event where some phases are time-defining while others are not: Pn on station SRK with a residual of -5.1 s was not used in the location, while PETK Pn with -1.5 s residual contributed to the solution as can be seen by the time defining flag T in column Def.

Example 1: Event where some phases are time-defining while others are not (ISF format). The abbreviations and units in this and the following (ISF) examples are: Err - origin time error, Smaj and Smin - semi major and minor axis of the epicenter error ellipse in km, Az - azimuth of error ellipse (degree), Depth (km), f for fixed, Ndef - number of defining phases, Nsta - number of defining stations, Gap - azimuthal gap (degree), Mdist - distance to closest station (degree), Qual (hypocentre) - analysis type and location method, Author - author of origin, Sta - station, Dist - epicentral distance (degree), EvAz - azimuth from event to station (degree), Tres - travel time residual (s), Azim - back azimuth (degree), Slow - slowness (s/degree), Sres - slowness residual (s/degree), Def - T is time defining flag, SNR - signal to noise ratio, Amp - amplitude (nm), Per - period of amplitude (s), Qual (phases) - direction of motion, manual (m) or automatic (a), onset quality, Magnitude - showing both the type and the value. Standards and formats can be found here: `http://www.isc.ac.uk/standards/`

```
Event 13918462 Kuril Islands
Date       Time        Err   RMS Latitude Longitude  Smaj  Smin  Az Depth   Err Ndef Nsta Gap  mdist  Mdist Qual   Author
2009/10/01 00:23:28.90              46.3900  153.3400                  49.0
     SKHL
2009/10/01 00:23:29.50   0.70       46.8400  152.8900   8.9   8.4  -1  30.0                                           JMA
2009/10/01 00:23:32.00   1.06       46.6490  152.7380  13.6   8.2  53  53.0          28                               MOS
2009/10/01 00:23:33.83   0.60 0.740 46.6669  152.6732  18.9  10.8 155  49.4   4.7    31      136   7.22  78.40     uk IDC
2009/10/01 00:23:31.67   0.55 2.580 46.2097  153.0627 11.81 6.113 144  48.0  4.49   102   86 136   3.77  78.93 m i ke ISC
 (#PRIME)

Magnitude  Err Nsta Author      OrigID
MPVA    5.0          SKHL      00764866
MSH     5.2          SKHL      00764866
MMM     5.1          JMA       15072871
mb      4.2       10 MOS       14469069
mb      3.7 0.1   18 IDC       16645279
mb1     4.0 0.1   21 IDC       16645279
mb1mx   3.9 0.1   30 IDC       16645279
mbtmp   4.0 0.1   21 IDC       16645279
MS      3.3 0.1    8 IDC       16645279
Ms1     3.3 0.1    8 IDC       16645279
ms1mx   3.1 0.1   47 IDC       16645279
mb      4.0 0.1   18 ISC       16764113
MS      3.5 0.1    5 ISC       16764113

Sta     Dist  EvAz Phase        Time      TRes  Azim AzRes   Slow   SRes Def   SNR       Amp   Per Qual Magnitude
KUR     3.77 256.8 Pn       00:24:28.9     1.7                           T__                         ci
KUR     3.77 256.8 Sn       00:25:14.6     4.4                           T__                         _i
SKR     4.92  23.3 Pn       00:24:37.6    -5.3                           ___                         _e
PETK    7.53  21.8 Pn       00:25:17.283  -1.5 185.7        13.00        T__  35.1       2.3  0.33  __
SONM   31.48 290.2 P        00:29:46.6    -2.2  59.5         8.50        T__   2.2       0.4  0.76  __ mb      3.3
SONM   31.48 290.2 LR       00:43:22.117       113.1        38.20        ___            76.5 18.28  __ MS      3.4
```

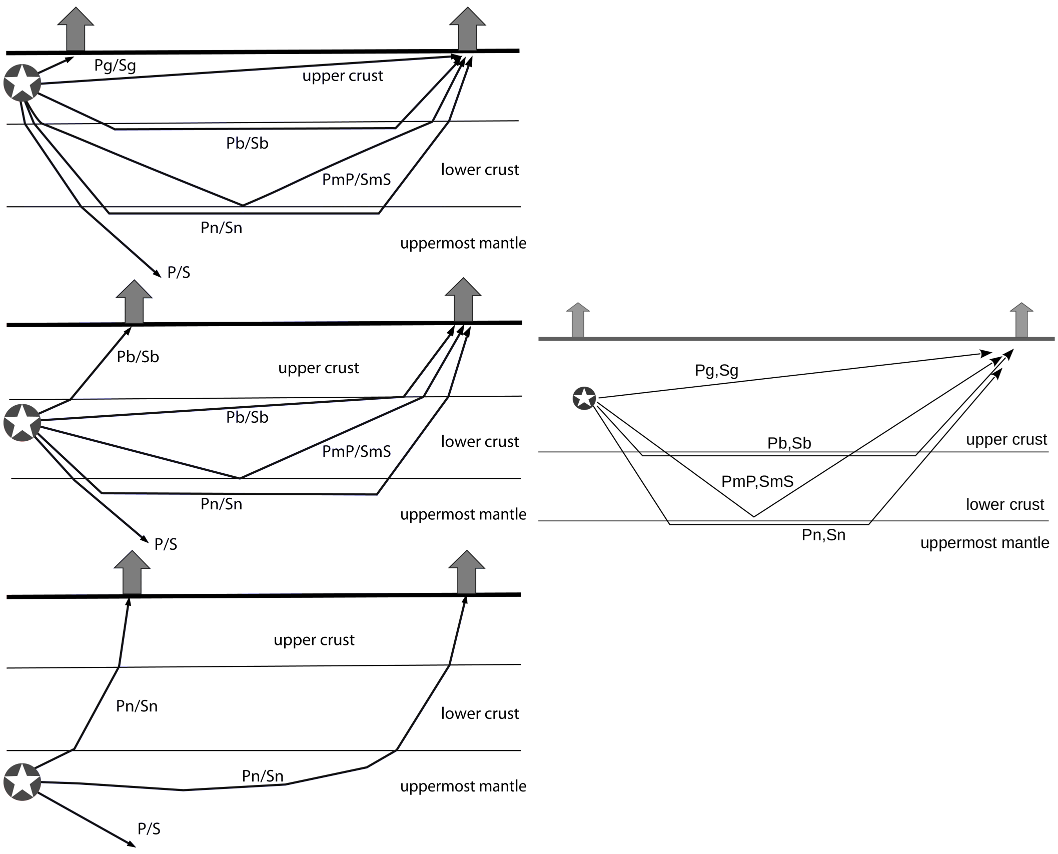

Figure 5.1: *Left: Phase definition in the ak135 model (after* Storchak et al., *2003, 2011;* Schweitzer et al., *2019), right: traditional phase definitions (e.g.* Aki and Richards, *2002;* Stein and Wysession, *2003).*

For some local phases the change of phase names gives an undesirable side effect. At short distances the main phases are Pg, Pb and Pn which traditionally are identified as seen in Figure 5.1 with Pn as a refracted wave along the Moho. However, the IASPEI definition of Pn follows the ak135 notation that includes any P wave bottoming in the uppermost mantle or an up-going P wave from a source in the uppermost mantle (`http://www.isc.ac.uk/standards/phases/`). This implies that for some distance/depths both Pb and Pn, in the ak135 definition, are what most location program would call Pg or P. The Pg phase in ak135 is what is traditionally called Pg. This change of definition from earlier practice was decided by the IASPEI Working Group on Standard Phase Names because the corresponding ak135 code did not differentiate between the classic Pn travelling as a headwave alongside the Moho and the branch of direct P that leaves a source in the uppermost mantle (Dmitry Storchak, personal communication).

For local earthquakes, the user will mostly use a standard location program (such as *Hypoinverse* (*Klein*, 2002) or *Hypocenter* used in SEISAN (*Lienert and Havskov*, 1995)) using a flat layer velocity model. Having the phases identified as Pb or Pn will then imply an identification which might not be in accordance with the local model or which cannot be calculated (Pn if the source is below Moho, Pb if the source is below Conrad). The Pb phase is rarely observed in practice and the corresponding Conrad layer might not be present in all models. So for local use Pb and Pn should be relabelled as P in order to get reliable locations (see Examples 2-4). The same is the case for the corresponding S-phases.

Example 2: The agency identified phases are shown in parenthesis. The agency phase identification is what traditionally would have been expected and the nearest station show Pg and Sg. In this case changing all Pn/Sn-phases to P and S will, when relocating, again identify the first two phases as g-types.

```
Event  14091935 Sichuan
Date         Time         Err    RMS Latitude Longitude   Smaj   Smin   Az   Depth   Err Ndef Nsta Gap   mdist   Mdist Qual    Author
2009/10/01 23:04:55.45    0.97 1.462   31.2363   104.1277 24.69 7.464 139   14.0f           9    7  94    0.45   58.57 m i ke ISC

Sta       Dist  EvAz Phase         Time       TRes  Azim AzRes    Slow    SRes Def
CD2       0.45 224.4 Pn(Pg)    23:05:07.4     -0.2                             T__
CD2       0.45 224.4 Sn(Sg)    23:05:14.5     -1.1                             T__
XAN       4.92  54.1 Pn(Pn)    23:06:09.6      0.6                             T__
XAN       4.92  54.1 Pg(Pg)    23:06:27.1     -2.5                             T__
XAN       4.92  54.1 Sn(Sn)    23:07:06.2      0.5                             T__
```

Example 3: In this event, all phases are labelled as Pn/Sn and a standard location program will put the event above Moho unless the program ignores the n. The original phases reported were all P and S. By removing the n, *Hypocenter* locates the event at 160 km depth. We do not know the local model or program used to get the agency's 86 km depth. Removing station JHO gives a 40 km depth so the depth is not well defined. These phases would traditionally have been called P/S. Note that the time defining flag is not set since the ISC did not locate the event and only calculated the residuals with the location fixed to the JMA solution.

```
Event  15487367
Date         Time          Err    RMS Latitude Longitude   Smaj   Smin   Az Depth    Err Ndef Nsta Gap   mdist   Mdist Qual    Author
2009/10/01 22:36:15.70    0.40          26.0000   140.6600    4.4    4.0   -1   86.0                                                JMA

Magnitude   Err Nsta Author       OrigID
       4.2             JMA        15073229

Sta       Dist  EvAz Phase         Time       TRes  Azim AzRes    Slow    SRes Def
JHHJ      1.50  65.0 Pn        22:36:41.4      0.2                             ___
JHHJ      1.50  65.0 Sn        22:37:00.9      0.3                             ___
CBIJ      1.75  51.0 Pn        22:36:44.7      0.2                             ___
CBIJ      1.75  51.0 Sn        22:37:07.3      1.0                             ___
BS01      8.63   1.7 Pn        22:38:15.3     -1.9                             ___
BS03      8.77 359.2 Pn        22:38:16.8     -2.7                             ___
JOD2      9.33 352.0 Pn        22:38:26.3     -1.0                             ___
JRY      10.10 351.8 Pn        22:38:35.8     -2.0                             ___
JAG      10.44 354.6 Pn        22:38:38.6     -3.9                             ___
JHO      10.58 359.6 Pn        22:38:39.7     -4.6                             ___
JHO      10.58 359.6 Sn        22:40:30.2    -10.7                             ___
```

Example 4: The nearest station in this example reports Pb (VLS) and a station further away reports Pg (AMT). Trying to relocate this event with *Hypocenter* and the ak135 model will ignore the first station (if flag for enforcing Pb and Pn is set) since it is too close for Pb. When using only P and S, all stations will be used. For more distant stations, Pn will be the first arrival instead of Pb, the phase at the closest station will be Pg and the RMS will be smaller compared to forcing the arrivals to be Pb. This shows that it can be problematic to label first arrivals Pg, Pb and Pn.

```
Event 15069387 Ionian Sea
Date         Time          Err    RMS Latitude Longitude  Smaj   Smin   Az Depth    Err Ndef Nsta Gap  mdist  Mdist Qual   Author
2009/10/01 23:04:09.70          0.400  38.0200   19.9700   8.5   11.0  -1  12.0   8.1    6      323                          ATH
2009/10/01 23:04:09.30          1.570  38.0200   19.9600f10000 10000       12.0f         6    5 323   0.52   1.88     uk
     CSEM

Magnitude  Err Nsta Author       OrigID
MD      3.2        5 ATH        14603884
MD      3.2          CSEM       16462702

Sta      Dist  EvAz Phase         Time      TRes  Azim AzRes   Slow   SRes Def
VLS      0.52  72.3 Pb       23:04:19.7                                    ___
VLS      0.52  72.3 Pb       23:04:19.7                                    ___
AMT      1.47 108.8 Pg       23:04:37.0                                    ___
AMT      1.47 108.8 Sb       23:04:57.1                                    ___
AMT      1.47 108.8 Pb       23:04:37.0                                    ___
AMT      1.47 108.8 Sb       23:04:57.1                                    ___
EFP      1.58  74.6 Pb       23:04:39.2                                    ___
EFP      1.58  74.6 Pb       23:04:39.2                                    ___
KLV      1.73  88.5 Pb       23:04:41.2                                    ___
KLV      1.73  88.5 Pn       23:04:41.2                                    ___
GUR      1.88  91.8 Pn       23:04:43.5                                    ___
GUR      1.88  91.8 Pn       23:04:43.5
```

Below is the SEISAN relocation forcing Pb, Sb and Pn. PN2 means refracted from interface 2 (Conrad) and PN3 is refracted from layer 3 (Moho).

Abbreviations are: hrmn - hour and minute, lat - latitude, long - longitude, depth is in km, no - number of stations, m - number of degrees of freedom, damp - damping, errln, errlt, errdp - error (km) in latitude, longitude and depth, respectively, stn - station, dist - distance (km), azm - azimuth(degree), ain - angle of incidence (degree), w - input weight, phas - given phase, calcphs - phase used by program, tsec - second of arrival, t-obs - observed travel time (s), t-cal - calculated travel time (s), res - residual (s), wt - weight used, di - importance of phase.

```
 date hrmn   sec      lat      long depth   no m    rms  damp erln erlt erdp
910 1 23 4 10.35 38 3.84N  19 58.1E  12.0*  10 2   0.87 0.000 27.4 20.4  0.0
stn   dist   azm  ain w phas     calcphs hrmn tsec  t-obs  t-cal    res   wt di
VLS     56  76.8      0 Pb               23 4 19.7    9.4
VLS     56  76.8      0 Pb               23 4 19.7    9.4
AMT    164 110.5 94.3 0 Pg       PG      23 4 37.0  26.65  28.40  -1.75 1.00  8
AMT    164 110.5 64.0 0 Sb       SN2     23 4 57.1  46.75  46.27   0.48 1.00 18
AMT    164 110.5 63.2 0 Pb       PN2     23 4 37.0  26.65  27.49  -0.84 1.00 11
AMT    164 110.5 64.0 0 Sb       SN2     23 4 57.1  46.75  46.27   0.48 1.00 18
EFP    174  76.0 63.2 0 Pb       PN2     23 4 39.2  28.85  29.01  -0.16 1.00 14
EFP    174  76.0 63.2 0 Pb       PN2     23 4 39.2  28.85  29.01  -0.16 1.00 14
KLV    192  90.0 63.2 0 Pb       PN2     23 4 41.2  30.85  31.71  -0.86 1.00  2
KLV    192  90.0 46.2 0 Pn       PN3     23 4 41.2  30.85  29.97   0.88 1.00  4
GUR    209  93.2 46.2 0 Pn       PN3     23 4 43.5  33.15  32.18   0.97 1.00  5
GUR    209  93.2 46.2 0 Pn       PN3     23 4 43.5  33.15  32.18   0.97 1.00  5
```

SEISAN output using just P and S:

```
 date hrmn   sec      lat      long depth   no m    rms  damp erln erlt erdp
910 1 23 4 11.59 38 6.32N  20  1.6E  12.0*  12 2   0.55 0.000 16.1 10.2  0.0
stn   dist   azm  ain w phas     calcphs hrmn tsec  t-obs  t-cal    res   wt di
VLS     50  80.7103.9 0 P        PG      23 4 19.7   8.11   8.88  -0.77 1.00 12
VLS     50  80.7103.9 0 P        PG      23 4 19.7   8.11   8.88  -0.77 1.00 12
AMT    161 112.7 46.2 0 P        PN3     23 4 37.0  25.41  26.17  -0.75 1.00 11
AMT    161 112.7 50.6 0 S        SN3     23 4 57.1  45.51  45.19   0.32 1.00 19
AMT    161 112.7 46.2 0 P        PN3     23 4 37.0  25.41  26.17  -0.75 1.00 11
AMT    161 112.7 50.6 0 S        SN3     23 4 57.1  45.51  45.19   0.32 1.00 19
EFP    168  77.2 46.2 0 P        PN3     23 4 39.2  27.61  27.01   0.61 1.00  5
EFP    168  77.2 46.2 0 P        PN3     23 4 39.2  27.61  27.01   0.61 1.00  5
KLV    186  91.5 46.2 0 P        PN3     23 4 41.2  29.61  29.35   0.27 1.00  1
KLV    186  91.5 46.2 0 P        PN3     23 4 41.2  29.61  29.35   0.27 1.00  1
GUR    204  94.6 46.2 0 P        PN3     23 4 43.5  31.91  31.59   0.33 1.00  1
GUR    204  94.6 46.2 0 P        PN3     23 4 43.5  31.91  31.59   0.33 1.00  1
```

To use the most reliable data it is recommended to give a full weight to phases that are time defining in an ISC solution as these phases will have been identified by ISCloc and will show acceptable residuals. However, non-defining phases should not be dismissed because of their larger residuals or no residuals (meaning that ISCloc was not able to identify this phase) as they might be a good fit when using another velocity model. ISCloc imposes hard limits on distance and depth, e.g., Pg phases above around 10 degrees distance will not fit ak135 and show either no or large residuals. Another example for this is PKPbc which can be misidentified outside its defined distance range as a different phase by ISCloc and show large residuals. ISC analysts then fix the phase manually back to PKPbc, which will result in no residual being shown as it cannot be calculated. Also note that depth phases will only be time defining when they are accompanied by a P phase on the same station. Thus, depth phases can be a perfectly good pick whilst being non-defining. In some cases, phases can have good residuals but do not contribute to an ISC solution yet as ISCloc stops after a certain number of iterations. These phases will likely become time defining after another run of ISCloc, which is usually done by ISC analysts during review if necessary. Nevertheless, some phases in the ISC Bulletin might have good residuals while being non-defining due to this effect.

For events that are not reviewed by the ISC there are no residuals in the ISC Bulletin. For these events all phases have to be used for relocation since we have no idea which phases were used by the local agency. However, as there is often not a consistent practice when picking Pg, Pb and Pn and corresponding S it might be necessary to also relabel these phases to just P and S.

Recommendation: For events relocated by the ISC, use all phases with a time defining flag. Other phases, from the same event, without a time defining flag but with a residual, should be included with a low weight. Phases without residuals should be included with zero weight so they can be evaluated after relocation. ISC reviewed events which are fixed to the agency location and reported with ak135 residuals should all be used since there is no time defining flag. For events not reviewed and located by the ISC, use all phases. Consider relabelling all crustal phases to P and S.

5.1.3 Back Azimuth and Slowness

The back azimuth (BAZ) can be useful for improving the epicenter location, particular for small events. The ISC reports the back azimuth determined by an agency but ISCloc does not use it in calculating locations and thus there is no quality check. Back azimuth from arrays are usually OK, at least for P, and could potentially be used. Occasionally, ISC analysts make use of back azimuth and slowness from arrays to confirm the phase association to an event if the phase readings are reported without a hypocentre. Slowness can be converted to apparent velocity and is useful for phase identification. However, currently the back azimuth must be removed or weighted out to not corrupt the relocation. Slowness is not used by many programs and, even for arrays, can be wrong.

Example 5: BAZ from arrays fit within about +/- 20 degrees. For H11S2, the back azimuth fits well but the slowness is completely wrong as a T-wave takes more than 0.7s to travel one degree. So be aware that automatic data from arrays might not always be reliable. Station AFI gives 3 different values for back azimuth where only 227 is correct.

```
Event 17141286 Tonga Islands
Date       Time        Err   RMS Latitude Longitude  Smaj  Smin  Az Depth   Err Ndef Nsta Gap  mdist  Mdist Qual   Author
2009/10/01 23:13:04.72   3.41 0.610 -15.2759 -173.6043 184.3  28.9 146   0.0f          5      210  49.68 145.

Magnitude  Err Nsta Author      OrigID
mb      3.7 0.1    4 IDC       16645498

Sta     Dist  EvAz Phase        Time      TRes  Azim AzRes   Slow   SRes Def
AFI     2.23  52.7 Pn       23:13:38.835  -4.2  76.4          9.10        ___
```

AFI	2.23	52.7	Sn	23:13:58.435	-12.9	227.1		22.50		___
AFI	2.23	52.7	LR	23:14:04.0		183.6		26.60		___
H11S2	38.76	329.3	T	00:01:16.715		152.1		0.70		___
WRA	49.68	256.7	P	23:21:58.55	-0.3	89.5		6.90		___
ASAR	49.96	251.8	P	23:22:00.7	-0.3	87.7		7.80		___
TXAR	80.71	56.2	P	23:25:23.15	2.9	224.0		5.20		___
PDAR	82.31	41.9	P	23:25:28.65	0.0	208.1		5.00		___
ILAR	82.36	11.2	P	23:25:27.5	-0.6	209.5		7.10		___
BRTR	145.94	320.9	PKPab	23:32:47.1	-0.2	118.6		1.50		___

Example 6: This event was not relocated by the ISC. Relocating it with SEISAN without using BAZ, gives nearly the same solution as IDC. Including the back azimuth from the most reliable P phases changes the location slightly but also shows that the BAZ values are not very reliable with up to 40 degree residuals on P and up to 98 degrees on other phases.

Abbreviations: IDC - IDC location, SEISAN - SEISAN location without BAZ, - -BAZ - SEISAN location with BAZ.

	Year	moda	hrmn	sec	lat	lon	depth	rms
IDC:	2009	1001	0003	12.4	-4.817	153.350	79.2	0.51
SEISAN:	2009	1001	0003	11.4	-4.818	153.350	70.5	0.52
--BAZ :	2009	1001	0003	11.4	-4.821	153.345	70.7	0.40

Event 17141139 New Ireland region

Date	Time	Err	RMS	Latitude	Longitude	Smaj	Smin	Az	Depth	Err	Ndef	Nsta	Gap	mdist	Mdist	Qual	Author	OrigID
2009/10/01	00:03:12.44	4.83	0.510	-4.8165	153.3501	28.9	19.3	48	79.2	39.6	15		177	7.66	150.83	uk	IDC	16645277

Magnitude		Err	Nsta	Author	OrigID
mb	3.7	0.1	10	IDC	16645277
mb1	3.9	0.1	11	IDC	16645277
mb1mx	3.7	0.1	21	IDC	16645277
mbtmp	3.8	0.1	11	IDC	16645277
ML	3.3	0.3	1	IDC	16645277
MS	3.6	0.2	1	IDC	16645277
Ms1	3.5	0.2	1	IDC	16645277
ms1mx	2.7	0.1	26	IDC	16645277

Sta	Dist	EvAz	Phase	Time	TRes	Azim	AzRes	Slow	SRes	Def	SNR	Amp	Per	Qual	Magnitude	
PMG	7.65	233.1	Pn	00:05:02.585	1.4	13.3		5.60		___	3.5	2.3	0.33	__	ML	3.3
PMG	7.65	233.1	Sn	00:06:26.335	-0.1	151.7		21.30		___	10.4	11.1	0.33	__		
DZM	21.33	144.7	P	00:07:52.7	-0.5	295.0		16.70		___	3.8	2.8	0.57	__	mb	3.6
WRA	23.85	229.3	P	00:08:18.75	0.1	53.6		9.80		___	17.9	2.2	0.50	__	mb	3.7
ASAR	26.51	223.1	P	00:08:43.05	0.3	57.5		9.20		___	6.8	0.5	0.43	__	mb	3.3
ASAR	26.51	223.1	PcP	00:12:06.119	0.2	112.8		1.70		___	4.4	0.2	0.34	__		
STKA	29.09	200.9	P	00:09:05.475	-0.2	39.7		12.30		___	5.4	1.2	0.58	__	mb	3.7
STKA	29.09	200.9	LR	00:21:17.31		25.7		37.30		___		108.4	19.41	__	MS	3.6
FITZ	30.13	241.8	P	00:09:14.687	-0.3	78.0		9.20		___	12.6	2.8	0.67	__	mb	4.0
RPZ	41.77	160.7	P	00:10:53.917	-0.1	301.0		5.90		___	5.2	9.6	0.71	__	mb	4.4
SONM	66.63	327.6	P	00:13:54.3	-0.4	153.5		5.80		___	2.9	0.3	0.52	__	mb	3.1
VNDA	72.79	178.1	P	00:14:32.2	0.3	341.3		7.30		___	9.1	2.3	0.72	__	mb	4.0
MKAR	80.70	318.8	P	00:15:17.5	0.5	96.9		7.10		___	12.6	0.4	0.43	__	mb	3.4
MKAR	80.70	318.8	pP	00:15:35.875	-1.1	134.1		5.20		___	3.6	0.6	0.83	__		
MAW	85.77	202.6	P	00:15:42.738	0.1	93.5		6.00		___	9.3	2.0	0.61	__	mb	4.1
TORD	150.83	288.4	PKPbc	00:22:56.325	-0.6	67.4		1.40		___	20.2	0.7	0.45	__		
TORD	150.83	288.4	PKPab	00:23:03.475	-0.9	62.5		2.40		___	9.3	0.4	0.45	__		

SEISAN BAZ residuals. *T-obs, t-cal and res are now in degrees.*

stn	dist	azm	ain	w	phas	calcphs	hrmn	tsec	t-obs	t-cal	res
PMG	851	233.1			BAZ-P				13.3	53.8	-40.55
PMG	851	233.1			BAZ-S				151.7	53.8	97.85
DZM	2374	144.7			BAZ-P				295.0	321.6	-26.63
WRA	2654	229.3			BAZ-P				53.6	53.4	0.18
ASAR	2951	223.2			BAZ-P				57.5	48.0	9.48
ASAR	2951	223.2			BAZ-PcP				112.8	48.0	64.78
STKA	3238	200.9			BAZ-P				39.7	24.7	15.02
STKA	3238	200.9			BAZ-LR				25.7	24.7	1.02
FITZ	3354	241.8			BAZ-P				78.0	67.4	10.61
RPZ	4650	160.7			BAZ-P				301.0	332.9	-31.94
SONM	7417	327.6			BAZ-P				153.5	127.5	26.00
VNDA	8103	178.1			BAZ-P				341.3	351.1	-9.83
MKAR	8983	318.8			BAZ-P				96.9	107.2	-10.33
MKAR	8983	318.8			BAZ-pP				134.1	107.2	26.87
MAW	9547	202.6			BAZ-P				93.5	92.3	1.22
TORD	16790	288.4			BAZ-PKPbc				67.4	76.1	-8.72

Recommendation: Weight out back azimuth or calculate residual and include if they fit. Often they do not.

5.1.4 Amplitudes

Amplitudes can cause a lot of confusion since different standards have been used and it is not always clear what correction has been applied by different agencies to produce the amplitude readings. This becomes very complex for magnitudes not calculated by the ISC. Amplitudes can be reported together with the phase reading and in that case there is no information on the time of the observations. Or they can be reported as 'amplitude phases'. Amplitude readings that follow the standard of the IASPEI Working Group on Magnitudes seem to be mostly correct in the ISC Bulletin (*IASPEI*; *Bormann and Dewey*, 2014). The unit is supposed to be nm ground displacement if the names include an A (such as AML) or nm/s if the name has a V (such as IVmBB), see `http://www.isc.ac.uk/standards/phases/#amplitude`. In addition, the ISC accepts amplitudes with the phase names P, pP, sP, AMB and pmax. Ideally only the latest IASPEI recommendation names should be used (it has been the standard for 8 years now) but that would severely limit the available data. The ISC only use amplitudes for mb and MS calculations so these amplitudes are checked and amplitudes that appear to be faulty are not used in the average. This is done by examining the station magnitude distribution (for mb and MS) during review for each event and spotting outliers and patterns. Usually the alpha trimmed median applied by ISCloc will dismiss outliers during magnitude calculations. Currently 39 types of magnitudes are reported to the ISC (see Section 7.5, p.66) and since the ISC is only calculating mb and MS, the input data (mainly amplitudes) for the remaining magnitudes are not checked.

Ml

Ml is not recalculated by the ISC and there seem to be many non standard amplitudes reported. In addition Ml scales for different regions vary so there is no way of calculating correct Ml without using different scales from different regions. The IASPEI standard (*Bormann and Dewey*, 2014) requires to calculate maximum ground displacement in nanometres using a filter that simulates the Wood Anderson (WA) instrument response. The magnitude relation is:

$$Ml_{iasp} = \log(A) + 1.11\log(R) + 0.00189R - 2.09, \tag{5.1}$$

where A is ground displacement in nm and R hypocentral distance in km.

So in order to use amplitudes for Ml calculations some selection must be done. If the standard IASPEI notation IAML is used the amplitudes seem OK in most cases. AML is used for non-standard displacement amplitude measurements and some of these do not fit well. Many amplitudes reported with the S or Sg phases also seem OK, but there are examples where they are off by a factor of e.g., 1000 so there is no guarantee they are correct. In a few cases, the amplitudes have been reported in mm on a Wood Anderson seismogram instead of nm ground displacement (ground displacement = WA displacement/2080). The ISC will convert the reported amplitudes to nm when parsing data into the database as this is the ISF standard unit for amplitudes. However, the ISC does not convert from WA to ground displacement as this cannot be reliably done with the various non-standard reported amplitudes. So be aware that amplitudes for Ml are given in nm but do not necessarily reflect ground displacement but could be the amplitude in nm on a Wood Anderson seismogram. Unfortunately, data are sometimes reported in the wrong unit. In obvious cases, such as values consistently being off by 1000, this will be fixed if spotted by the ISC. Maximum amplitude is often reported on both P and S for short distances but there is no standard magnitude scale which can be used with these P-amplitudes. Amplitudes for Ml are not checked by the ISC, however it seems that amplitudes from trustworthy agencies are OK. IMS (International Monitoring System by CTBTO) arrays may report amplitudes that they use for Ml. However often they cannot be used since they may be non standard, often reported on both P and S beams so they give a wrong Ml if used with the standard scale. Amplitudes reported with AML seem mostly correct, but not always, see Examples 7-11. So in the end, only a fraction of the amplitudes for Ml reported by the ISC can generally be relied upon.

Example 7: The amplitudes seem to be too large by a factor of 1000 when initially calculating Ml and might have been reported in nm and not in micrometre as was indicated, but they were likely reported as Wood Anderson amplitudes. The comment says that amplitudes are in micrometres. However, when parsing the data into the ISC database amplitudes are converted into nanometres and comments like these should be ignored. The ISC aims to remove those comments and for the example below (and other events) this has now been done.

```
Event   600896052 Greece-Albania border region
Date         Time         Err    RMS Latitude Longitude  Smaj  Smin  Az Depth   Err Ndef Nsta Gap  mdist  Mdist Qual  Author
2011/02/01 01:48:46.50         1.540  39.9775   20.9862f 9999 10000       17.8f         12    7 128   0.27   1.41    ke CSEM
2011/02/01 01:48:46.55         0.460  39.9775   20.9862   6.3   0.9 167  17.8   6.3   12      111   0.27   1.42    ke ATH

(Event not reviewed by the ISC)
(Analyst: Ch.Ventouzi ML Amplitudes are expressed in micrometres All distances are expressed in km)

Magnitude  Err Nsta Author      OrigID
ML     1.2         3 CSEM       601687637
ML     1.2         3 ATH        600844792

Sta      Dist  EvAz Phase        Time      TRes  Azim AzRes   Slow   SRes Def   SNR       Amp   Per Qual Magnitude
MEV      0.27 135.8 P        01:48:52.95                                 ___                          __
MEV      0.27 135.8 P        01:48:53.0                                  ___                          __
JAN      0.34 198.1 AML      01:49:00.83                                 ___        116400.0  0.12  __ ML     1.5
NEST     0.44   6.3 P        01:48:54.89                                 ___                          __
NEST     0.44   6.3 S        01:49:02.3                                  ___                          __
NEST     0.44   6.3 AML      01:49:04.34                                 ___         32200.0  0.34  __ ML     1.1
NEST     0.44   6.3 AML      01:49:04.4                                  ___         22900.0  0.30  __ ML     1.0
```

Table 5.1: *Calculating Ml assuming amplitudes reported as ground displacement (Ml_iasp) gives the wrong magnitudes while assuming Wood Anderson seismogram amplitudes by dividing the amplitude by 2080 (ML_iasp_WA) yields the reported magnitudes. Amp is amplitude and R is hypocentral distance.*

Station	Phase	R (km)	Amp (nm)	Reported Ml	Ml_iasp	Ml_iasp_WA
JAN	AML	42	116,400	1.5	4.9	1.6
NEST	AML	52	32,200	1.1	4.4	1.1
NEST	AML	52	22,900	1.0	4.3	1.0

Example 8: Both AML and IAML amplitudes are reported for the same station by two different agencies and only IAML reported in ground displacement. Although both station magnitudes are a bit high compared to the reported network magnitudes.

```
Event   609928377 Northwestern Balkan Peninsula
Date         Time         Err    RMS Latitude Longitude  Smaj  Smin  Az Depth   Err Ndef Nsta Gap  mdist  Mdist Qual   Author
2016/12/23 23:39:23.90   0.40          42.5070   18.5170   0.1   0.0        6.0   1.9   40   22        0.24   3.69      ke BEO
2016/12/23 23:39:24.00   0.50          42.5500   18.4000  6.67 3.336  -1  13.9   3.1    9    9                        MED_RCMT
2016/12/23 23:39:23.99   0.63 2.013   42.5231   18.5002 2.212 1.716  26  15.6  4.07  959  722  19   0.08 124.03 m i ke ISC

Magnitude  Err Nsta Author      OrigID

ML     3.8 0.1   15 IDC         608075296
ML     4.2 0.3  134 ROM         611235664
Ml     4.4          TIR         09993780
ML     4.0 0.2   11 PDG         09127985
ML     4.1       19 BEO         11703260
ML     4.5       18 RHSSO       08424384
Ml     4.3 0.4   37 LDG         08023407
ML     3.8 0.1    5 THE         08488814
ML     4.4          VIE         08401194
```

```
Sta       Dist  EvAz Phase        Time       TRes  Azim AzRes   Slow   SRes Def   SNR       Amp   Per Qual Magnitude
LJU       4.53 322.3 Pn        23:40:34.61    2.7                          T__
LJU       4.53 322.3 Sn        23:41:28.33    4.0                          T__
LJU       4.53 322.3 IAML      23:42:05.37                                 ___           1504.0  1.40
LJU       4.53 322.3 Pn        23:40:34.77    2.8                          T__
LJU       4.53 322.3 AML                                                   ___        7540000.0  1.20  __
```

Table 5.2: *Calculating Ml assuming amplitudes reported as ground displacement (Ml_ iasp) gives the wrong magnitude for the AML phase while assuming Wood Anderson seismogram amplitudes by dividing the amplitude by 2080 (ML_ iasp_ WA) yields the reported magnitude for the AML phase. Amp is amplitude and R is hypocentral distance.*

Station	Phase	R (km)	Amp (nm)	Reported Ml	Ml_iasp	Ml_iasp_WA
LJU	IAML	504	1,504	5.4	5.0	1.7
LJU	AML	504	7,540,000		8.7	5.4

Example 9: Event has wrong IAML amplitudes on BOJS and LJU. Both seem to be 100 times too large.

```
Event   616652085 Albania
Date        Time          Err   RMS Latitude Longitude  Smaj  Smin  Az Depth   Err Ndef Nsta Gap  mdist  Mdist Qual   Author
2017/07/03 11:18:18.80   1.19        41.1270   20.8170   0.5   0.5  56  11.0         186                                 MOS
2017/07/03 11:18:19.40   0.20        41.0100   20.8000                    12.3   0.5  313  136                           GCMT
2017/07/03 11:18:19.74   0.55 1.722  41.1794   20.8816 1.932 1.635  51   6.9  3.43 1138 1022  11   0.09 122.17 m i ke ISC

Ml      5.2           TIR       09994118
ML      4.1 0.1    10 IDC       13271224
ML      4.9           SKO       11823055
ML      4.8 0.1    13 PDG       13408058
Ml      4.3 0.4    23 LDG       08896013
ML      4.9 0.2    16 THE       09736238
ML      4.7        17 BEO       11783323

Sta       Dist  EvAz Phase        Time       TRes  Azim AzRes   Slow   SRes Def   SNR       Amp   Per Qual Magnitude
BOJS      5.96 318.4 IAML      11:22:07.14                                 ___          17602.0  4.90
LJU       6.70 318.6 IAML      11:22:20.38                                 ___           8779.0  3.90
```

Table 5.3: *Calculating Ml assuming amplitudes reported as ground displacement (Ml_ iasp) gives the wrong magnitude for the two IAML phases while dividing amplitude by 100 (ML_ iasp_ 100) yields the reported magnitudes. Amp is amplitude and R is hypocentral distance.*

Station	Phase	R (km)	Amp (nm)	Reported Ml	Ml_iasp	Ml_iasp_100
BOJS	IAML	663	17,602		6.5	4.5
LJU	IAML	42	8,779		6.5	4.5

Example 10: Stations TTG (phase Sg) and CEME (Phase Sg) report amplitudes with 4476 and 554 nm respectively while PUK (phase AMP) and BCI (phase AMP) report 1.0 and 2.9 nm, respectively. TTG and CEME give a reasonable magnitude (average 2.5) using the Hutton and Boore scale (*Hutton and Boore*, 1987), while PUK and BCO give an average of 0.3. Assuming the amplitudes for PUK and BCO are mm on a Wood Anderson seismogram, we can convert to nm. Now the average magnitude is 2.9 for PUK and BCI. The average Ml reported for this event is 2.4 so 2.9 seems a bit high: Some agencies use the wrong Wood Anderson gain of 2800 instead of 2080, if this is the case, the average magnitude would have been 2.8. In this case the error was easy to spot, but whether the amplitude has been calculated with the correct Wood Anderson gain, or not is still in doubt. This of course is only a problem if the agency reports amplitude in mm on a Wood Anderson seismogram.

```
Event  611449844 Northwestern Balkan Peninsula
Date       Time        Err   RMS Latitude Longitude  Smaj  Smin  Az Depth   Err Ndef Nsta Gap  mdist  Mdist Qual   Author
2015/01/03 22:17:02.34          0.220  42.4562    19.2903    1.4              6.7  20.0                                TIR
2015/01/03 22:17:03.20   0.03 0.030  42.4391    19.2842    0.0    0.0    0  14.6   0.1   32   16  86  0.02 1.25      ke PDG
2015/01/03 22:17:03.61   0.79 0.814  42.4529    19.3017   2.92 2.534  48  16.9  4.72   69   63  38  0.04 1.28      ke IASPEI
2015/01/03 22:17:04.40   0.20        42.4650    19.3270    0.0    0.0      14.0   2.6   23   15      0.06 2.56      ke BEO
2015/01/03 22:17:03.92   0.76 0.972  42.4563    19.3140   2.57 2.213  52  15.2  4.61  113   63  39  0.05 6.05 m i ke ISC

Magnitude  Err Nsta Author     OrigID
Ml     2.6          TIR        609057730
ML     2.4 0.3   14 PDG        609096920
ML     2.5       12 RHSSO      608421240
ML     2.2       13 BEO        606738973

Sta     Dist  EvAz Phase        Time      TRes  Azim AzRes   Slow   SRes Def   SNR       Amp   Per
TTG     0.05 239.0 Pg       22:17:05.7    -1.1                           T__
TTG     0.05 239.0 Sg       22:17:07.8    -0.8                           T__          4476.2
CEME    0.31 287.3 Pg       22:17:09.1    -1.3                           T__
CEME    0.31 287.3 Sg       22:17:14.1    -0.7                           T__           554.2
BCI     0.56  98.9 Pg       22:17:14.16   -0.9  98.0                     T__
BCI     0.56  98.9 Sb       22:17:22.82   -0.6  98.0                     T__
BCI     0.56  98.9 AMP                          98.0                     ___             2.9  0.28
PUK     0.60 133.7 Pg       22:17:14.67   -1.0 132.0                     T__
PUK     0.60 133.7 Sg       22:17:23.65    0.0 132.0                     T__
PUK     0.60 133.7 AMP                         132.0                     ___             1.0  0.11
```

Example 11: All 5 stations that report amplitudes (with Sg) give too low Ml station magnitudes (average value 0.1) versus the reported network Ml 1.3. Assuming this to be mm on a Wood Anderson seismogram, the magnitude would be 2.9 which is too high. So it is not clear what amplitude is reported.

```
Event 13826378 France
Date       Time        Err   RMS Latitude Longitude  Smaj  Smin  Az Depth   Err Ndef Nsta Gap  mdist  Mdist Qual   Author
2009/10/01 00:26:51.10   0.06 0.250  45.2844     3.7749    1.5    1.0  67   3.0f              99   0.24   2.24    ke LDG
2009/10/01 00:26:51.60   0.29 0.400  45.3400     3.8300    0.0    0.0   0   5.0f         10    5 210   0.20   0.87    ke STR
2009/10/01 00:26:50.60   0.14 0.560  45.2685     3.7666    3.2    2.2  64   5.0f         20   10  96   0.25   2.22    ke CSEM
 (Event not reviewed by the ISC)

Magnitude  Err Nsta Author      OrigID
Ml     1.4 0.2    5 LDG       12452567
Ml     1.4 0.0      STR       14928018
ML     1.3 0.2    5 CSEM      16462244

Sta     Dist  EvAz Phase        Time      TRes  Azim AzRes   Slow   SRes Def   SNR       Amp   Per  Qual    ML
VIVF    0.76 122.4 Sg       00:27:15.2                               ___             1.5  0.22  _e ML  1.6
LASF    1.19 176.9 Sg       00:27:28.9                               ___             0.3  0.27  _e ML  1.2
CAF     1.25 254.7 Sg       00:27:30.9                               ___             0.2  0.24  _e ML  1.1
AVF     1.55 349.4 Sg       00:27:39.1                               ___             0.2  0.24  _e ML  1.3
MTLF    2.23 210.5 Sg       00:28:01.4                               ___             0.2  0.26  _e ML  1.4
```

Recommendation: Only use amplitudes from IAML phases. In a few cases even IAML can be wrong though. Use AML phases with caution. If the user wants to use other amplitudes, they should be checked by calculating magnitudes for distances around 50-200 km using the standard California scale and compared to what the corresponding agency has reported.

mb

In general amplitudes for mb are correct and are easily selected as the ones used by the ISC. The ISC strictly calculates mb only when the distance is larger than 20 degrees so P amplitudes at shorter distances are not used. The very wide spread SeisComP system (*Hanka et al.*, 2010; `https://geofon.gfz-potsdam.de/software/seiscomp/`) uses a magnitude scale mb extended to shorter distances (J. Saul, personal communication, 2016). The IASPEI standard is to use IAmb while an earlier standard was to use AMB, still used by many. In addition, the ISC accepts amplitudes with the phase names P, pP, sP and pmax. The non standard pmax (not in the IASPEI phase list) is still reported by Russia (MOS) and China (BJI) for mb but was more common in the past. Ideally only the latest IASPEI recommendation IAmb should be used but that would severely limit the available data. Arrays have their own non standard mb scales like mbtmp and the corresponding amplitudes cannot always be used with the standard mb scale.

Example 12: IMS use of mbtmp. The amplitude at station CMAR is associated with a magnitude in the IMS bulletin but in the ISC Bulletin, the distance is too short for ISCloc to calculate the magnitude. So in the ISC Bulletin, we do not know what kind of amplitude it is. For observations with distances larger than 20 degrees, the amplitudes are used for mb.

```
ISC 611831815

CMAR   13.54  12.0 Pn        19:50:18.95   -0.1 198.5        13.60         T__  23.9       1.4  0.33  __
CMAR   13.54  12.0 Lg        19:54:11.852       187.8        32.80         ___   4.1       0.9  0.33  __
CMAR   13.54  12.0 LR        19:55:43.827       195.0        38.60         ___        2514.9 18.14  __
CMAR   13.54  12.0                                                         ___             6.3  0.79  __
KAPI   25.77 112.7 P         19:52:37.619   0.0 259.7         8.40         T__  14.4     128.9  1.02  __ mb      5.5

IDC 14091935

CMAR   13.44  12.1 Pn        19:50:18.950   1.8 198.5  -1.1   13.6   -0.3 T__  23.9       1.4  0.33 a__ ML      4.8
                                                                                           6.3  0.79     mbtmp   4.3
CMAR   13.44  12.1 Lg        19:54:11.852  -0.1 187.8  -7.8   32.8    1.0 T__   4.1       0.9  0.33 ___
CMAR   13.44  12.1 LR        19:55:43.827   1.5 195.0   2.3   38.6    0.1 ___        2514.9 18.14 a__ Ms
KAPI   25.82 112.9 P         19:52:37.619  -0.6 259.7 -33.2    8.4   -0.7 T__  14.4     128.9  1.02 a__ mbtmp   5.6
                                                                                         128.9  1.02     mb      5.6
```

Example 13: Not all mb in the ISC Bulletin are correct. In this event two stations report too high amplitudes. However, they are not contributing to the average as the ISC uses an alpha trimmed median. There is no indication in the ISF file that they have not been used though and the user must also do some checking.

```
Event 13918464 Bougainville-Solomon Islands region
Date       Time         Err   RMS Latitude Longitude  Smaj  Smin  Az Depth   Err Ndef Nsta Gap  mdist  Mdist Qual   Author
2009/10/01 07:02:26.00   0.35 1.408   -8.7896  159.4114 8.341 7.490  63 121.5  3.04  267  204  28   0.83 157.71 m i se ISC

Magnitude  Err Nsta Author      OrigID
mb      4.8       18 NEIC      15372161
mb      4.8 0.1   57 ISC       16764170

Sta     Dist  EvAz Phase        Time      TRes  Azim AzRes   Slow   SRes Def   SNR       Amp   Per Qual
ASAR   28.54 235.7 P        07:08:09.35   -1.1  65.3        10.30        T__  48.0       5.0  0.40  __ mb      4.5
AFI    28.69 102.9 P        07:08:08.16   -3.7                           T__           297.2  0.80  _e mb      6.0
BBOO   32.22 218.8 P        07:08:43.02    0.3                           T__           474.3  0.80  _e mb      6.3
```

Recommendation: Use all amplitudes where the ISC or others have calculated mb and use all amplitudes given by the IAmb. For events with an ISC hypocentre, station magnitudes are calculated by ISCloc, while for events with an agency's hypocentre as prime the station magnitudes are those reported by the agency. It is assumed that the user's software automatically does not use data outside the valid distance range. For stations outside the correct station range, accept all amplitudes on phases accepted by the ISC since they are likely correct, but be aware that they have not been checked by the ISC. Consider using an alpha trimmed median (20%) like ISCloc does to sort out any outliers.

mB

Broadband mb, IASPEI name mB_BB, here we use mB: The IASPEI phase name is IVmB_BB indicating that the amplitude is in velocity. There are very few reported to the ISC, probably because it is not implemented in most processing software. For November 2018 there were a total of 545 observations, all from SEISAN users. The ISC is not yet using these amplitudes.

Example 14: Agency BJI reports magnitudes mb and mB. We assume mB is broadband mB but the event does not show the corresponding IVmb_BB phases and it seems the amplitude is reported as AMB at station WMQ. The magnitude relation for mB is

$$mB = \log(V_{max}/2\pi) + Q(\Delta, h) - 3.0, \tag{5.2}$$

where V_{max} is ground velocity in nm/s recorded on a broad band sensor proportional to velocity and Q is a correction function dependent on distance Δ and depth h (*Bormann and Dewey*, 2014). In the classic relation, $(V_{max}/2\pi)$ is equivalent to $(A/T)_{max}$.

Strictly speaking the amplitude should be in velocity $V = 410$ nm/s and then $mB = \log(V/2\pi)+$ correction but that is almost the same as assuming displacement $A = 410$ nm and calculating $mB = \log(410 \text{ nm}/5.8 \text{ s})+$correction. So in this example it is hard to know what unit is used unless we assume it to be displacement since IVmb_BB has not been used. The event has several Chinese stations with similar reports but they are not used by the ISC since the period is too high. So ISC data probably contains more data for mB, but they are hard to find as, if not using IVmb_BB amplitudes, there is no way of knowing how the amplitude was picked. If the period is above 3 s it is likely that the amplitude is for mB. China uses the mB magnitude scale regularly (*Bormann et al.*, 2009), but probably reporting displacement and period instead of velocity.

```
Event 13918464 Bougainville-Solomon Islands region
Date       Time        Err   RMS Latitude Longitude  Smaj  Smin  Az Depth   Err Ndef Nsta Gap  mdist  Mdist Qual   Author
2009/10/01 07:02:14.80        0.780  -8.6100  159.1900                    31.0           42       323  55.80  88.20     uk BJI
2009/10/01 07:02:26.00   0.35 1.408  -8.7896  159.4114 8.341 7.490  63 121.5  3.04  267  204  28   0.83 157.71 m i se ISC

Magnitude  Err Nsta Author      OrigID
mb      4.9       37 BJI       13450879
mB      5.3       18 BJI       13450879
Ms      5.0       17 BJI       13450879
mb      4.8 0.1   57 ISC       16764170

Sta      Dist  EvAz Phase         Time      TRes  Azim AzRes   Slow   SRes Def   SNR       Amp   Per Qual Magnitude

MCK     82.13  20.6 P        07:14:32.49   -0.4                             T__            30.9  1.00  _e mb     5.1
IMA2    82.13  17.5 P        07:14:32.83   -0.1                             T__                        _e
WMQ     83.12 316.2 P        07:14:38.4    -0.1                             T__                        _e
WMQ     83.12 316.2 AMB                                                     ___            11.0  0.80  __ mb     4.8
WMQ     83.12 316.2 AMB                                                     ___           410.0  5.80  __
WMQ     83.12 316.2 LR                                                      ___           280.0 20.00  __
```

Recommendation: Use all IVmB_BB amplitudes. Amplitudes for mB with period above 3 s are most likely in displacement as reporting amplitudes in velocity instead of a displacement and corresponding period suggests that the reporter uses IASPEI standards and thus would likely report the correct phase names.

MS

Amplitudes for the classic MS are reported with phase names like M, MLR, L, LR and AMS while the IASPEI standard is IAMs_20 indicated that it ideally should be read within the period range 18-22 s. Many amplitudes used by the ISC are not in the 18-22 s range but they are still used as the ISC accepts periods in the range 10 to 60 s.

However, the requirement that the event is shallow (depth $<$ 60 km) and in the distance range of 20 to 160 degrees is followed. So MS calculation does not completely follow the IASPEI standard.

Recommendation: Use all amplitudes for which the ISC calculated a MS magnitude and all of the IAMs_20 amplitudes. It is assumed that the user's software automatically does not use data outside the valid distance range and depth range. Data with the above phase names can still be included with caution. Abnormal magnitudes must be filtered out by the user's software.

MS_BB

Broadband MS, IASPEI name is Ms_BB, here we use MS_BB: The IASPEI phase name is IVMs_BB indicating that the amplitude is in velocity. Since it can be used in distance range 2 to 160 degrees and period 3 to 60 s it should have a much wider use. It is particularly useful for larger regional events where mb and MS cannot be used due to the short distances and Ml being inaccurate. There are very few IVMs_BB reported to the ISC: For November 2018, there are 227, all from SEISAN users. The ISC is not yet using these amplitudes. It seems that BJI calculates MS_BB.

Recommendation: Use all IVMs_BB amplitudes.

Mc or Md

Coda magnitudes from contributing agencies are given but the coda length is not stored. The IASPEI standard is to mark the end of the coda with phase name END from which the coda length and coda magnitude can be calculated. Only if the END phase is used will the ISC store the coda. However they seem not to be reported very often and the ISC has only about 100,000 observations in total, nearly all from Italy (ROM). The END phase has been implemented in SEISAN version 12.0 so there will probably be more in the future although coda magnitudes are used much less than they used to.

Recommendation: Use all END phases.

5.1.5 Summary

Using ISC data presents only a few problems for telseismic phases and magnitudes mb and MS. For local events, where data is often more inhomogeneous, phase names Pg, Pn and Pb should be changed to P and S respectively.

Amplitude data for Ml should be checked before use although most data for IAML phases are OK.

For all phases it is best to use data that is time-defining or has a time residual if relocated by the ISC. Other phases from ISC located events should initially be weighted out. For events not located by the ISC all phases should be used.

5.1.6 Suggestions for Improved ISC Reporting

Jens: Calculate residuals for back azimuth, even if not used, so the user can find reliable observations. Or better, start using back azimuth, then maybe more IDC only events could be located by ISC.

Kathrin/ISC: *The ISC only recently finished the Rebuild project where we recalculated our entire Bulletin between 1964 to 2010 with ISCloc and ak135 to make the Bulletin consistent (ISCloc was implemented in 2009). Changing our location procedure now and introducing another inconsistency is very* *unlikely to happen for some time. This would be a very non-trivial change that would require a lot of staff time.*

Jens: Calculate Ml for reported amplitudes up to 100 km and flag values outside reasonable limits. Up to 100 km there is little difference between different regional scales so the Ml should be reasonable correct. Or better, calculate Ml using Hutton and Boore and report. Indicate large outliers.

Kathrin/ISC: *As described above, Ml amplitudes come in a variety of standards that would require a lot of staff time to sort out and confirm. Unfortunately, it is not viable for us to do so at the moment. Should we decide to calculate a Ml_ISC magnitude this might change. In addition, currently ISF has no way to flag magnitude outliers so this would require some format changes.*

Jens: Calculate magnitude for broadband MS and mb.

Kathrin/ISC: *When time and funding allows we plan to tackle calculating additional magnitudes other than mb and MS.*

Jens: Make available the phases reported to the ISC also in ISF format so the user can see what has changed.

Kathrin/ISC: *As this already is available in QuakeMl format adding it to ISF is not a priority at the moment.*

Jens: Flag events not processed by the ISC.

Kathrin/ISC: *We are in the process of implementing this.*

The ISC is grateful for all feedback. Please contact us for questions, comments and suggestions for improving our data sets and services, or should you find any faults in our data (`http://www.isc.ac.uk/contact/`).

Acknowledgments

We thank James Harris and Domenico Di Giacomo for their help with queries about the ISC database, ISCloc and ISC magnitudes and Natalia Poiata for her helpful comments on the manuscript.

References

Aki, K. and P. G. Richards (2002), Quantitative seismology, Second Edition, University Science Books, Sausalito, ISBN 0-935702-96-2, 704 pp.

Bondar, I. and D. Storchak (2011), Improved location procedures at the International Seismological Centre, *Geophys. J. Int.*, *186*(3), 1220–1244, `https://doi.org/10.1111/j.1365-246X.2011.05107.x`.

Bormann, P., R. Liu, Z. Xu, K. Ren, L. Zhang and S. Wendt (2009), First Application of the New IASPEI Teleseismic Magnitude Standards to Data of the China National Seismographic Network, *Bull. Seismol. Soc. Am.*, 99, 1868–1891, https://doi.org/10.1785/0120080010.

Bormann, P. and J.W. Dewey (2014), The new IASPEI standards for determining magnitudes from digital data and their relation to classical magnitudes, In: Bormann, P. (Ed.), *New Manual of Seismological Observatory Practice 2 (NMSOP-2)*, Potsdam, Deutsches GeoForschungsZentrum GFZ, 1-44, https://doi.org/10.2312/GFZ.NMSOP-2_IS_3.3.

Hanka, W., J. Saul, B. Weber, J. Becker, P. Harjadi, Fauzi and GITEWS Seismology Group (2010), Real-time earthquake monitoring for tsunami warning in the Indian Ocean and beyond, *Nat. Hazards Earth Syst. Sci.*, *10*, 2611-–2622, https://doi.org/10.5194/nhess-10-2611-2010,2010.

Havskov, J., P. Voss and L. Ottemöller (2020), Seismological observatory software: Thirty years of SEISAN, *Seismol. Res. Lett.*, *91*, 1846–1852, https://doi.org/10.1785/0220190313.

Hutton, L. K. and D. M. Boore (1987), The ML scale in southern California, *Bull. Seismol. Soc. Am.*, *77*, 2074-–2094.

IASPEI, Working Group on Magnitudes, http://www.iaspei.org/commissions/commission-on-seismological-observation-and-interpretation/Summary_WG_recommendations_20130327.pdf

Kennett, B.L.N, E.R. Engdahl and R. Buland (1995), Constraints on seismic velocities in the Earth from traveltimes, *Geophys. J. Int.*, *122*(1), 108–124, https://doi.org/10.1111/j.1365-246X.1995.tb03540.x.

Klein, F. W. (2002), User's guide to HYPOINVERSE-2000, a Fortran program to solve for earthquake locations and magnitudes, *Open-File Report 2002-171*, US Geological Survey, https://doi.org/10.3133/ofr02171.

Lienert, B. and J. Havskov (1995), A Computer Program for Locating Earthquakes Both Locally and Globally, *Seismol. Res. Lett.*, *66*(5), 26-36, https://doi.org/10.1785/gssrl.66.5.26.

Schweitzer J., D.A. Storchak and P. Borman (2019), Seismic Phase Nomenclature: The IASPEI Standard, In: Gupta H. (eds), *Encyclopedia of Solid Earth Geophysics, Encyclopedia of Earth Sciences Series*, Springer, Cham, https://doi.org/10.1007/978-3-030-10475-7_11-1.

Stein, S. and M. Wysession (2003), Introduction to Seismology, Earthquakes and Earth Structure, Blackwell Publishing, Oxford, 498 pp.

Storchak, D.A., J. Schweitzer and P. Bormann (2003), The IASPEI Standard Seismic Phase List, *Seismol. Res. Lett.*, *74*(6), 761–772, https://doi.org/10.1785/gssrl.74.6.761.

Storchak D.A., J. Schweitzer and P. Bormann (2011), Seismic Phase Names: IASPEI Standard, In: Gupta H.K. (eds) *Encyclopedia of Solid Earth Geophysics. Encyclopedia of Earth Sciences Series*, Springer, Dordrecht, https://doi.org/10.1007/978-90-481-8702-7_11.

6

Summary of Seismicity, January – June 2019

The first half of 2019 saw seven earthquakes with magnitudes larger than 7 (see Tab. 6.1). The largest event was the M_W 8 Peru earthquake on 26 May 2019 (07:41:14.36 UTC, 5.8927°S, 75.2457°W, 125.5 km depth, 2935 stations (ISC)). It was a normal-faulting earthquake at intermediate depth at the eastern end of the flat part of the subducting Nazca plate underneath Peru, where the slab rebends and sinks to greater depths (*Liu and Yao*, 2020; *Hu et al.*, 2021; *Jiménez et al.*, 2021; *Ye et al.*, 2020). Studies reveal a complex rupture process and suggest the event resulted from extensional stress generated by slab bending (*Hu et al.*, 2021; *Liu and Yao*, 2020; *Jiménez et al.*, 2021). *Ye et al.* (2020) found that the aftershock productivity of the 2019 Peru earthquake is very low for a large intermediate-depth earthquake but similar to that for other large Peruvian intraslab events, suggesting regionally homogeneous faulting systems and a relatively uniform stress state in the nearly horizontal slab.

The event that was referenced most in the ISC Event Bibliography (*Di Giacomo et al.*, 2014; *International Seismological Centre*, 2021) currently with 17 articles was the M_W 5.7 Changning event in China on 17 June 2019 (14:55:46.22 UTC, 28.3585°N, 104.9248°E, 17.4 km depth, 2106 Stations (ISC)). The earthquake was the largest and the most damaging event in the Changning area causing high casualties and economic losses (e.g., *Li et al.*, 2020; *Zhang et al.*, 2020). The event occurred in an area with low background seismicity (e.g., *Li et al.*, 2021; *Jiang et al.*, 2020) and is located close to shale gas and salt mining production. Several studies suggest that fluid injection for salt mining might have triggered this event (e.g. *Li et al.*, 2021;, *Zhang et al.*, 2020; *Li et al.*, 2020; *Yang et al.*, 2021).

The number of events in this Bulletin Summary categorised by type are given in Table 6.2.

Figure 6.1 shows the number of moderate and large earthquakes in the first half of 2019. The distribution of the number of earthquakes should follow the Gutenberg-Richter law.

Figures 6.2 to 6.6 show the geographical distribution of moderate and large earthquakes in various magnitude ranges.

Table 6.1: *Summary of the earthquakes of magnitude Mw ≥ 7 between January and June 2019.*

Date	lat	lon	depth	Mw	Flinn-Engdahl Region
2019-05-26 07:41:14	-5.89	-75.25	125	8.0	Northern Peru
2019-05-14 12:58:26	-4.20	152.62	15	7.6	New Britain region
2019-02-22 10:17:22	-2.28	-77.01	149	7.5	Peru-Ecuador border region
2019-06-24 02:53:39	-6.39	129.25	221	7.3	Banda Sea
2019-06-15 22:55:02	-30.81	-178.02	38	7.3	Kermadec Islands
2019-05-06 21:19:36	-7.00	146.45	140	7.1	Eastern New Guinea region
2019-03-01 08:50:42	-14.68	-70.06	265	7.1	Central Peru

Table 6.2: *Summary of events by type between January and June 2019.*

damaging earthquake	1
felt earthquake	84
known earthquake	225684
known chemical explosion	9467
known induced event	2470
known mine explosion	2454
known rockburst	411
known experimental explosion	181
suspected collapse	7
suspected earthquake	35363
suspected chemical explosion	5573
suspected induced event	147
suspected mine explosion	6005
suspected rockburst	151
suspected experimental explosion	167
suspected ice-quake	114
unknown	2
total	288281

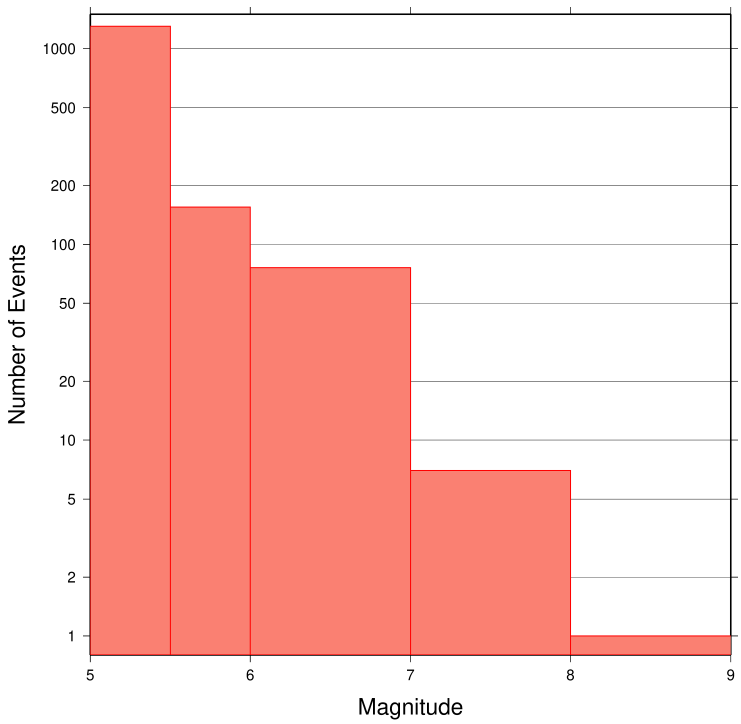

Figure 6.1: *Number of moderate and large earthquakes between January and June 2019. The non-uniform magnitude bias here correspond with the magnitude intervals used in Figures 6.2 to 6.6.*

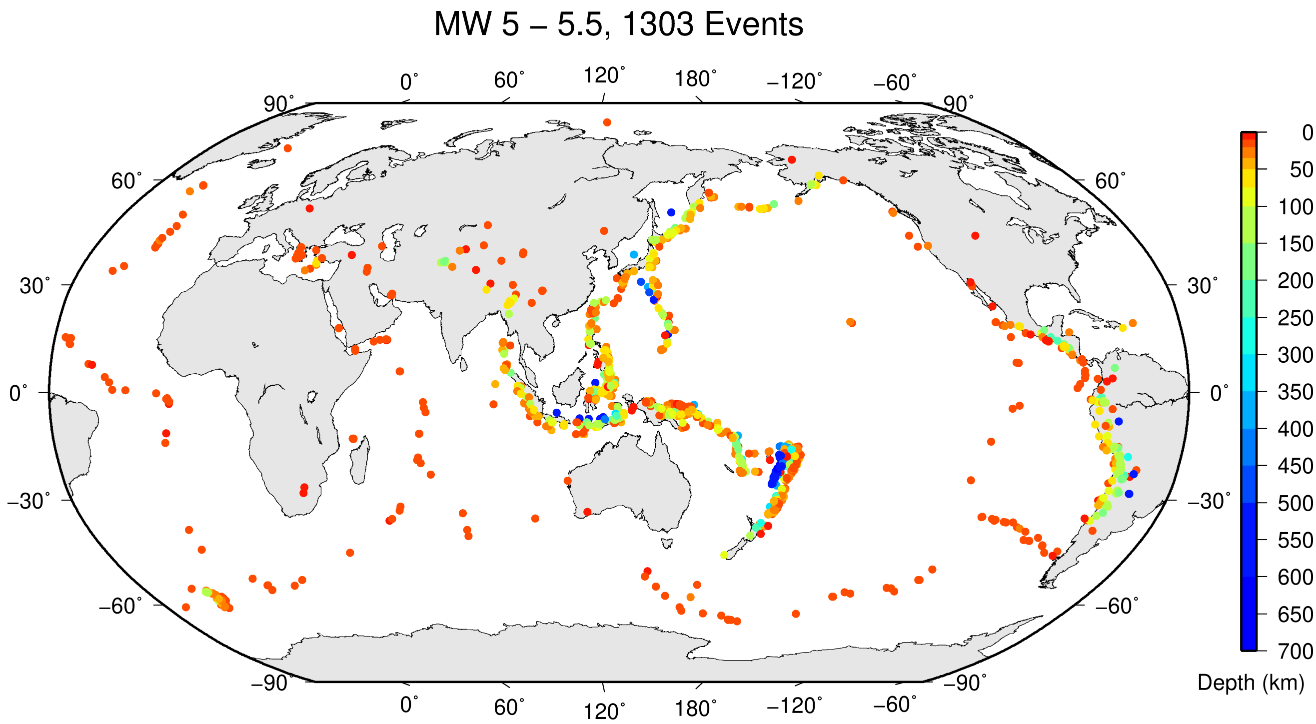

Figure 6.2: *Geographic distribution of magnitude 5-5.5 earthquakes between January and June 2019.*

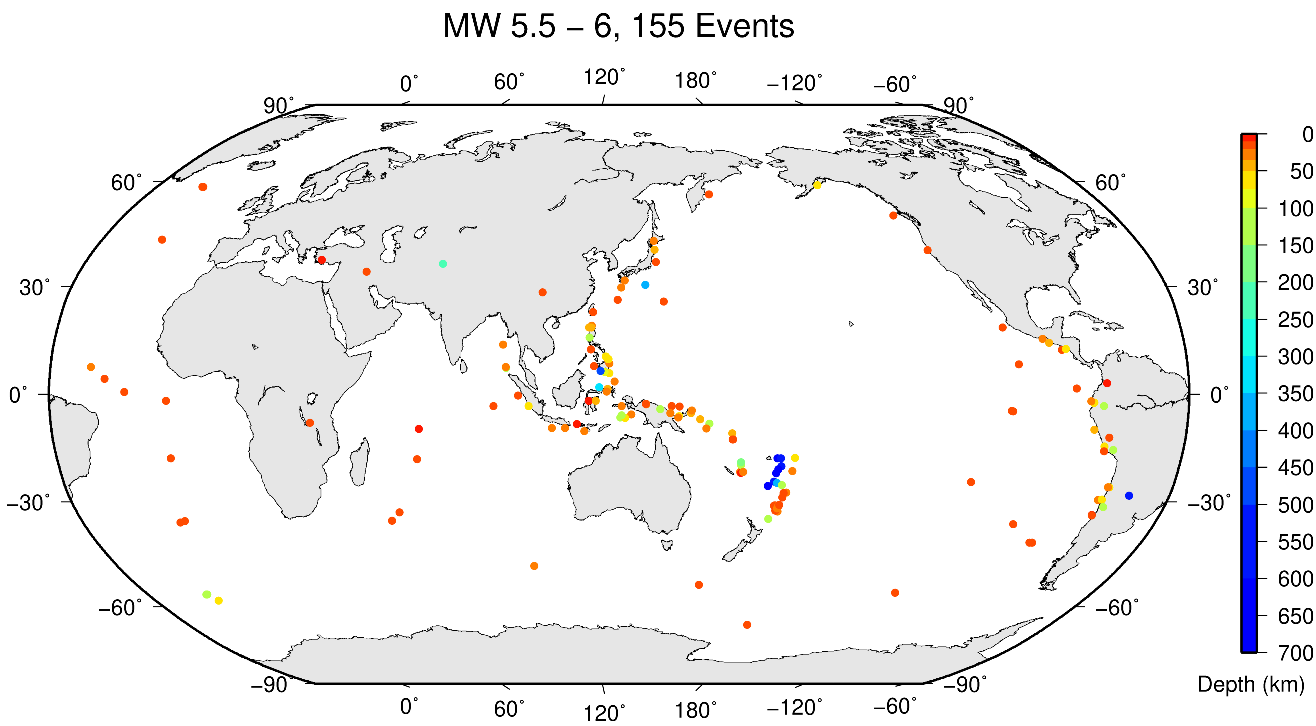

Figure 6.3: *Geographic distribution of magnitude 5.5-6 earthquakes between January and June 2019.*

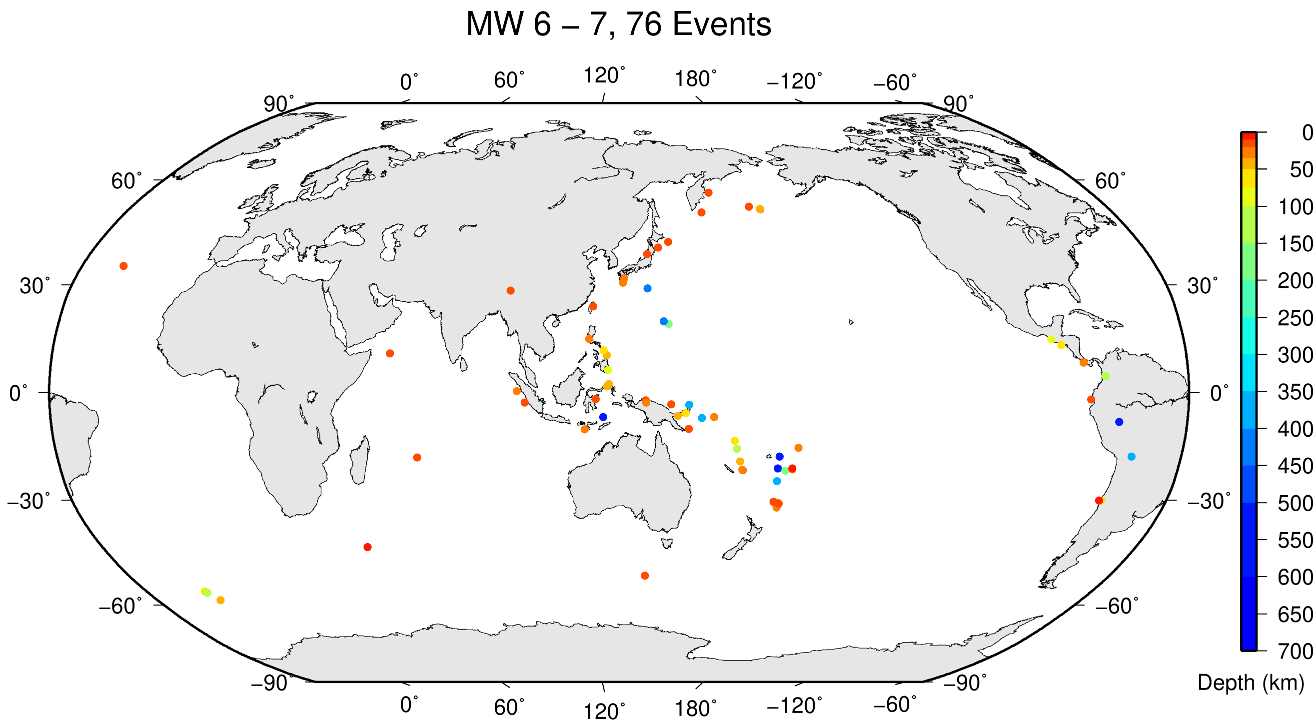

Figure 6.4: *Geographic distribution of magnitude 6-7 earthquakes between January and June 2019.*

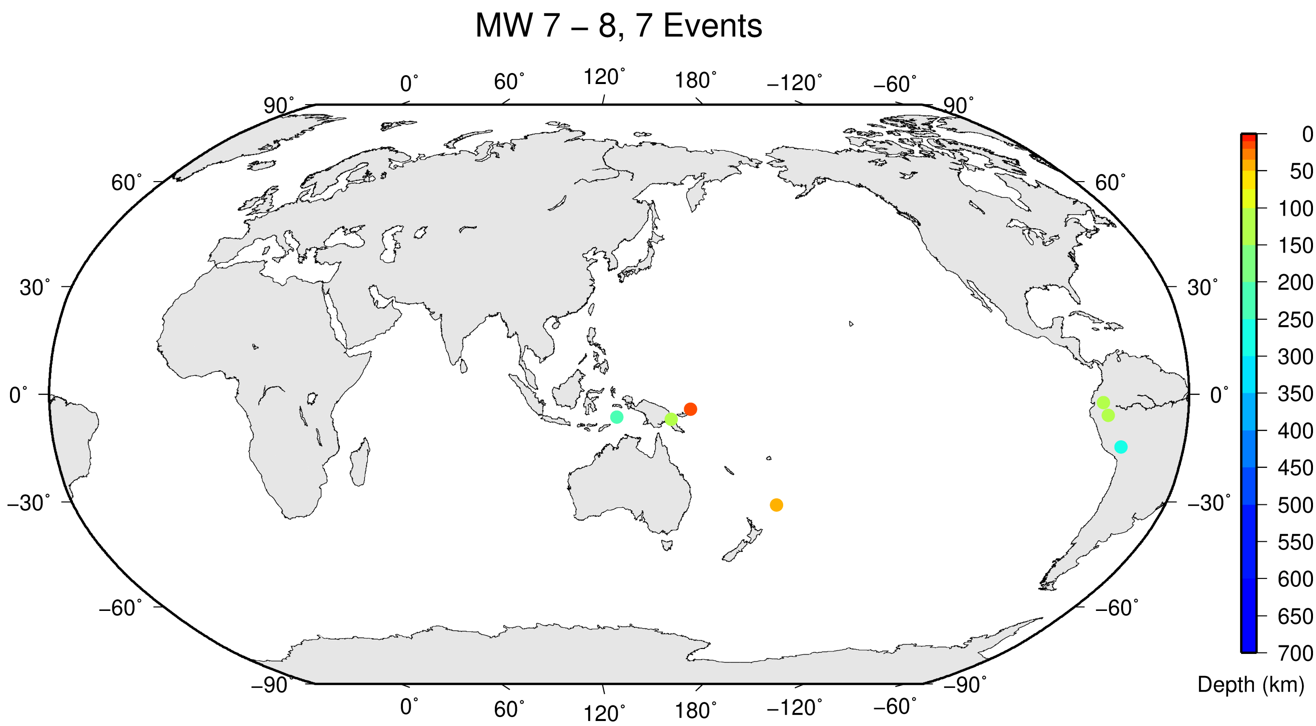

Figure 6.5: *Geographic distribution of magnitude 7-8 earthquakes between January and June 2019.*

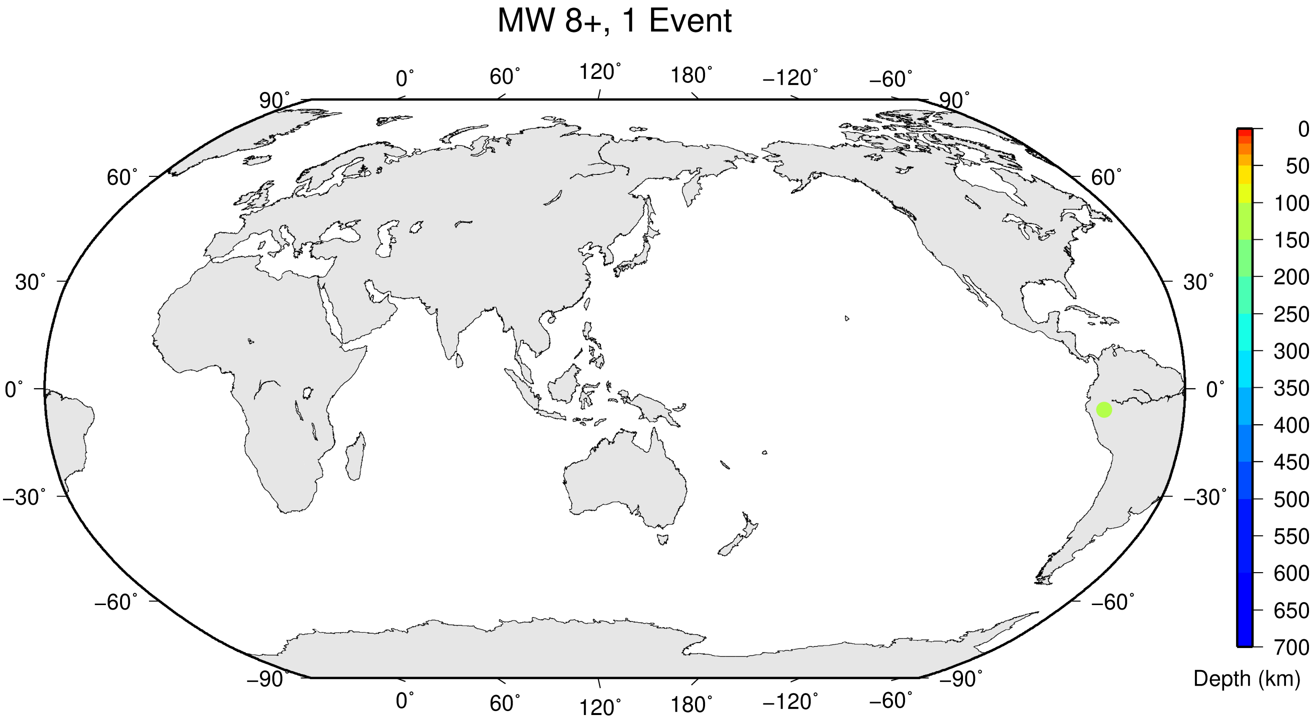

Figure 6.6: *Geographic distribution of magnitude 8+ earthquakes between January and June 2019.*

References

Di Giacomo, D., D.A. Storchak, N. Safronova, P. Ozgo, J. Harris, R. Verney and I. Bondár (2014), A New ISC Service: The Bibliography of Seismic Events, *Seismol. Res. Lett.*, *85*(2), 354–360, `https://doi.org/10.1785/0220130143`.

Hu, Y., Y. Yagi, R. Okuwaki and K. Shimizu (2021), Back-propagating rupture evolution within a curved slab during the 2019 Mw 8.0 Peru intraslab earthquake, *Geophys. J. Int*, *227*(3),1602–1611, `https://doi.org/10.1093/gji/ggab303`.

International Seismological Centre (2021), On-line Event Bibliography, `https://doi.org/10.31905/EJ3B5LV6`.

Jiang, D., S. Zhang and Rui Ding (2020), Surface deformation and tectonic background of the 2019 Ms 6.0 Changning earthquake, Sichuan basin, SW China, *J Asian Earth Sci*, *200*, 104493, `https://doi.org/10.1016/j.jseaes.2020.104493`.

Jiménez, C., N. Luna, N. Moreno and M. Saaveda J. (2021), Seismic source characteristics of the intermediate-depth and intraslab 2019 northern Peru earthquake (Mw 8.0), *J Seismol*, *25*, `https://doi.org/10.1007/s10950-021-09996-x`.

Li, W., S. Ni, Ch. Zang and R. Chu (2020), Rupture Directivity of the 2019 Mw 5.8 Changning, Sichuan, China, Earthquake and Implication for Induced Seismicity, *Bull. Seismol. Soc. Am*, *110*(5), 2138–2153, `https://doi.org/10.1785/0120200013`.

Li, T., J. Sun, Y. Bao, Y. Zhan, Z.K. Shen, X. Xu and C. Lasserre (2021), The 2019 Mw 5.8 Changning, China earthquake: A cascade rupture of fold-accommodation faults induced by fluid injection, *Tectonophysics*, *801*, 228721, `https://doi.org/10.1016/j.tecto.2021.228721`.

Liu, W. and H. Yao (2020), Rupture process of the 26 May 2019 Mw 8.0 northern Peru intermediate-depth earthquake and insights into its mechanism, *Geophys. Res. Lett*, *47*, e2020GL087167, `https://doi.org/10.1029/2020GL087167`.

Yang, Y.-H., J.-Ch. Hu, Q. Chen, X. Lei, J. Zhao, W. Li, R. Xu and Ch.-Y. Chiu (2021), Shallow slip of blind fault associated with the 2019 Ms 6.0 Changning earthquake in fold-and-thrust belt in salt mines of Southeast Sichuan, China, *Geophys. J. Int.*, *224*, 909–922, `https://doi.org/10.1093/gji/ggaa488`.

Ye, L., T. Lay and H. Kanamori (2020), Anomalously low aftershock productivity of the 2019 MW 8.0 energetic intermediate-depth faulting beneath Peru, *Earth Planet. Sci. Lett.*, *549*, `https://doi.org/10.1016/j.epsl.2020.116528`.

Zhang, B., J. Lei and G. Zhang (2020), Seismic evidence for influences of deep fluids on the 2019 Changning Ms 6.0 earthquake, Sichuan basin, SW China, *J Asian Earth Sci*, *200*, 104492, `https://doi.org/10.1016/j.jseaes.2020.104492`.

7

Statistics of Collected Data

7.1 Introduction

The ISC Bulletin is based on the parametric data reports received from seismological agencies around the world. With rare exceptions, these reports include the results of waveform review done by analysts at network data centres and observatories. These reports include combinations of various bulletin elements such as event hypocentre estimates, moment tensors, magnitudes, event type and felt and damaging data as well as observations of the various seismic waves recorded at seismic stations.

Data reports are received in different formats that are often agency specific. Once an authorship is recognised, the data are automatically parsed into the ISC database and the original reports filed away to be accessed when necessary. Any reports not recognised or processed automatically are manually checked, corrected and re-processed. This chapter describes the data that are received at the ISC before the production of the reviewed Bulletin.

Notably, the ISC integrates all newly received data reports into the automatic ISC Bulletin (available on-line) soon after these reports are made available to ISC, provided it is done before the submission deadline that currently stands at 12 months following an event occurrence.

With data constantly being reported to the ISC, even after the ISC has published its review, the total data shown as collected, in this chapter, is limited to two years after the time of the associated reading or event, i.e. any hypocentre data collected two years after the event are not reflected in the figures below.

7.2 Summary of Agency Reports to the ISC

A total of 149 agencies have reported data for January 2019 to June 2019. The parsing of these reports into the ISC database is summarised in Table 7.1.

Table 7.1: *Summary of the parsing of reports received by the ISC from a total of 149 agencies, containing data for this summary period.*

	Number of reports
Total collected	3953
Automatically parsed	2796
Manually parsed	1145

Data collected by the ISC consists of multiple data types. These are typically one of:

- Bulletin, hypocentres with associated phase arrival observations.

- Catalogue, hypocentres only.
- Unassociated phase arrival observations.

In Table 7.2, the number of different data types reported to the ISC by each agency is listed. The number of each data type reported by each agency is also listed. Agencies reporting indirectly have their data type additionally listed for the agency that reported it. The agencies reporting indirectly may also have 'hypocentres with associated phases' but with no associated phases listed - this is because the association is being made by the agency reporting directly to the ISC. Summary maps of the agencies and the types of data reported are shown in Figure 7.1 and Figure 7.2.

Table 7.2: *Agencies reporting to the ISC for this summary period. Entries in bold are for new or renewed reporting by agencies since the previous six-month period.*

Agency	Country	Directly or indirectly reporting (D/I)	Hypocentres with associated phases	Hypocentres without associated phases	Associated phases	Unassociated phases	Amplitudes
TIR	Albania	D	832	0	17296	33	4445
CRAAG	Algeria	D	185	0	1378	86	0
LPA	Argentina	D	0	0	0	423	0
SJA	Argentina	D	3443	4	109266	222	26836
NSSP	Armenia	D	51	0	1096	0	0
AUST	Australia	D	1101	0	66205	0	57954
CUPWA	Australia	D	51	0	731	1	0
IDC	Austria	D	18367	2	592009	0	546249
VIE	Austria	D	4575	100	45174	342	45249
AZER	Azerbaijan	D	169	0	7256	0	0
UCC	Belgium	D	1222	0	8162	19	2216
LPZ	Bolivia	I ECX	12	0	0	0	0
SCB	Bolivia	D	764	0	9545	11	1631
RHSSO	Bosnia and Herzegovina	D	1005	14	18656	6847	0
BGSI	Botswana	D	422	0	4547	0	1043
OSUNB	Brazil	D	136	0	6182	0	0
VAO	Brazil	D	879	23	22870	0	0
SOF	Bulgaria	D	266	0	3661	1881	0
OTT	Canada	D	1001	14	29237	0	4110
PGC	Canada	I OTT	431	0	15765	0	0
GUC	Chile	D	3993	112	96620	6226	29290
BJI	China	D	1344	21	126257	36375	88734
ASIES	Chinese Taipei	D	0	156	0	0	0
TAP	Chinese Taipei	D	16242	0	793580	0	0
RSNC	Colombia	D	13743	157	246840	181	32055
UCR	Costa Rica	D	554	0	23443	12	0
ZAG	Croatia	D	0	0	0	27022	0
SSNC	Cuba	D	957	0	19790	12	7963
NIC	Cyprus	D	375	0	10884	0	4501
IPEC	Czech Republic	D	432	13	3039	18959	1395
PRU	Czech Republic	D	3726	14	36059	180	8270
WBNET	Czech Republic	D	350	0	6949	0	6939
KEA	Democratic People's Republic of Korea	D	115	0	1590	0	859
DNK	Denmark	D	2323	1291	30735	25478	8275
OSPL	Dominican Republic	D	857	0	10609	0	3366
SDD	Dominican Republic	D	1456	0	29613	0	10997
IGQ	Ecuador	D	164	0	10119	0	0
HLW	Egypt	D	431	0	3337	0	0
SNET	El Salvador	D	1393	4	27156	20	2572
EST	Estonia	I HEL	244	23	0	0	0
FIA0	Finland	I HEL	8	0	0	0	0
HEL	Finland	D	7652	964	194568	0	36227
CSEM	France	I PJWWP	2336	301	0	0	0
IPGP	France	D	0	133	0	0	0

Table 7.2: *(continued)*

Agency	Country	Directly or indirectly reporting (D/I)	Hypocentres with associated phases	Hypocentres without associated phases	Associated phases	Unassociated phases	Amplitudes
LDG	France	D	2546	66	32367	0	14311
STR	France	D	4971	1	105191	80	0
PPT	French Polynesia	D	1175	11	10512	105	10595
TIF	Georgia	D	0	76	0	1347	0
AWI	Germany	D	4382	0	18510	640	8735
BGR	Germany	D	639	250	17595	0	5815
BNS	Germany	I BGR	0	19	0	0	0
BRG	Germany	D	0	0	0	10358	3613
BUG	Germany	I BGR	2	48	0	0	0
CLL	Germany	D	8	0	261	8235	2941
GDNRW	Germany	I BGR	1	9	0	0	0
GFZ	Germany	I KRSZO	18	4	0	0	0
HLUG	Germany	I BGR	5	5	0	0	0
LEDBW	Germany	I BGR	20	5	0	0	0
ATH	Greece	D	12821	37	344848	0	103656
THE	Greece	D	3050	0	66457	2891	29884
UPSL	Greece	D	0	14	0	0	0
GCG	Guatemala	D	5765	308	46606	149	4404
HKC	Hong Kong	D	0	0	0	33	0
KRSZO	Hungary	D	516	371	9590	0	3372
REY	Iceland	D	32	0	1201	0	0
HYB	India	D	622	1	1729	0	211
NDI	India	D	587	502	21888	78	8327
DJA	Indonesia	D	6955	94	96829	0	95375
TEH	Iran	D	5695	0	47443	0	0
THR	Iran	D	94	0	2142	0	848
ISN	Iraq	D	486	0	4001	0	1130
DIAS	Ireland	D	0	0	0	599	0
GII	Israel	D	2112	25	42580	361	0
GEN	Italy	D	550	0	11325	8	0
MED_RCMT	Italy	D	0	158	0	0	0
RISSC	Italy	D	3	0	45	0	0
ROM	Italy	D	8412	218	686602	237139	452253
TRI	Italy	D	0	0	0	9953	0
JSN	Jamaica	D	152	0	451	4	0
JMA	Japan	D	94027	2967	643955	0	14095
NIED	Japan	D	0	599	0	0	0
SYO	Japan	D	0	0	0	2054	0
JSO	Jordan	D	101	13	1646	0	32
NNC	Kazakhstan	D	8340	0	88155	0	82389
SOME	Kazakhstan	D	4246	228	50167	0	43078
KNET	Kyrgyzstan	D	1004	0	8389	0	2744
KRNET	Kyrgyzstan	D	2282	0	47322	0	0
LVSN	Latvia	D	179	0	2796	0	1673
GRAL	Lebanon	D	197	0	1947	953	0
LIT	Lithuania	D	651	573	5250	211	0
MCO	Macao, China	D	0	0	0	31	0
TAN	**Madagascar**	**D**	**1749**	**14**	**22617**	**0**	**0**
GSDM	Malawi	D	0	0	0	136	0
ECX	Mexico	D	878	0	20342	0	4099
MEX	Mexico	D	13586	150	253318	472	0
MOLD	Moldova	D	0	0	0	2091	963
PDG	Montenegro	D	449	2	9288	0	4715
CNRM	Morocco	D	1524	0	16395	0	0
NAM	Namibia	D	8	0	90	6	23
DMN	Nepal	D	152	0	2538	0	973
DBN	Netherlands	I BGR	0	2	0	0	0
NOU	New Caledonia	D	4530	0	90185	0	3346
WEL	New Zealand	D	12786	98	402158	64	309222
CATAC	Nicaragua	D	2660	2351	63110	65520	0
SKO	North Macedonia	D	597	0	8593	2231	1578
BER	Norway	D	2300	1720	51796	5222	13920
NAO	Norway	D	2491	931	6199	0	2286
OMAN	Oman	D	533	0	31096	0	0
UPA	Panama	D	1163	0	20707	9	719
ARE	Peru	I RSNC	1	0	0	0	0

Table 7.2: *(continued)*

Agency	Country	Directly or indirectly reporting (D/I)	Hypocentres with associated phases	Hypocentres without associated phases	Associated phases	Unassociated phases	Amplitudes
MAN	Philippines	D	0	37	0	0	0
QCP	Philippines	D	0	0	0	206	0
PJWWP	Poland	D	118	0	262	1	17
WAR	Poland	D	0	0	0	7051	342
IGIL	Portugal	D	722	0	3549	0	1164
INMG	Portugal	D	2180	0	137482	12871	39751
SVSA	Portugal	D	1292	0	41116	6610	29240
BELR	Republic of Belarus	D	0	0	0	26283	8529
CFUSG	Republic of Crimea	D	87	1	1773	756	1513
KMA	Republic of Korea	D	23	0	432	0	0
BUC	Romania	D	598	40	14813	55439	3175
ASRS	Russia	D	94	3809	3122	0	1109
BYKL	Russia	D	48	0	6576	0	2147
DRS	Russia	I MOS	193	169	0	0	0
FCIAR	Russia	D	177	1	1555	633	488
IDG	Russia	I MOS	0	27	0	0	0
KOLA	Russia	D	2193	152	21318	32	0
KRSC	Russia	D	1022	0	32682	0	0
MIRAS	Russia	D	34	4	1076	0	446
MOS	Russia	D	2811	4358	323869	1	110690
NERS	Russia	D	69	1	1388	0	671
NORS	Russia	I MOS	28	167	0	0	0
SKHL	Russia	D	1210	1285	25454	0	11253
VKMS	Russia	I MOS	0	18	0	0	0
YARS	Russia	D	423	71	4627	0	3558
SGS	Saudi Arabia	D	2772	0	44723	26	0
BEO	Serbia	D	1292	10	26602	0	0
BRA	Slovakia	D	0	0	0	20122	0
LJU	Slovenia	D	1484	16	21172	3173	7709
PRE	South Africa	D	1934	0	44692	584	14925
MDD	Spain	D	3321	0	75801	0	20127
MRB	Spain	D	1378	0	27751	254	12434
SFS	Spain	D	1124	0	18736	17	0
UPP	Sweden	D	2373	1220	30770	0	0
ZUR	Switzerland	D	766	3	12790	0	8245
BKK	Thailand	D	178	1	1264	0	1990
TRN	Trinidad and Tobago	D	1457	7	17389	31393	0
TUN	Tunisia	D	41	1	204	3	0
AFAD	Turkey	D	12595	6	299070	0	108871
ISK	Turkey	D	9254	0	152206	2047	86807
AEIC	U.S.A.	I NEIC	1805	1084	70153	0	0
ANF	U.S.A.	I IRIS	312	532	0	0	0
BUT	U.S.A.	I NEIC	0	76	1641	0	0
GCMT	U.S.A.	D	0	2438	0	0	0
HVO	U.S.A.	I NEIC	243	8	13620	0	0
IRIS	U.S.A.	D	1984	532	295795	0	0
LDO	U.S.A.	I NEIC	0	17	198	0	0
NCEDC	U.S.A.	I NEIC	79	17	9084	0	0
NEIC	U.S.A.	D	16507	8558	1532544	0	835239
PAS	U.S.A.	I NEIC	75	6	12246	0	0
PMR	**U.S.A.**	**I IRIS**	**14**	**0**	**0**	**0**	**0**
PNSN	U.S.A.	D	0	68	0	0	0
REN	U.S.A.	I NEIC	72	29	3490	0	0
RSPR	U.S.A.	D	2485	1008	46265	0	0
SEA	U.S.A.	I NEIC	35	0	1930	0	0
SLM	U.S.A.	I NEIC	2	58	1489	0	0
TXNET	**U.S.A.**	**D**	**12650**	**202**	**115190**	**4561**	**39592**
UUSS	U.S.A.	I NEIC	110	17	2114	0	0
MCSM	Ukraine	D	1468	240	25756	0	14955
SIGU	Ukraine	D	22	25	659	0	355
DSN	United Arab Emirates	D	480	0	6584	0	0
BGS	United Kingdom	D	283	27	8309	0	3291

Table 7.2: *(continued)*

Agency	Country	Directly or indirectly reporting (D/I)	Hypocentres with associated phases	Hypocentres without associated phases	Associated phases	Unassociated phases	Amplitudes
ISC-PPSM	**United Kingdom**	**D**	**0**	**103**	**0**	**0**	**0**
ISU	Uzbekistan	D	635	2	4216	29	0
FUNV	Venezuela	D	1202	0	10855	0	0
PLV	Viet Nam	D	48	9	525	0	244
BUL	Zimbabwe	D	325	0	2758	47	0

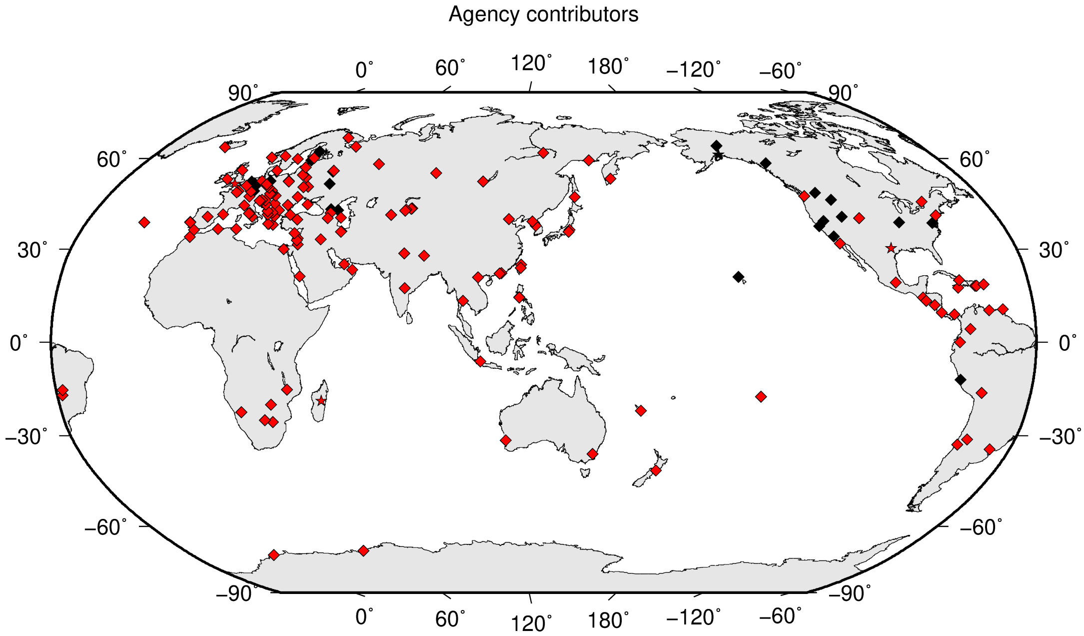

Figure 7.1: *Map of agencies that have contributed data to the ISC for this summary period. Agencies that have reported directly to the ISC are shown in red. Those that have reported indirectly (via another agency) are shown in black. Any new or renewed agencies, since the last six-month period, are shown by a star. Each agency is listed in Table 7.2.*

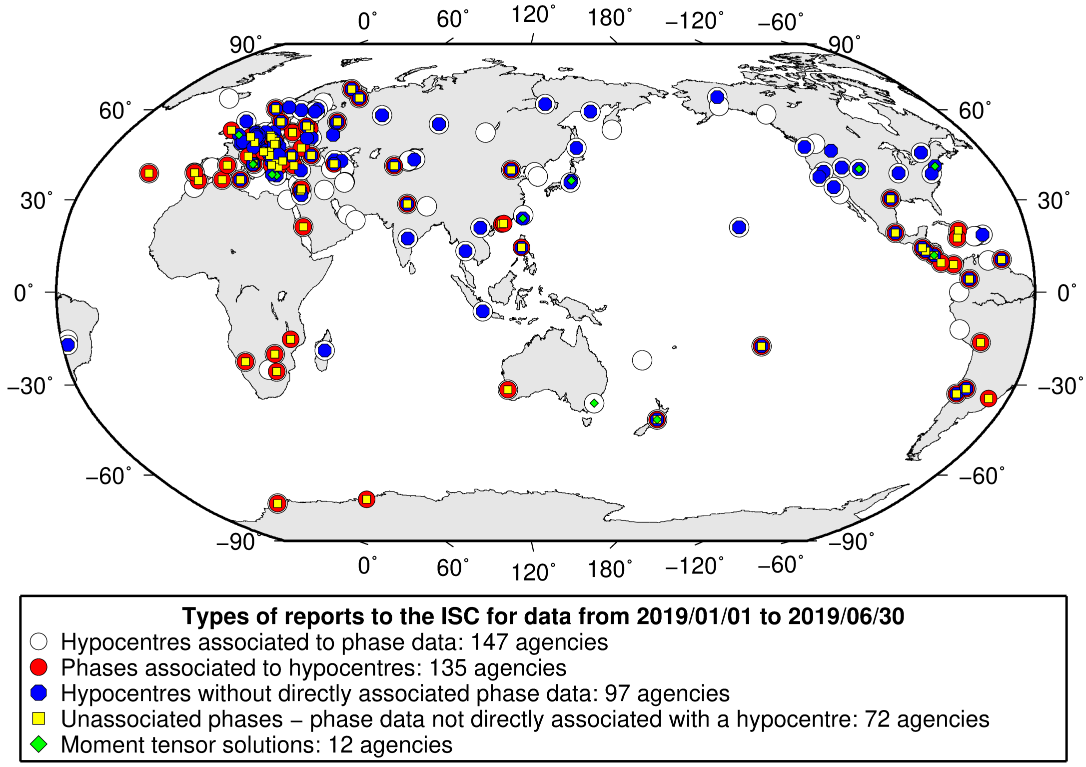

Figure 7.2: *Map of the different data types reported by agencies to the ISC. A full list of the data types reported by each agency is shown in Table 7.2.*

7.3 Arrival Observations

The collection of phase arrival observations at the ISC has increased dramatically with time. The increase in reported phase arrival observations is shown in Figure 7.3.

The reports with phase data are summarised in Table 7.3. This table is split into three sections, providing information on the reports themselves, the phase data, and the stations reporting the phase data. A map of the stations contributing these phase data is shown in Figure 7.4.

The ISC encourages the reporting of phase arrival times together with amplitude and period measurements whenever feasible. Figure 7.5 shows the percentage of events for which phase arrival times from each station are accompanied with amplitude and period measurements.

Figure 7.6 indicates the number of amplitude and period measurement for each station.

Together with the increase in the number of phases (Figure 7.3), there has been an increase in the number of stations reported to the ISC. The increase in the number of stations is shown in Figure 7.7. This increase can also be seen on the maps for stations reported each decade in Figure 7.8.

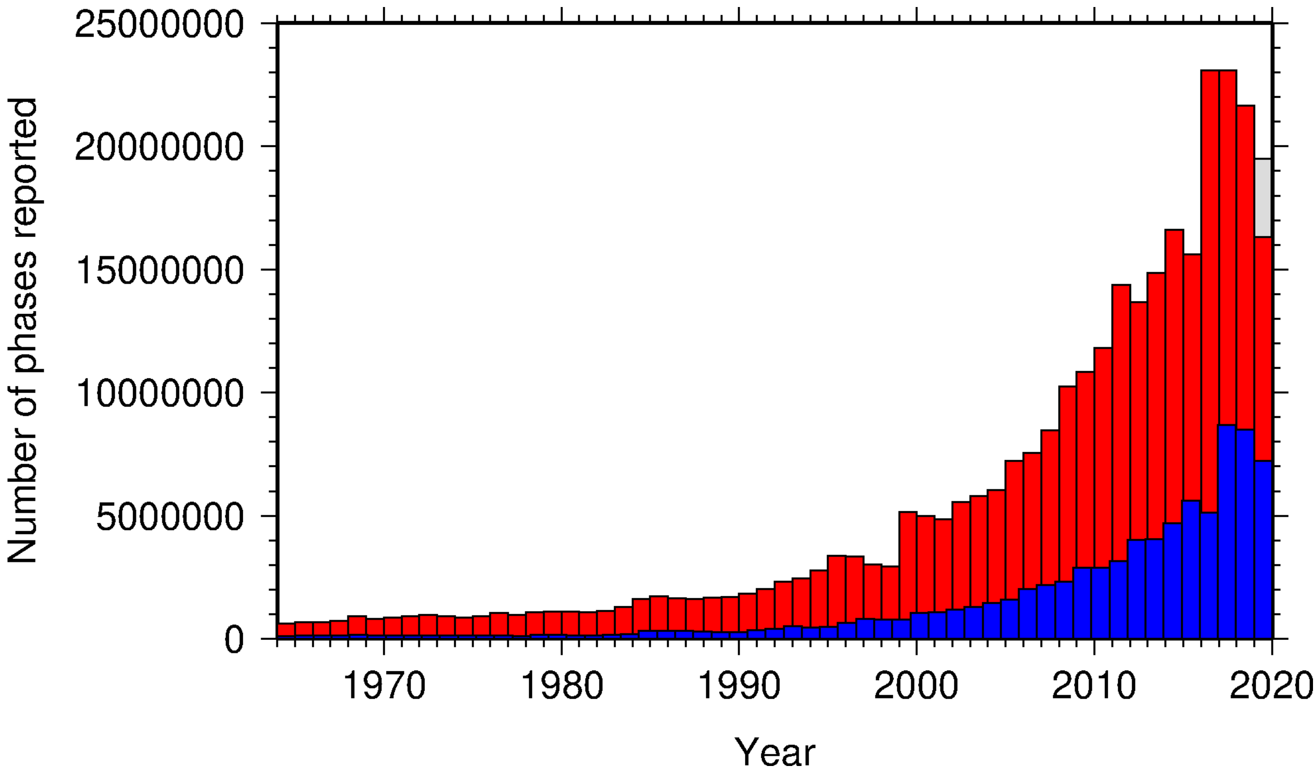

Figure 7.3: *Histogram showing the number of phases (red) and number of amplitudes (blue) collected by the ISC for events each year since 1964. The data in grey covers the current period where data are still being collected before the ISC review takes place and is accurate at the time of publication.*

Table 7.3: *Summary of reports containing phase arrival observations.*

Reports with phase arrivals	3509
Reports with phase arrivals including amplitudes	2930
Reports with only phase arrivals (no hypocentres reported)	164
Total phase arrivals received	9898553
Total phase arrival-times received	9176879
Number of duplicate phase arrival-times	746663 (8.1%)
Number of amplitudes received	3481796
Stations reporting phase arrivals	9637
Stations reporting phase arrivals with amplitude data	5488
Max number of stations per report	2199

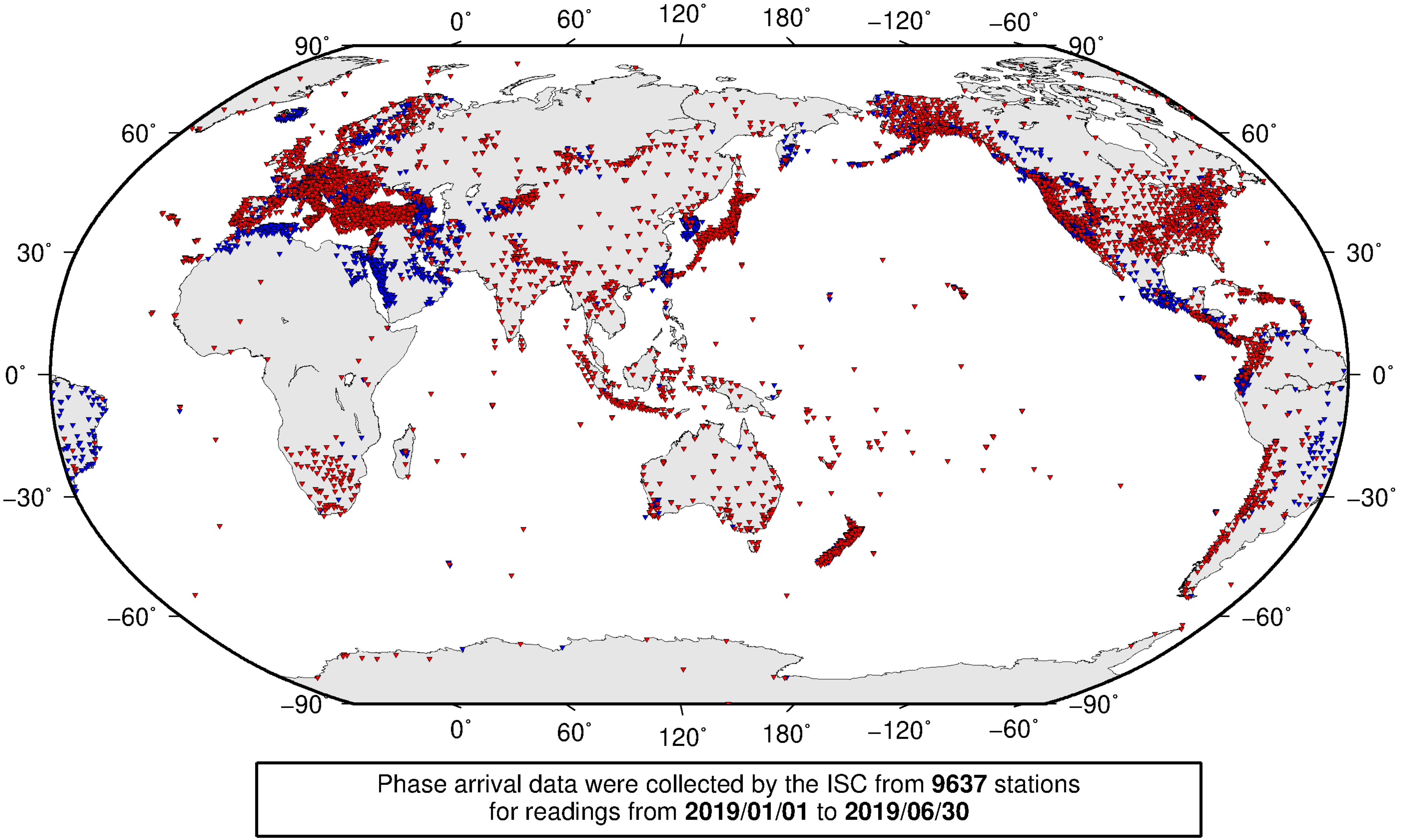

Figure 7.4: *Stations contributing phase data to the ISC for readings from January 2019 to the end of June 2019. Stations in blue provided phase arrival times only; stations in red provided both phase arrival times and amplitude data.*

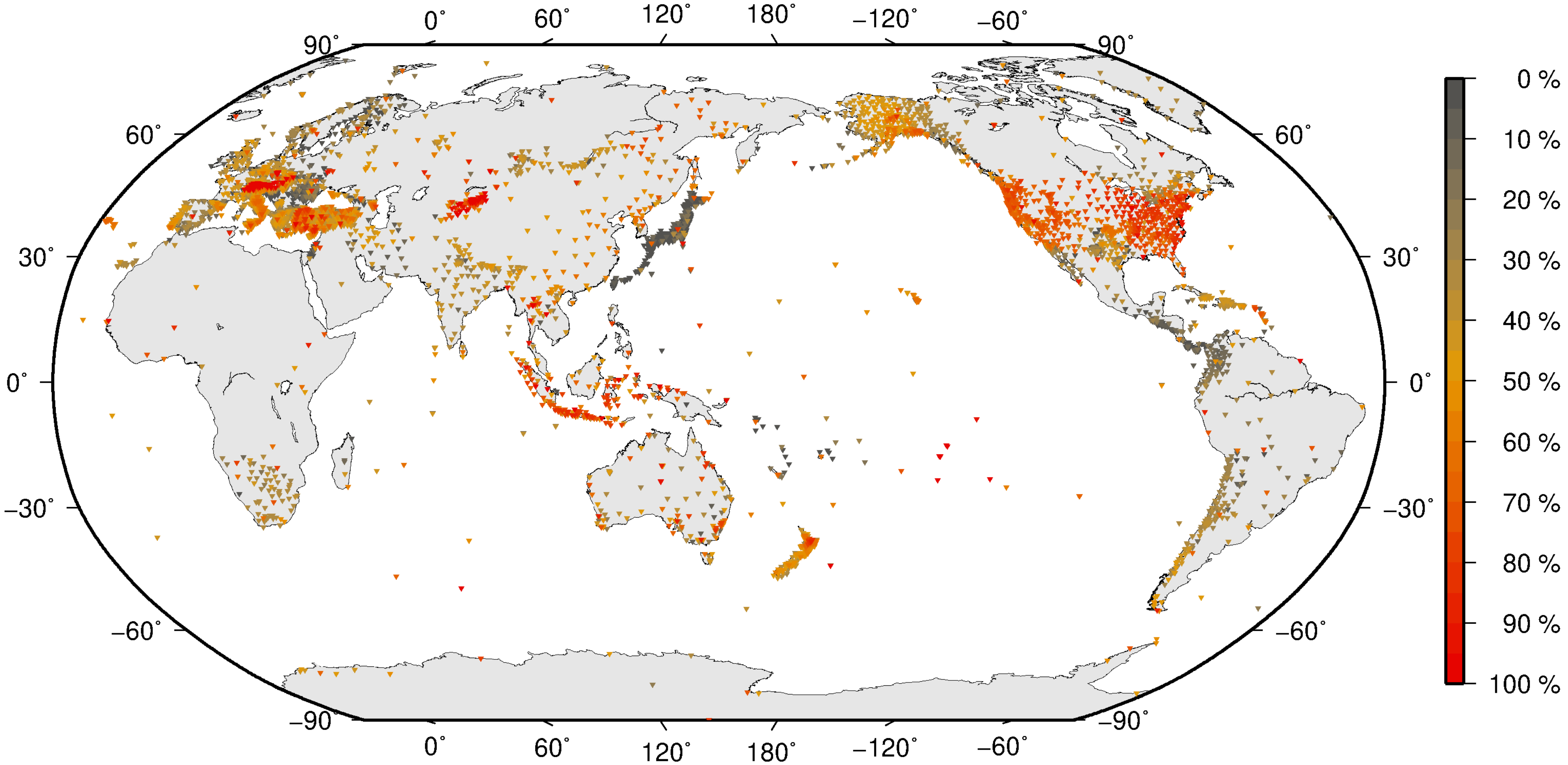

Amplitude data were collected by the ISC from **5439** stations sent by **87** agencies for readings from **2019/01/01** to **2019/06/30**

Figure 7.5: *Percentage of events for which phase arrival times from each station are accompanied with amplitude and period measurements.*

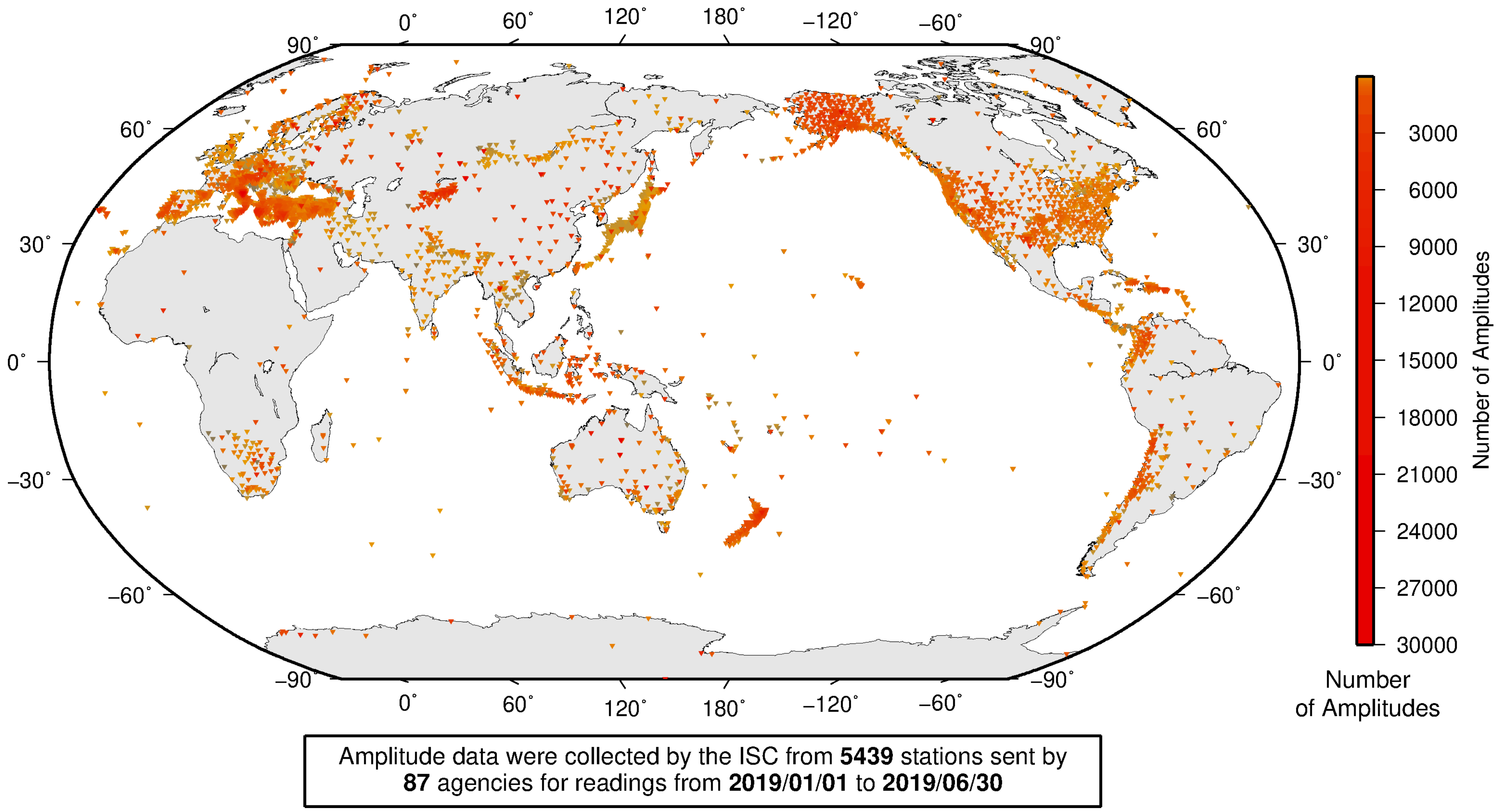

Figure 7.6: *Number of amplitude and period measurements for each station.*

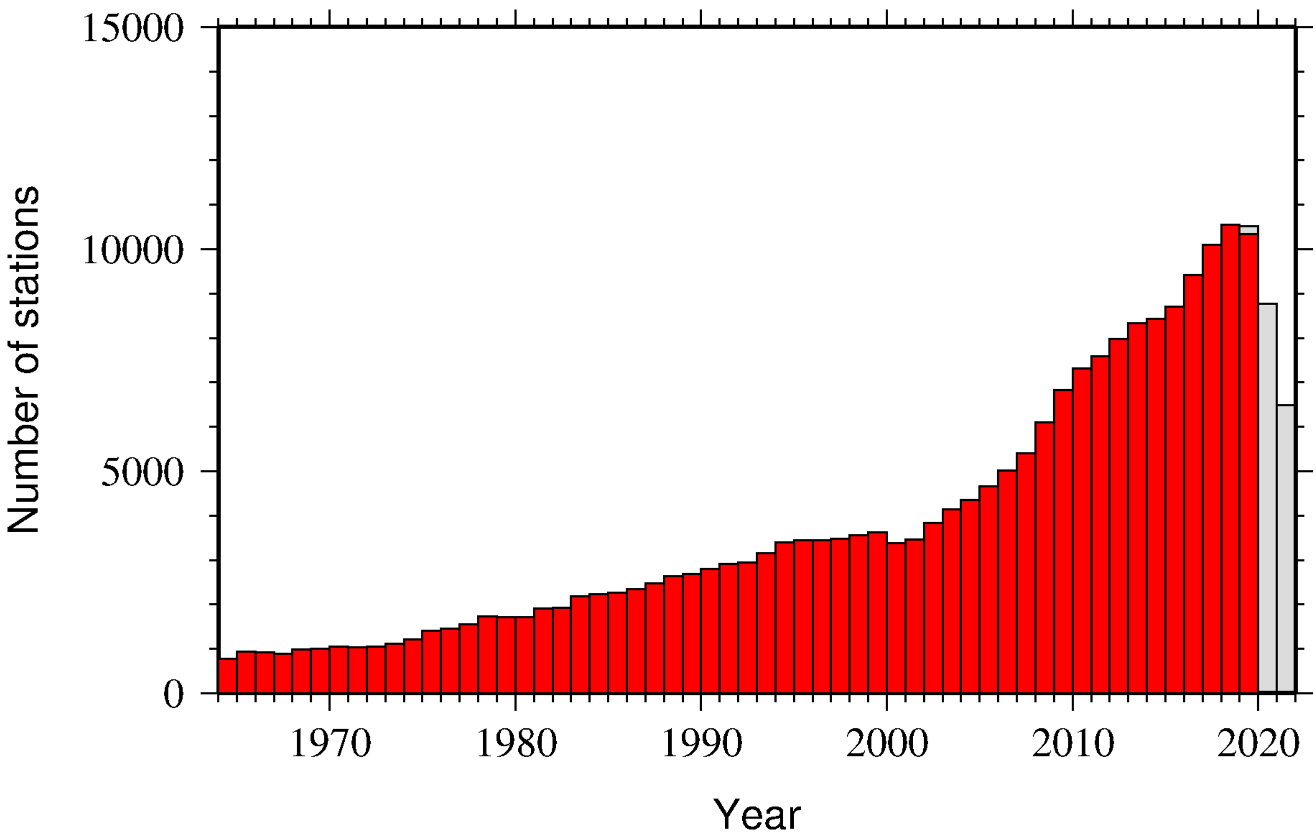

Figure 7.7: *Histogram showing the number of stations reporting to the ISC each year since 1964. The data in grey covers the current period where station information is still being collected before the ISC review of events takes place and is accurate at the time of publication.*

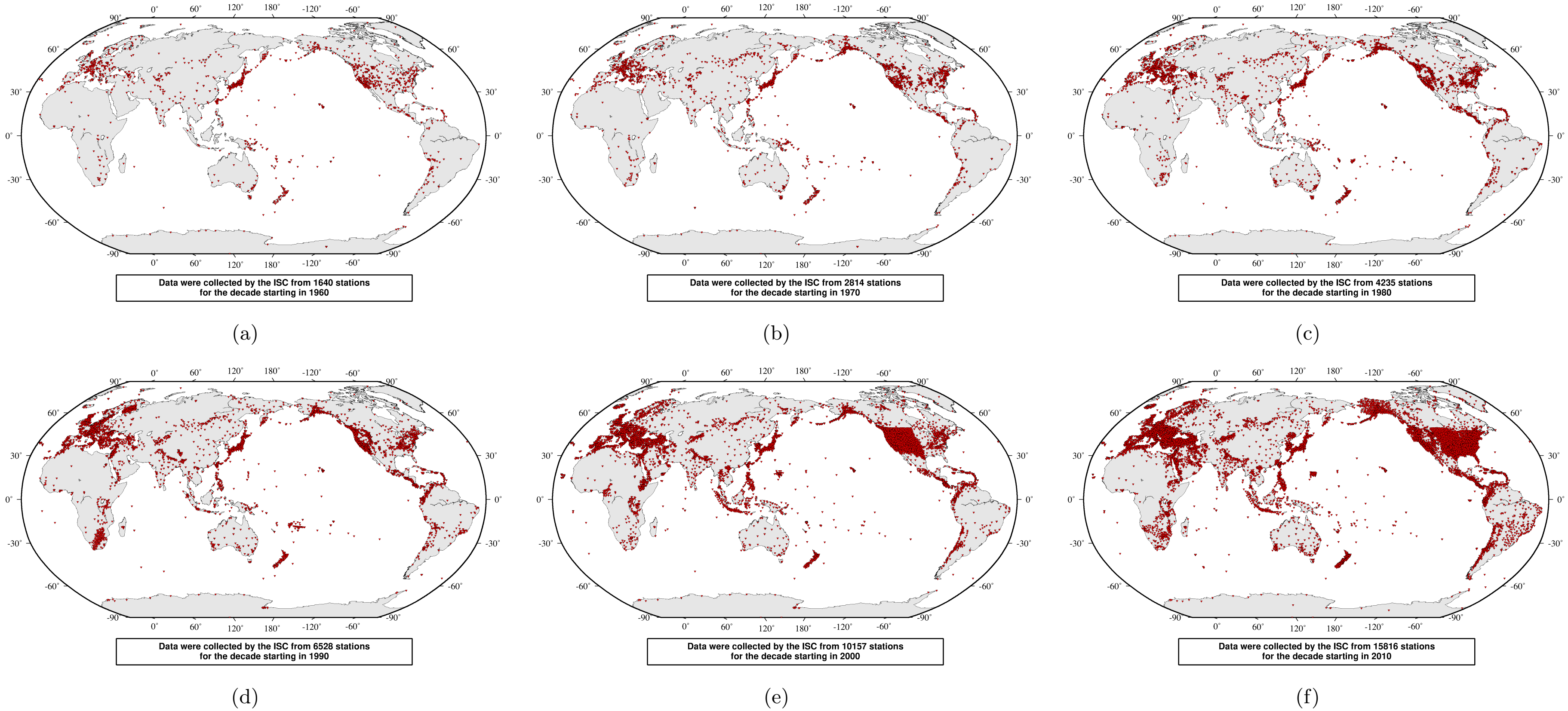

Figure 7.8: *Maps showing the stations reported to the ISC for each decade since 1960. Note that the last map covers a shorter time period.*

7.4 Hypocentres Collected

The ISC Bulletin groups multiple estimates of hypocentres into individual events, with an appropriate prime hypocentre solution selected. The collection of these hypocentre estimates are described in this section.

The reports containing hypocentres are summarised in Table 7.4. The number of hypocentres collected by the ISC has also increased significantly since 1964, as shown in Figure 7.9. A map of all hypocentres reported to the ISC for this summary period is shown in Figure 7.10. Where a network magnitude was reported with the hypocentre, this is also shown on the map, with preference given to reported values, first of M_W followed by M_S, m_b and M_L respectively (where more than one network magnitude was reported).

Table 7.4: *Summary of the reports containing hypocentres.*

Reports with hypocentres	3789
Reports of hypocentres only (no phase readings)	444
Total hypocentres received	422039
Number of duplicate hypocentres	16116 (3.8%)
Agencies determining hypocentres	163

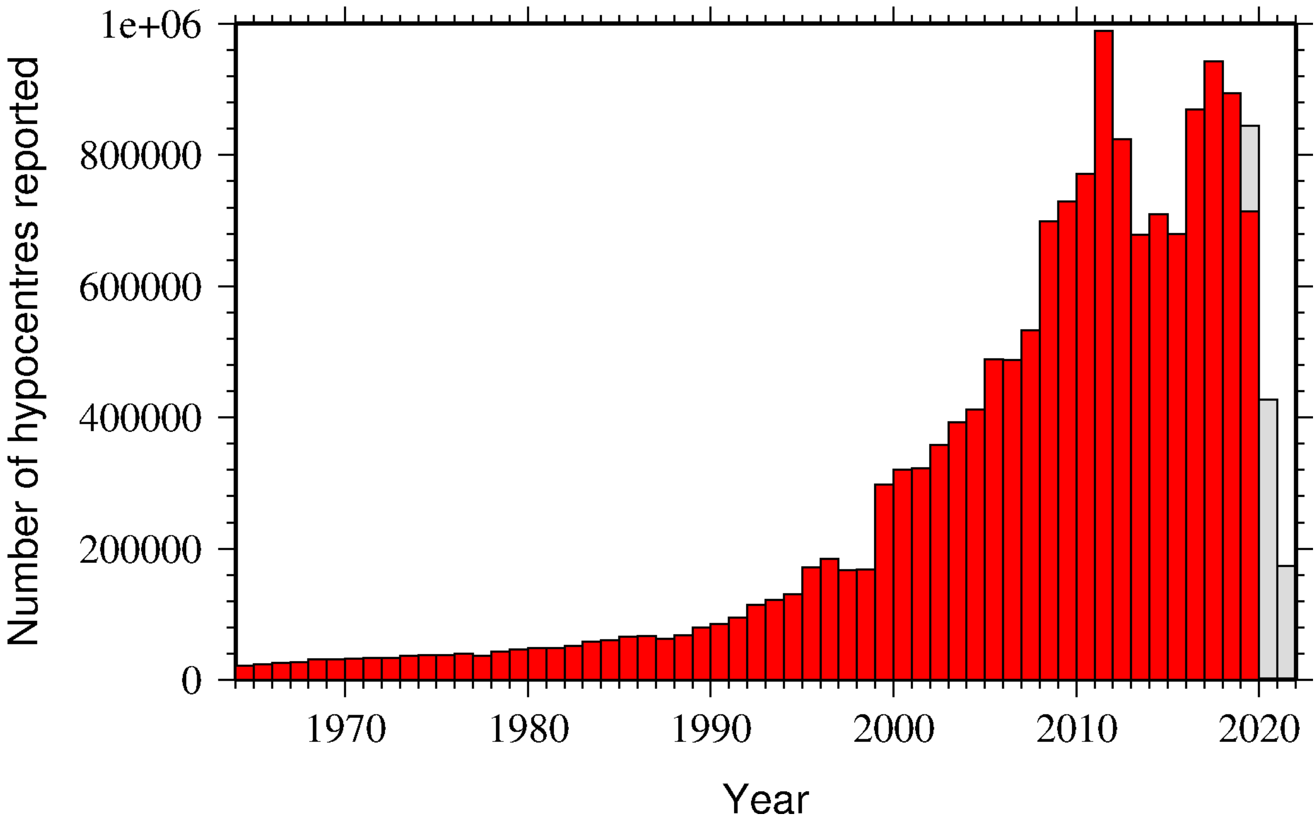

Figure 7.9: *Histogram showing the number of hypocentres collected by the ISC for events each year since 1964. For each event, multiple hypocentres may be reported.*

All the hypocentres that are reported to the ISC are automatically grouped into events, which form the basis of the ISC Bulletin. For this summary period 442880 hypocentres (including ISC) were grouped

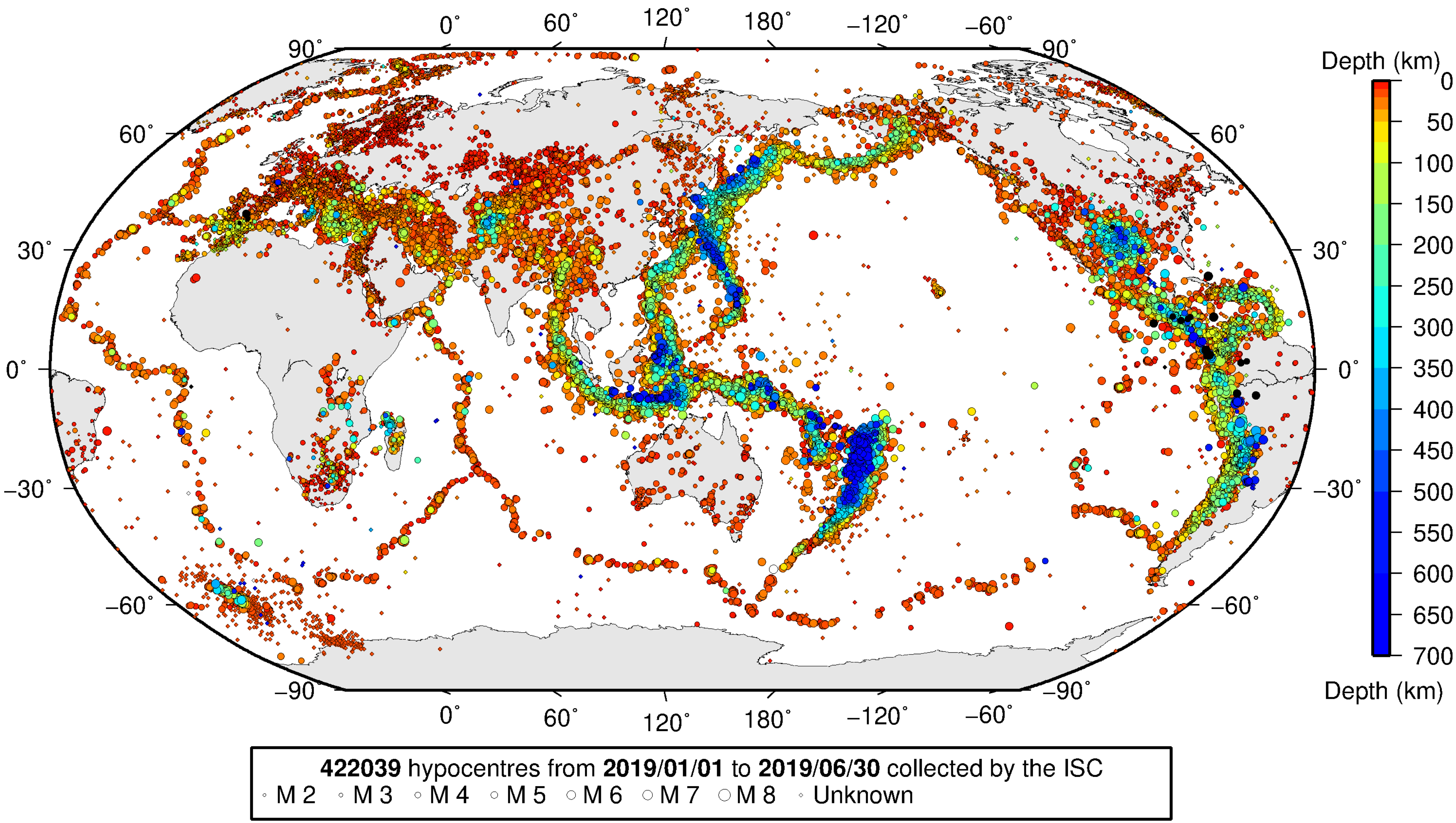

Figure 7.10: *Map of all hypocentres collected by the ISC. The scatter shows the large variation of the multiple hypocentres that are reported for each event. The magnitude corresponds with the reported network magnitude. If more than one network magnitude type was reported, preference was given to values of* M_W*,* M_S*,* m_b *and* M_L *respectively. Compare with Figure 8.2*

into 306106 events, the largest of these having 53 hypocentres in one event. The total number of events shown here is the result of an automatic grouping algorithm, and will differ from the total events in the published ISC Bulletin, where both the number of events and the number of hypocentre estimates will have changed due to further analysis. The process of grouping is detailed in Section 10.1.3. Figure 8.2 on page 78 shows a map of all prime hypocentres.

7.5 Collection of Network Magnitude Data

Data contributing agencies normally report earthquake hypocentre solutions along with magnitude estimates. For each seismic event, each agency may report one or more magnitudes of the same or different types. This stems from variability in observational practices at regional, national and global level in computing magnitudes based on a multitude of wave types. Differences in the amplitude measurement algorithm, seismogram component(s) used, frequency range, station distance range as well as the instrument type contribute to the diversity of magnitude types. Table 7.5 provides an overview of the complexity of reported network magnitudes reported for seismic events during the summary period.

Table 7.5: *Statistics of magnitude reports to the ISC; M – average magnitude of estimates reported for each event.*

	M<3.0	3.0≤M<5.0	M≥5.0
Number of seismic events	225733	44810	500
Average number of magnitude estimates per event	1.4	3.1	22.8
Average number of magnitudes (by the same agency) per event	1.2	1.8	3.0
Average number of magnitude types per event	1.3	2.4	10.7
Number of magnitude types	26	39	33

Table 7.6 gives the basic description, main features and scientific paper references for the most commonly reported magnitude types.

Table 7.6: *Description of the most common magnitude types reported to the ISC.*

Magnitude type	Description	References	Comments
M	Unspecified		Often used in real or near-real time magnitude estimations
mB	Medium-period and Broad-band body-wave magnitude	*Gutenberg* (1945a); *Gutenberg* (1945b); *IASPEI* (2005); *IASPEI* (2013); *Bormann et al.* (2009); *Bormann and Dewey* (2012)	
mb	Short-period body-wave magnitude	*IASPEI* (2005); *IASPEI* (2013); *Bormann et al.* (2009); *Bormann and Dewey* (2012)	Classical mb based on stations between 21°-100° distance

Table 7.6: *continued*

Magnitude type	Description	References	Comments
mb1	Short-period body-wave magnitude	*IDC* (1999) and references therein	Reported only by the IDC; also includes stations at distances less than 21°
mb1mx	Maximum likelihood short-period body-wave magnitude	*Ringdal* (1976); *IDC* (1999) and references therein	Reported only by the IDC
mbtmp	short-period body-wave magnitude with depth fixed at the surface	*IDC* (1999) and references therein	Reported only by the IDC
mbLg	Lg-wave magnitude	*Nuttli* (1973); *IASPEI* (2005); *IASPEI* (2013); *Bormann and Dewey* (2012)	Also reported as MN
Mc	Coda magnitude		
MD (Md)	Duration magnitude	*Bisztricsany* (1958); *Lee et al.* (1972)	
ME (Me)	Energy magnitude	*Choy and Boatwright* (1995)	Reported only by NEIC
MJMA	JMA magnitude	*Tsuboi* (1954)	Reported only by JMA
ML (Ml)	Local (Richter) magnitude	*Richter* (1935); *Hutton and Boore* (1987); *IASPEI* (2005); *IASPEI* (2013)	
MLSn	Local magnitude calculated for Sn phases	*Balfour et al.* (2008)	Reported by PGC only for earthquakes west of the Cascadia subduction zone
MLv	Local (Richter) magnitude computed from the vertical component		Reported only by DJA and BKK
MN (Mn)	Lg-wave magnitude	*Nuttli* (1973); *IASPEI* (2005)	Also reported as mbLg
MS (Ms)	Surface-wave magnitude	*Gutenberg* (1945c); *Vaněk et al.* (1962); *IASPEI* (2005)	Classical surface-wave magnitude computed from station between 20°-160° distance
Ms1	Surface-wave magnitude	*IDC* (1999) and references therein	Reported only by the IDC; also includes stations at distances less than 20°
ms1mx	Maximum likelihood surface-wave magnitude	*Ringdal* (1976); *IDC* (1999) and references therein	Reported only by the IDC

Table 7.6: *continued*

Magnitude type	Description	References	Comments
Ms7	Surface-wave magnitude	*Bormann et al.* (2007)	Reported only by BJI and computed from records of a Chinese-made long-period seismograph in the distance range 3°-177°
MW (Mw)	Moment magnitude	*Kanamori* (1977); *Dziewonski et al.* (1981)	Computed according to the *IASPEI* (2005) and *IASPEI* (2013) standard formula
Mw(mB)	Proxy Mw based on mB	*Bormann and Saul* (2008)	Reported only by DJA and BKK
Mwp	Moment magnitude from P-waves	*Tsuboi et al.* (1995)	Reported only by DJA and BKK and used in rapid response
mbh	Unknown		
mbv	Unknown		
MG	Unspecified type		Contact contributor
Mm	Unknown		
msh	Unknown		
MSV	Unknown		

Table 7.7 lists all magnitude types reported, the corresponding number of events in the ISC Bulletin and the agency codes along with the number of earthquakes.

Table 7.7: *Summary of magnitude types in the ISC Bulletin for this summary period. The number of events with values for each magnitude type is listed. The agencies reporting these magnitude types are listed, together with the total number of values reported.*

Magnitude type	Events	Agencies reporting magnitude type (number of values)
M	17462	WEL (11934), ASRS (3793), CATAC (1473), BKK (158), IDG (27), VKMS (18), PRU (15), INMG (14), YARS (12), MOS (9), TAN (5), SKHL (4), MIRAS (4), TXNET (4), NERS (1)
mb	24201	IDC (16328), NEIC (6937), NNC (4223), KRNET (2280), DJA (1744), MOS (1690), VIE (1673), BJI (1103), RSNC (561), NOU (450), VAO (398), BGR (228), NAO (195), OMAN (124), MCSM (112), CATAC (84), MDD (80), AUST (74), CFUSG (61), BKK (55), NDI (44), MAN (36), DSN (27), INMG (25), THR (22), SIGU (16), OSUNB (15), SFS (10), IGIL (8), PPT (8), PDG (5), DNK (4), CRAAG (3), THE (3), BER (2), WEL (2), PGC (1), AZER (1), SSNC (1), ROM (1), BGS (1)
mB	2333	BJI (1117), DJA (814), WEL (406), RSNC (287), CATAC (67), BKK (48), NOU (3), OSUNB (2), KEA (1), SFS (1), ASRS (1)
mb(Pn)	431	BER (431)
mB_BB	26	BGR (26)

Table 7.7: *Continued.*

Magnitude type	Events	Agencies reporting magnitude type (number of values)
mb_Lg	3644	MDD (3209), NEIC (430), OTT (14)
mBc	10	RSNC (10)
mbR	64	VAO (64)
mbtmp	18109	IDC (18109)
Mc	47	KRSC (47)
MC	1	AFAD (1)
MD	12421	RSPR (2723), GCG (2086), LDG (1900), TRN (1452), SDD (1438), SSNC (818), GII (687), ECX (548), JMA (375), TIR (375), HLW (325), SOF (254), UPA (233), GRAL (197), ROM (177), MEX (133), PDG (84), JSN (79), SLM (60), PNSN (57), BUG (48), TUN (38), UUSS (24), JSO (21), HVO (17), NCEDC (12), SNET (9), LVSN (5), DNK (4), SJA (2), BGSI (1), STR (1), AUST (1), NEIC (1)
Mjma	191	BKK (158), JSO (15), CATAC (8), RSNC (8), DJA (3), WEL (1)
ML	133920	TAP (16241), RSNC (13658), ATH (12703), AFAD (12279), WEL (11421), IDC (10301), ISK (9253), ROM (8203), HEL (7736), NEIC (4974), GUC (4044), SJA (3374), UPP (3095), SGS (2764), VIE (2756), AEIC (2467), THE (2322), INMG (2182), KOLA (2101), PRE (1916), LDG (1728), SFS (1671), DNK (1489), SDD (1430), SNET (1380), MRB (1376), BER (1356), BEO (1289), LJU (1275), KRSC (1022), RHSSO (1004), CNRM (862), OSPL (856), SSNC (821), TIR (784), SCB (761), ECX (759), TXNET (722), BUC (598), ANF (587), SKO (533), GEN (487), ISN (484), IGIL (433), IPEC (432), HLW (415), GCG (392), PDG (384), AUST (383), WBNET (350), YARS (329), NIC (323), PGC (311), NAO (306), UPA (306), TAN (287), NDI (263), HVO (233), KNET (210), OMAN (185), BGSI (184), LVSN (178), DSN (170), AZER (169), BJI (168), BKK (157), UCC (156), ASIES (156), BGR (130), BGS (124), CRAAG (119), NOU (104), UUSS (101), REN (99), BUT (76), PAS (72), PPT (70), DMN (62), PLV (55), BUG (50), NCEDC (45), KEA (44), THR (43), MAN (37), SEA (37), CUPWA (35), MIRAS (34), KRSZO (30), OTT (28), JSO (25), BNS (19), LDO (17), CATAC (8), FIA0 (8), RSPR (7), CLL (6), DJA (4), MCSM (3), RISSC (3), CSEM (1), VAO (1), MEX (1), PMR (1)
MLh	1429	THE (713), ZUR (616), ASRS (93), RSNC (7)
MLSn	136	PGC (136)
MLv	27888	WEL (12043), DJA (6188), STR (4969), CATAC (1499), NOU (1202), RSNC (1162), SFS (862), BKK (167), IGQ (147), MCSM (122), JSO (56), OSUNB (8), PPT (6), AUST (1)
MN	501	OTT (501)
mpv	4624	NNC (4624)
MPVA	245	MOS (215), NORS (195)
mR	72	OSUNB (72)

Table 7.7: *Continued.*

Magnitude type	Events	Agencies reporting magnitude type (number of values)
MS	7952	IDC (7822), BJI (905), MOS (452), BGR (122), NSSP (51), VIE (38), MAN (36), OMAN (32), INMG (19), SOME (18), IGIL (4), GUC (4), DSN (3), BER (1), KEA (1)
Ms(BB)	19	RSNC (11), CATAC (4), DJA (2), JSO (2)
Ms7	901	BJI (901)
Ms_20	174	NEIC (174)
Ms_VX	1	NEIC (1)
MV	92411	JMA (92411)
MW	9707	SJA (2924), SDD (1353), GCMT (1219), FUNV (1173), UPA (626), NIED (599), UCR (464), AFAD (306), SSNC (304), NDI (254), SCB (233), GCG (225), ASIES (156), PGC (142), IPGP (131), BER (102), WEL (97), JMA (82), MED_RCMT (79), DJA (43), ATH (27), ROM (14), UPSL (14), RSNC (9), INMG (9), GUC (5), AZER (4), OSUNB (3), PLV (3), GFZ (2), MEX (1), IEC (1)
Mw(mB)	488	WEL (378), CATAC (62), BKK (48), SFS (1)
Mwb	173	NEIC (173)
MwMwp	23	CATAC (20), BKK (3)
Mwp	281	DJA (186), RSNC (76), CATAC (20), OMAN (9), BKK (5), ROM (1)
Mwpd	1	ROM (1)
Mwr	341	NEIC (251), GUC (42), NCEDC (33), SLM (25), PAS (9), OTT (7), REN (2), BUC (1), UUSS (1)
Mws	478	GII (478)
Mww	609	NEIC (609), GUC (1)

The most commonly reported magnitude types are short-period body-wave, surface-wave, local (or Richter), moment, duration and JMA magnitude type. For a given earthquake, the number and type of reported magnitudes greatly vary depending on its size and location. The large earthquake of October 25, 2010 gives an example of the multitude of reported magnitude types for large earthquakes (Listing 7.1). Different magnitude estimates come from global monitoring agencies such as the IDC, NEIC and GCMT, a local agency (GUC) and other agencies, such as MOS and BJI, providing estimates based on the analysis of their networks. The same agency may report different magnitude types as well as several estimates of the same magnitude type, such as NEIC estimates of Mw obtained from W-phase, centroid and body-wave inversions.

Listing 7.1: *Example of reported magnitudes for a large event*

```
Event   15264887 Southern Sumatera
   Date       Time        Err   RMS Latitude Longitude  Smaj  Smin  Az Depth   Err Ndef Nsta Gap  mdist  Mdist Qual   Author      OrigID
2010/10/25 14:42:22.18   0.27 1.813  -3.5248  100.1042 4.045 3.327  54  20.0  1.37 2102 2149  23   0.76 176.43 m i de ISC       01346132
 (#PRIME)

Magnitude  Err Nsta Author      OrigID
mb      6.1       61 BJI       15548963
mB      6.9       68 BJI       15548963
Ms      7.7       85 BJI       15548963
Ms7     7.5       86 BJI       15548963
mb      5.3 0.1   48 IDC       16686694
mb1     5.3 0.1   51 IDC       16686694
mb1mx   5.3 0.0   52 IDC       16686694
mbtmp   5.3 0.1   51 IDC       16686694
ML      5.1 0.2    2 IDC       16686694
MS      7.1 0.0   31 IDC       16686694
Ms1     7.1 0.0   31 IDC       16686694
ms1mx   6.9 0.1   44 IDC       16686694
mb      6.1      243 ISCJB     01677901
```

```
MS      7.3       228 ISCJB      01677901
M       7.1       117 DJA        01268475
mb      6.1 0.2   115 DJA        01268475
mB      7.1 0.1   117 DJA        01268475
MLv     7.0 0.2    26 DJA        01268475
        7.1 0.4   117 DJA        01268475
Mwp     6.9 0.2   102 DJA        01268475
mb      6.4        49 MOS        16742129
MS      7.2        70 MOS        16742129
mb      6.5       110 NEIC       01288303
ME      7.3           NEIC       01288303
MS      7.3       143 NEIC       01288303
MW      7.7           NEIC       01288303
MW      7.8       130 GCMT       00125427
mb      5.9           KLM        00255772
ML      6.7           KLM        00255772
MS      7.6           KLM        00255772
mb      6.4        20 BGR        16815854
Ms      7.2         2 BGR        16815854
mb      6.3 0.3   250 ISC        01346132
MS      7.3 0.1   237 ISC        01346132
```

An example of a relatively small earthquake that occurred in northern Italy for which we received magnitude reports of mostly local and duration type from six agencies in Italy, France and Austria is given in Listing 7.2.

Listing 7.2: *Example of reported magnitudes for a small event*

```
Event 15089710 Northern Italy
   Date       Time        Err   RMS Latitude Longitude  Smaj  Smin  Az Depth   Err Ndef Nsta Gap  mdist  Mdist Qual   Author      OrigID
2010/08/08 15:20:46.22   0.94 0.778  45.4846    8.3212 2.900 2.539 110  28.6  9.22  172  110  82   0.41   5.35 m i ke ISC        01249414
 (#PRIME)

Magnitude  Err Nsta Author      OrigID
ML      2.4       10 ZUR       15925566
Md      2.6 0.2   19 ROM       16861451
Ml      2.2 0.2    9 ROM       16861451
ML      2.5          GEN       00554757
ML      2.6 0.3   28 CSEM      00554756
Md      2.3 0.0    3 LDG       14797570
Ml      2.6 0.3   32 LDG       14797570
```

Figure 7.11 shows a distribution of the number of agencies reporting magnitude estimates to the ISC according to the magnitude value. The peak of the distribution corresponds to small earthquakes where many local agencies report local and/or duration magnitudes. The number of contributing agencies rapidly decreases for earthquakes of approximately magnitude 5.5 and above, where magnitudes are mostly given by global monitoring agencies.

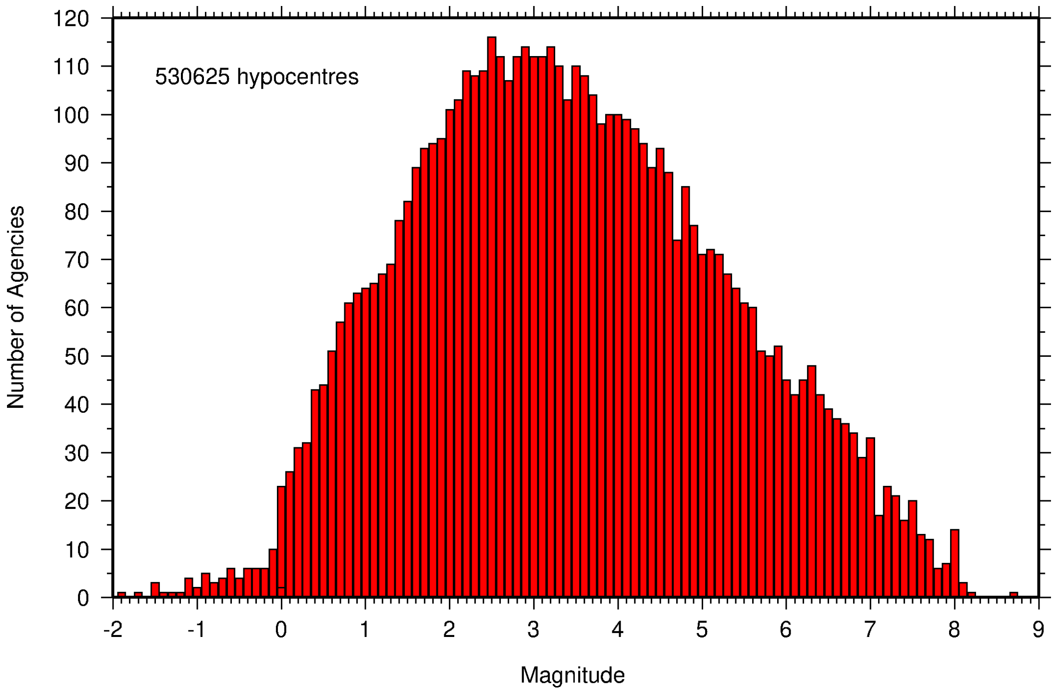

Figure 7.11: *Histogram showing the number of agencies that reported network magnitude values. All magnitude types are included.*

7.6 Moment Tensor Solutions

The ISC Bulletin publishes moment tensor solutions, which are reported to the ISC by other agencies. The collection of moment tensor solutions is summarised in Table 7.8. A histogram showing all moment tensor solutions collected throughout the ISC history is shown in Figure 7.12. Several moment tensor solutions from different authors and different moment tensor solutions calculated by different methods from the same agency may be present for the same event.

Table 7.8: *Summary of reports containing moment tensor solutions.*

Reports with Moment Tensors	399
Total moment tensors received	19180
Agencies reporting moment tensors	12

The number of moment tensors for this summary period, reported by each agency, is shown in Table 7.9. The moment tensor solutions are plotted in Figure 7.13.

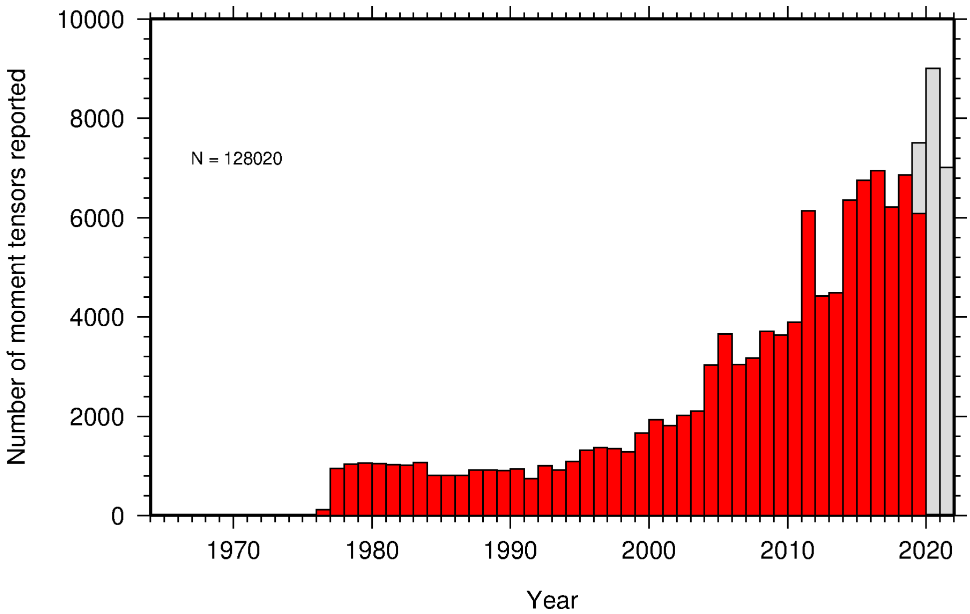

Figure 7.12: *Histogram showing the number of moment tensors reported to the ISC since 1964. The regions in grey represent data that are still being actively collected.*

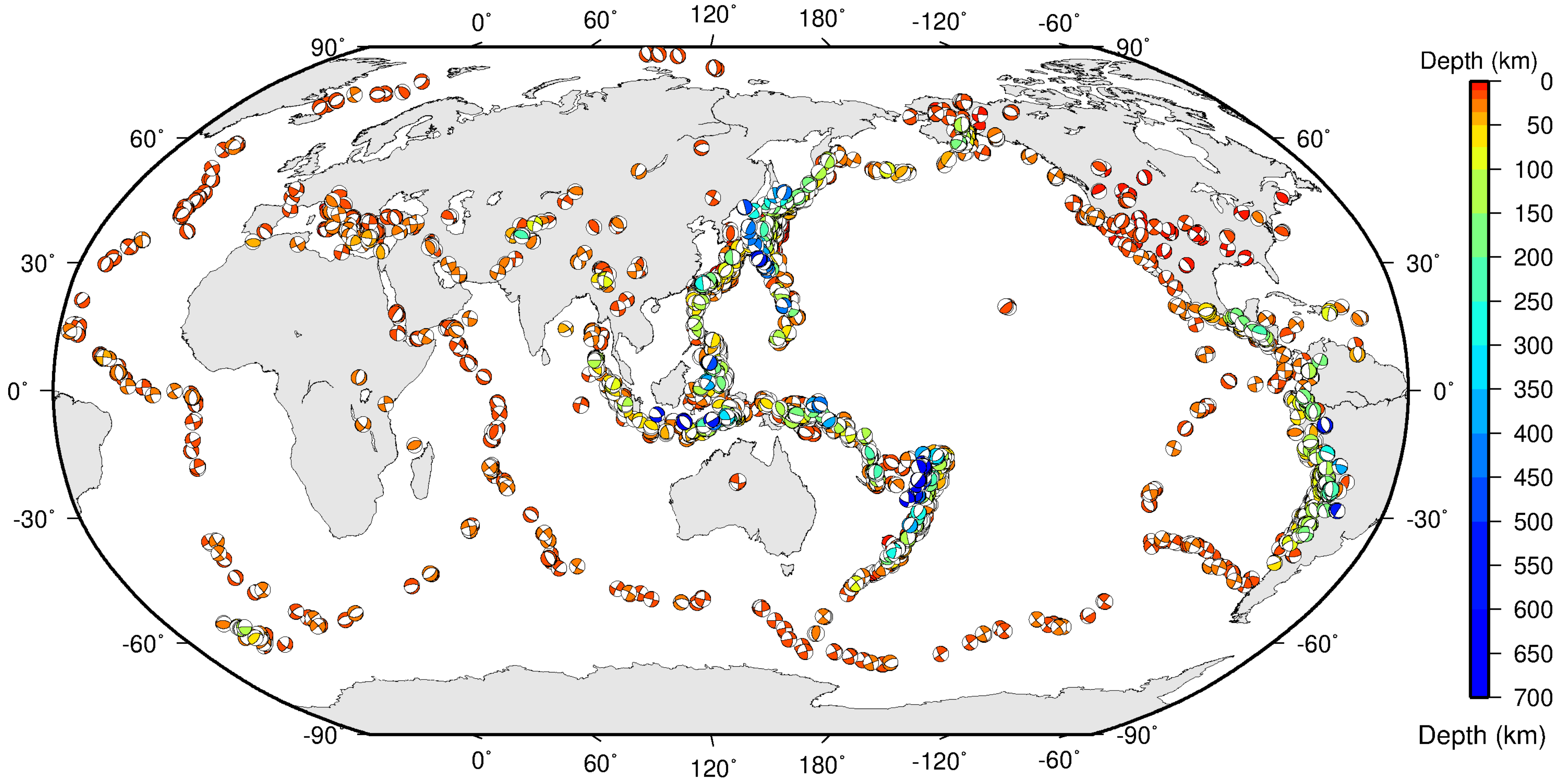

ISC Bulletin: **3447** focal mechanism solutions for **2223** events from **2019/01/01** to **2019/06/30**

Figure 7.13: *Map of all moment tensor solutions in the ISC Bulletin for this summary period.*

Table 7.9: Summary of moment tensor solutions in the ISC Bulletin reported by each agency.

Agency	Number of moment tensor solutions
GCMT	1219
NEIC	1047
ISC	792
NIED	599
TAN	288
IPGP	261
ASIES	156
ISC-PPSM	103
UPA	98
WEL	97
CATAC	92
MED_RCMT	79
PNSN	57
UCR	41
ATH	27
ROM	14
UPSL	14
MOS	12
ECX	10
SDD	3
IEC	2
BER	2

7.7 Timing of Data Collection

Here we present the timing of reports to the ISC. Please note, this does not include provisional alerts, which are replaced at a later stage. Instead, it reflects the final data sent to the ISC. The absolute timing of all hypocentre reports, regardless of magnitude, is shown in Figure 7.14. In Figure 7.15 the reports are grouped into one of six categories - from within three days of an event origin time, to over one year. The histogram shows the distribution with magnitude (for hypocentres where a network magnitude was reported) for each category, whilst the map shows the geographic distribution of the reported hypocentres.

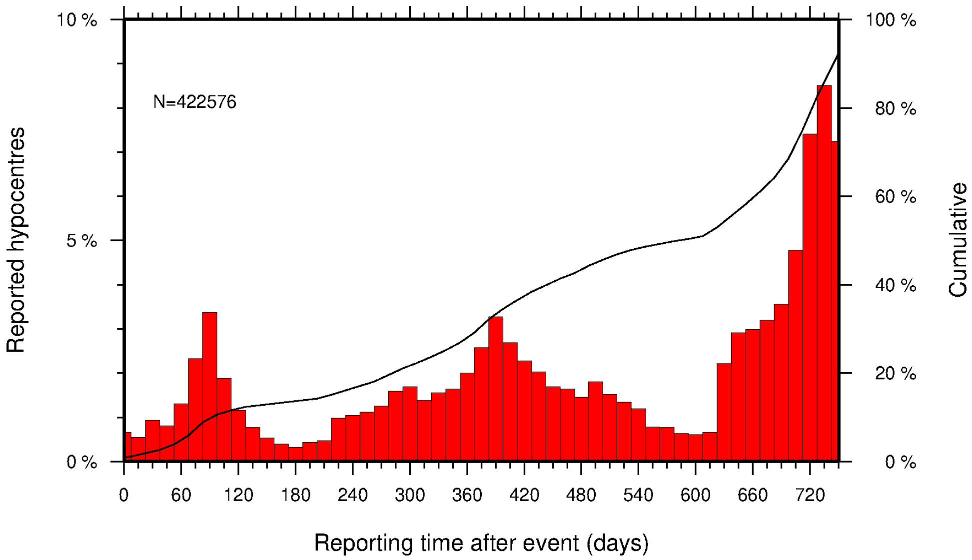

Figure 7.14: *Histogram showing the timing of final reports of the hypocentres (total of N) to the ISC. The cumulative frequency is shown by the solid line.*

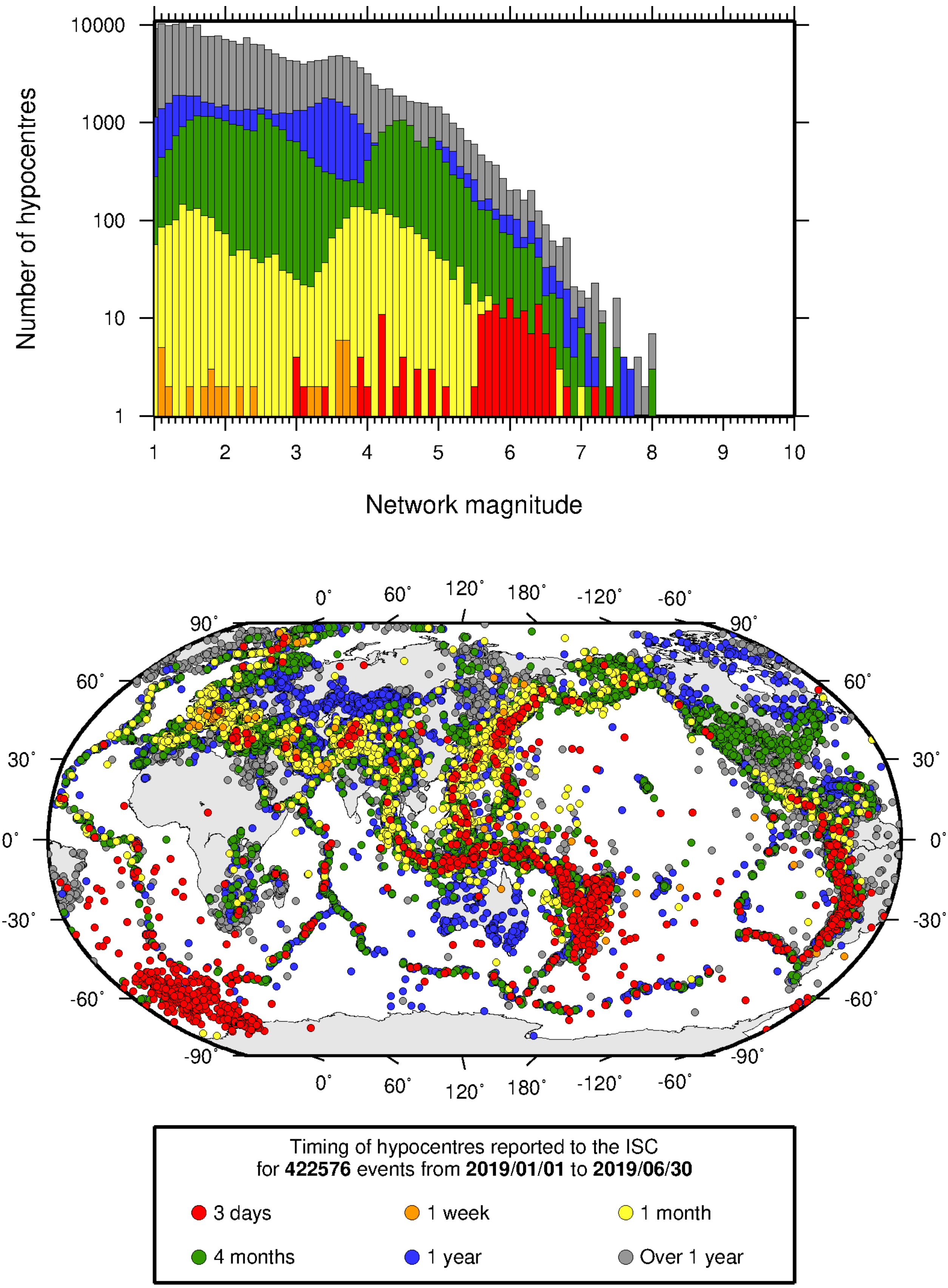

Figure 7.15: *Timing of hypocentres reported to the ISC. The colours show the time after the origin time that the corresponding hypocentre was reported. The histogram shows the distribution with magnitude. If more than one network magnitude was reported, preference was given to a value of M_W followed by M_S, m_b and M_L respectively; all reported hypocentres are included on the map. Note: early reported hypocentres are plotted over later reported hypocentres, on both the map and histogram.*

8

Overview of the ISC Bulletin

This chapter provides an overview of the seismic event data in the ISC Bulletin. We indicate the differences between all ISC events and those ISC events that are reviewed or located. We describe the wealth of phase arrivals and phase amplitudes and periods observed at seismic stations worldwide, reported in the ISC Bulletin and often used in the ISC location and magnitude determination. Finally, we make some comparisons of the ISC magnitudes with those reported by other agencies, and discuss magnitude completeness of the ISC Bulletin.

8.1 Events

The ISC Bulletin had 288285 reported events in the summary period between January and June 2019. Some 90% (261136) of the events were identified as earthquakes, the rest (27149) were of anthropogenic origin (including mining and other chemical explosions, rockbursts and induced events) or of unknown origin. As discussed in Section 10.1.3, typically about 15% of the events are selected for ISC review, and about half of the events selected for review are located by the ISC. In this summary period 10% of the events were reviewed and 7% of the events were located by the ISC. For events that are not located by the ISC, the prime hypocentre is identified according to the rules described in Section 10.1.3.

Of the 10147514 reported phase observations, 36% are associated to ISC-reviewed events, and 33% are associated to events selected for ISC location. Note that all large events are reviewed and located by the ISC. Since large events are globally recorded and thus reported by stations worldwide, they will provide the bulk of observations. This explains why only about one-fifth of the events in any given month is reviewed although the number of phases associated to reviewed events has increased nearly exponentially in the past decades.

Figure 8.1 shows the daily number of events throughout the summary period. Figure 8.2 shows the locations of the events in the ISC Bulletin; the locations of ISC-reviewed and ISC-located events are shown in Figures 8.3 and 8.4, respectively.

Figure 8.5 shows the hypocentral depth distributions of events in the ISC Bulletin for the summary period. The vast majority of events occur in the Earth's crust. Note that the peaks at 0, 10, 35 km, and at every 50 km intervals deeper than 100 km are artifacts of analyst practices of fixing the depth to a nominal value when the depth cannot be reliably resolved.

Figure 8.6 shows the depth distribution of free-depth solutions in the ISC Bulletin. The depth of a hypocentre reported to the ISC is assumed to be determined as a free parameter, unless it is explicitly labelled as a fixed-depth solution. On the other hand, as described in Section 10.1.4, the ISC locator attempts to get a free-depth solution if, and only if, there is resolution for the depth in the data, i.e. if there is a local network and/or sufficient depth-sensitive phases are reported.

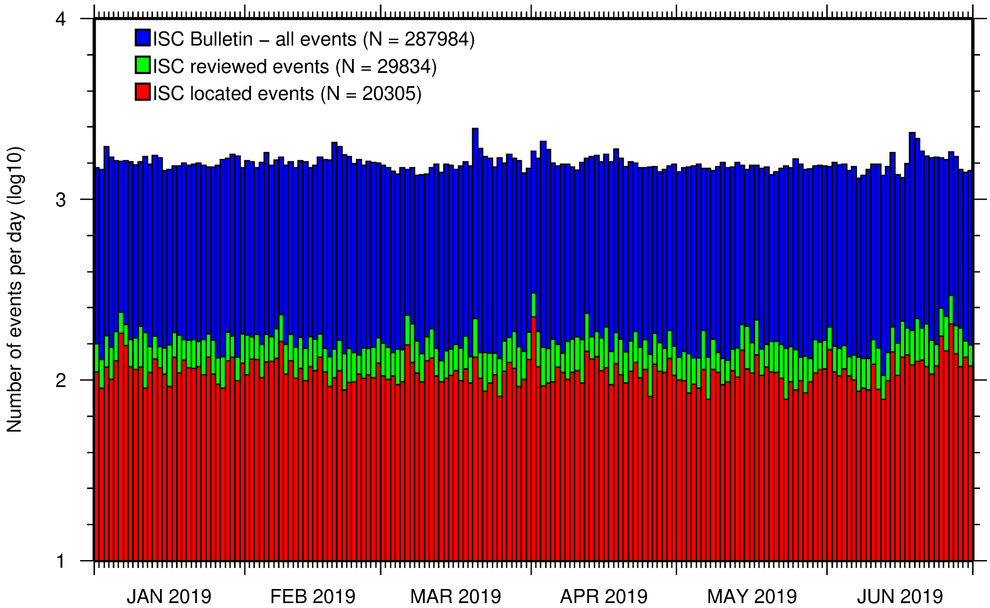

Figure 8.1: *Histogram showing the number of events in the ISC Bulletin for the current summary period. The vertical scale is logarithmic.*

Figure 8.7 shows the depth distribution of fixed-depth solutions in the ISC Bulletin. Except for a fraction of events whose depth is fixed to a shallow depth, this set comprises mostly ISC-located events. If there is no resolution for depth in the data, the ISC locator fixes the depth to a value obtained from the ISC default depth grid file, or if no default depth exists for that location, to a nominal default depth assigned to each Flinn-Engdahl region (see details in Section 10.1.4). During the ISC review editors are inclined to accept the depth obtained from the default depth grid, but they typically change the depth of those solutions that have a nominal (10 or 35 km) depth. When doing so, they usually fix the depth to a round number, preferably divisible by 50.

For events selected for ISC location, the number of stations typically increases as arrival data reported by several agencies are grouped together and associated to the prime hypocentre. Consequently, the network geometry, characterised by the secondary azimuthal gap (the largest azimuthal gap a single station closes), is typically improved. Figure 8.8 illustrates that the secondary azimuthal gap is indeed generally smaller for ISC-located events than that for all events in the ISC Bulletin. Figure 8.9 shows the distribution of the number of associated stations. For large events the number of associated stations is usually larger for ISC-located events than for any of the reported event bulletins. On the other hand, events with just a few reporting stations are rarely selected for ISC location. The same is true for the number of defining stations (stations with at least one defining phase that were used in the location). Figure 8.10 indicates that because the reported observations from multiple agencies are associated to the prime, large ISC-located events typically have a larger number of defining stations than any of the reported event bulletins.

The formal uncertainty estimates are also typically smaller for ISC-located events. Figure 8.11 shows the distribution of the area of the 90% confidence error ellipse for ISC-located events during the summary period. The distribution suffers from a long tail indicating a few poorly constrained event locations. Nevertheless, half of the events are characterised by an error ellipse with an area less than 190 km^2, 90% of the events have an error ellipse area less than 1412 km^2, and 95% of the events have an error ellipse

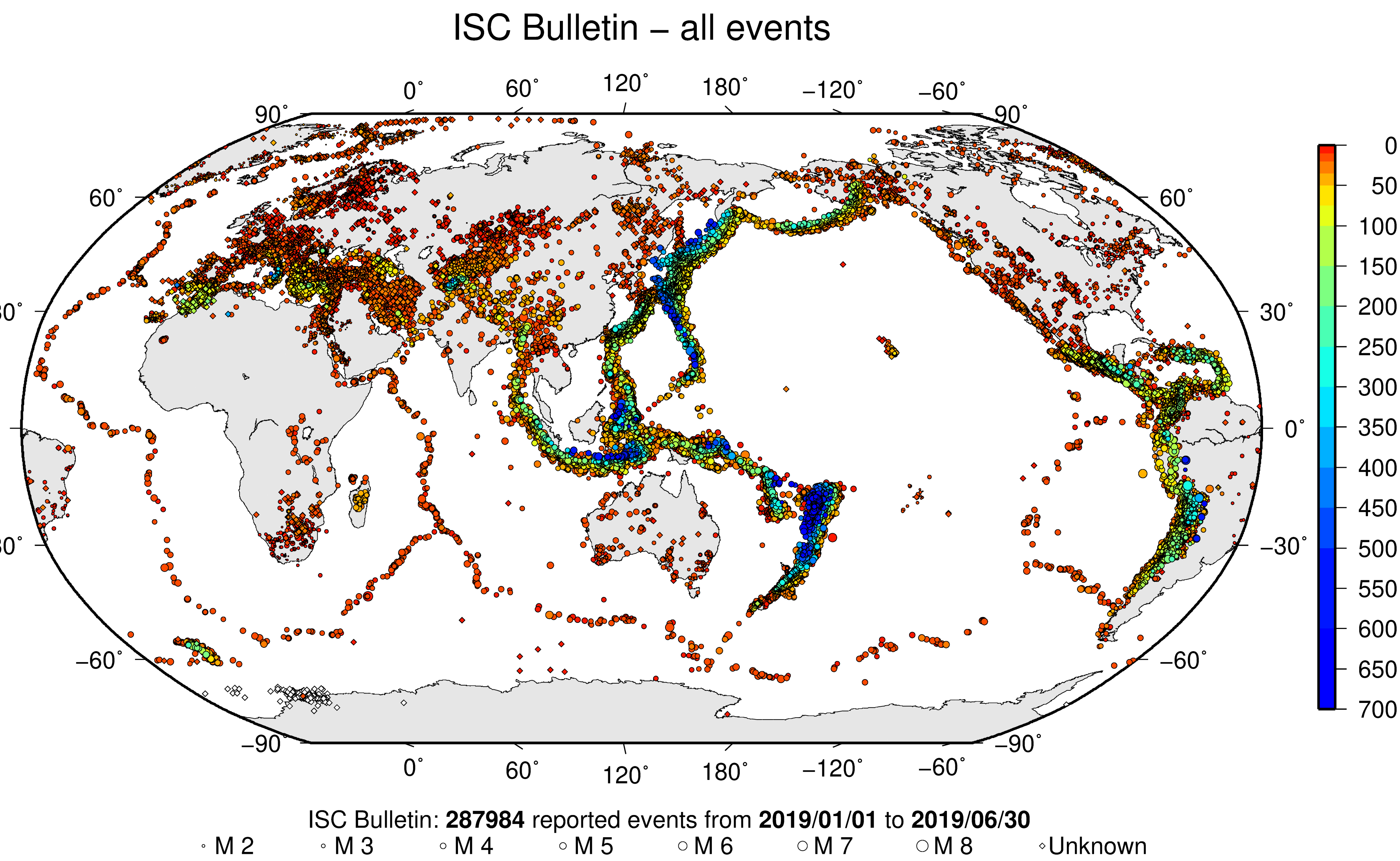

Figure 8.2: *Map of all events in the ISC Bulletin. Prime hypocentre locations are shown. Compare with Figure 7.10.*

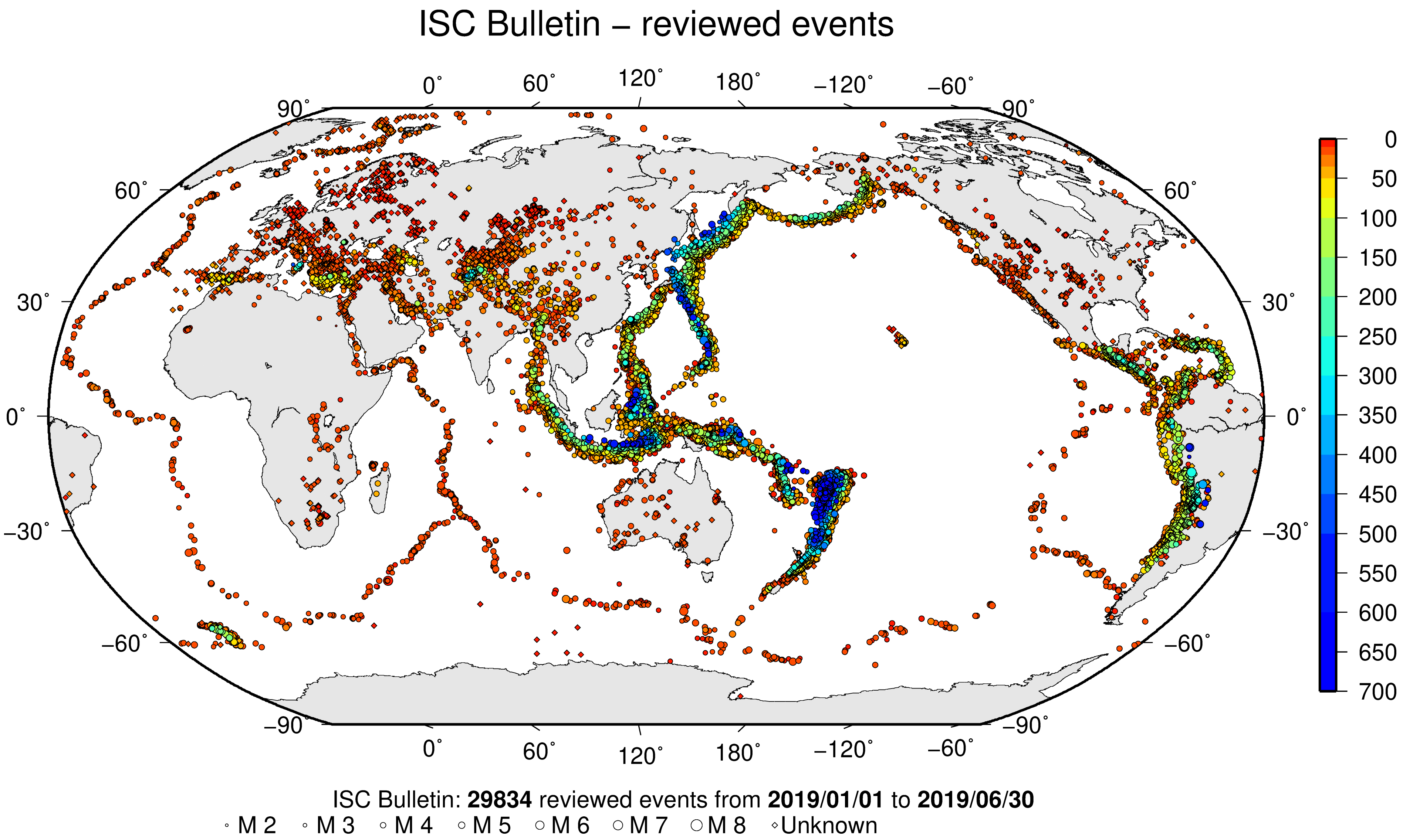

Figure 8.3: *Map of all events reviewed by the ISC for this time period. Prime hypocentre locations are shown.*

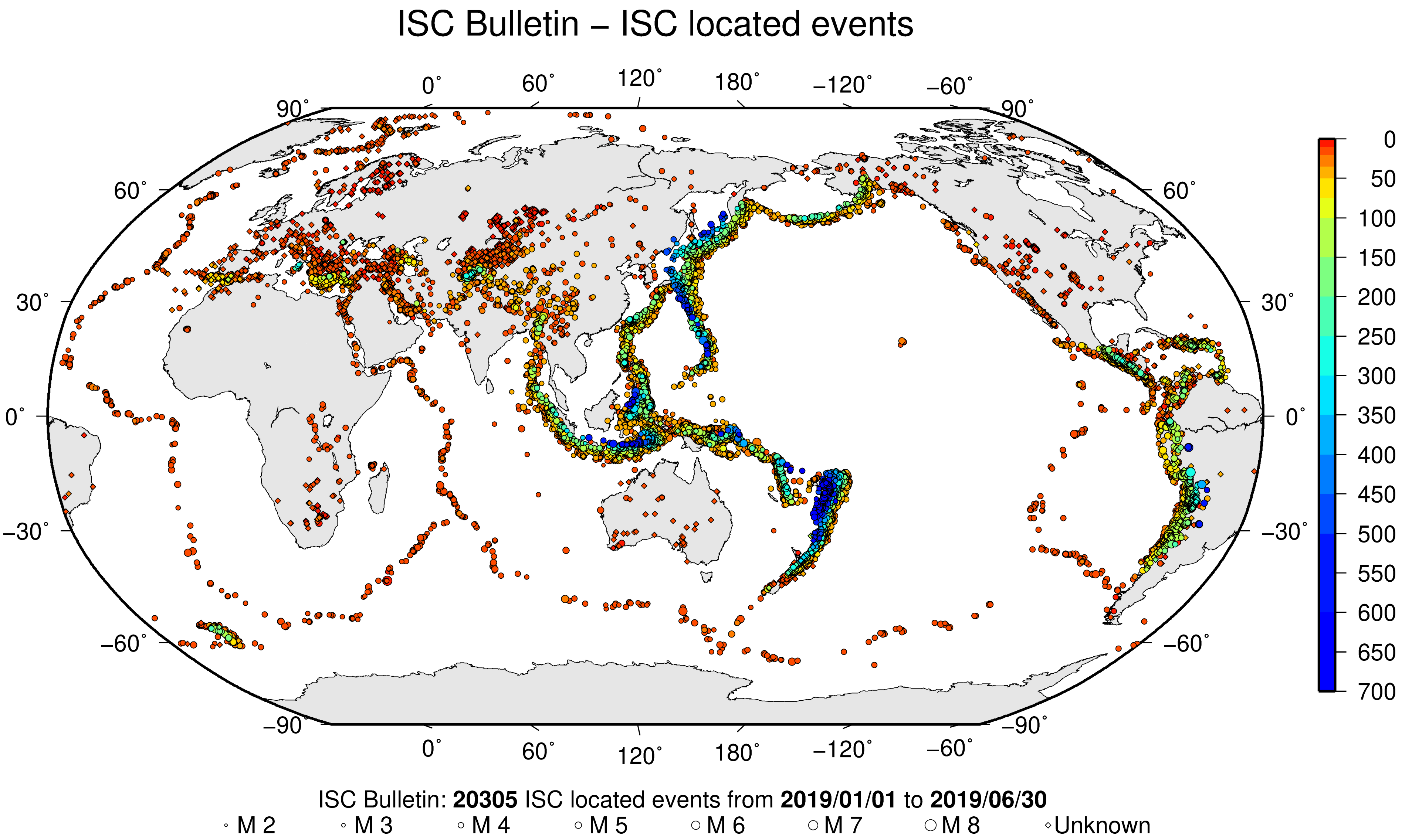

Figure 8.4: *Map of all events located by the ISC for this time period. ISC determined hypocentre locations are shown.*

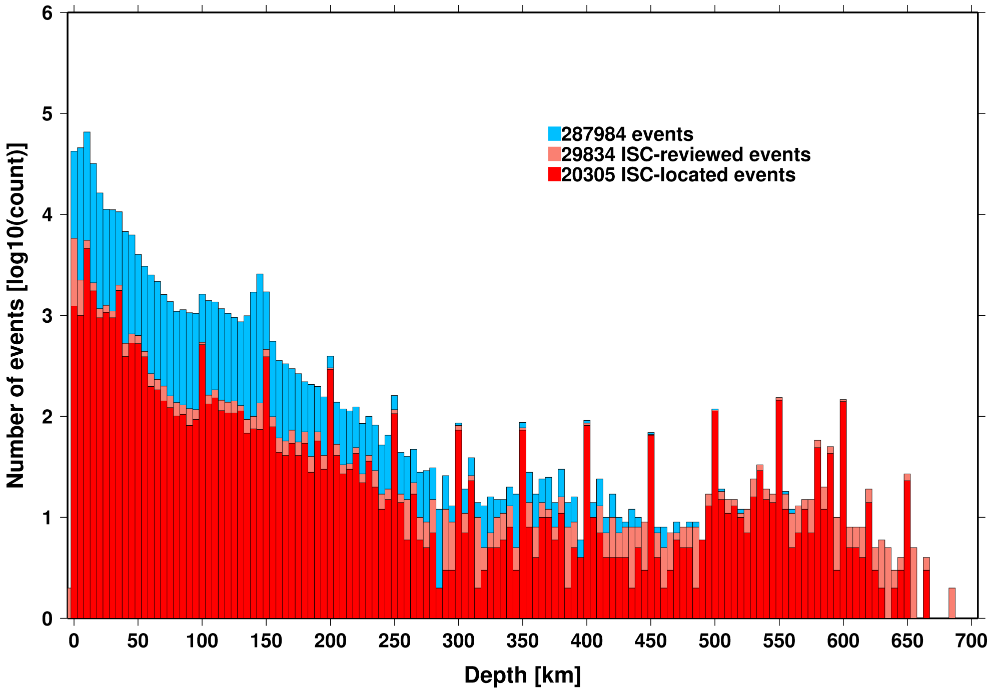

Figure 8.5: *Distribution of event depths in the ISC Bulletin (blue) and for the ISC-reviewed (pink) and the ISC-located (red) events during the summary period. All ISC-located events are reviewed, but not all reviewed events are located by the ISC. The vertical scale is logarithmic.*

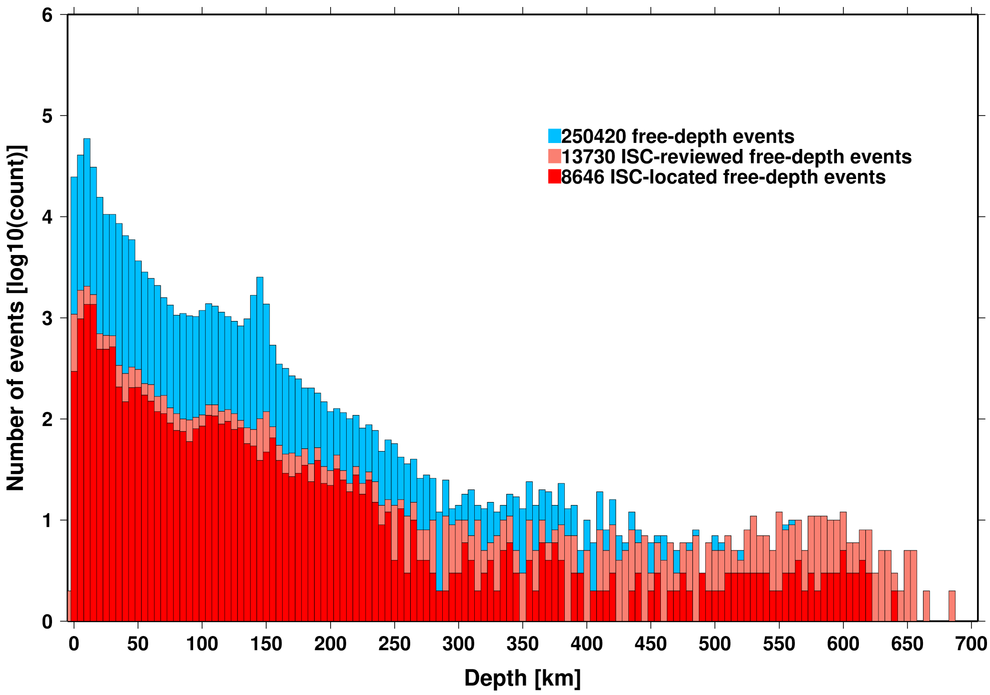

Figure 8.6: *Hypocentral depth distribution of events where the prime hypocentres are reported/located with a free-depth solution in the ISC Bulletin. The vertical scale is logarithmic.*

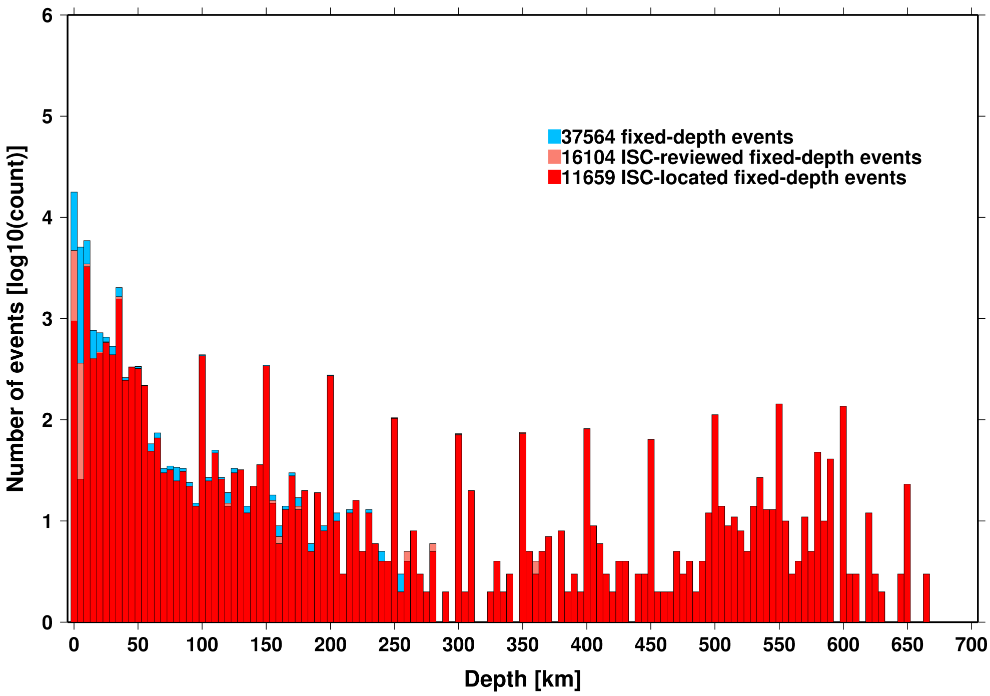

Figure 8.7: *Hypocentral depth distribution of events where the prime hypocentres are reported/located with a fixed-depth solution in the ISC Bulletin. The vertical scale is logarithmic.*

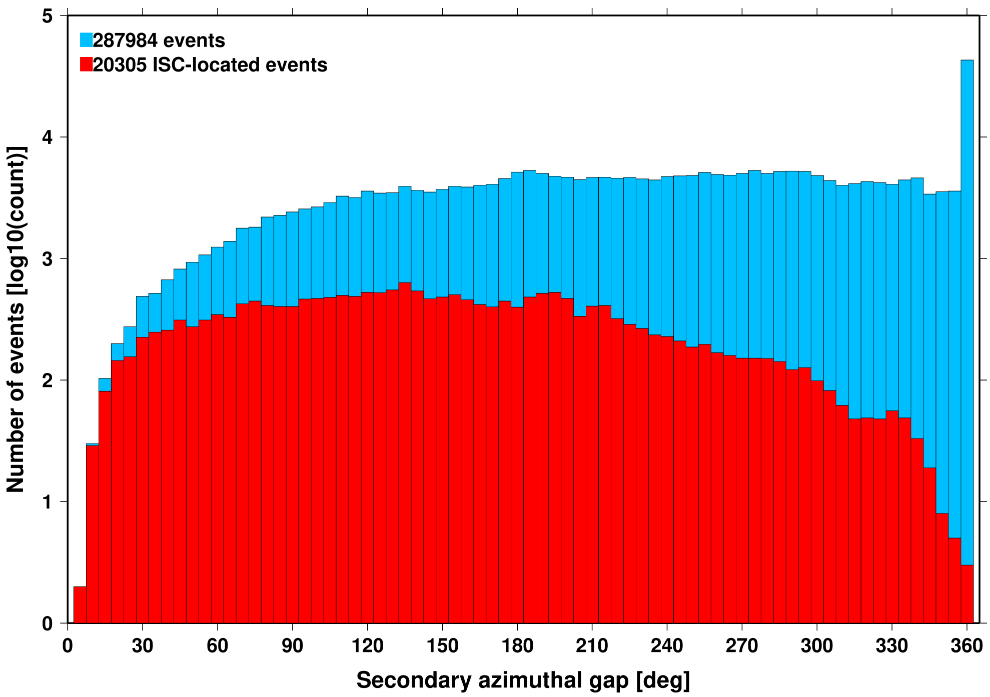

Figure 8.8: *Distribution of secondary azimuthal gap for events in the ISC Bulletin (blue) and those selected for ISC location (red). The vertical scale is logarithmic.*

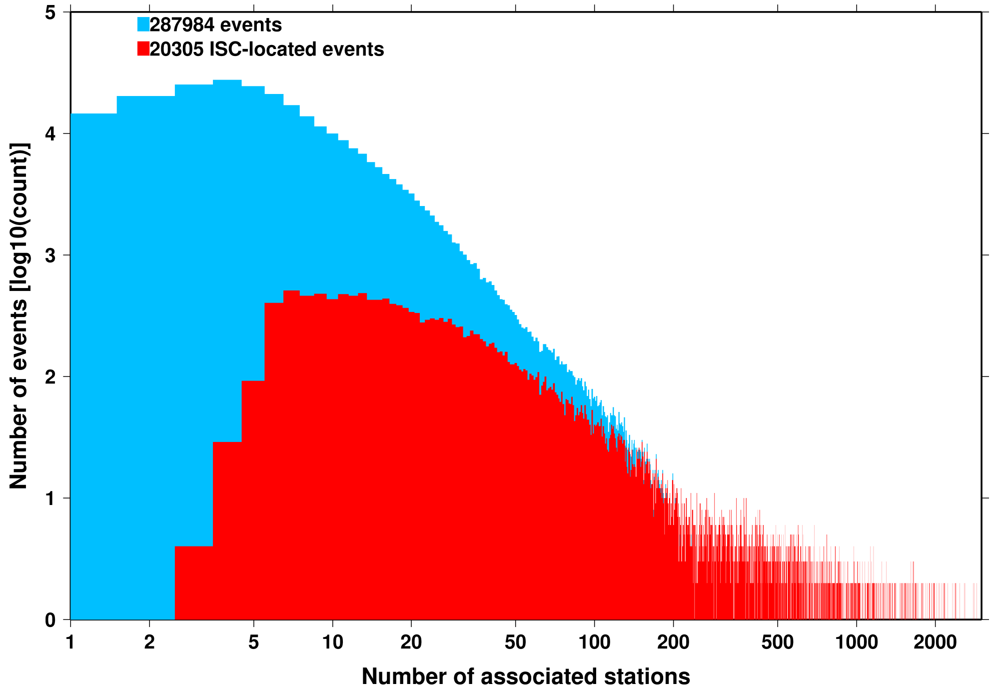

Figure 8.9: *Distribution of the number of associated stations for events in the ISC Bulletin (blue) and those selected for ISC location (red). The vertical scale is logarithmic.*

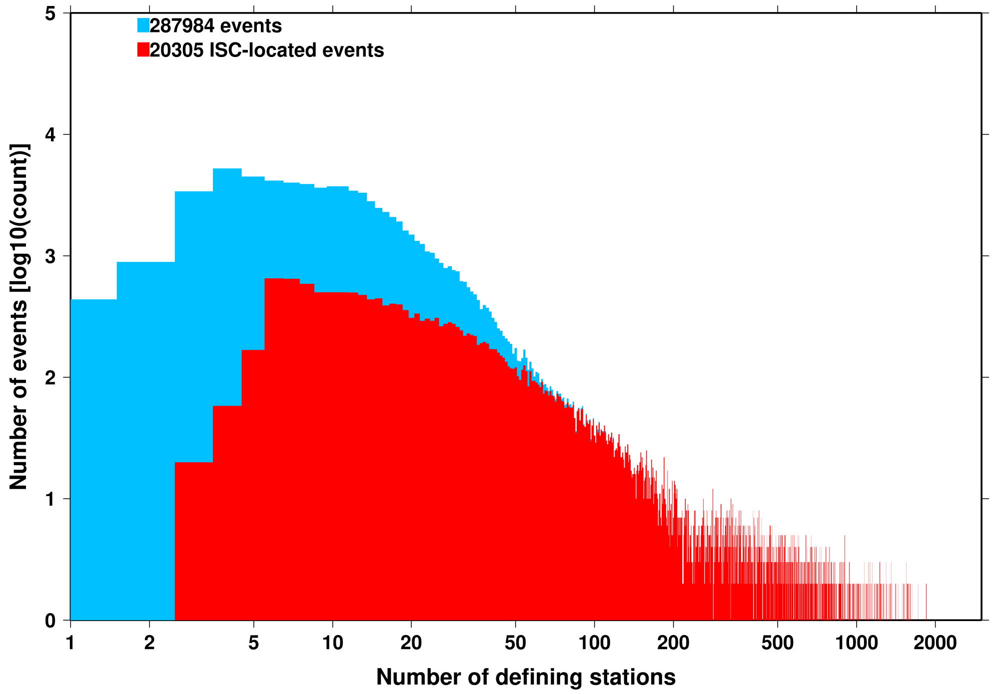

Figure 8.10: *Distribution of the number of defining stations for events in the ISC Bulletin (blue) and those selected for ISC location (red). The vertical scale is logarithmic.*

area less than 2523 km^2.

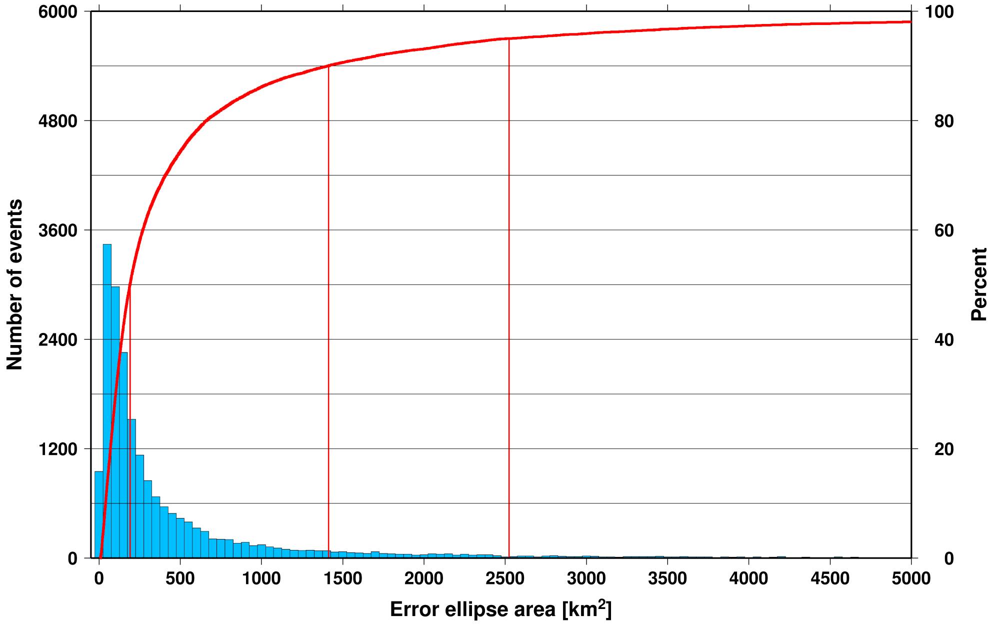

Figure 8.11: *Distribution of the area of the 90% confidence error ellipse of the ISC-located events. Vertical red lines indicate the 50th, 90th and 95th percentile values.*

Figure 8.12 shows one of the major characteristic features of the ISC location algorithm (Bondár and Storchak, 2011). Because the ISC locator accounts for correlated travel-time prediction errors due to unmodelled velocity heterogeneities along similar ray paths, the area of the 90% confidence error ellipse does not decrease indefinitely with increasing number of stations, but levels off once the information carried by the network geometry is exhausted, thus providing more realistic uncertainty estimates.

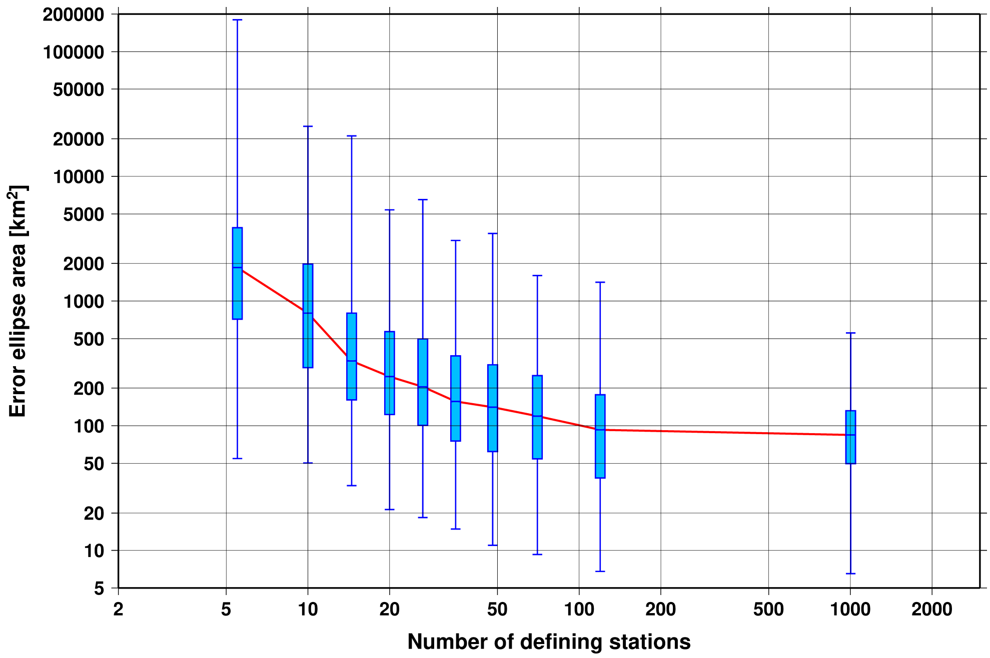

Figure 8.12: *Box-and-whisker plot of the area of the 90% confidence error ellipse of the ISC-located events as a function of the number of defining stations. Each box represents one-tenth-worth of the total number of data. The red line indicates the median 90% confidence error ellipse area.*

8.2 Seismic Phases and Travel-Time Residuals

The number of phases that are associated to events over the summary period in the ISC Bulletin is shown in Figure 8.13. Phase types and their total number in the ISC Bulletin is shown in the Appendix, Table 10.3. A summary of phase types is indicated in Figure 8.14.

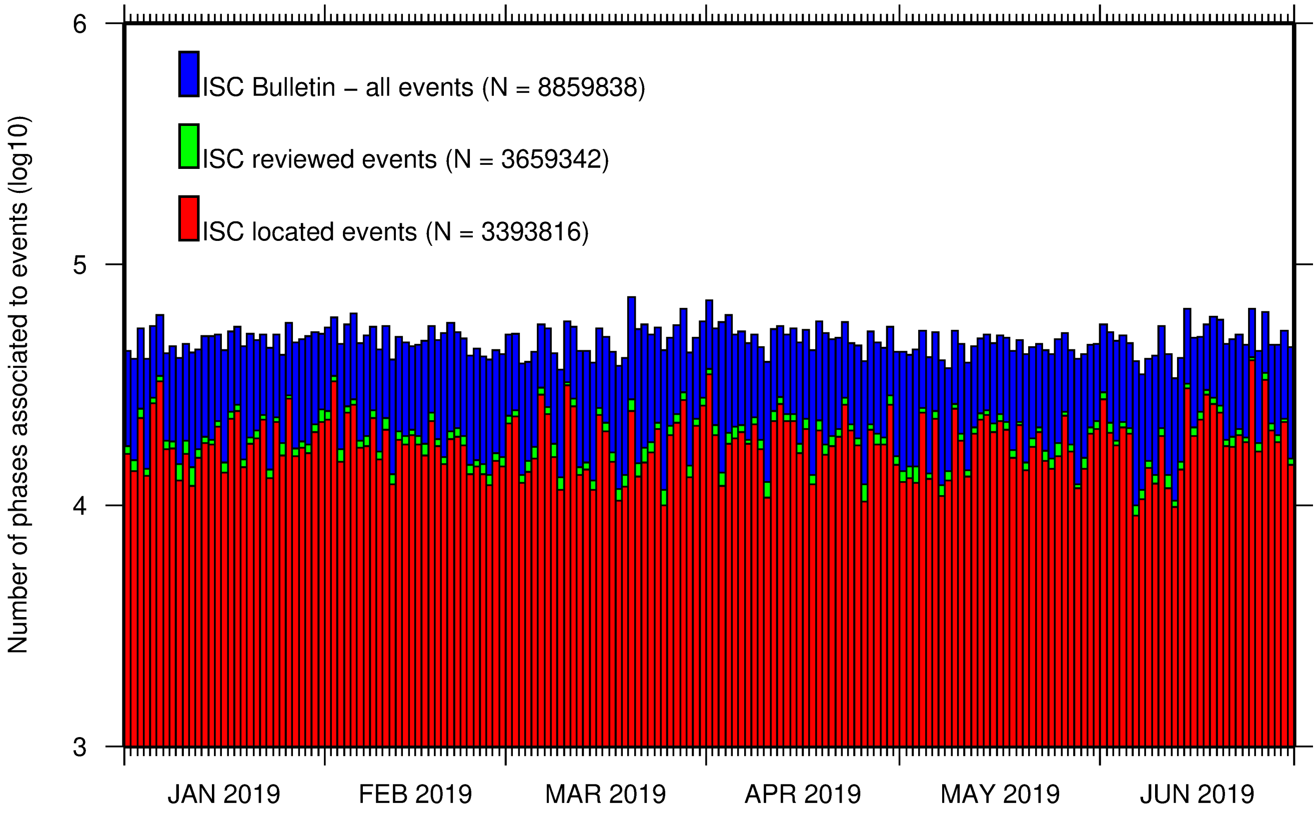

Figure 8.13: *Histogram showing the number of phases (N) that the ISC has associated to events within the ISC Bulletin for the current summary period.*

In computing ISC locations, the current (for events since 2009) ISC location algorithm (*Bondár and Storchak*, 2011) uses all *ak135* phases where possible. Within the Bulletin, the phases that contribute to an ISC location are labelled as *time defining*. In this section, we summarise these time defining phases.

In Figure 8.15, the number of defining phases is shown in a histogram over the summary period. Each defining phase is listed in Table 8.1, which also provides a summary of the number of defining phases per event. A pie chart showing the proportion of defining phases is shown in Figure 8.16. Figure 8.17 shows travel times of seismic waves. The distribution of residuals for these defining phases is shown for the top five phases in Figures 8.18 through 8.22.

Table 8.1: *Numbers of 'time defining' phases (N) within the ISC Bulletin for 20305 ISC located events.*

Phase	Number of 'defining' phases	Number of events	Max per event	Median per event
P	976198	13696	2241	14
Pn	600282	18465	847	16
Sn	196206	15697	272	6
Pb	90320	8072	112	6
Pg	64550	6273	197	6
Sb	56471	7612	108	4
PKPdf	55343	4324	942	2
S	49474	3636	525	3

Table 8.1: *(continued)*

Phase	Number of 'defining' phases	Number of events	Max per event	Median per event
Sg	48274	5759	124	5
PKiKP	30526	3286	556	2
PKPbc	24221	3441	222	2
PKPab	16915	2664	195	2
PcP	13987	3802	75	2
Pdif	11527	1124	471	2
PP	10234	1113	289	2
pP	9971	1400	246	3
SS	4839	1084	67	2
ScP	4323	1145	128	2
SKSac	4171	472	124	2
sP	3628	1082	55	2
PKKPbc	2473	471	85	2
pwP	1598	567	55	2
PnPn	1165	584	11	1
ScS	1154	314	27	2
SnSn	1095	571	10	1
pPKPdf	1048	324	47	1
SKPbc	934	307	18	2
sS	764	415	10	1
P'P'df	686	183	25	2
SKiKP	632	293	28	1
PKKPdf	586	246	32	1
PKKPab	583	245	35	1
pPKPbc	431	212	14	1
PS	418	178	32	1
pPKPab	356	143	36	1
SP	304	53	65	2
SKSdf	276	131	41	1
sPKPdf	230	156	9	1
PcS	222	134	7	1
SKKSac	187	99	11	1
sPKPab	185	67	14	1
SKPab	184	110	7	1
SKPdf	137	57	20	1
SKKPbc	132	47	11	2
Sdif	126	59	29	1
PnS	107	84	5	1
pPKiKP	98	44	16	1
sPKPbc	95	70	5	1
PKSdf	88	39	9	1
pS	86	79	3	1
pPdif	64	36	5	1
SKKSdf	44	42	2	1
P'P'bc	15	10	2	2
SKKPab	13	11	2	1
SPn	11	8	4	1
SKKPdf	7	7	1	1
PbPb	7	5	2	1
sPKiKP	6	6	1	1
sPdif	5	5	1	1
sSKSac	5	3	3	1
P'P'ab	5	5	1	1
SbSb	3	3	1	1
sPn	3	3	1	1
pPn	3	1	3	3
S'S'ac	2	2	1	1
PKKSbc	1	1	1	1
PKSab	1	1	1	1
sSdif	1	1	1	1
SgSg	1	1	1	1

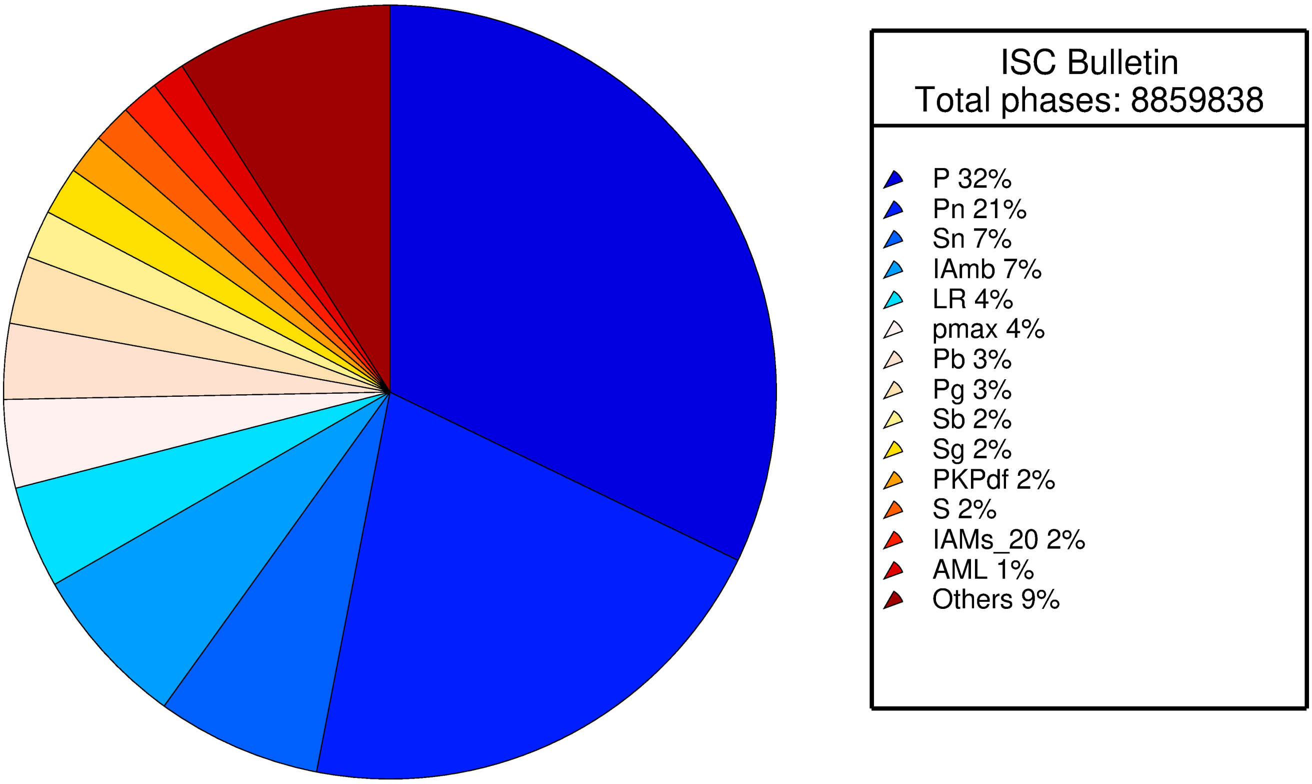

Figure 8.14: *Pie chart showing the fraction of various phase types in the ISC Bulletin for this summary period.*

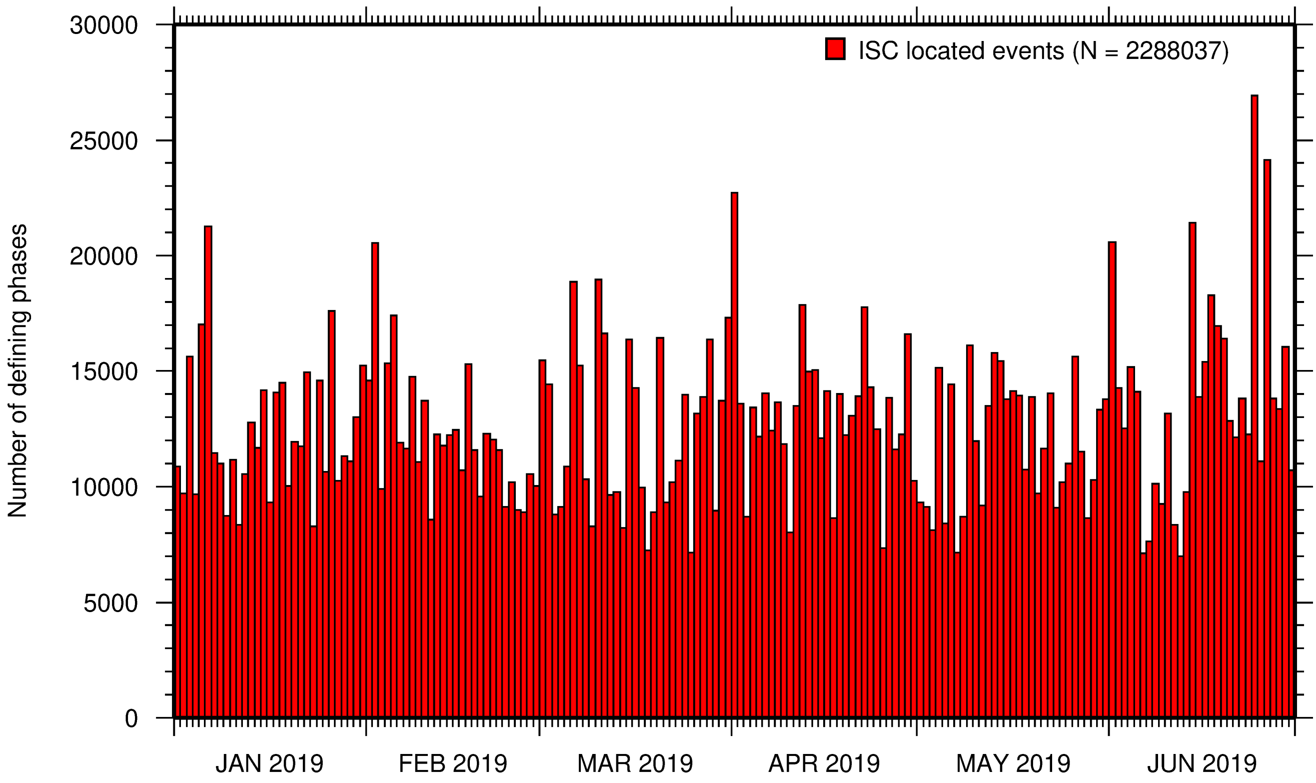

Figure 8.15: *Histogram showing the number of defining phases in the ISC Bulletin, for events located by the ISC.*

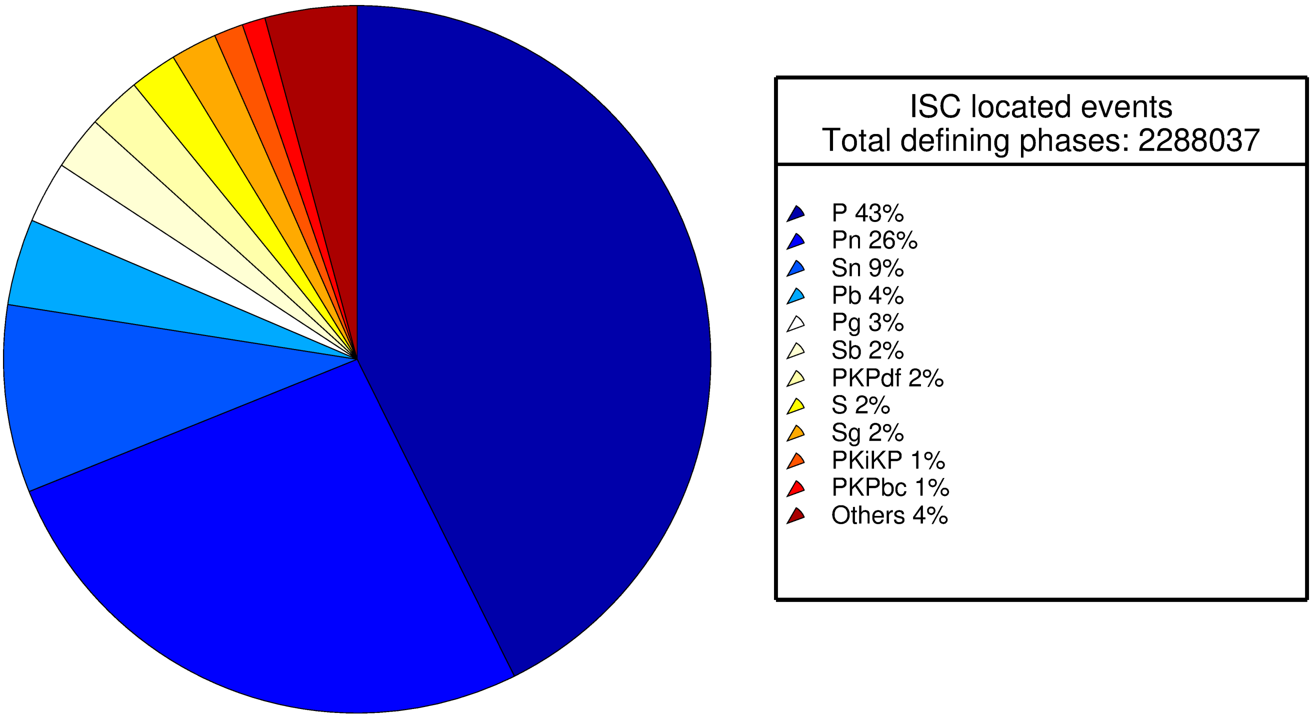

Figure 8.16: *Pie chart showing the defining phases in the ISC Bulletin, for events located by the ISC. A complete list of defining phases is shown in Table 8.1.*

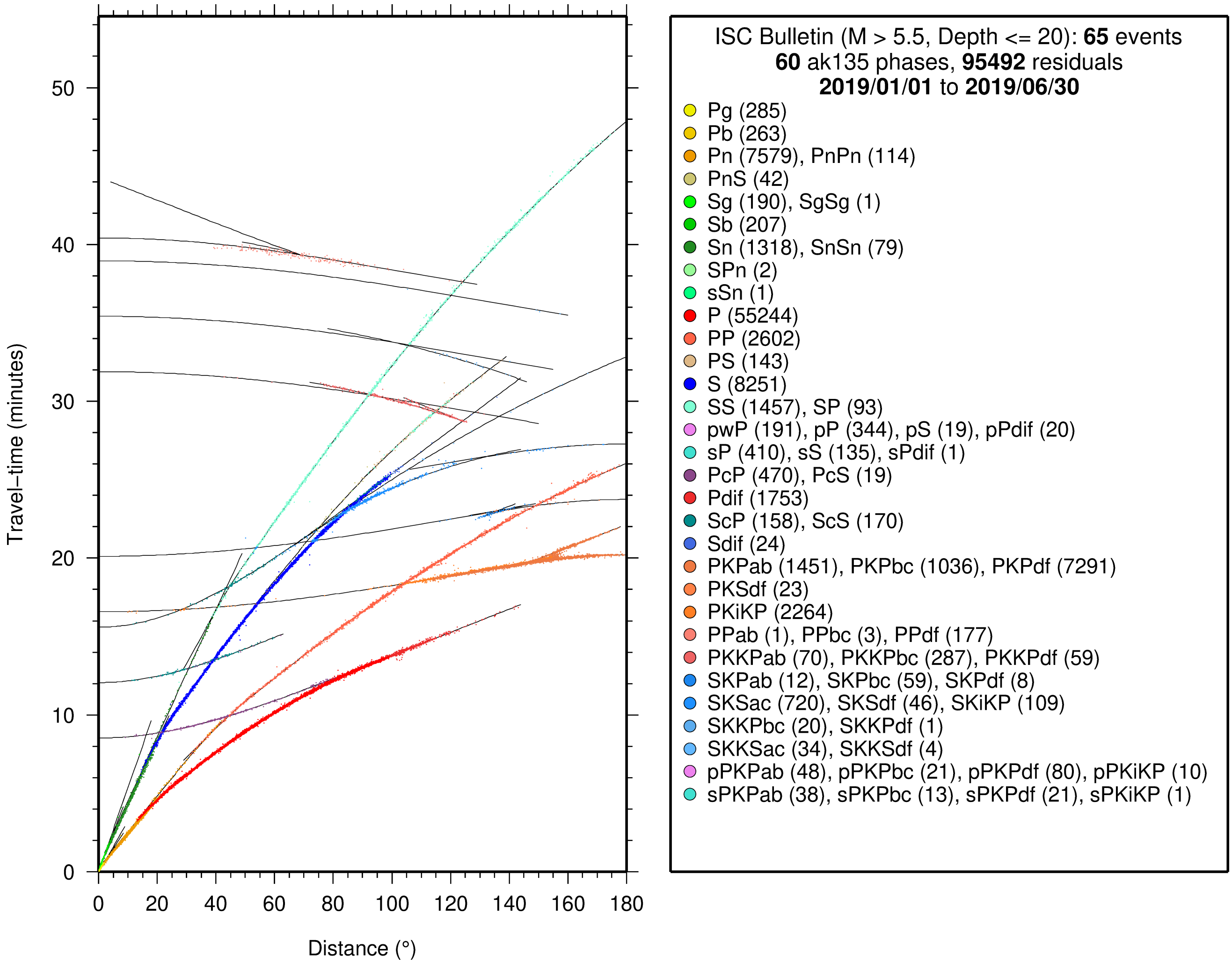

Figure 8.17: *Distribution of travel-time observations in the ISC Bulletin for events with M > 5.5 and depth less than 20 km. The travel-time observations are shown relative to a 0 km source and compared with the theoretical ak135 travel-time curves (solid lines). The legend lists the number of each phase plotted.*

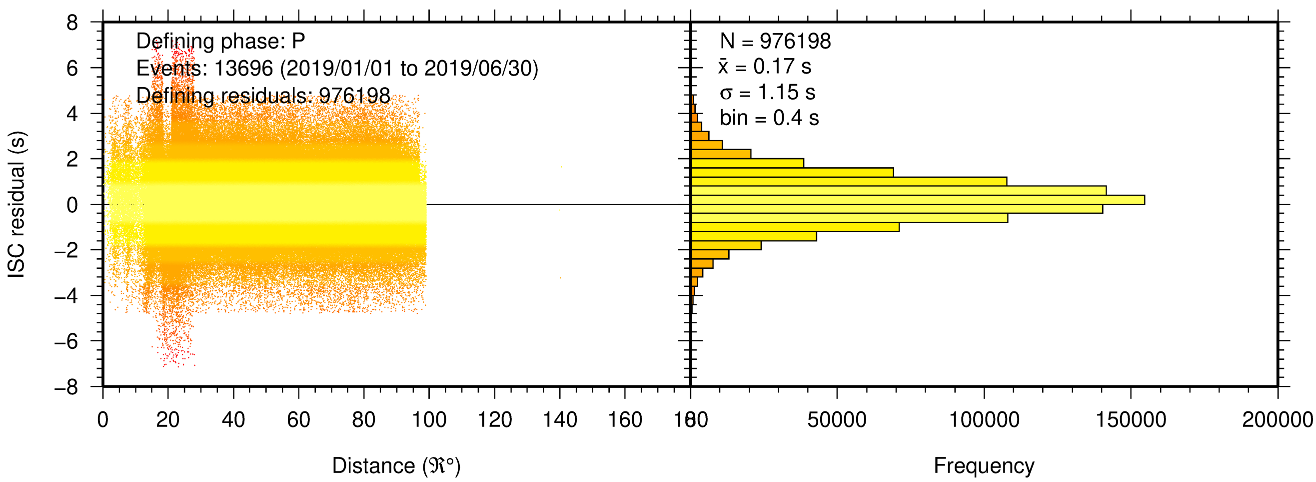

Figure 8.18: *Distribution of travel-time residuals for the defining P phases used in the computation of ISC located events in the Bulletin.*

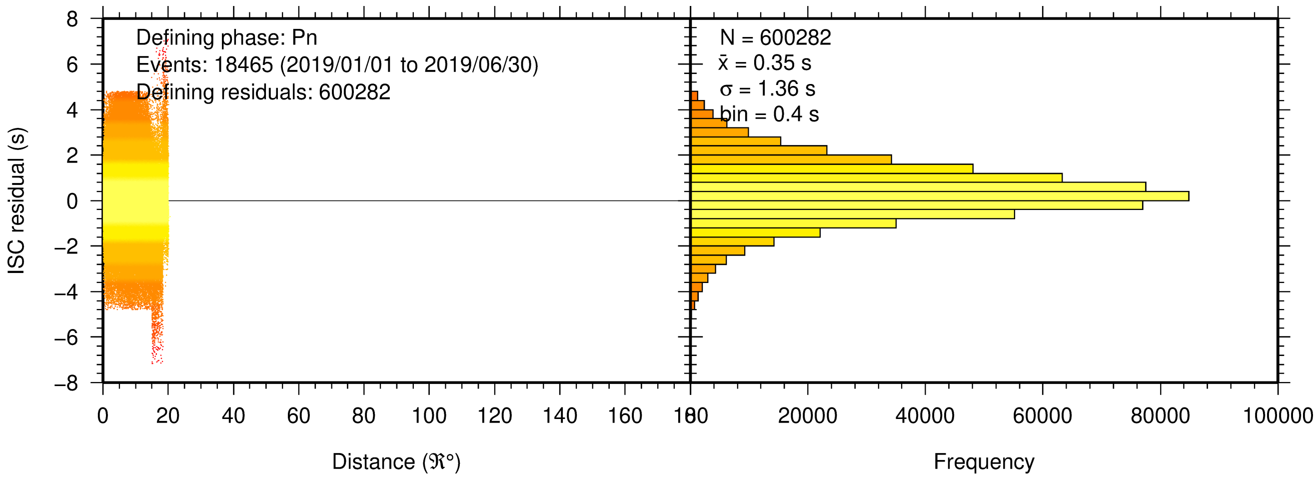

Figure 8.19: *Distribution of travel-time residuals for the defining Pn phases used in the computation of ISC located events in the Bulletin.*

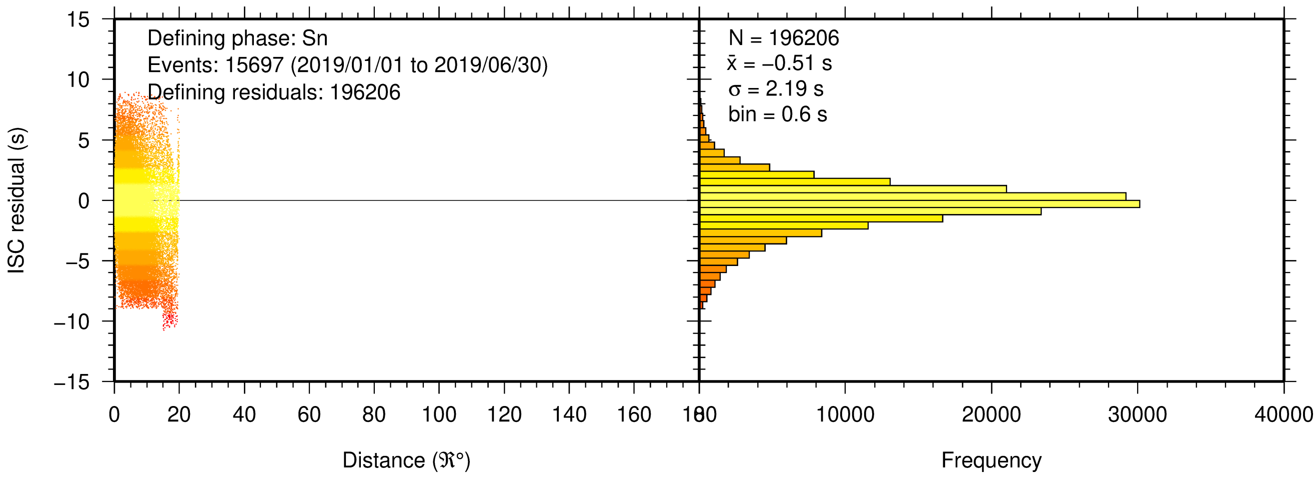

Figure 8.20: *Distribution of travel-time residuals for the defining Sn phases used in the computation of ISC located events in the Bulletin.*

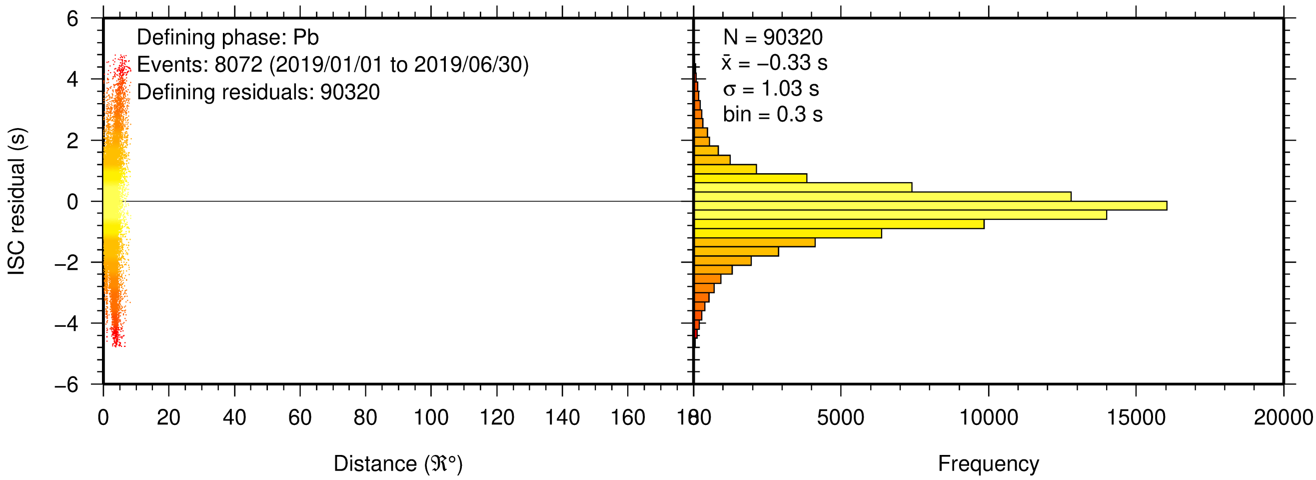

Figure 8.21: *Distribution of travel-time residuals for the defining Pb phases used in the computation of ISC located events in the Bulletin.*

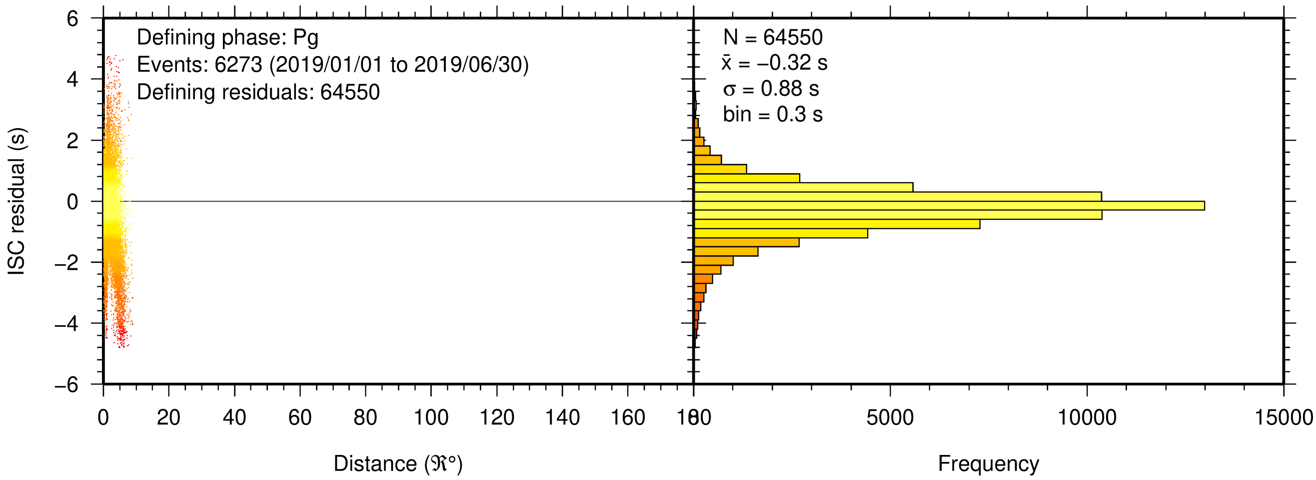

__Figure 8.22:__ Distribution of travel-time residuals for the defining Pg phases used in the computation of ISC located events in the Bulletin.

8.3 Seismic Wave Amplitudes and Periods

The ISC Bulletin contains a variety of seismic wave amplitudes and periods measured by reporting agencies. For this Bulletin Summary, the total of collected amplitudes and periods is 3481796 (see Section 7.3). For the determination of the ISC magnitudes MS and mb, only a fraction of such data can be used. Indeed, the ISC network magnitudes are computed only for ISC located events. Here we recall the main features of the ISC procedure for MS and mb computation (see detailed description in Section 10.1.4). For each amplitude-period pair in a reading the ISC algorithm computes the magnitude (a reading can include several amplitude-period measurements) and the reading magnitude is assigned to the maximum A/T in the reading. If more than one reading magnitude is available for a station, the station magnitude is the median of the reading magnitudes. The network magnitude is computed then as the 20% alpha-trimmed median of the station magnitudes (at least three required). MS is computed for shallow earthquakes (depth $\leq$ 60 km) only and using amplitudes and periods on all three components (when available) if the period is within 10-60 s and the epicentral distance is between 20° and 160°. mb is computed also for deep earthquakes (depth down to 700 km) but only with amplitudes on the vertical component measured at periods $\leq$ 3 s in the distance range 21°-100°.

Table 8.2 is a summary of the amplitude and period data that contributed to the computation of station and ISC MS and mb network magnitudes for this Bulletin Summary.

Table 8.2: *Summary of the amplitude-period data used by the ISC Locator to compute MS and mb.*

	MS	mb
Number of amplitude-period data	165460	476937
Number of readings	145675	472799
Percentage of readings in the ISC located events with qualifying data for magnitude computation	16.2	42.6
Number of station magnitudes	141417	437730
Number of network magnitudes	3493	12444

A small percentage of the readings with qualifying data for MS and mb calculation have more than one amplitude-period pair. Notably, only 16% of the readings for the ISC located (shallow) events included qualifying data for MS computation, whereas for mb the percentage is much higher at 43%. This is due to the seismological practice of reporting agencies. Agencies contributing systematic reports of amplitude and period data are listed in Appendix Table 10.4. Obviously the ISC Bulletin would benefit if more agencies included surface wave amplitude-period data in their reports.

Figure 8.23 shows the distribution of the number of station magnitudes versus distance. For mb there is a significant increase in the distance range 70°-90°, whereas for MS most of the contributing stations are below 100°. The increase in number of station magnitude between 70°-90° for mb is partly due to the very dense distribution of seismic stations in North America and Europe with respect to earthquake occurring in various subduction zones around the Pacific Ocean.

Finally, Figure 8.24 shows the distribution of network MS and mb as well as the median number of stations for magnitude bins of 0.2. Clearly with increasing magnitude the number of events is smaller but with a general tendency of having more stations contributing to the network magnitude.

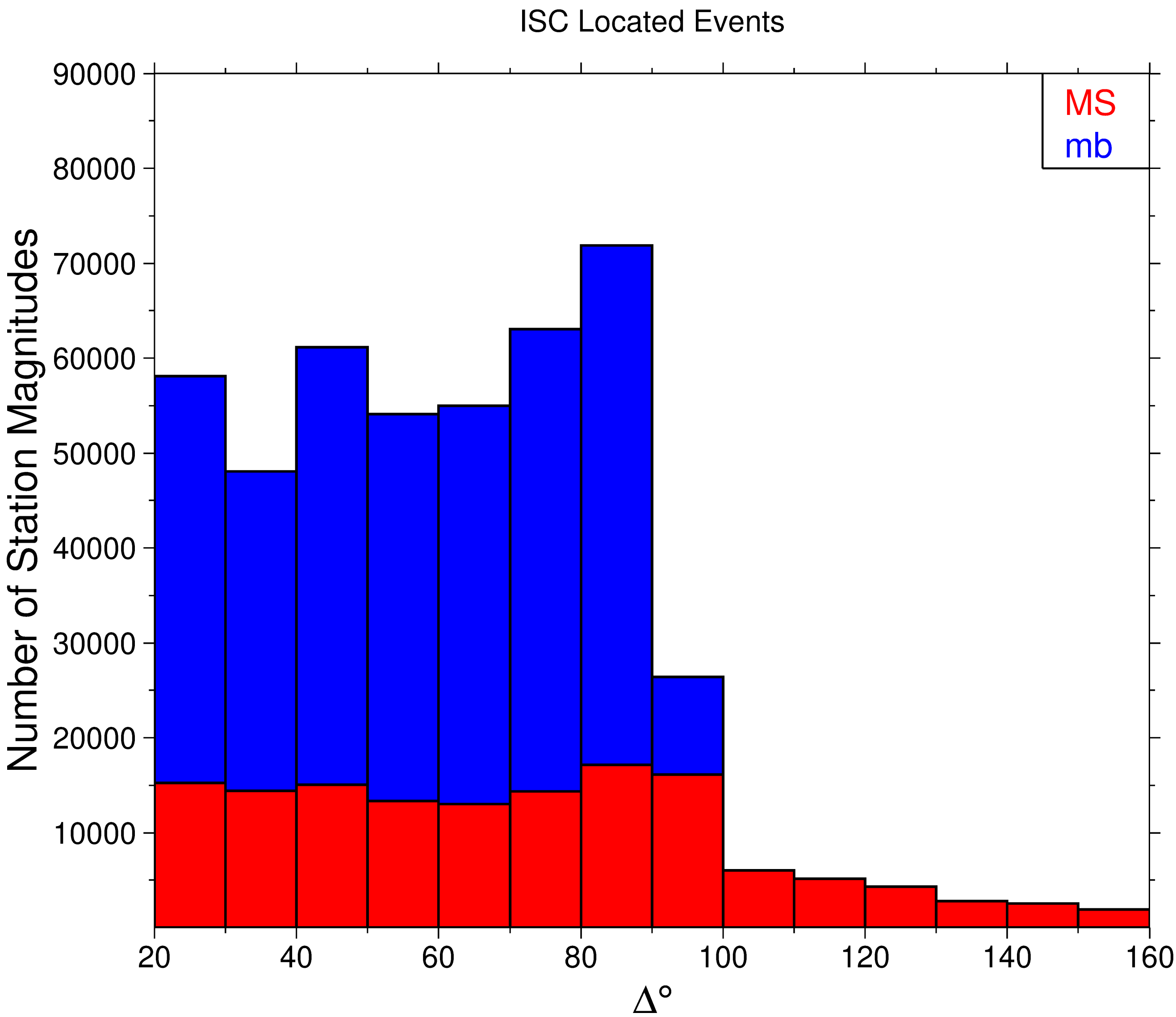

Figure 8.23: *Distribution of the number of station magnitudes computed by the ISC Locator for mb (blue) and MS (red) versus distance.*

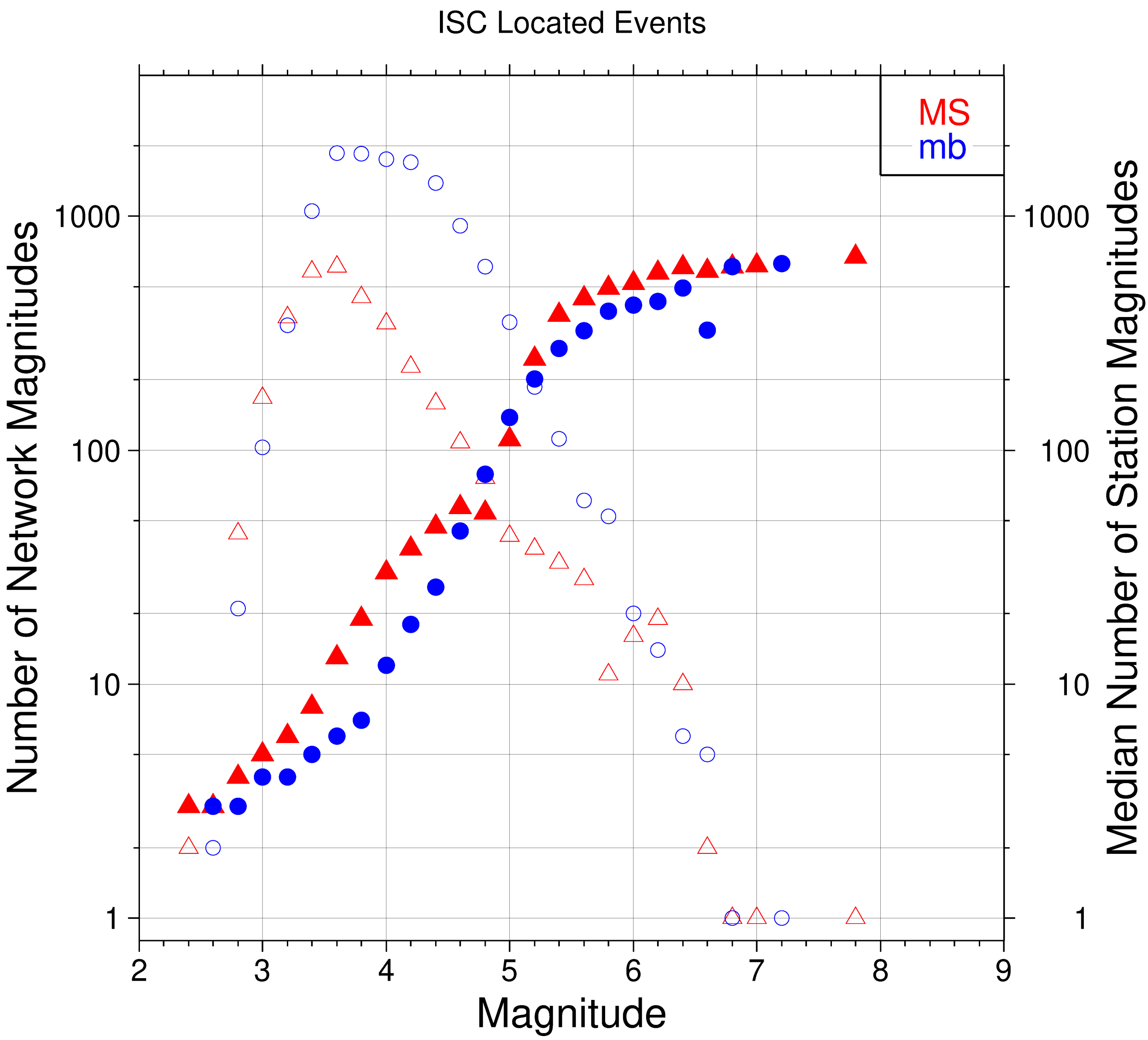

Figure 8.24: *Number of network magnitudes (open symbols) and median number of stations magnitudes (filled symbols). Blue circles refer to mb and red triangles to MS. The width of the magnitude interval δM is 0.2, and each symbol includes data with magnitude in $M \pm \delta M/2$.*

8.4 Completeness of the ISC Bulletin

We define the magnitude of completeness (hereafter M_C) as the lowest magnitude threshold above which all events are believed to be recorded. The Bulletin with events bigger than the defined M_C is assumed to be complete.

Until Issue 53, Volume II (July - December 2016) of the Summary of the ISC an estimation of M_C was computed only with the maximum curvature technique (*Woessner and Wiemer*, 2005). After the completion of the Rebuild Project and relocation of ISC hypocenters from data years 1964 to 2010 (*Storchak et al.*, 2017), the estimate of M_C for the entire ISC Bulletin is re-computed using four catalogue based methodologies (*Adamaki*, 2017, and references therein): the previously used maximum curvature for comparison (maxC), Mc based on the b-value stability (MBS technique), the Goodness of Fit Test with a 90% level of fit (GFT90) and the modified Goodness of Fit Test (mGFT). Further details on each of these methodologies and their statistical behaviour can be found in *Leptokaropoulos et al.* (2018).

The magnitudes of completeness of the ISC Bulletin for this Summary period is shown in Figure 8.25. How M_C varies for the ISC Bulletin over the years is shown in Figure 8.26. The step change in 1996 corresponds with the inclusion of the Prototype IDC (EIDC) Bulletin, followed by the Reviewed Event Bulletin (REB) of the IDC.

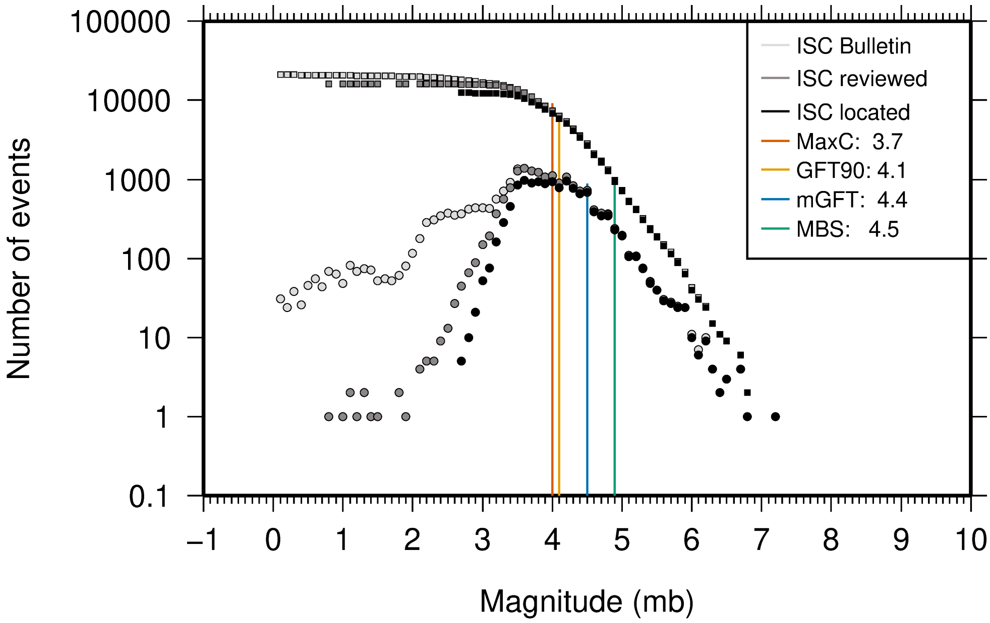

Figure 8.25: *Frequency and cumulative frequency magnitude distribution for all events in the ISC Bulletin, ISC reviewed events and events located by the ISC. The magnitude of completeness (M_C) is shown for the ISC Bulletin. Note: only events with values of mb are represented in the figure.*

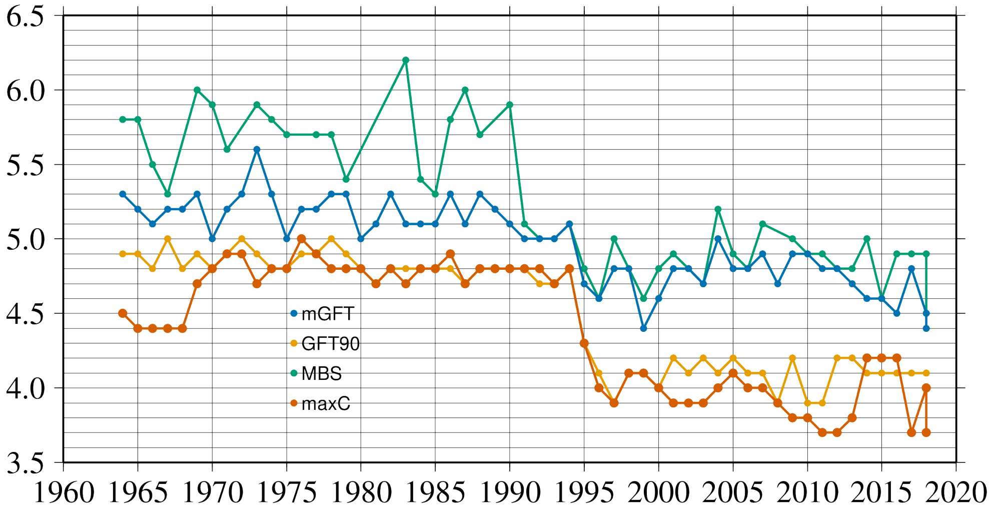

Figure 8.26: *Variation of magnitude of completeness (M_C) for each year in the ISC Bulletin. Note: M_C is calculated only using those events with values of mb.*

8.5 Magnitude Comparisons

The ISC Bulletin publishes network magnitudes reported by multiple agencies to the ISC. For events that have been located by the ISC, where enough amplitude data has been collected, the MS and mb magnitudes are calculated by the ISC (MS is computed only for depths $\leq$ 60 km). In this section, ISC magnitudes and some other reported magnitudes in the ISC Bulletin are compared.

The comparison between MS and mb computed by the ISC locator for events in this summary period is shown in Figure 8.27, where the large number of data pairs allows a colour coding of the data density. The scatter in the data reflects the fundamental differences between these magnitude scales.

Similar plots are shown in Figure 8.28 and 8.29, respectively, for comparisons of ISC mb and ISC MS with M_W from the GCMT catalogue. Since M_W is not often available below magnitude 5, these distributions are mostly for larger, global events. Not surprisingly, the scatter between mb and M_W is larger than the scatter between MS and M_W. Also, the saturation effect of mb is clearly visible for earthquakes with $M_W > 6.5$. In contrast, MS scales well with $M_W > 6$, whereas for smaller magnitudes MS appears to be systematically smaller than M_W.

In Figure 8.30 ISC values of mb are compared with all reported values of mb, values of mb reported by NEIC and values of mb reported by IDC. Similarly in Figure 8.31, ISC values of MS are compared with all reported values of MS, values of MS reported by NEIC and values of MS reported by IDC. There is a large scatter between the ISC magnitudes and the mb and MS reported by all other agencies.

The scatter decreases both for mb and MS when ISC magnitudes are compared just with NEIC and IDC magnitudes. This is not surprising as the latter two agencies provide most of the amplitudes and periods used by the ISC locator to compute MS and mb. However, ISC mb appears to be smaller than NEIC mb for $mb < 4$ and larger than IDC mb for $mb > 4$. Since NEIC does not include IDC amplitudes, it seems these features originate from observations at the high-gain, low-noise sites reported by the IDC. For the MS comparisons between ISC and NEIC a similar but smaller effect is observed for $MS < 4.5$, whereas a good scaling is generally observed for the MS comparisons between ISC and IDC.

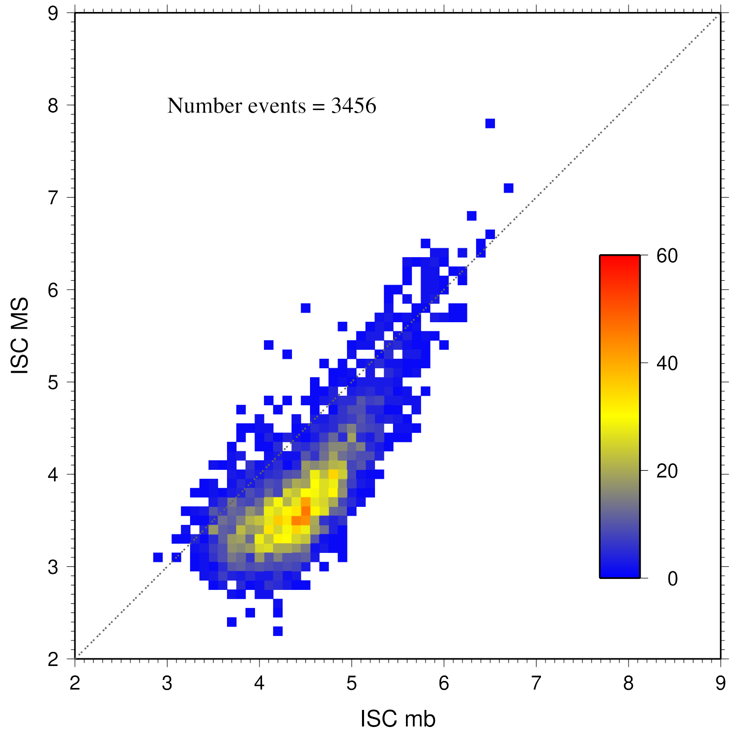

Figure 8.27: *Comparison of ISC values of MS with mb for common event pairs.*

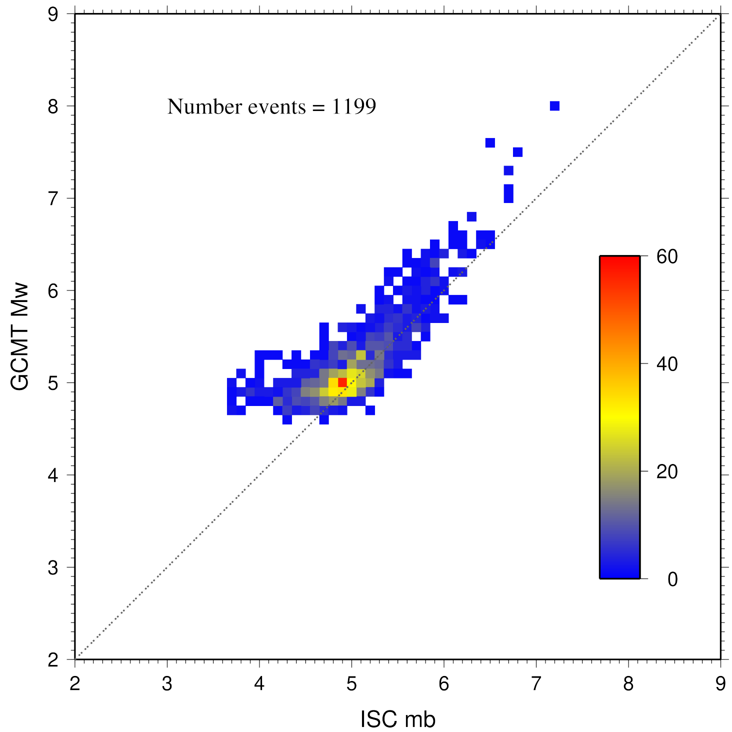

Figure 8.28: *Comparison of ISC values of mb with GCMT* M_W *for common event pairs.*

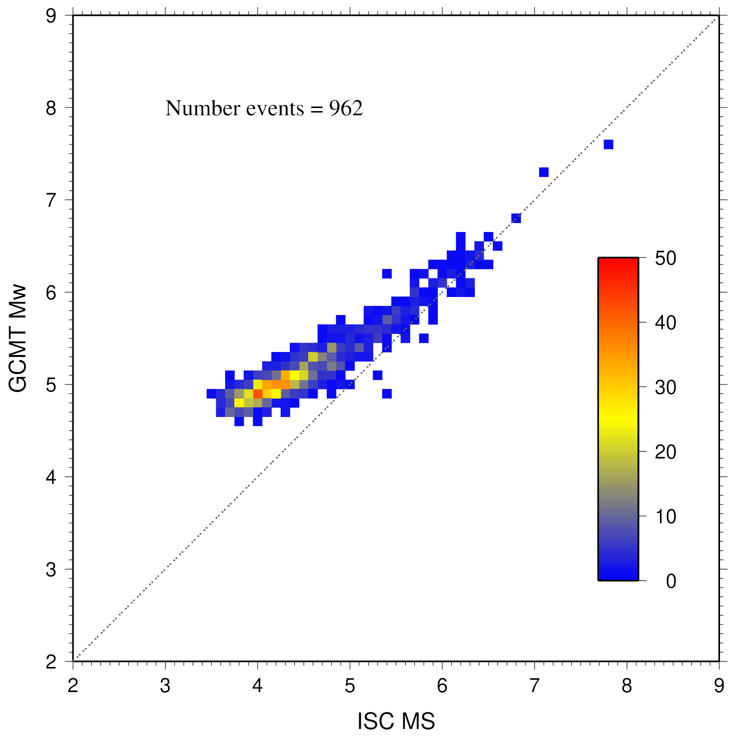

Figure 8.29: *Comparison of ISC values of MS with GCMT M_W for common event pairs.*

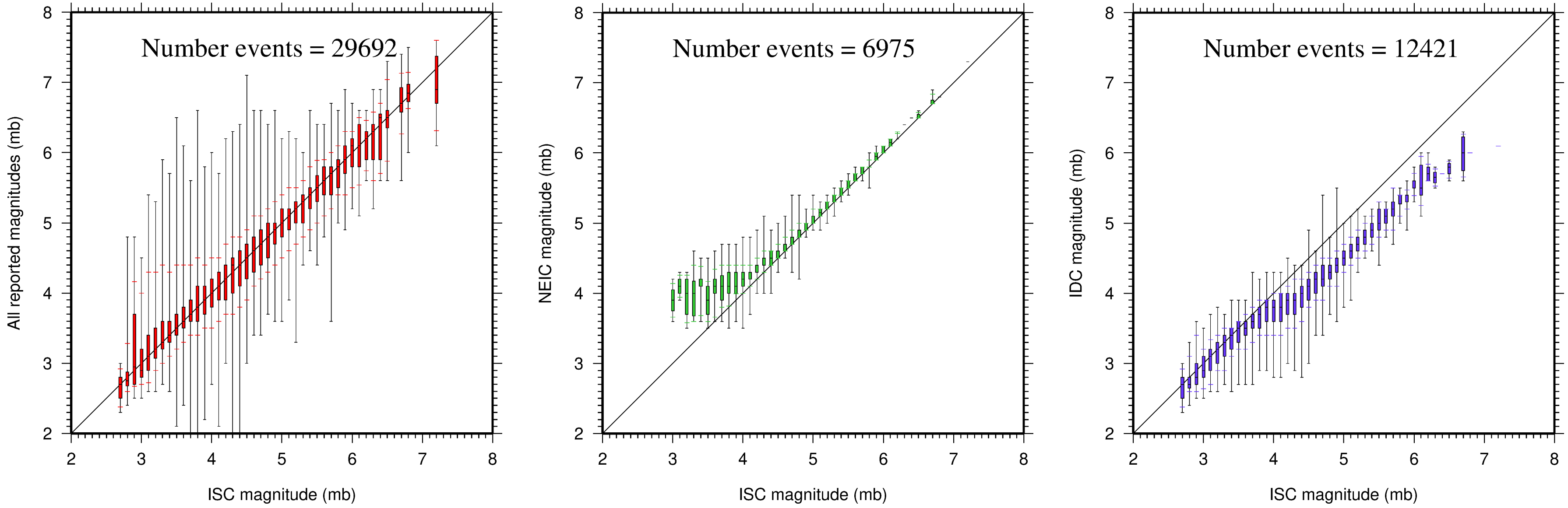

(a) (b) (c)

Figure 8.30: *Comparison of ISC magnitude data (mb) with additional agency magnitudes (mb). The statistical summary is shown in box-and-whisker plots where the 10th and 90th percentiles are shown in addition to the max and min values. (a): All magnitudes reported; (b): NEIC magnitudes; (c): IDC magnitudes.*

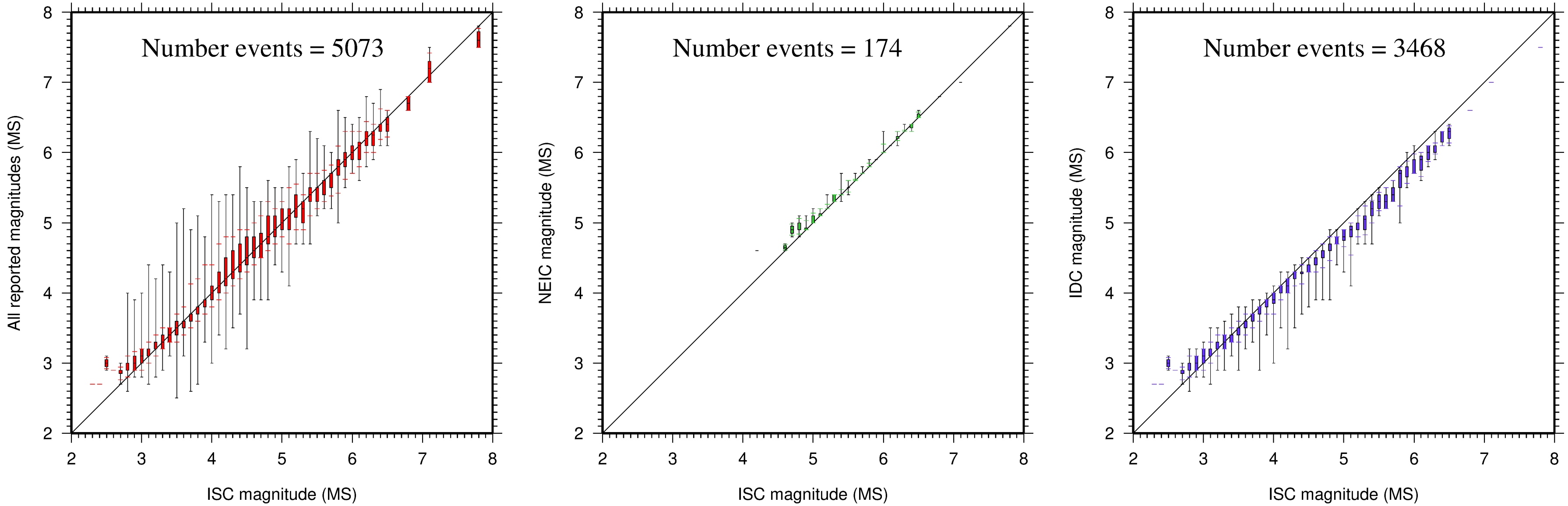

(a) (b) (c)

Figure 8.31: *Comparison of ISC magnitude data (MS) with additional agency magnitudes (MS). The statistical summary is shown in the box-and-whisker plots where the 10th and 90th percentiles are shown in addition to the max and min values. (a): All magnitudes reported; (b): NEIC magnitudes; (c): IDC magnitudes.*

9

The Leading Data Contributors

For the current six-month period, 149 agencies reported related bulletin data. Although we are grateful for every report, we nevertheless would like to acknowledge those agencies that made the most useful or distinct contributions to the contents of the ISC Bulletin. Here we note those agencies that:

- provided a comparatively large volume of parametric data (see Section 9.1),
- reported data that helped quite considerably to improve the quality of the ISC locations or magnitude determinations (see Section 9.2),
- helped the ISC by consistently reporting data in one of the standard recognised formats and in-line with the ISC data collection schedule (see Section 9.3).

We do not aim to discourage those numerous small networks who provide comparatively smaller yet still most essential volumes of regional data regularly, consistently and accurately. Without these reports the ISC Bulletin would not be as comprehensive and complete as it is today.

9.1 The Largest Data Contributors

We acknowledge the contribution of IDC, NEIC, MOS, BJI, GCMT, DJA, NOU, NAO and a few others (Figure 9.1) that reported the majority of moderate to large events recorded at teleseismic distances. The contributions of NEIC, IDC, MEX, DJA and several others are also acknowledged with respect to smaller seismic events. The contributions of JMA, TAP, RSNC, AFAD, ATH and a number of others are also acknowledged with respect to small seismic events. Note that the NEIC bulletin accumulates a contribution of all regional networks in the USA. Several agencies monitoring highly seismic regions routinely report large volumes of small to moderate magnitude events, such as those in Japan, Chinese Taipei, Turkey, Italy, Greece, New Zealand, Mexico and Columbia. Contributions of small magnitude events by agencies in regions of low seismicity, such as Finland are also gratefully received.

We also would like to acknowledge contributions of those agencies that report a large portion of arrival time and amplitude data (Figure 9.2). For small magnitude events, these are local agencies in charge of monitoring local and regional seismicity. For moderate to large events, contributions of IDC, USArray, NEIC, MOS are especially acknowledged. Notably, three agencies (IDC, NEIC and MOS) together reported over 70% of all amplitude measurements made for teleseismically recorded events. We hope that other agencies would also be able to update their monitoring routines in the future to include the amplitude reports for teleseismic events compliant with the IASPEI standards.

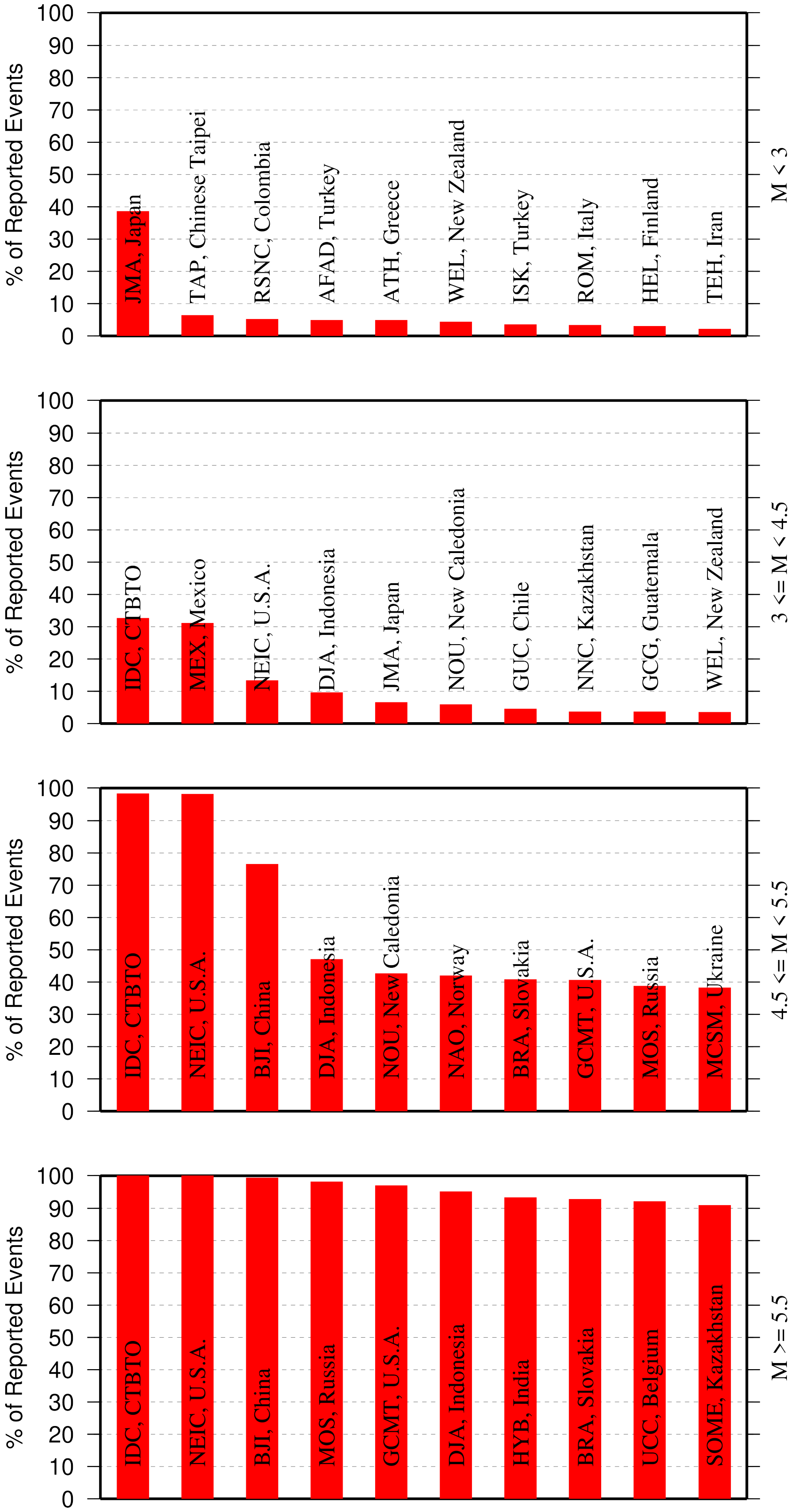

Figure 9.1: *Frequency of events in the ISC Bulletin for which an agency reported at least one item of data: a moment tensor, a hypocentre, a station arrival time or an amplitude. The top ten agencies are shown for four magnitude intervals.*

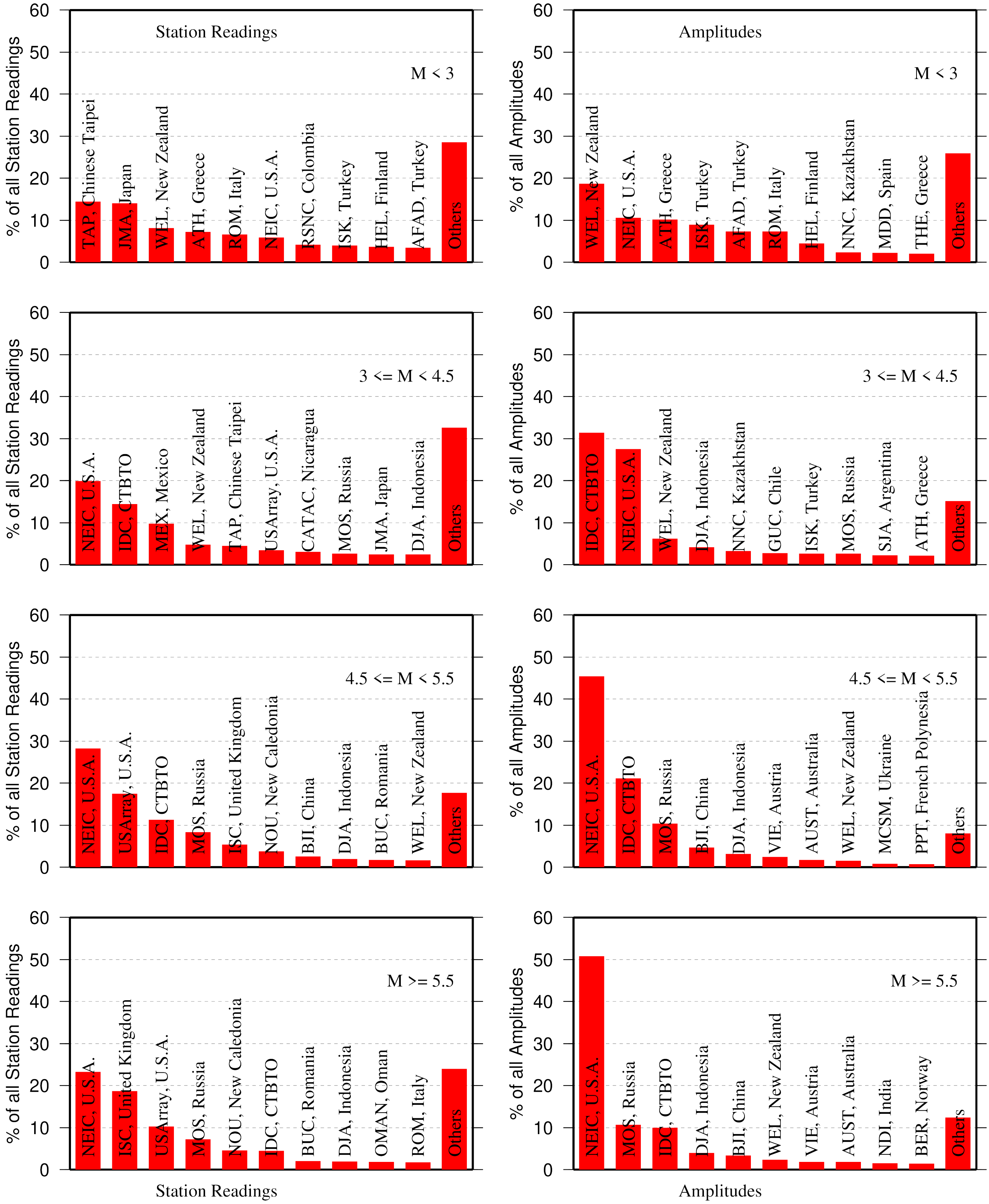

Figure 9.2: *Contributions of station arrival time readings (left) and amplitudes (right) of agencies to the ISC Bulletin. Top ten agencies are shown for four magnitude intervals.*

9.2 Contributors Reporting the Most Valuable Parameters

One of the main ISC duties is to re-calculate hypocentre estimates for those seismic events where a collective wealth of all station reports received from all agencies is likely to improve either the event location or depth compared to the hypocentre solution from each single agency. For areas with a sparse local seismic network or an unfavourable station configuration, readings made by other networks at teleseismic distances are very important. All events near mid-oceanic ridges as well as those in the majority of subduction zones around the world fall into this category. Hence we greatly appreciate the effort made by many agencies that report data for remote earthquakes (Figure 9.3). For some agencies, such as the IDC and the NEIC, it is part of their mission. For instance, the IDC reports almost every seismic event that is large enough to be recorded at teleseismic distance (20 degrees and beyond). This is largely because the International Monitoring System of primary arrays and broadband instruments is distributed at quiet sites around the world in order to be able to detect possible violations of the Comprehensive Nuclear-Test-Ban Treaty. The NEIC reported over 40% of those events as their mission requires them to report events above magnitude 4.5 outside the United States of America. For other agencies reporting distant events it is an extra effort that they undertake to notify their governments and relief agencies as well as to help the ISC and academic research in general. Hence these agencies usually report on the larger magnitude events. BJI, NAO, MOS, NOU, BRA, VIE, CLL and AWI each reported individual station arrivals for several percent of all relevant events. We encourage other agencies to report distant events to us.

In addition to the first arriving phase we encourage reporters to contribute observations of secondary seismic phases that help constrain the event location and depth: S, Sn, Sg and pP, sP, PcP (Figure 9.4). We expect though that these observations are actually made from waveforms, rather than just predicted by standard velocity models and modern software programs. It is especially important that these arrivals are manually reviewed by an operator (as we know takes place at the IDC and NEIC), as opposed to some lesser attempts to provide automatic phase readings that are later rejected by the ISC due to a generally poor quality of unreviewed picking.

Another important long-term task that the ISC performs is to compute the most definitive values of

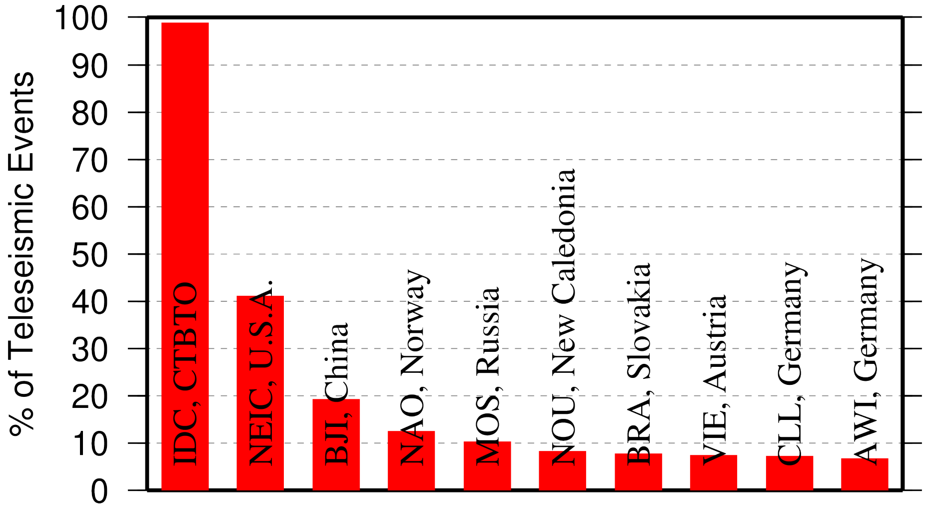

Figure 9.3: *Top ten agencies that reported teleseismic phase arrivals for a large portion of ISC events.*

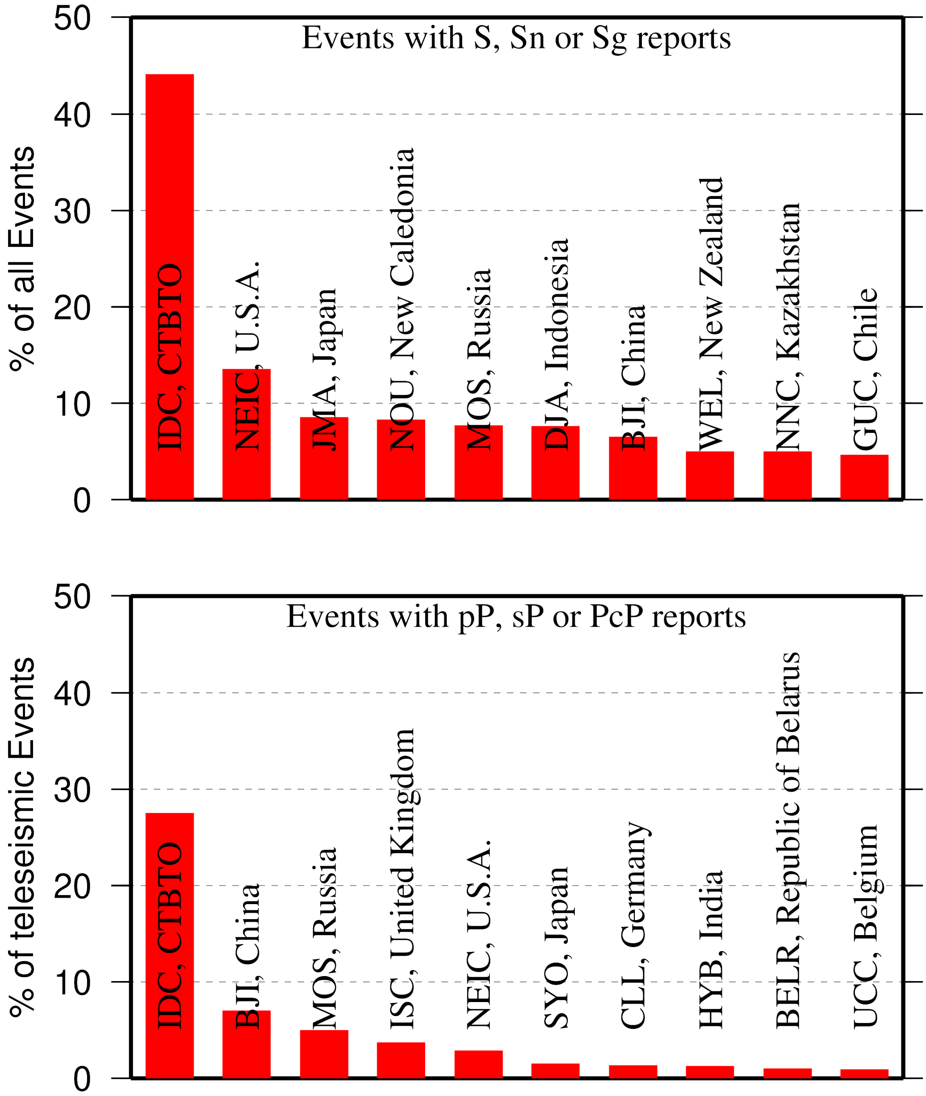

Figure 9.4: *Top ten agencies that reported secondary phases important for an accurate epicentre location (top) and focal depth determination (bottom).*

MS and mb network magnitudes that are considered reliable due to removal of outliers and consequent averaging (using alpha-trimmed median) across the largest network of stations, generally not feasible for a single agency. Despite concern over the bias at the lower end of mb introduced by the body wave amplitude data from the IDC, other agencies are also known to bias the results. This topic is further discussed in Section 8.5.

Notably, the IDC reports almost 100% of all events for which MS and mb are estimated. This is due to the standard routine that requires determination of body and surface wave magnitudes useful for discrimination purposes. NEIC, BJI, MOS, NAO, PRU, CLL and a few other agencies (Figure 9.5) are also responsible for the majority of the amplitude and period reports that contribute towards the ISC magnitudes.

The ISC only recently started to determine source mechanisms in addition to those reported by other agencies. For moment tensor magnitudes we rely on reports from other agencies (Figure 9.6).

Among other event parameters the ISC Bulletin also contains information on event type. We cannot

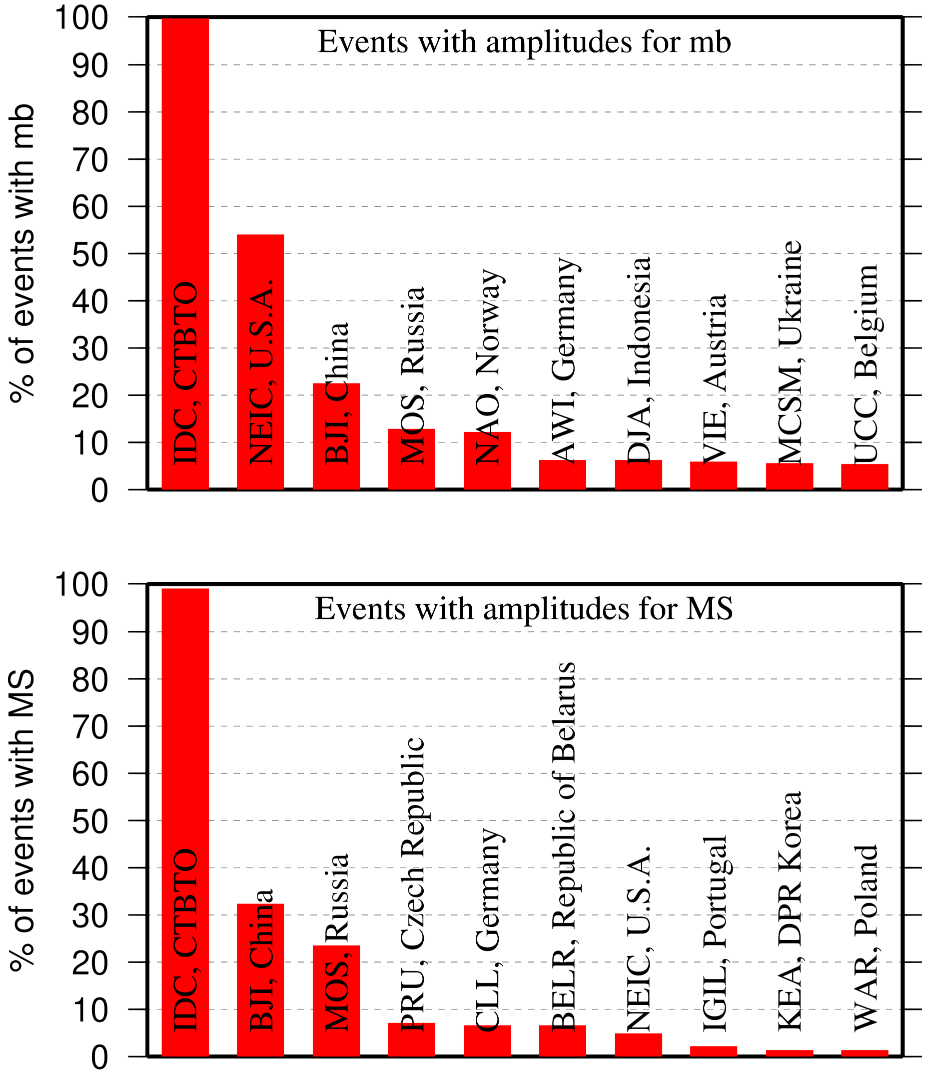

Figure 9.5: *Agencies that report defining body (top) and surface (bottom) wave amplitudes and periods for the largest fraction of those ISC Bulletin events with MS/mb determinations.*

independently verify the type of each event in the Bulletin and thus rely on other agencies to report the event type to us. Practices of reporting non-tectonic events vary greatly from country to country. Many agencies do not include anthropogenic events in their reports. Suppression of such events from reports to the ISC may lead to a situation where a neighbouring agency reports the anthropogenic event as an earthquake for which expected data are missing. This in turn is detrimental to ISC Bulletin users studying natural seismic hazard. Hence we encourage all agencies to join the agencies listed on Figure 9.7 and several others in reporting both natural and anthropogenic events to the ISC.

The ISC Bulletin also contains felt and damaging information when local agencies have reported it to us. Agencies listed on Figure 9.8 provide such information for the majority of all felt or damaging events in the ISC Bulletin.

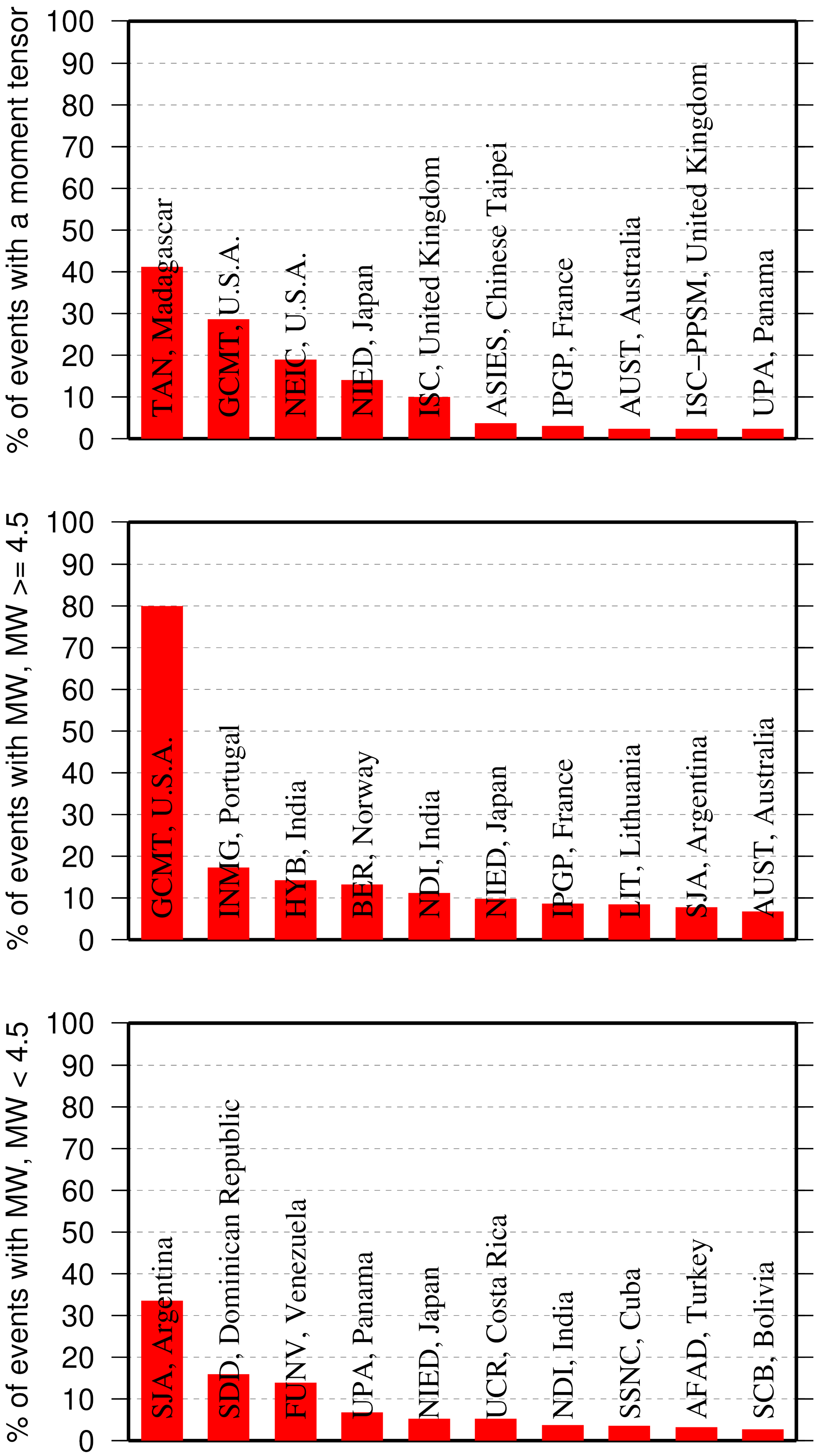

Figure 9.6: *Top ten agencies that most frequently report determinations of seismic moment tensor (top) and moment magnitude (middle/bottom for M greater/smaller than 4.5).*

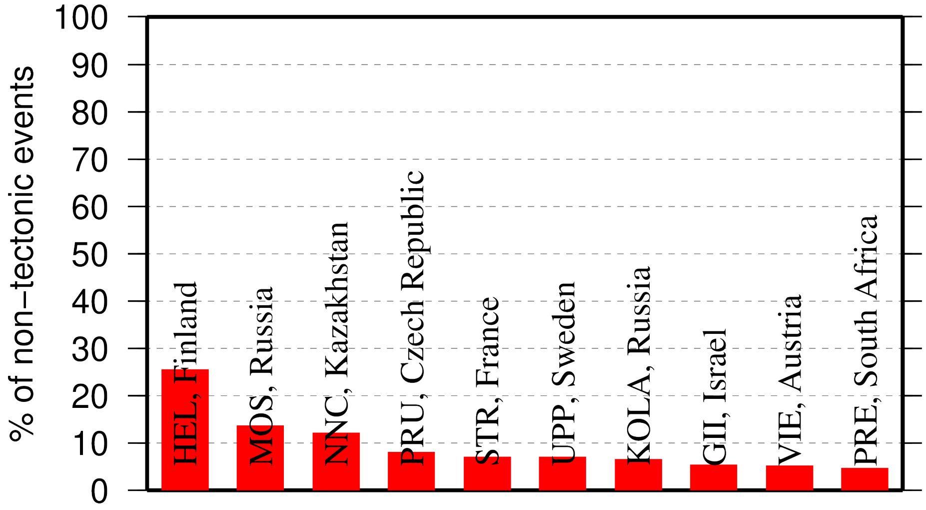

Figure 9.7: *Top ten agencies that most frequently report non-tectonic seismic events to the ISC.*

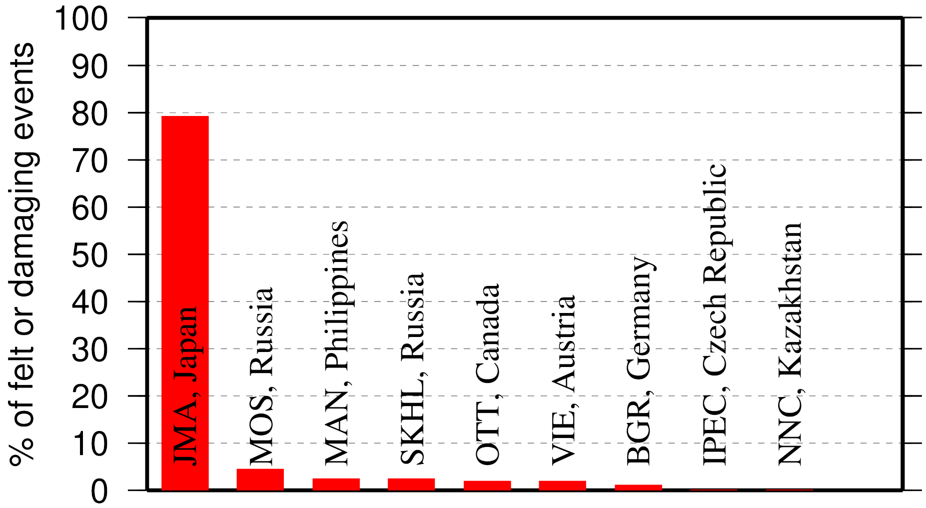

Figure 9.8: *Top ten agencies that most frequently report macroseismic information to the ISC.*

9.3 The Most Consistent and Punctual Contributors

During this six-month period, 33 agencies reported their bulletin data in one of the standard seismic formats (ISF, IMS, GSE, Nordic or QuakeML) and within the current 12-month deadline. Here we must reiterate that the ISC accepts reviewed bulletin data after a final analysis as soon as they are ready. These data, even if they arrive before the deadline, are immediately parsed into the ISC database, grouped with other data and become available to the ISC users on-line as part of the preliminary ISC Bulletin. There is no reason to wait until the deadline to send the data to the ISC. Table 9.1 lists all agencies that have been helpful to the ISC in this respect during the six-month period.

Table 9.1: *Agencies that contributed reviewed bulletin data to the ISC in one of the standard international formats before the submission deadline.*

Agency Code	Country	Average Delay from real time (days)
ZUR	Switzerland	15
ATH	Greece	22
WEL	New Zealand	25
IDC	Austria	31
IGIL	Portugal	31
ECX	Mexico	31
KNET	Kyrgyzstan	32
NAO	Norway	37
BUC	Romania	39
LDG	France	57
ISK	Turkey	84
NEIC	U.S.A.	106
ISN	Iraq	108
VIE	Austria	114
PPT	French Polynesia	119
TIR	Albania	120
THE	Greece	123
BER	Norway	133
BGSI	Botswana	135
KEA	Democratic People's Republic of Korea	137
BGS	United Kingdom	143
INMG	Portugal	145
BJI	China	183
MDD	Spain	208
AUST	Australia	218
BYKL	Russia	285
STR	France	291
AFAD	Turkey	297
IPEC	Czech Republic	310
TEH	Iran	318
UCC	Belgium	320
PRU	Czech Republic	337
OMAN	Oman	347

10

Appendix

10.1 ISC Operational Procedures

10.1.1 Introduction

The relational database at the ISC is the primary source for the ISC Bulletin. This database is also the source for the ISC web-based search, the ISC CD-ROMs and this printed Summary. The ISC database is also mirrored at several institutions such as the Data Management Center of the Incorporated Research Institutions for Seismology (IRIS DMC), Earthquake Research Institute (ERI) of the University of Tokyo and a few others.

The database holds information about ISC events, both natural and anthropogenic. Information on each event may include hypocentre estimates, moment tensors, event type, felt and damaging reports and associated station observations reported by different agencies and grouped together per physical event.

The majority of the ISC events (∼80%) are small and are not reviewed by the ISC analysts. Those that are reviewed (∼20%, usually magnitude greater than 3.5) may or may not include an ISC hypocentre solution and magnitude estimates. The decision depends on whether the wealth of combined information from several agencies as compared to the data of each single agency alone warrants the ISC location. The events are called ISC events regardless of whether they have been reviewed or located by the ISC or not.

All events located by the ISC are reviewed by the ISC analysts but not the other way round. Analyst review involves an examination of the integrity of all reported parametric information. It does not involve review of waveforms. Even if waveforms from all of the ∼6,000 stations included in a typical recent month of the ISC Bulletin were freely available, it would be an unmanageable task to inspect them all.

We shall now describe briefly current processes and procedures involved in producing the Bulletin of the International Seismological Centre. These have been developed from former practices described in the Introduction to earlier issues of the ISC Bulletin to account for modern methods and technologies of data collection and analysis.

10.1.2 Data Collection

Parametric data, mainly comprising seismic event hypocentre solutions, phase arrival observations and associated magnitude data, are now mostly emailed to the ISC (seismo@isc.ac.uk) by agencies around the world. Other macroseismic and source information associated with seismic events may also be incorporated in accordance with modern standards. The process of data collection at the ISC involves the automatic parsing of these data into the ISC relational database. The ISC now has over 200 individual parsers to account for legacy and current bulletin data formats used by data reporters.

Figure 10.1 shows the 313 agencies that have reported bulletin data to the ISC, directly or via regional data centres, during the entire period of the ISC existence: these agencies are also listed in Table 10.2 of the Appendix. In Figure 10.1, corresponding countries are shown shaded in red. Please note that the continent of Antarctica appears white on the map despite a steady stream of bulletin data from Antarctic stations: the agencies that run these stations are based elsewhere.

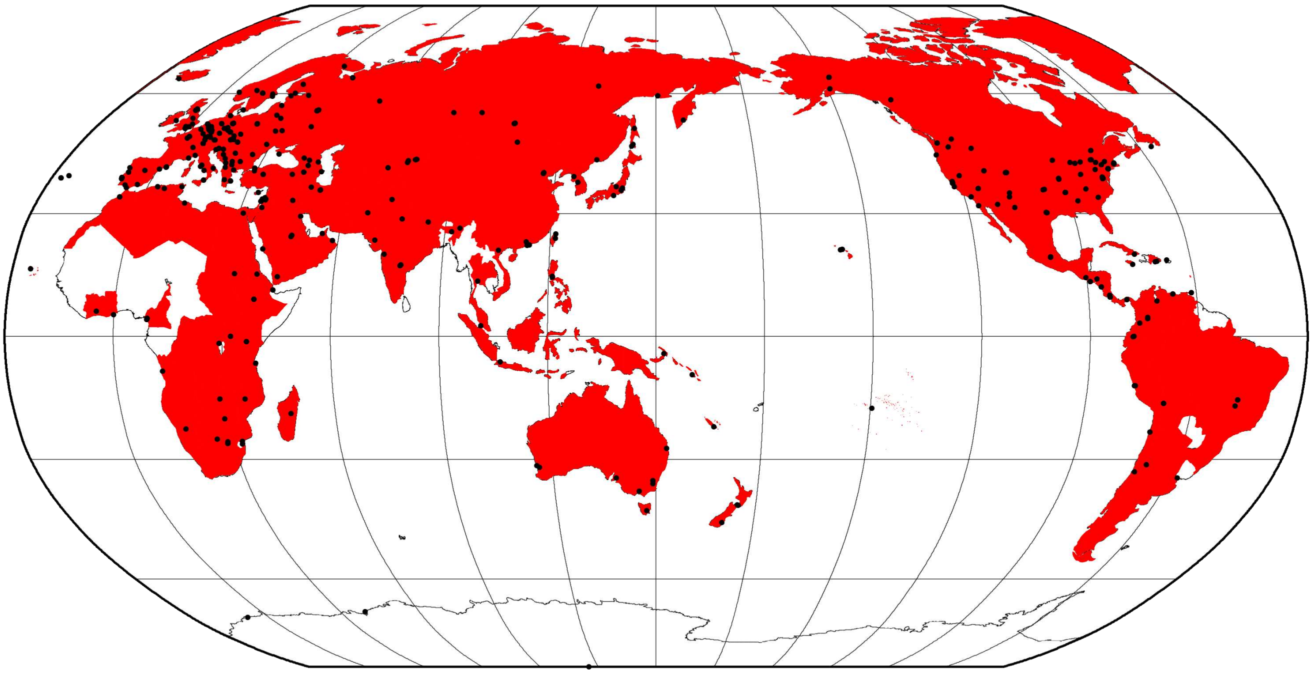

Figure 10.1: *Map of 313 agencies and corresponding countries that have reported seismic bulletin data to the ISC at least once during the entire period of the ISC operations, either directly or via regional data centres. Corresponding countries are shaded in red.*

10.1.3 ISC Automatic Procedures

Grouping

Grouping is the automatic process by which the many hypocentre solutions sent by the agencies reporting to the ISC for the same physical event are merged together into a single ISC event. This process possibly begins with an alert message and ends before a final review by ISC analysts. The process periodically runs through a set time interval of the input data stream, typically one day, looking for hypocentres in newly received data that are not yet grouped into an ISC event. Thus it considers only data more recent than the last data month reviewed by the ISC analysts. Immediately after grouping the seismic arrival associator is run on the same time interval, dealing with new phase arrival data not associated with any hypocentre.

The first stage of grouping gets a score where possible for each hypocentre to determine whether the reported hypocentre will be considered to be the primary estimate, or prime, for an ISC event. This score is based on the station arrival times reported in association with the hypocentre in four epicentral distance zones that characterise the networks of stations reporting:

1. Whole network
2. Local, 0 - 150 km
3. Near-regional, 3° - 10°
4. Teleseismic, 28° - 180°

For each distance zone, the azimuthal gap, the secondary azimuthal gap (the largest azimuthal gap filled by a single station), the minimum and maximum epicentral distance and number of stations are all used to calculate the value of dU, the normalised absolute deviation from best fitting uniformly distributed stations (*Bondár and McLaughlin*, 2009a). Clearly, this procedure can only use:

1. Bulletin data with hypocentres and sufficient associated seismic arrivals
2. Data for stations that are in the International Registry (IR)
3. Station data that are actually reported to ISC: CENC (China), for example, reports at most 24 stations, whilst many more may have been used to determine the hypocentre.

The hypocentres are then each considered in turn for grouping using one of two methods, the first by searching for a similar hypocentre, and the second by searching for the best fit of the reported phase arrival data that are associated with the candidate hypocentre. The method chosen for a reporter is based on feedback gained from ISC analysts.

For finding similar hypocentres, three sets of limits for origin-time difference and epicentral separation are used according to the type of bulletin data, be it alert, provisional or final: these limits are, respectively:

- ± 2 minutes and 10°
- ± 2 minutes and 4°
- ± 1 minutes and 2°

If there is no overlap with the hypocentre of an existing ISC event, a new event is formed. For each candidate hypocentre, a proximity score is otherwise calculated based on differences in time, t, and distance, s, between the candidate hypocentre and a hypocentre in an event with which it could potentially be grouped.

Proximity score $= 2 - (dt/dt_{max}) - (ds/ds_{max})$

where ds_{max} is the maximum distance between hypocentres and dt_{max} the maximum difference in origin time.

As long as there is no duplication of hypocentre (with the same author, origin time and location within tight limits) the candidate hypocentre together with the associated phase data is grouped with the prime hypocentre of the event and the initial dU score is used to reassess the prime hypocentre designation. Apparent duplicated hypocentre estimations, including preliminary solutions relayed by other agencies, need to be assessed to determine whether they should really be split between different events. Should there be two or more equally valid events, these can be assessed in turn and may eventually be merged together.

Grouping by fit of the associated phase arrival data is simpler. The residuals of the arrival data are calculated using ak135 travel times for all suitable prime hypocentres within the widest proximity limits given above for similar hypocentres. The hypocentre and associated phase arrival data is then grouped with the event with the best fitting prime hypocentre, which may similarly be re-designated according to the dU scores. Associations of phase arrival data are updated to be with the prime hypocentre estimate of each ISC event.

It follows that a hypocentre and associated phase arrival data submitted by a reporter will have the reported hypocentre set as the prime hypocentre in the ISC event if no other submitted hypocentre estimate is a closer match. It follows also that a hypocentre submitted without phase data can only be grouped with a similar hypocentre. Generally, early arriving data may be superseded by later arriving data: the data will still be in the ISC database but be deprecated, that is, marked as being no longer useful for further processes.

Association

Association is the automatic procedure, run routinely after grouping, that links reported phase arrivals at IR stations with the prime hypocentres of ISC events. As grouping took care of those phases associated with reported hypocentres, by associating the phases to the respective prime hypocentres of the ISC events without further checks, this procedure is only required for phase arrival observations that were sent without any association of event made for them by the reporter. Currently only 5% of arrival data is sent unassociated compared with 25% ten years ago.

If a phase arrival is found to be very similar to another already reported, it is placed in the same event, otherwise the procedure below is followed.

For associating a phase arrival, suitable events are sought with prime hypocentre origin-times in the window 40 minutes before and 100 s after the arrival time. For each phase arrival and prime hypocentre an ak135 travel-time residual is calculated for either the reported arrival phase name or an alternative from a default list if appropriate. Possible timing errors that are multiples of 60 s (a minute) are considered if the phase arrival is at a station not known to be digitally recording. A reporting likelihood is then determined based on the reported event magnitude: a magnitude default of 3.0 is used if no magnitude is given.

A final score is calculated from the residuals, from the likelihood of the phase observations for the magnitude of the event and from the S-P misfit. A phase arrival along with all other phase arrivals in that reading for the station is then associated with the prime hypocentre with the best score. If no suitable match is found, the reading remains unassociated but may be used at some later stage.

Thresholding

Thresholding is the process determining which events are to be reviewed by the ISC analysts. In former times, before email transmission of data was convenient, all events were reviewed, with magnitudes nearly always 3.5 or above. Nowadays, data contributors are encouraged to send all their data, which are stored in the ISC database. The overwhelming amount of data, including that for many more smaller events and from many more seismograph stations, led to the advent of ISC Comprehensive Bulletin, for all events, and the ISC Reviewed Bulletin, for selected events reviewed by ISC analysts. Thresholding has been under constant review since the start of the 1999 data year.

Several criteria are considered to decide which events merit review. Once a decision is made, whether or not an event is to be reviewed, further criteria are not considered.

In this section, M is the maximum magnitude reported by any agency for the event. The sequence of tests in the automatic decision process for reviewing events is currently:

- All events reported by the International Data Centre (IDC) of the Comprehensive Nuclear-Test-Ban Treaty Organization (CTBTO) are reviewed.
- If M is greater than or equal to 3.5, the event is reviewed.
- If M is less than 2.5, the event is not reviewed.
- If M is unknown, the number of data sources of hypocentres and phase arrivals is used. Care is taken here to avoid counting indirect reports arriving via agencies such as NEIC, CSEM and CASC, which compile regional and global data:
  - If the number of hypocentre authors is greater than two and the maximum epicentral distance of arrival data is greater than 10°, the event is reviewed.
  - If the number of arrival authors is greater than two and the maximum epicentral distance of arrival data is greater than 10°, the event is reviewed.
  - Otherwise the event is not reviewed.
- If M is between 2.5 and 3.5:
  - If the number of hypocentre and seismic arrival authors is less than two, the event is not reviewed.
  - If any bulletin contributing to the event has at least ten stations within 3° and the secondary azimuthal gap (the largest azimuthal gap filled by a single station) is less than 135°, the event is not reviewed.

Location by the ISC

The automatic processes group and associate incoming data into ISC events as indicated above. These data are available to users before review by the ISC analysts but there will be no ISC hypocentre solutions for any of the events. The candidate events due for review by the ISC analysts are determined by the thresholding process, which is why many smaller events remain without an ISC hypocentre solution even after the analyst review.

Several further checks of the data are made in preparation for the analyst review, and initial trial estimates for ISC hypocentres are then generated using the accumulated data. If sufficiently robust, the ISC hypocentre estimation will be retained and be made the prime solution for the event, but this, of course, will itself be subject to the analyst review.

It is important to note that not all reviewed events will have an ISC hypocentre. At least one of the criteria listed below must be met for an initial ISC location of a reviewed event to be made:

- All events with an IDC hypocentre, unless IDC is the only hypocentre author and there are less than six associated phases.
- Two or more reporters of data
- Phase data at epicentral distance $\geq 20°$

The ISC locator also needs an intial seed location; in all events except those with eight or more reporters of data where the existing prime is used, this is calculated using a Neighbourhood Algorithm (NA) (*Sambridge*, 1999; *Sambridge and Kennett*, 2001). More information about the ISC location algorithm and initial seed is given in the next section.

10.1.4 ISC Location Algorithm

The new ISC location algorithm is described in detail in *Bondár and Storchak* (2011) (doi: 10.1111/j.1365-246X.2011.05107.x, Manual www.isc.ac.uk/iscbulletin/iscloc/); here we give a short summary of the major features. Ever since the ISC came into existence in 1964, it has been committed to providing a homogeneous bulletin that benefits scientific research. Hence the location algorithm used by the ISC, except for some minor modifications, has remained largely unchanged for the past 40 years (*Adams et al.*, 1982; *Bolt*, 1960). While the ISC location procedures have served the scientific community well in the past, they can certainly be improved.

Linearised location algorithms are very sensitive to the initial starting point for the location. The old procedures made the assumption that a good initial hypocentre is available among the reported hypocentres. However, there is no guarantee that any of the reported hypocentres are close to the global minimum in the search space. Furthermore, attempting to find a free-depth solution was futile when the data had no resolving power for depth (e.g. when the first arrival is not within the inflection point of the P travel-time curve). When there was no depth resolution, the algorithm would simply pick a point on the origin time – depth trade-off curve. The old ISC locator assumed that the observational errors are independent. The recent years have seen a phenomenal growth both in the number of reported events and phases, owing to the ever-increasing number of stations worldwide. Similar ray paths will produce correlated travel-time prediction errors due to unmodelled heterogeneities in the Earth, resulting in underestimated location uncertainties and for unfavourable network geometries, location bias. Hence, accounting for correlated travel-time prediction errors becomes imperative if we want to improve (or simply maintain) location accuracy as station networks become progressively denser. Finally, publishing network magnitudes that may have been derived from a single station measurement was rather prone to producing erroneous event magnitude estimates.

To meet the challenge imposed by the ever-increasing data volume from heavily unbalanced networks we introduced a new ISC location algorithm to ensure the efficient handling of data and to further improve the location accuracy of events reviewed by the ISC. The new ISC location algorithm

- Uses all ak135 (*Kennett et al.*, 1995) predicted phases (including depth phases) in the location;
- Obtains the initial hypocentre guess via the Neighbourhood Algorithm (NA) (*Sambridge*, 1999; *Sambridge and Kennett*, 2001);
- Performs iterative linearised inversion using an *a priori* estimate of the full data covariance matrix to account for correlated model errors (*Bondár and McLaughlin*, 2009b);
- Attempts a free-depth solution if and only if there is depth resolution, otherwise it fixes the depth to a region-dependent default depth;
- Scales uncertainties to 90% confidence level and calculates location quality metrics for various distance ranges;
- Obtains a depth-phase depth estimate based on reported surface reflections via depth-phase stacking (*Murphy and Barker*, 2006);
- Provides robust network magnitude estimates with uncertainties.

Seismic Phases

One of the major advantages of using the ak135 travel-time predictions (*Kennett et al.*, 1995) is that they do not suffer from the baseline difference between P, S and PKP phases compared with the Jeffreys-Bullen tables (*Jeffreys and Bullen*, 1940). Furthermore, ak135 offers an abundance of phases from the IASPEI Standard Seismic List (*Storchak et al.*, 2003; 2011) that can be used in the location, most notably the PKP branches and depth-sensitive phases. Elevation and ellipticity corrections (*Dziewonski and Gilbert*, 1976; *Engdahl et al.*, 1998; *Kennett et al.*, 1996), using the WG84 ellipsoid parameters, are added to the ak135 predictions. For depth phases, bounce point (elevation correction at the surface reflection point) and water depth (for pwP) corrections are calculated using the algorithm of *Engdahl et al.* (1998). We use the ETOPO1 global relief model (*Amante and Eakins*, 2009) to obtain the elevation or the water depth at the bounce point.

Phase picking errors are described by *a priori* measurement error estimates derived from the inspection of the distribution of ground truth residuals (residuals calculated with respect to the ground truth location) from the IASPEI Reference Event List (*Bondár and McLaughlin*, 2009a). For phases that do not have a sufficient number of observations in the ground truth database we establish *a priori* measurement errors so that the consistency of the relative weighting schema is maintained. First-arriving P-type phases (P, Pn, Pb, Pg) are picked more accurately than later phases, so their measurement error estimates are the smallest, 0.8 s. The measurement error for first-arriving S-phases (S, Sn, Sb, Sg) is set to 1.5 s.

Phases traversing through or reflecting from the inner/outer core of the Earth have somewhat larger (1.3 s for PKP, PKS, PKKP, PKKS and P'P' branches as well as PKiKP, PcP and PcS, and 1.8 s for SKP, SKS, SKKP, SKKS and S'S' branches as well as SKiKP, ScP and ScS) measurement error estimates to account for possible identification errors among the various branches. Free-surface reflections and conversions (PnPn, PbPb, PgPg, PS, PnS, PgS and SnSn, SbSb, SgSg, SP, SPn, SPg) are observed less frequently and with larger uncertainty, and therefore suffer from large, 2.5 s, measurement errors. Similarly, a measurement error of 2.8 s is assigned to the longer period and typically emergent diffracted phases (Pdif, Sdif, PKPdif). The *a priori* measurement error for the commonly observed depth phases (pP, sP, pS, sS and pwP) is set to 1.3 s, while the remaining depth phases (pPKP, sPKP, pSKS, sSKS branches and pPb, sPb, sSb, pPn, sPn, sSn) have the measurement error estimate set to 1.8 s. We set the measurement error estimate to 2.5 s for the less reliable depth phases (pPg, sPg, sSg, pPdif, pSdif, sPdif and sSdif). Note that we also allow for distance-dependent measurement errors. For instance, to account for possible phase identification errors at far-regional distances the *a priori* measurement error for Pn and P is increased from 0.8 s to 1.2 s and for Sn and S from 1.5 s to 1.8 s between 15° and 28°. The measurement errors between 40° and 180° are set to 1.3 s and 1.8 s for the prominent PP and SS arrivals respectively, but they are increased to 1.8 s and 2.5 s between 25° and 40°.

The relative weighting scheme (Figure 10.2) described above ensures that arrivals picked less reliably or prone to phase identification errors are down-weighted in the location algorithm. Since the ISC works with reported parametric data with wildly varying quality, we opted for a rather conservative set of *a priori* measurement error estimates.

Correlated Travel-Time Prediction Error Structure

Most location algorithms, either linearised or non-linear, assume that all observational errors are independent. This assumption is violated when the separation between stations is less than the scale length of local velocity heterogeneities. When correlated travel-time prediction errors are present, the data covariance matrix is no longer diagonal, and the redundancy in the observations reduces the effective number of degrees of freedom. Thus, ignoring the correlated error structure inevitably results in underestimated location uncertainty estimates. For events located by an unbalanced seismic network this may also lead to a biased location estimate. *Chang et al.* (1983) demonstrated that accounting for correlated error structure in a linearised location algorithm is relatively straightforward once an estimate of the non-diagonal data covariance matrix is available. To determine the data covariance matrix we follow the approach described by *Bondár and McLaughlin* (2009b). They assume that the similarity between ray paths is well approximated by the station separation. This simplifying assumption allows for the estimation of covariances between station pairs from a generic P variogram model derived from ground truth residuals. Because the overwhelming number of phases in the ISC Bulletin is teleseismic P, we expect that the generic variogram model will perform reasonably well anywhere on the globe.

Since in this representation the covariances depend only on station separations, the covariance matrix (and its inverse) needs to be calculated only once. We assume that different phases owing to the different ray paths they travel along as well as station pairs with a separation larger than 1000 km are uncorrelated. Hence, the data covariance matrix is a sparse, block-diagonal matrix. Furthermore, if the stations in each phase block are ordered by their nearest neighbour distance, the phase blocks themselves become

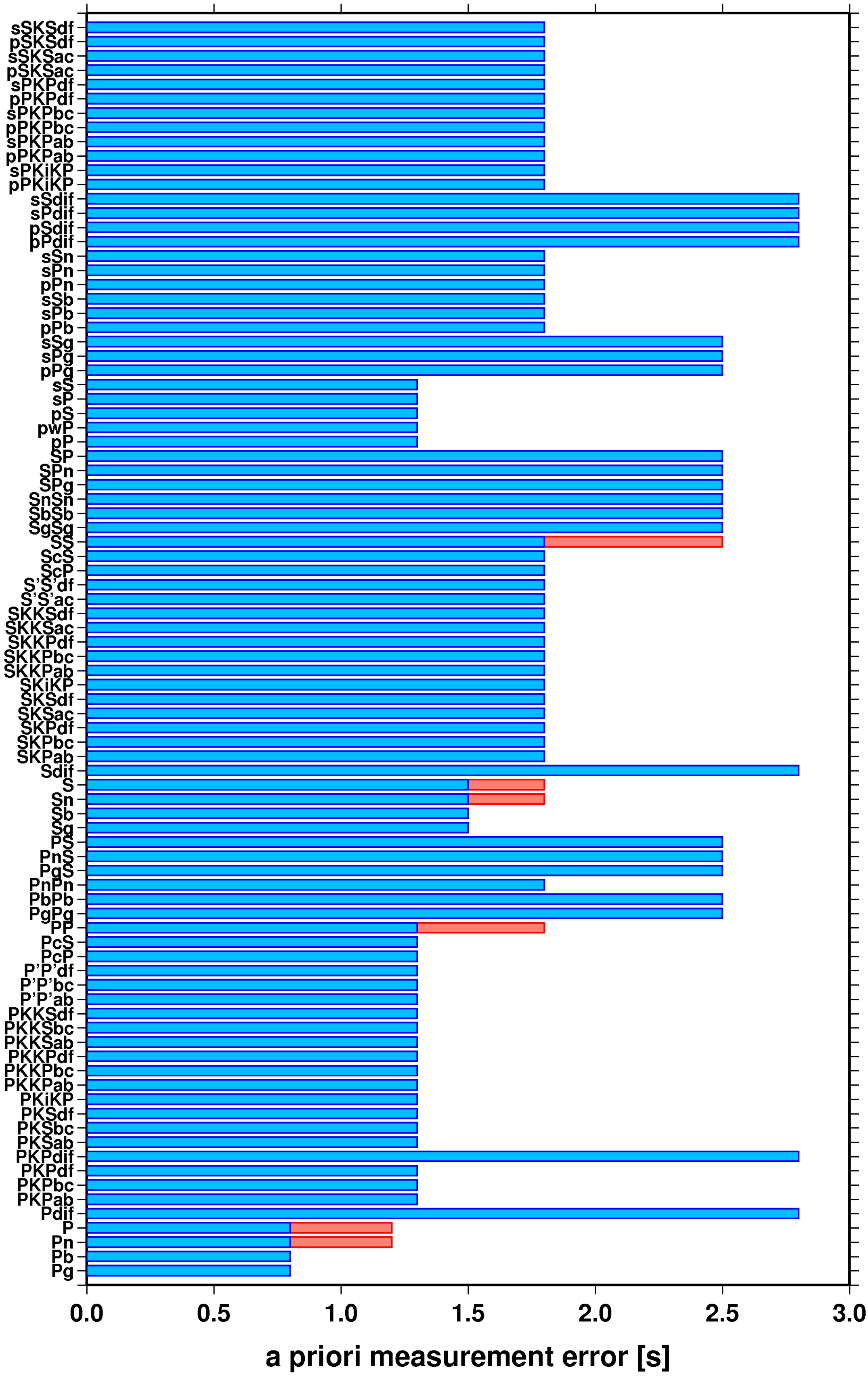

Figure 10.2: A priori *measurement error estimates for phases used in the location algorithm. The red coloured errors are distance-dependent, which are applied for distances when phase identification errors may occur (see text).*

block-diagonal. To reduce the computational time of inverting large matrices we exploit the inherent block-diagonal structure by inverting the covariance matrix block-by-block. The *a priori* measurement error variances are added to the diagonal of the data covariance matrix.

Depth Resolution

In principle, depth can be resolved if there is a mixture of upgoing and downgoing waves emanating from the source, that is, if there are stations covering the distance range where the vertical partial derivative of the travel-time of the first-arriving phase changes sign (local networks), or if there are phases with vertical slowness of opposite sign (depth phases). Core reflections, such as PcP, and to a lesser extent, secondary phases (S in particular) could also help in resolving the depth.

We developed a number of criteria to test whether the reported data for an event have sufficient depth resolution:

- local network: one or more stations within 0.2° with time-defining phases
- depth phases: five or more time-defining depth phases reported by at least two agencies (to reduce a chance of misinterpretation by a single inexperienced analyst)
- core reflections: five or more time-defining core reflections (PcP, ScS) reported by at least two agencies
- local/near regional S: five or more time-defining S and P pairs within 3°

We attempt a free-depth solution if any of the above criteria are satisfied; otherwise we fix the depth to a default depth dependent on the epicentre location. This will preferably be the grid depth based on the ISC default depth grid (Figure 10.3). Where no grid depth is available the default depth is set to either 10 km or 35 km based on the GRN (See Figure 10.4. A list of GRN's can be found in Section 10.2.2). The default depth grid was derived from the EHB (*Engdahl et al.*, 1998) free-depth solutions, including the fixed-depth EHB earthquakes that were flagged as having reliable depth estimate (personal communication with Bob Engdahl), as well as from free-depth solutions obtained by the new locator when locating the entire ISC Bulletin data-set. As Figure 10.3 indicates, the default depth grid provides a reasonable depth estimate where seismicity is well established. Note that the depths of known anthropogenic events and landslides are fixed to the surface.

Depth-Phase Stack

While we use depth phases directly in the location, the depth-phase stacking method (*Murphy and Barker*, 2006) provides an independent means to obtain robust depth estimates. Because the depth obtained from the depth-phase stacking method implicitly depends on the epicentre itself, we perform the depth-phase stack only twice: first, with respect to the initial location in order to obtain a reasonable starting point for the depth in the grid search described in the following section; second, with respect to the final location to obtain the final estimate for the depth-phase constrained depth.

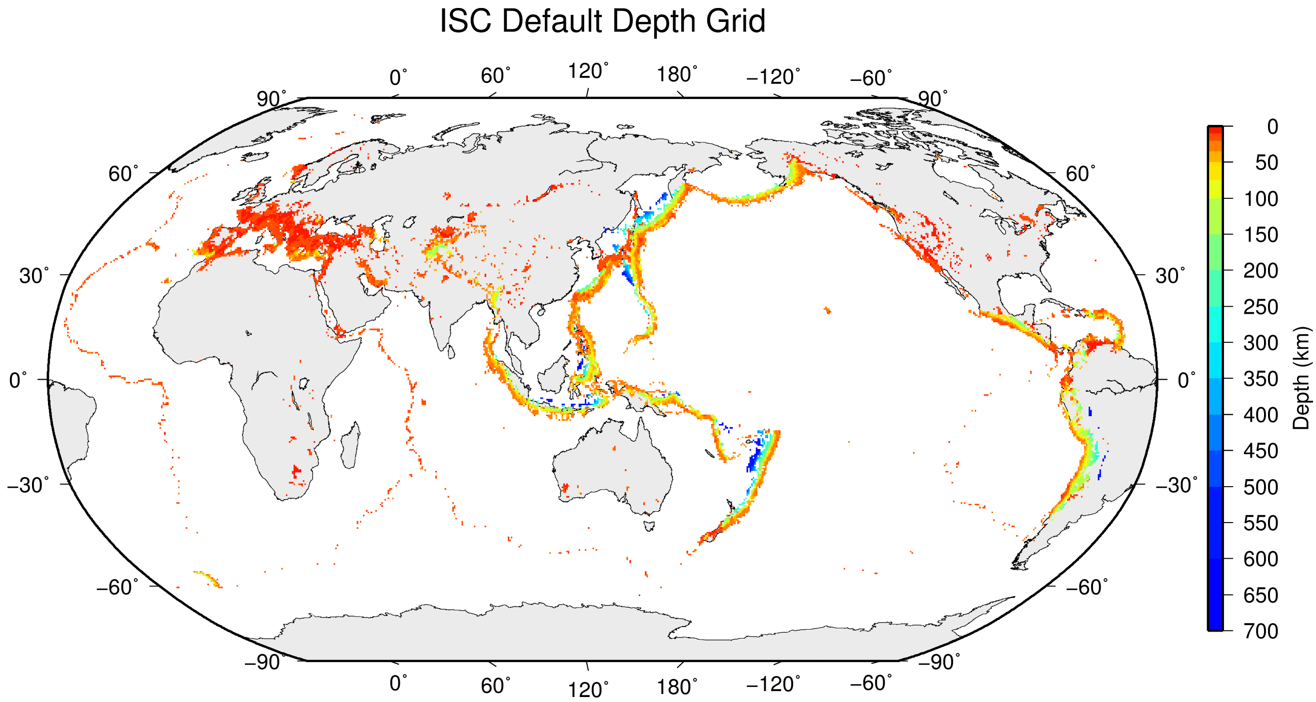

__Figure 10.3:__ Default depths on a 0.5×0.5 degree grid derived from EHB free-depth solutions and EHB events flagged as reliable depth, as well as free-depth solutions from the entire ISC Bulletin located with the new locator.

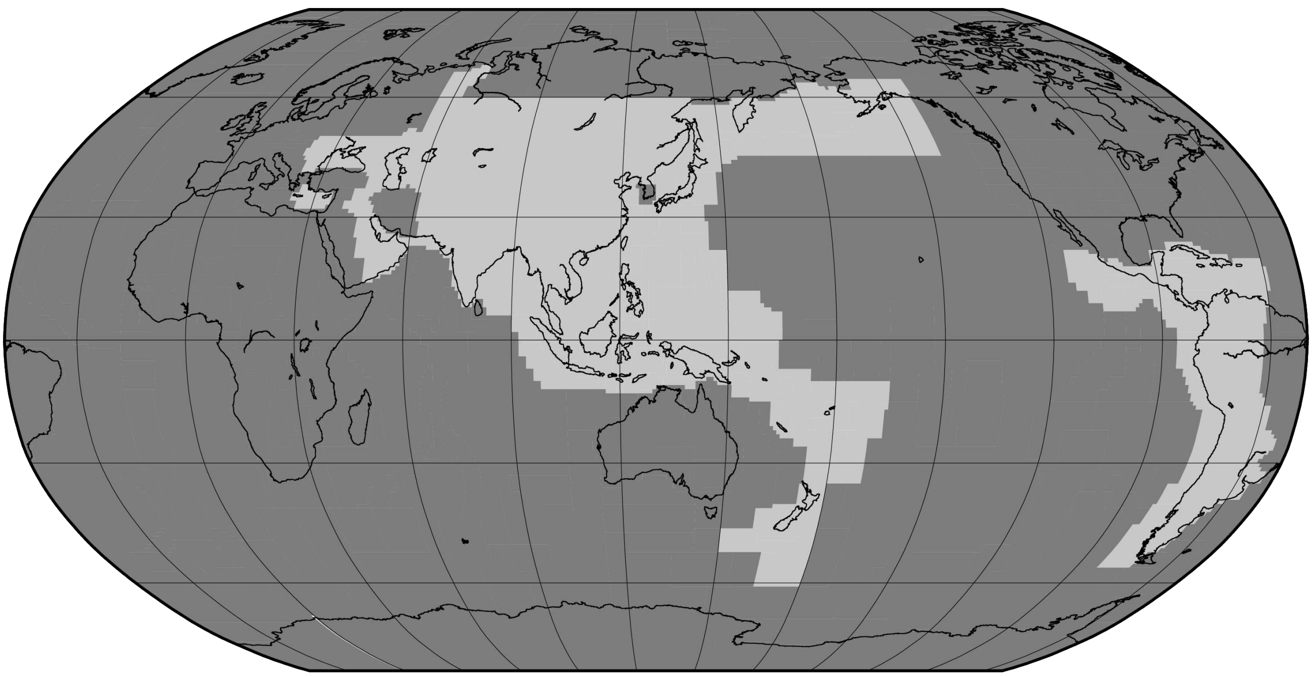

__Figure 10.4:__ Default depths by Flinn-Engdahl geographic regions. Dark grey regions are set to 10 km and light grey to 35 km

Initial Hypocentre

For poorly recorded events the reported hypocentres may exhibit a large scatter and they could suffer from large location errors, especially if they are only recorded teleseismically. In order to obtain a good initial hypocentre guess for the linearised location algorithm we employ the Neighbourhood Algorithm (NA) (*Sambridge*, 1999; *Sambridge and Kennett*, 2001). NA is a nonlinear grid search method capable of exploring a large search space and rapidly closing in on the global optimum. *Kennett* (2006) discusses in detail the NA algorithm and its use for locating earthquakes.

We perform a search around the median of reported hypocentre parameters with a generously defined search region – within a 2° radius circle around the median epicentre, 10 s around the median origin time and 150 km around the median reported depth. These default search parameters were obtained by trial-and-error runs to achieve a compromise between execution time and allowance for gross errors in the median reported hypocentre parameters. Note that if our test for depth resolution fails, we fix the depth to the region-dependent default depth. The initial hypocentre estimate will be the one with the smallest L1-norm misfit among the NA trial hypocentres. Once close to the global optimum, we proceed with the linearised location algorithm to obtain the final solution and corresponding formal uncertainties.

Iterative Linearised Location Algorithm

We adopt the location algorithm described in detail in *Bondár and McLaughlin* (2009b). Recall that in the presence of correlated travel-time prediction errors the data covariance matrix is no longer diagonal. Using the singular value decomposition of the data covariance matrix we construct a projection matrix that orthogonalises the data set and projects redundant observations into the null space. In other words, we solve the inversion problem in the eigen coordinate system in which the transformed observations are independent.

The model covariance matrix yields the four-dimensional error ellipsoid whose projections provide the two-dimensional error ellipse and one-dimensional errors for depth and origin time. These uncertainties are scaled to the 90% confidence level. Note that since we projected the system of equations into the eigen coordinate system, the number of independent observations is less than the total number of observations. Hence, the estimated location error ellipses necessarily become larger, providing a more realistic representation of the location uncertainties. The major advantage of this approach is that the projection matrix is calculated only once for each event location.

Validation Tests

To demonstrate improvements due to the new location procedures, we located some 7,200 GT0-5 events in the IASPEI Reference Event List (*Bondár and McLaughlin*, 2009a) both with the old ISC locator (which constitutes the baseline) and with the new location algorithm. We also located the entire (1960-2010) ISC Bulletin, including four years of the International Seismological Summary (ISS, the predecessor of the ISC) catalogue (*Villaseñor and Engdahl*, 2005; 2007).

The location of GT events demonstrated that the new ISC location algorithm provides small but consistent location improvements, considerable improvements in depth determination and significantly more accurate formal uncertainty estimates. Even using a 1-D model and a variogram model that fits teleseismic observations we could achieve realistic uncertainty estimates, as the 90% confidence error ellipses cover the true locations 80-85% of the time. The default depth grid provides reasonable depth estimates where there is seismicity. We have shown that the location and depth accuracy obtained by the new algorithm matches or surpasses the EHB accuracy.

We noted above that the location improvements for the ground truth events are consistent, but minor. This is not surprising as most of the events in the IASPEI Reference Event List are very well-recorded with a small azimuthal gap and dominated by P-type phases. In these circumstances we could expect significant location improvements only for heavily unbalanced networks where large numbers of correlated ray paths conspire to introduce location bias. On the other hand, the ISC Bulletin represents a plethora of station configurations ranging from reasonable to the most unfavourable network geometries. Hence, we could expect more dramatic location improvements when locating the entire ISC Bulletin. Although in this case we cannot measure the improvement in location accuracy due to the lack of ground truth information, we show that with the new locator we obtain significantly better clustering of event locations (Figure 10.5), thus providing an improved view of the seismicity of the Earth.

Magnitude Calculation

Currently the ISC locator calculates body and surface wave magnitudes. MS is calculated for shallow events (depth $<$ 60 km) only. At least three station magnitudes are required for a network (mb or MS) magnitude. The network magnitude is defined as the median of the station magnitudes, and its uncertainty is defined as the standard median absolute deviation (SMAD) of the alpha-trimmed (*alpha* $=$ 20%) station magnitudes.

The station magnitude is defined as the median of reading magnitudes for a station. The reading magnitude is defined as the magnitude computed from the maximal log(A/T) in a reading. Amplitude magnitudes are calculated for each reported amplitude-period pair.

Body-Wave Magnitudes

Body-wave magnitudes are calculated for each reported amplitude-period pair, provided that the phase is in the list of phases that can contribute to mb (P, pP, sP, AMB, IAmb, pmax), the station is between the epicentral distances $21 - 100°$ and the period is less than 3 s.

A reading contains all parametric data reported by a single agency for an event at a station, and it may have several reported amplitude and periods. The amplitudes are measured as zero-to-peak values in nanometres. For each pair an amplitude mb is calculated.

$$mb_{amp} = log(A/T) + Q(\Delta, h) - 3 \tag{10.1}$$

If no amplitude-period pairs are reported for a reading, the body-wave magnitude is calculated using the reported logat values for $log(A/T)$.

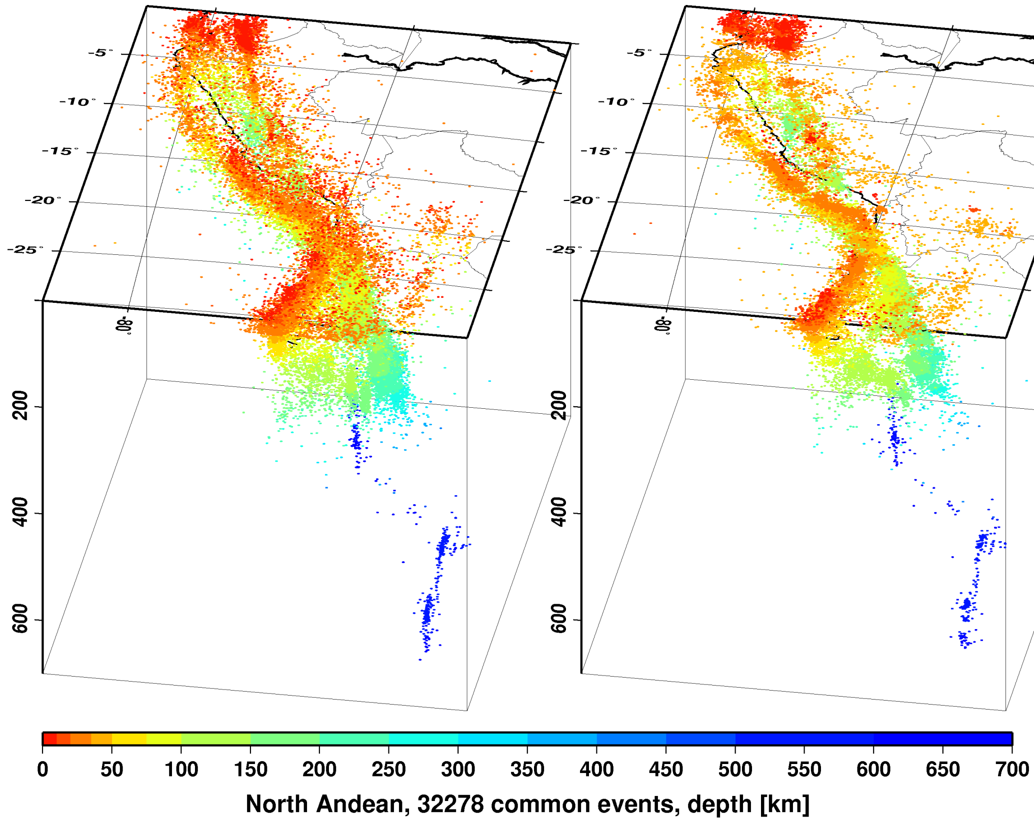

(a)

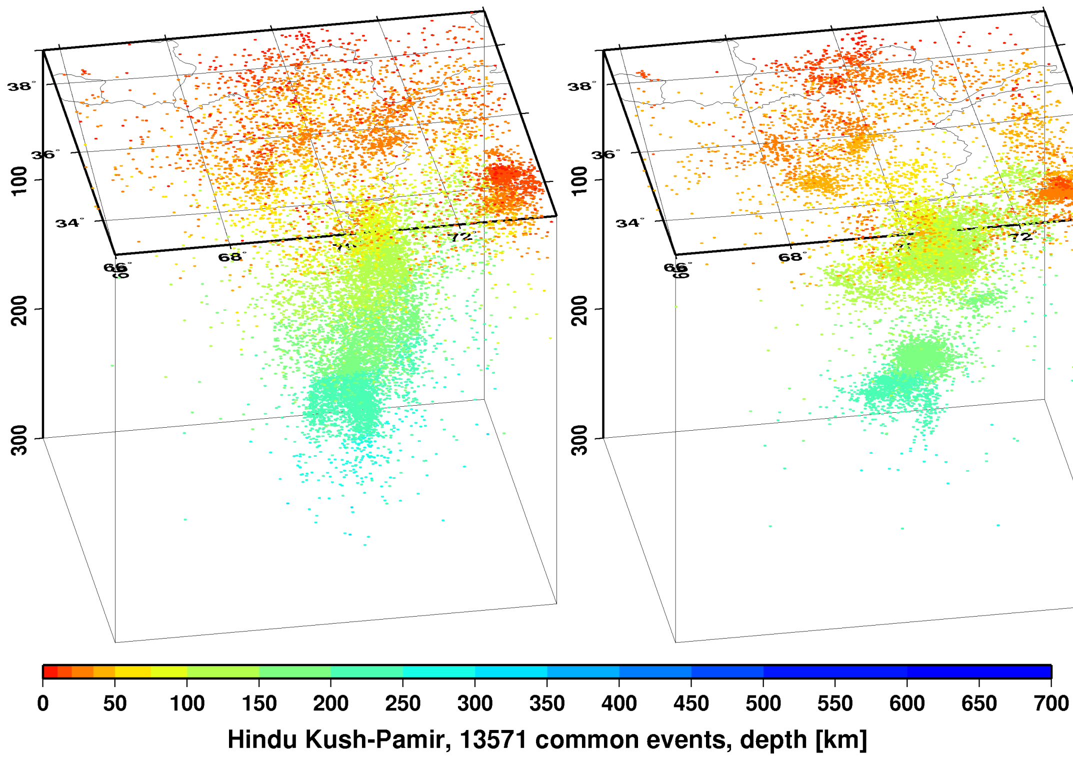

(b)

Figure 10.5: *Comparison of seismicity maps for common events in the reviewed ISC Bulletin (old locator, left) and the located ISC Bulletin (new locator, right) for the North Andean (a) and Hindu Kush - Pamir regions (b). The events are better clustered when located with the new locator.*

$$mb_{amp} = logat + Q(\Delta, h) - 3 \tag{10.2}$$

where the magnitude attenuation $Q(\Delta, h)$ value is calculated using the Gutenberg-Richter tables (*Gutenberg and Richter*, 1956).

For each reading the ISC locator finds the reported amplitude-period pair for which A/T is maximal:

$$mb_{rd} = log(max(A/T)) + Q(\Delta, h) - 3 \tag{10.3}$$

Or, if no amplitude-period pairs were reported for the reading:

$$mb_{rd} = max(logat) + Q(\Delta, h) - 3 \tag{10.4}$$

Several agencies may report data from the same station. The station magnitude is defined as the median of the reading magnitudes for a station.

$$mb_{sta} = median(mb_{rd}) \tag{10.5}$$

Once all station mb values are determined, the station magnitudes are sorted and the lower and upper alpha percentiles are made non-defining. The network mb and its uncertainty are then calculated as the median and the standard median absolute deviation (SMAD) of the alpha-trimmed station magnitudes, respectively.

Surface-Wave Magnitudes

Surface-wave magnitudes are calculated for each reported amplitude-period pair, provided that the phase is in the list of phases that can contribute to MS (*AMS, IAMs_20, LR, MLR, M, L*), the station is between the epicentral distances $20 - 160°$ and the period is between $10 - 60$ s.

For each reported amplitude-period pair MS is calculated using the Prague formula (*Vaněk et al.*, 1962). Amplitude MS is calculated for each component (Z, E, N) separately.

$$MS_{amp} = log(A/T) + 1.66 * log(\Delta) + 0.3 \tag{10.6}$$

To calculate the reading MS, the ISC locator first finds the reported amplitude-period pair for which A/T is maximal on the vertical component.

$$MS_Z = log(max(A_Z/T_Z)) + 1.66 * log(\Delta) + 0.3 \tag{10.7}$$

Then it finds the max(A/T) for the E and N components for which the period measured on the horizontal components is within ±5s from the period measured on the vertical component.

$$MS_E = log(max(A_E/T_E)) + 1.66 * log(\Delta) + 0.3 \quad (10.8)$$

$$MS_N = log(max(A_N/T_N)) + 1.66 * log(\Delta) + 0.3 \quad (10.9)$$

The horizontal MS is calculated as

$$max(A/T)h = \begin{cases} \sqrt{2(max(A_E/T_E))^2} & \text{if } MS_N \text{ does not exist} \\ \sqrt{(max(A_E/T_E))^2 + (max(A_N/T_N))^2} & \text{if } MS_E \text{ and } MS_N \text{ exist} \\ \sqrt{2(max(A_N/T_N))^2} & \text{if } MS_E \text{ does not exist} \end{cases} \quad (10.10)$$

$$MS_H = log(max(A/T)_H) + 1.66 * log(\Delta) + 0.3 \quad (10.11)$$

The reading MS is defined as

$$MS = \begin{cases} (MS_Z + MS_H)/2 & \text{if } MS_Z \text{ and } MS_H \text{ exist} \\ MS_H & \text{if } MS_Z \text{ does not exist} \\ MS_Z & \text{if } MS_H \text{ does not exist} \end{cases} \quad (10.12)$$

Several agencies may report data from the same station. The station magnitude is defined as the median of the reading magnitudes for a station.

$$MS_{sta} = median(MS_{rd}) \quad (10.13)$$

Once all station MS values are determined, the station magnitudes are sorted and the lower and upper alpha percentiles are made non-defining. The network MS and its uncertainty are calculated as the median and the standard median absolute deviation (SMAD) of the alpha-trimmed station magnitudes, respectively.

10.1.5 Review Process

Typically, for each month, the ISC analysts now review approximately 10-20% of the events in the ISC database, currently 3,500-5,000 per data month. This review is done about 24 months behind real time to allow for the comprehensive collection of data from networks and data centres worldwide.

Users of the ISC Bulletin can be assured that all ISC Bulletin events with an ISC hypocentre solution have been reviewed by the ISC analysts. Not all reviewed events will end up having an ISC hypocentre solution, but events that have not been reviewed are flagged accordingly.

At the beginning of analysis of each data month, events that need to be reviewed by an analyst are flagged based on the thresholding procedure described in Section 10.1.3. These events are split into daily blocks on average consisting of 100 – 150 to events. They are then analysed and if necessary edited by an analyst. After all blocks in a data month have been reviewed, they are being assessed again by a different analyst to spot any potential inconsistencies that might have been overlooked in the first run.

Analysis is done with the help of the Visual Bulletin Analysis System (VBAS) developed at ISC. For each event it shows the reported hypocentres, magnitudes and phase arrivals as well as an ISC solution for the hypocentre, if there is one, along with phase arrival-time residuals and error estimates. Amongst other visual aids, VBAS plots graphs of travel time curves, seismicity maps, depth distributions of reported hypocentres and station geometry.

The analysts have the capability to execute a variety of commands that can be used to merge or split events, to move phase arrivals or hypocentres from one event to another or to modify the reported phase names. There are also several commands to change the starting depth or location in the location algorithm.

The main tasks in reviewing the ISC Bulletin are to:

1. Check that the grouping of hypocentres and association of phase arrivals is appropriate.
2. Check that the depth and location is appropriate for the region and reported phase arrivals.
3. Check that no data are missing for an event, given the region and magnitude, and that included data are appropriate.
4. Examine the phase arrival-time residuals to check that the ISC hypocentre solution is appropriate.
5. Look for outliers in the observations and for misassociated phases.
6. Check that the azimuthal coverage for ISC hypocentres is at least 45 deg.

As well as examining each event closely, it is also important to scan the hypocentres and phase arrivals of adjacent events, close in time and space, to ensure that there is uniformity in the composition of the events. In some cases, two events should be merged into one event, as apparent in some other case. In other cases, one apparent event needs to be split into two events, when the automatic grouping has erroneously created one event with more than one reported hypocentre out of the observations for two real events that are distinct but closely occurring.

Misassociated phase arrivals are returned to the unassociated data stream, if not immediately placed by the analyst in another event where they belong, These unassociated phases are then available to be associated with some other event if the time and location is appropriate. The analysts also check that no phase is associated to more than one event.

Towards the end of the monthly analysis, the ISC 'Search' procedure runs, attempting to build events from the remaining set of unassociated phase arrivals. The algorithm is based on the methodology of *Engdahl and Gunst* (1966). Candidate events are validated or rejected by attempting to find ISC hypocentres for them using the ISC locator. The surviving events are then reviewed. Those events with phase arrival observations reported by stations from at least two networks are added to the ISC Bulletin if the solutions meet the standards set by the ISC analysts. These events have only an ISC determination of hypocentre.

At the end of analysis for a data month, a set of final checks is run for quality control, with the results reviewed by an analyst and the defects rectified. These are checks for inconsistencies and errors to ensure the general integrity of the ISC Bulletin.

10.1.6 Probabilistic Point Source Model (ISC-PPSM)

From data month January 2019 we have begun routinely calculating the earthquake moment tensor, source time function (STF) and depth for moderate magnitude (M_W 5.8 – 7.2) earthquakes. The resulting catalogue is refered to as ISC-PPSM (International Seismological Centre - Probabilistic Point Source Model). This point source calculation is performed using a Bayesian inversion technique based on the methods proposed by *Stähler and Sigloch* (2014; 2016). There are three main purposes of the ISC-PPSM catalogue:

1. Quantifying the uncertainties in the earthquake moment tensor.
2. Providing new constraints on the earthquake STF, along with full error estimation.
3. Adding new depth resolution, especially for relatively shallow ($<$ 40 km depth) moderate magnitude earthquakes, where surface reflected depth phases are subsumed into the earthquake STF.

The first purpose is motivated by the range of moment tensor solutions that can be reported by different agencies or methods for the same earthquake (e.g., *Lentas et al.* (2019)). It is clear that given the variability in the data and methods these different earthquake mechanisms may not be reconciled in all cases. Instead, we aim to quantify the full range of plausible earthquake mechanisms for a given event.

The second role of the ISC-PPSM catalogue is to provide new parameterised estimates of the earthquake STF. By parameterising the STF, we allow the range of plausible STFs to be assessed, but also reduce the sensitivity to near source reverberations (such as water depth phases). It is hoped that this will provide a new resource for full waveform tomographic studies, as well as earthquake physics studies.

Thirdly, and of most significance to the wider ISC operations, ISC-PPSM offers new depth resolution for remote shallow moderate magnitude earthquakes, where the depth of an ISC hypocentre would otherwise be fixed to a default or grid depth (e.g., *Bondár and Storchak* (2011)). As ISC-PPSM solves for both the earthquake depth and STF, the tradeoffs between depth and STF length are directly addressed. In cases where no free depth solution is possible, the ISC-PPSM depth can be fixed to by an analyst during the review process.

To allow the ISC-PPSM depth to be used in the main ISC review process, we calculate preliminary ISC-PPSM results ahead of the review process. For the preliminary ISC-PPSM result, the earthquake latitude and longitude are fixed to the USGS-PDE epicenter. After the main ISC review process, we recalculate the ISC-PPSM solution at the location of the reviewed ISC epicenter. After checking that the revised ISC-PPSM depths are consistent with any earthquake depths that were fixed to preliminary ISC-PPSM, we publish the revised ISC-PPSM solution. If the depths are not consistent to within 1 km, we relocate the ISC hypocentre at the revised ISC-PPSM depth.

10.1.7 History of Operational Changes

The following operational changes are listed here for historical archiving purpose. Some of them have effectively become irrelevant as a result of further changes.

- From data-month January 2001 onwards, both P and S groups of arrival times are used in location.
- From data-month September 2002 onwards, the printed ISC Bulletins have been generated directly from the ISC Relational Database.
- From data-month October 2002, a new location program ISCloc has been used in operations. Also, the IASPEI standard phase list has now been adopted by the ISC. Please see Section 10.2.1 for details.
- From data-month January 2003 onwards, an updated regionalisation scheme has been adopted (*Young et al.*, 1996).
- From data-month January 2006 the ISC hypocentres are computed using the *ak135* earth velocity model (*Kennett et al.*, 1995) and then reviewed by ISC seismologists. The ISC still produces the hypocentre solutions based on Jeffreys-Bullen travel time tables (agency code ISCJB), yet these solutions are no longer reviewed.

  Currently, the ISC is re-computing the entire ISC Bulletin as part of the Rebuild Project using *ak135* and the new location program (Section 10.1.4) in order to assure homogeneity and consistency of the data in the ISC Bulletin.
- From data-month January 2009, a new location program (*Bondár and Storchak*, 2011) has been used in operations. The new program uses all predicted *ak135* phases and accounts for correlated model errors. An overview of the location algorithm is provided in this volume (Section 10.1.4).
- As of February 2020, the ISC Bulletin for the period 1964-2010 has been completely rebuilt (*Storchak et al.*, 2017; 2020): all ISC hypocentres and magnitude have been recalculated using the algorithm by *Bondár and Storchak* (2011); many new previously unavailable datasets added based on extensive international correspondence with networks, data centres, temporary deployment managers and individual researchers; the Bulletin has been cleaned from phantom and poorly constrained events; many station readings have been added or corrected.

10.2 IASPEI Standards

10.2.1 Standard Nomenclature of Seismic Phases

The following list of seismic phases was approved by the IASPEI Commission on Seismological Observation and Interpretation (CoSOI) and adopted by IASPEI on 9th July 2003. More details can be found in *Storchak et al.* (2003) and *Storchak et al.* (2011). Ray paths for some of these phases are shown in Figures 10.6–10.11.

Crustal Phases	
Pg	At short distances, either an upgoing P wave from a source in the upper crust or a P wave bottoming in the upper crust. At larger distances also, arrivals caused by multiple P-wave reverberations inside the whole crust with a group velocity around 5.8 km/s.
Pb	Either an upgoing P wave from a source in the lower crust or a P wave bottoming in the lower crust (alt: P*)

Pn	Any P wave bottoming in the uppermost mantle or an upgoing P wave from a source in the uppermost mantle
PnPn	Pn free-surface reflection
PgPg	Pg free-surface reflection
PmP	P reflection from the outer side of the Moho
PmP*N*	PmP multiple free surface reflection; *N* is a positive integer. For example, PmP2 is PmPPmP.
PmS	P to S reflection/conversion from the outer side of the Moho
Sg	At short distances, either an upgoing S wave from a source in the upper crust or an S wave bottoming in the upper crust. At larger distances also, arrivals caused by superposition of multiple S-wave reverberations and SV to P and/or P to SV conversions inside the whole crust.
Sb	Either an upgoing S wave from a source in the lower crust or an S wave bottoming in the lower crust (alt: S*)
Sn	Any S wave bottoming in the uppermost mantle or an upgoing S wave from a source in the uppermost mantle
SnSn	Sn free-surface reflection
SgSg	Sg free-surface reflection
SmS	S reflection from the outer side of the Moho
SmS*N*	SmS multiple free-surface reflection; *N* is a positive integer. For example, SmS2 is SmSSmS.
SmP	S to P reflection/conversion from the outer side of the Moho
Lg	A wave group observed at larger regional distances and caused by superposition of multiple S-wave reverberations and SV to P and/or P to SV conversions inside the whole crust. The maximum energy travels with a group velocity of approximately 3.5 km/s
Rg	Short-period crustal Rayleigh wave

Mantle Phases

P	A longitudinal wave, bottoming below the uppermost mantle; also an upgoing longitudinal wave from a source below the uppermost mantle
PP	Free-surface reflection of P wave leaving a source downward
PS	P, leaving a source downward, reflected as an S at the free surface. At shorter distances the first leg is represented by a crustal P wave.
PPP	Analogous to PP
PPS	PP which is converted to S at the second reflection point on the free surface; travel time matches that of PSP
PSS	PS reflected at the free surface
PcP	P reflection from the core-mantle boundary (CMB)
PcS	P converted to S when reflected from the CMB
PcP*N*	PcP reflected from the free surface *N* - 1 times; *N* is a positive integer. For example PcP2 is PcPPcP.
P*z*+P	(alt: P*z*P) P reflection from outer side of a discontinuity at depth *z*; *z* may be a positive numerical value in km. For example, P660+P is a P reflection from the top of the 660 km discontinuity.
P*z*-P	P reflection from inner side of a discontinuity at depth *z*. For example, P660-P is a P reflection from below the 660 km discontinuity, which means it is precursory to PP.
P*z*+S	(alt:P*z*S) P converted to S when reflected from outer side of discontinuity at depth *z*
P*z*-S	P converted to S when reflected from inner side of discontinuity at depth *z*
PScS	P (leaving a source downward) to ScS reflection at the free surface
Pdif	P diffracted along the CMB in the mantle (old: Pdiff)
S	Shear wave, bottoming below the uppermost mantle; also an upgoing shear wave from a source below the uppermost mantle
SS	Free-surface reflection of an S wave leaving a source downward
SP	S, leaving a source downward, reflected as P at the free surface. At shorter distances the second leg is represented by a crustal P wave.
SSS	Analogous to SS

SSP	SS converted to P when reflected from the free surface; travel time matches that of SPS
SPP	SP reflected at the free surface
ScS	S reflection from the CMB
ScP	S converted to P when reflected from the CMB
ScSN	ScS multiple free-surface reflection; N is a positive integer. For example ScS2 is ScSScS.
Sz+S	S reflection from outer side of a discontinuity at depth z; z may be a positive numerical value in km. For example S660+S is an S reflection from the top of the 660 km discontinuity. (alt: SzS)
Sz-S	S reflection from inner side of discontinuity at depth z. For example, S660-S is an S reflection from below the 660 km discontinuity, which means it is precursory to SS.
Sz+P	(alt: SzP) S converted to P when reflected from outer side of discontinuity at depth z
Sz-P	S converted to P when reflected from inner side of discontinuity at depth z
ScSP	ScS to P reflection at the free surface
Sdif	S diffracted along the CMB in the mantle (old: Sdiff)

Core Phases

PKP	Unspecified P wave bottoming in the core (alt: P')
PKPab	P wave bottoming in the upper outer core; ab indicates the retrograde branch of the PKP caustic (old: PKP2)
PKPbc	P wave bottoming in the lower outer core; bc indicates the prograde branch of the PKP caustic (old: PKP1)
PKPdf	P wave bottoming in the inner core (alt: PKIKP)
PKPpre	A precursor to PKPdf due to scattering near or at the CMB (old: PKhKP)
PKPdif	P wave diffracted at the inner core boundary (ICB) in the outer core
PKS	Unspecified P wave bottoming in the core and converting to S at the CMB
PKSab	PKS bottoming in the upper outer core
PKSbc	PKS bottoming in the lower outer core
PKSdf	PKS bottoming in the inner core
P'P'	Free-surface reflection of PKP (alt: PKPPKP)
P'*N*	PKP reflected at the free surface *N* - 1 times; *N* is a positive integer. For example, P'3 is P'P'P'. (alt: PKP*N*)
P'*z*-P'	PKP reflected from inner side of a discontinuity at depth *z* outside the core, which means it is precursory to P'P'; *z* may be a positive numerical value in km
P'S'	(alt: PKPSKS) PKP converted to SKS when reflected from the free surface; other examples are P'PKS, P'SKP
PS'	P (leaving a source downward) to SKS reflection at the free surface (alt: PSKS)
PKKP	Unspecified P wave reflected once from the inner side of the CMB
PKKPab	PKKP bottoming in the upper outer core
PKKPbc	PKKP bottoming in the lower outer core
PKKPdf	PKKP bottoming in the inner core
P*N*KP	P wave reflected *N* - 1 times from inner side of the CMB; *N* is a positive integer.
PKKPpre	A precursor to PKKP due to scattering near the CMB
PKiKP	P wave reflected from the inner core boundary (ICB)
PK*N*IKP	P wave reflected *N* - 1 times from the inner side of the ICB
PKJKP	P wave traversing the outer core as P and the inner core as S
PKKS	P wave reflected once from inner side of the CMB and converted to S at the CMB
PKKSab	PKKS bottoming in the upper outer core
PKKSbc	PKKS bottoming in the lower outer core
PKKSdf	PKKS bottoming in the inner core
PcPP'	PcP to PKP reflection at the free surface; other examples are PcPS', PcSP', PcSS', PcPSKP, PcSSKP. (alt: PcPPKP)
SKS	unspecified S wave traversing the core as P (alt: S')
SKSac	SKS bottoming in the outer core
SKSdf	SKS bottoming in the inner core (alt: SKIKS)
SPdifKS	SKS wave with a segment of mantleside Pdif at the source and/or the receiver side of the ray path (alt: SKPdifS)
SKP	Unspecified S wave traversing the core and then the mantle as P
SKPab	SKP bottoming in the upper outer core
SKPbc	SKP bottoming in the lower outer core
SKPdf	SKP bottoming in the inner core
S'S'	Free-surface reflection of SKS (alt: SKSSKS)
S'*N*	SKS reflected at the free surface *N* - 1 times; *N* is a positive integer
S'*z*-S'	SKS reflected from inner side of discontinuity at depth *z* outside the core, which means it is precursory to S'S'; *z* may be a positive numerical value in km.
S'P'	(alt: SKSPKP) SKS converted to PKP when reflected from the free surface; other examples are S'SKP, S'PKS.
S'P	(alt: SKSP) SKS to P reflection at the free surface
SKKS	Unspecified S wave reflected once from inner side of the CMB
SKKSac	SKKS bottoming in the outer core
SKKSdf	SKKS bottoming in the inner core
S*N*KS	S wave reflected *N* - 1 times from inner side of the CMB; *N* is a positive integer.

SKiKS	S wave traversing the outer core as P and reflected from the ICB
SKJKS	S wave traversing the outer core as P and the inner core as S
SKKP	S wave traversing the core as P with one reflection from the inner side of the CMB and then continuing as P in the mantle
SKKPab	SKKP bottoming in the upper outer core
SKKPbc	SKKP bottoming in the lower outer core
SKKPdf	SKKP bottoming in the inner core
ScSS'	ScS to SKS reflection at the free surface; other examples are ScPS', ScSP', ScPP', ScSSKP, ScPSKP. (alt: ScSSKS)

Near-source Surface reflections (Depth Phases)

pP*y*	All P-type onsets (P*y*), as defined above, which resulted from reflection of an upgoing P wave at the free surface or an ocean bottom. WARNING: The character *y* is only a wild card for any seismic phase, which could be generated at the free surface. Examples are pP, pPKP, pPP, pPcP, etc.
sP*y*	All P*y* resulting from reflection of an upgoing S wave at the free surface or an ocean bottom; for example, sP, sPKP, sPP, sPcP, etc.
pS*y*	All S-type onsets (S*y*), as defined above, which resulted from reflection of an upgoing P wave at the free surface or an ocean bottom; for example, pS, pSKS, pSS, pScP, etc.
sS*y*	All S*y* resulting from reflection of an upgoing S wave at the free surface or an ocean bottom; for example, sSn, sSS, sScS, sSdif, etc.
pwP*y*	All P*y* resulting from reflection of an upgoing P wave at the ocean's free surface
pmP*y*	All P*y* resulting from reflection of an upgoing P wave from the inner side of the Moho

Surface Waves

L	Unspecified long-period surface wave
LQ	Love wave
LR	Rayleigh wave
G	Mantle wave of Love type
G*N*	Mantle wave of Love type; *N* is integer and indicates wave packets traveling along the minor arcs (odd numbers) or major arc (even numbers) of the great circle
R	Mantle wave of Rayleigh type
R*N*	Mantle wave of Rayleigh type; *N* is integer and indicates wave packets traveling along the minor arcs (odd numbers) or major arc (even numbers) of the great circle
PL	Fundamental leaking mode following P onsets generated by coupling of P energy into the waveguide formed by the crust and upper mantle SPL S wave coupling into the PL waveguide; other examples are SSPL, SSSPL.

Acoustic Phases

H	A hydroacoustic wave from a source in the water, which couples in the ground
HPg	H phase converted to Pg at the receiver side
HSg	H phase converted to Sg at the receiver side
HRg	H phase converted to Rg at the receiver side
I	An atmospheric sound arrival which couples in the ground
IPg	I phase converted to Pg at the receiver side
ISg	I phase converted to Sg at the receiver side
IRg	I phase converted to Rg at the receiver side
T	A tertiary wave. This is an acoustic wave from a source in the solid earth, usually trapped in a low-velocity oceanic water layer called the SOFAR channel (SOund Fixing And Ranging).
TPg	T phase converted to Pg at the receiver side
TSg	T phase converted to Sg at the receiver side
TRg	T phase converted to Rg at the receiver side

Amplitude Measurement Phases

The following set of amplitude measurement names refers to the IASPEI Magnitude Standard (see www.iaspei.org/commissions/CSOI/Summary_of_WG_recommendations.pdf) compliance to which is indicated by the presence of leading letter I. The absence of leading letter I indicates that a measurement is non-standard. Letter A indicates a measurement in nm made on a displacement seismogram, whereas letter V indicates a measurement in nm/s made on a velocity seismogram.

IAML	Displacement amplitude measured according to the IASPEI standard for local magnitude ML
IAMs_20	Displacement amplitude measured according to IASPEI standard for surface-wave magnitude $MS(20)$
IVMs_BB	Velocity amplitude measured according to IASPEI standard for broadband surface-wave magnitude $MS(BB)$
IAmb	Displacement amplitude measured according to IASPEI standard for short-period teleseismic body-wave magnitude mb
IVmB_BB	Velocity amplitude measured according to IASPEI standard for broadband teleseismic body-wave magnitude $mB(BB)$
AX_IN	Displacement amplitude of phase of type X (e.g., PP, S, etc), measured on an instrument of type IN (e.g., SP - short-period, LP - long-period, BB - broadband)
VX_IN	Velocity amplitude of phase of type X and instrument of type IN (as above)
A	Unspecified displacement amplitude measurement
V	Unspecified velocity amplitude measurement
AML	Displacement amplitude measurement for nonstandard local magnitude
AMs	Displacement amplitude measurement for nonstandard surface-wave magnitude
Amb	Displacement amplitude measurement for nonstandard short-period body-wave magnitude
AmB	Displacement amplitude measurement for nonstandard medium to long-period body-wave magnitude
END	Time of visible end of record for duration magnitude

Unidentified Arrivals

x	unidentified arrival (old: i, e, NULL)
rx	unidentified regional arrival (old: i, e, NULL)
tx	unidentified teleseismic arrival (old: i, e, NULL)
Px	unidentified arrival of P type (old: i, e, NULL, (P), P?)
Sx	unidentified arrival of S type (old: i, e, NULL, (S), S?)

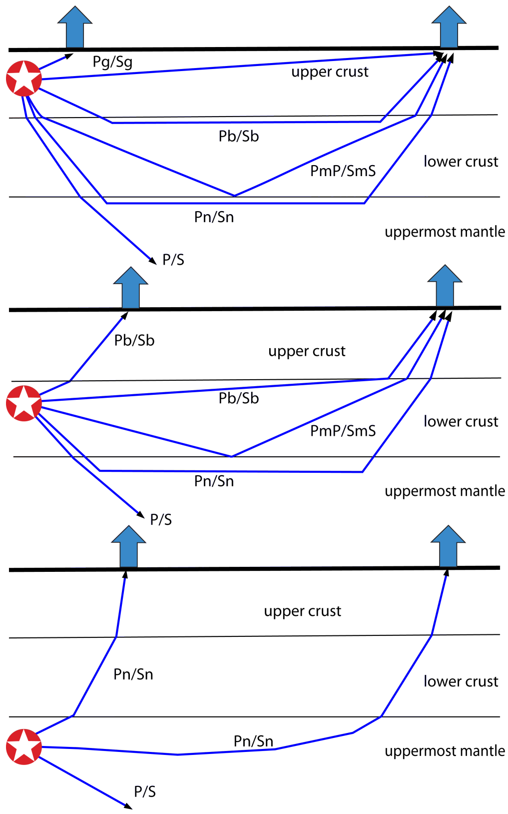

Figure 10.6: *Seismic 'crustal phases' observed in the case of a two-layer crust in local and regional distance ranges (0°<D< about 20°) from the seismic source in the: upper crust (top); lower crust (middle); and uppermost mantle (bottom).*

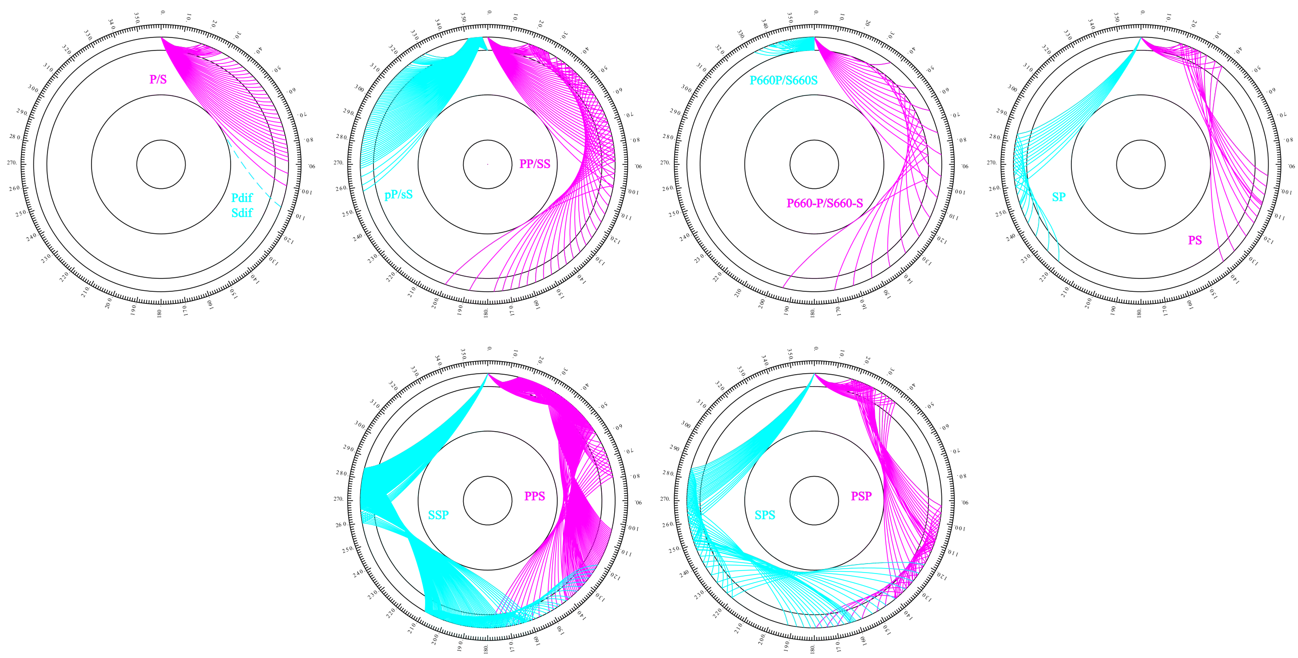

Figure 10.7: *Mantle phases observed at the teleseismic distance range D > about 20°.*

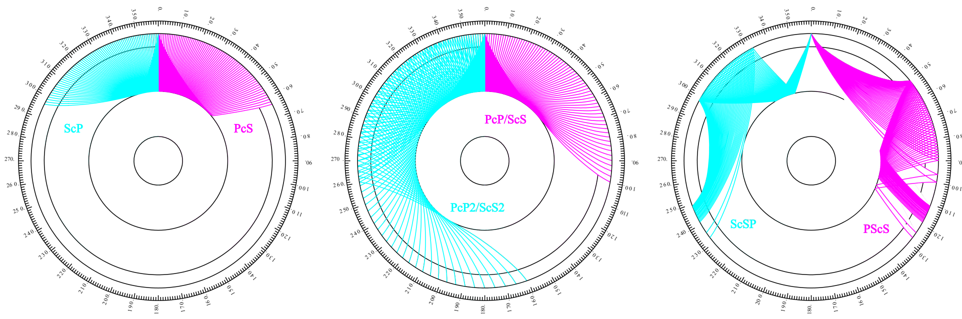

Figure 10.8: *Reflections from the Earth's core.*

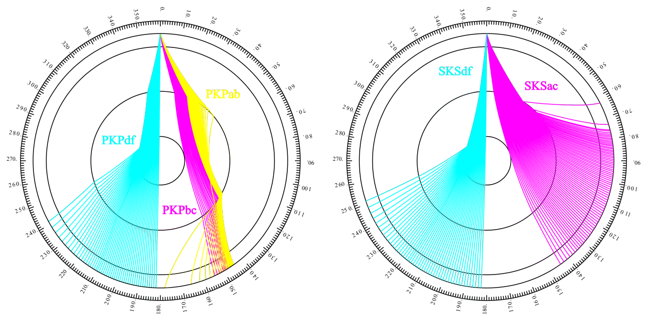

Figure 10.9: *Seismic rays of direct core phases.*

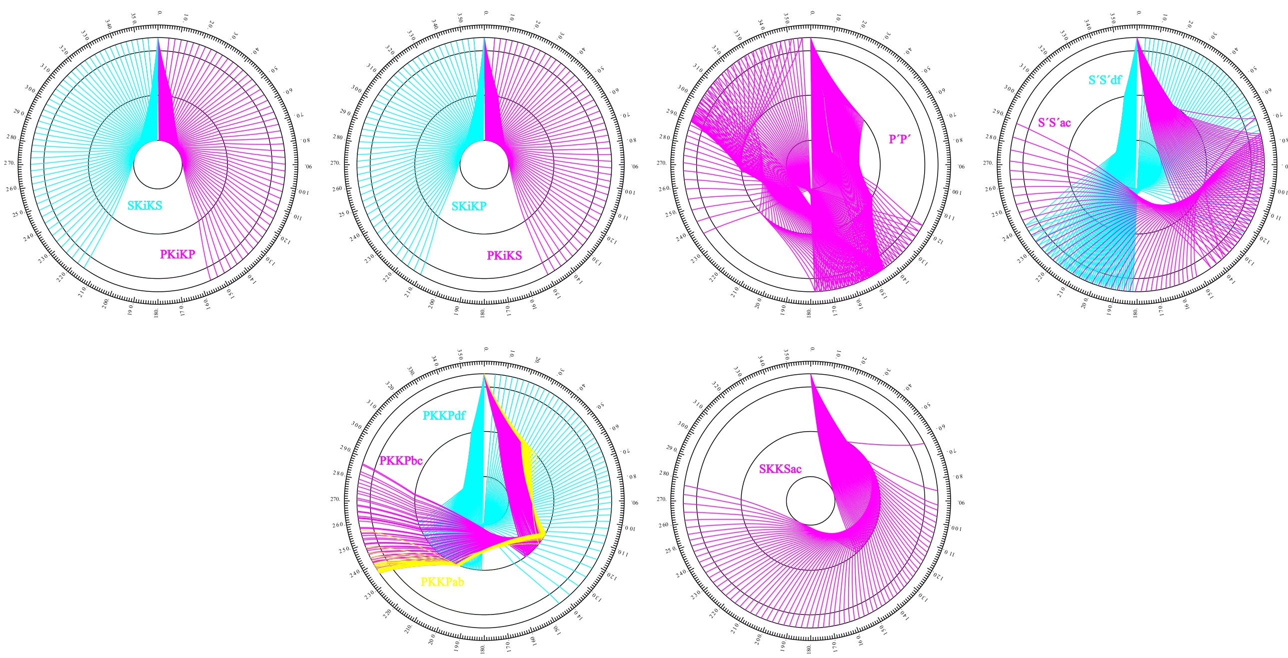

Figure 10.10: *Seismic rays of single-reflected core phases.*

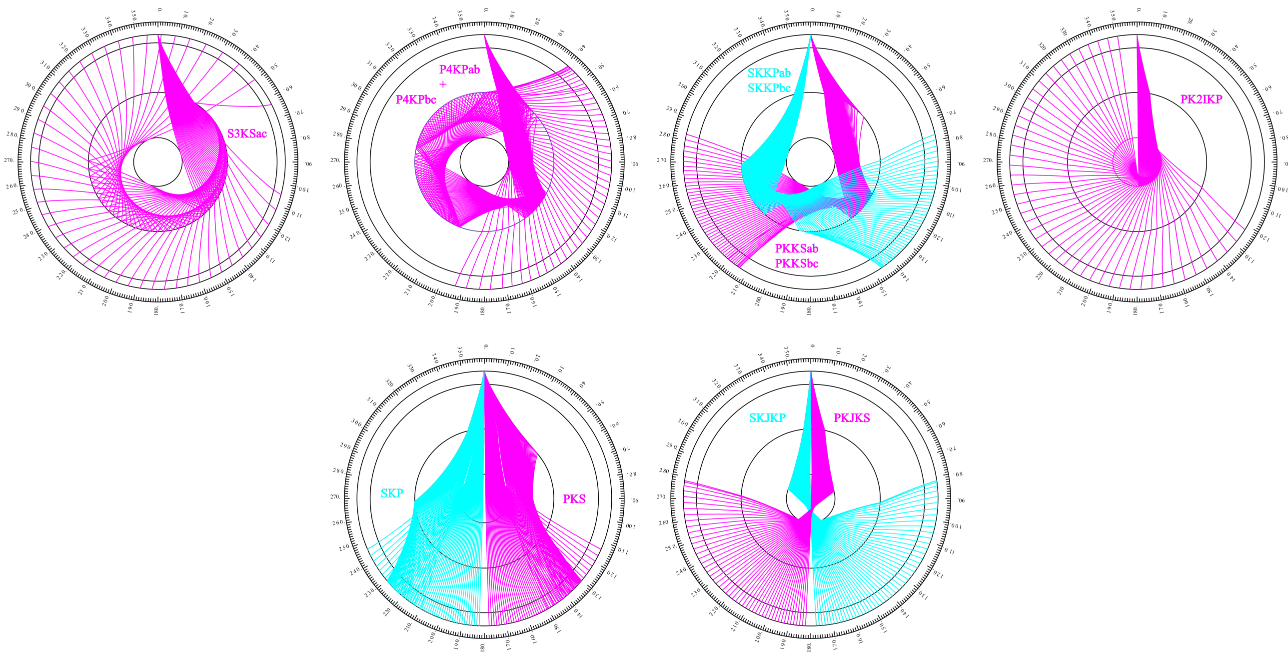

Figure 10.11: *Seismic rays of multiple-reflected and converted core phases.*

10.2.2 Flinn-Engdahl Regions

The Flinn-Engdahl regions were first proposed by *Flinn and Engdahl* (1965), with the standard defined by *Flinn et al.* (1974). The latest version of the schema, published by *Young et al.* (1996), divides the Earth into 50 seismic regions (Figure 10.12), which are further subdivided producing a total of 754 geographical regions (listed below). The geographic regions are numbered 1 to 757 with regions 172, 299 and 550 no longer in use. The boundaries of these regions are defined at one-degree intervals.

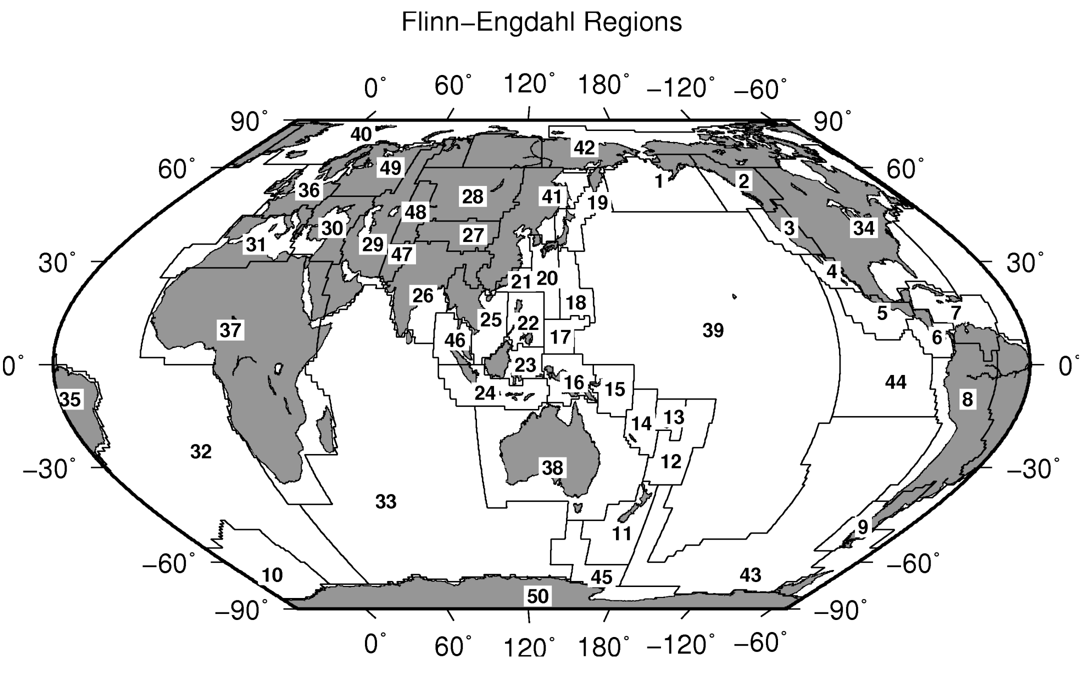

Figure 10.12: *Map of all Flinn-Engdahl seismic regions.*

Seismic Region 1
Alaska-Aleutian Arc
1. Central Alaska
2. Southern Alaska
3. Bering Sea
4. Komandorsky Islands region
5. Near Islands
6. Rat Islands
7. Andreanof Islands
8. Pribilof Islands
9. Fox Islands
10. Unimak Island region
11. Bristol Bay
12. Alaska Peninsula
13. Kodiak Island region
14. Kenai Peninsula
15. Gulf of Alaska
16. South of Aleutian Islands
17. South of Alaska

Seismic Region 2
Eastern Alaska to Vancouver Island
18. Southern Yukon Territory
19. Southeastern Alaska
20. Off coast of southeastern Alaska
21. West of Vancouver Island
22. Queen Charlotte Islands region
23. British Columbia
24. Alberta
25. Vancouver Island region
26. Off coast of Washington
27. Near coast of Washington
28. Washington-Oregon border region
29. Washington

Seismic Region 3
California-Nevada Region
30. Off coast of Oregon
31. Near coast of Oregon
32. Oregon
33. Western Idaho
34. Off coast of northern California
35. Near coast of northern California
36. Northern California
37. Nevada
38. Off coast of California
39. Central California
40. California-Nevada border region
41. Southern Nevada
42. Western Arizona
43. Southern California
44. California-Arizona border region
45. California-Baja California border region
46. Western Arizona-Sonora border region

Seismic Region 4
Lower California and Gulf of California
47. Off west coast of Baja California
48. Baja California
49. Gulf of California
50. Sonora
51. Off coast of central Mexico
52. Near coast of central Mexico

Seismic Region 5
Mexico-Guatemala Area
53. Revilla Gigedo Islands region
54. Off coast of Jalisco
55. Near coast of Jalisco
56. Near coast of Michoacan
57. Michoacan
58. Near coast of Guerrero
59. Guerrero
60. Oaxaca
61. Chiapas
62. Mexico-Guatemala border region
63. Off coast of Mexico
64. Off coast of Michoacan
65. Off coast of Guerrero
66. Near coast of Oaxaca
67. Off coast of Oaxaca
68. Off coast of Chiapas
69. Near coast of Chiapas
70. Guatemala
71. Near coast of Guatemala
730. Northern East Pacific Rise

Seismic Region 6
Central America
72. Honduras
73. El Salvador
74. Near coast of Nicaragua
75. Nicaragua
76. Off coast of central America
77. Off coast of Costa Rica
78. Costa Rica
79. North of Panama
80. Panama-Costa Rica border region
81. Panama
82. Panama-Colombia border region
83. South of Panama

Seismic Region 7
Caribbean Loop
84. Yucatan Peninsula
85. Cuba region
86. Jamaica region
87. Haiti region
88. Dominican Republic region
89. Mona Passage
90. Puerto Rico region
91. Virgin Islands
92. Leeward Islands
93. Belize
94. Caribbean Sea
95. Windward Islands
96. Near north coast of Colombia
97. Near coast of Venezuela
98. Trinidad
99. Northern Colombia
100. Lake Maracaibo
101. Venezuela
731. North of Honduras

Seismic Region 8
Andean South America
102. Near west coast of Colombia
103. Colombia
104. Off coast of Ecuador
105. Near coast of Ecuador
106. Colombia-Ecuador border region
107. Ecuador
108. Off coast of northern Peru
109. Near coast of northern Peru
110. Peru-Ecuador border region
111. Northern Peru
112. Peru-Brazil border region
113. Western Brazil
114. Off coast of Peru
115. Near coast of Peru
116. Central Peru
117. Southern Peru
118. Peru-Bolivia border region
119. Northern Bolivia
120. Central Bolivia
121. Off coast of northern Chile
122. Near coast of northern Chile
123. Northern Chile
124. Chile-Bolivia border region
125. Southern Bolivia
126. Paraguay
127. Chile-Argentina border region
128. Jujuy Province
129. Salta Province
130. Catamarca Province
131. Tucuman Province
132. Santiago del Estero Province
133. Northeastern Argentina
134. Off coast of central Chile
135. Near coast of central Chile
136. Central Chile
137. San Juan Province
138. La Rioja Province
139. Mendoza Province

140. San Luis Province
141. Cordoba Province
142. Uruguay

Seismic Region 9
Extreme South America
143. Off coast of southern Chile
144. Southern Chile
145. Southern Chile-Argentina border region
146. Southern Argentina

Seismic Region 10
Southern Antilles
147. Tierra del Fuego
148. Falkland Islands region
149. Drake Passage
150. Scotia Sea
151. South Georgia Island region
152. South Georgia Rise
153. South Sandwich Islands region
154. South Shetland Islands
155. Antarctic Peninsula
156. Southwestern Atlantic Ocean
157. Weddell Sea
732. East of South Sandwich Islands

Seismic Region 11
New Zealand Region
158. Off west coast of North Island
159. North Island
160. Off east coast of North Island
161. Off west coast of South Island
162. South Island
163. Cook Strait
164. Off east coast of South Island
165. North of Macquarie Island
166. Auckland Islands region
167. Macquarie Island region
168. South of New Zealand

Seismic Region 12
Kermadec-Tonga-Samoa Area
169. Samoa Islands region
170. Samoa Islands
171. South of Fiji Islands
172. West of Tonga Islands (REGION NOT IN USE)
173. Tonga Islands
174. Tonga Islands region
175. South of Tonga Islands
176. North of New Zealand
177. Kermadec Islands region
178. Kermadec Islands
179. South of Kermadec Islands

Seismic Region 13
Fiji Area
180. North of Fiji Islands
181. Fiji Islands region
182. Fiji Islands

Seismic Region 14
Vanuatu (New Hebrides)
183. Santa Cruz Islands region
184. Santa Cruz Islands
185. Vanuatu Islands region
186. Vanuatu Islands
187. New Caledonia
188. Loyalty Islands
189. Southeast of Loyalty Islands

Seismic Region 15
Bismarck and Solomon Islands
190. New Ireland region
191. North of Solomon Islands
192. New Britain region
193. Bougainville-Solomon Islands region
194. D'Entrecasteaux Islands region
195. South of Solomon Islands

Seismic Region 16
New Guinea
196. Irian Jaya region
197. Near north coast of Irian Jaya
198. Ninigo Islands region
199. Admiralty Islands region
200. Near north coast of New Guinea
201. Irian Jaya
202. New Guinea
203. Bismarck Sea
204. Aru Islands region
205. Near south coast of Irian Jaya
206. Near south coast of New Guinea
207. Eastern New Guinea region
208. Arafura Sea

Seismic Region 17
Caroline Islands to Guam
209. Western Caroline Islands
210. South of Mariana Islands

Seismic Region 18
Guam to Japan
211. Southeast of Honshu
212. Bonin Islands region
213. Volcano Islands region
214. West of Mariana Islands
215. Mariana Islands region
216. Mariana Islands

Seismic Region 19
Japan-Kurils-Kamchatka
217. Kamchatka Peninsula
218. Near east coast of Kamchatka Peninsula
219. Off east coast of Kamchatka Peninsula
220. Northwest of Kuril Islands
221. Kuril Islands
222. East of Kuril Islands
223. Eastern Sea of Japan
224. Hokkaido region
225. Off southeast coast of Hokkaido
226. Near west coast of eastern Honshu
227. Eastern Honshu
228. Near east coast of eastern Honshu
229. Off east coast of Honshu
230. Near south coast of eastern Honshu

Seismic Region 20
Southwestern Japan and Ryukyu Islands
231. South Korea
232. Western Honshu
233. Near south coast of western Honshu
234. Northwest of Ryukyu Islands
235. Kyushu
236. Shikoku
237. Southeast of Shikoku
238. Ryukyu Islands
239. Southeast of Ryukyu Islands
240. West of Bonin Islands
241. Philippine Sea

Seismic Region 21
Taiwan
242. Near coast of southeastern China
243. Taiwan region
244. Taiwan
245. Northeast of Taiwan
246. Southwestern Ryukyu Islands
247. Southeast of Taiwan

Seismic Region 22
Philippines
248. Philippine Islands region
249. Luzon
250. Mindoro
251. Samar
252. Palawan
253. Sulu Sea
254. Panay

255. Cebu
256. Leyte
257. Negros
258. Sulu Archipelago
259. Mindanao
260. East of Philippine Islands

Seismic Region 23
Borneo-Sulawesi
261. Borneo
262. Celebes Sea
263. Talaud Islands
264. North of Halmahera
265. Minahassa Peninsula, Sulawesi
266. Northern Molucca Sea
267. Halmahera
268. Sulawesi
269. Southern Molucca Sea
270. Ceram Sea
271. Buru
272. Seram

Seismic Region 24
Sunda Arc
273. Southwest of Sumatera
274. Southern Sumatera
275. Java Sea
276. Sunda Strait
277. Jawa
278. Bali Sea
279. Flores Sea
280. Banda Sea
281. Tanimbar Islands region
282. South of Jawa
283. Bali region
284. South of Bali
285. Sumbawa region
286. Flores region
287. Sumba region
288. Savu Sea
289. Timor region
290. Timor Sea
291. South of Sumbawa
292. South of Sumba
293. South of Timor

Seismic Region 25
Myanmar and Southeast Asia
294. Myanmar-India border region
295. Myanmar-Bangladesh border region
296. Myanmar
297. Myanmar-China border region
298. Near south coast of Myanmar
299. Southeast Asia (REGION NOT IN USE)
300. Hainan Island
301. South China Sea
733. Thailand
734. Laos
735. Kampuchea
736. Vietnam
737. Gulf of Tongking

Seismic Region 26
India-Xizang-Szechwan-Yunnan
302. Eastern Kashmir
303. Kashmir-India border region
304. Kashmir-Xizang border region
305. Western Xizang-India border region
306. Xizang
307. Sichuan
308. Northern India
309. Nepal-India border region
310. Nepal
311. Sikkim
312. Bhutan
313. Eastern Xizang-India border region
314. Southern India
315. India-Bangladesh border region
316. Bangladesh
317. Northeastern India
318. Yunnan
319. Bay of Bengal

Seismic Region 27
Southern Xinjiang to Gansu
320. Kyrgyzstan-Xinjiang border region
321. Southern Xinjiang
322. Gansu
323. Western Nei Mongol
324. Kashmir-Xinjiang border region
325. Qinghai

Seismic Region 28
Alma-Ata to Lake Baikal
326. Southwestern Siberia
327. Lake Baykal region
328. East of Lake Baykal
329. Eastern Kazakhstan
330. Lake Issyk-Kul region
331. Kazakhstan-Xinjiang border region
332. Northern Xinjiang
333. Tuva-Buryatia-Mongolia border region
334. Mongolia

Seismic Region 29
Western Asia
335. Ural Mountains region
336. Western Kazakhstan
337. Eastern Caucasus
338. Caspian Sea
339. Northwestern Uzbekistan
340. Turkmenistan
341. Iran-Turkmenistan border region
342. Turkmenistan-Afghanistan border region
343. Turkey-Iran border region
344. Iran-Armenia-Azerbaijan border region
345. Northwestern Iran
346. Iran-Iraq border region
347. Western Iran
348. Northern and central Iran
349. Northwestern Afghanistan
350. Southwestern Afghanistan
351. Eastern Arabian Peninsula
352. Persian Gulf
353. Southern Iran
354. Southwestern Pakistan
355. Gulf of Oman
356. Off coast of Pakistan

Seismic Region 30
Middle East-Crimea-Eastern Balkans
357. Ukraine-Moldova-Southwestern Russia region
358. Romania
359. Bulgaria
360. Black Sea
361. Crimea region
362. Western Caucasus
363. Greece-Bulgaria border region
364. Greece
365. Aegean Sea
366. Turkey
367. Turkey-Georgia-Armenia border region
368. Southern Greece
369. Dodecanese Islands
370. Crete
371. Eastern Mediterranean Sea
372. Cyprus region
373. Dead Sea region
374. Jordan-Syria region
375. Iraq

Seismic Region 31
Western Mediterranean Area
376. Portugal
377. Spain

378. Pyrenees
379. Near south coast of France
380. Corsica
381. Central Italy
382. Adriatic Sea
383. Northwestern Balkan Peninsula
384. West of Gibraltar
385. Strait of Gibraltar
386. Balearic Islands
387. Western Mediterranean Sea
388. Sardinia
389. Tyrrhenian Sea
390. Southern Italy
391. Albania
392. Greece-Albania border region
393. Madeira Islands region
394. Canary Islands region
395. Morocco
396. Northern Algeria
397. Tunisia
398. Sicily
399. Ionian Sea
400. Central Mediterranean Sea
401. Near coast of Libya

Seismic Region 32
Atlantic Ocean

402. North Atlantic Ocean
403. Northern Mid-Atlantic Ridge
404. Azores Islands region
405. Azores Islands
406. Central Mid-Atlantic Ridge
407. North of Ascension Island
408. Ascension Island region
409. South Atlantic Ocean
410. Southern Mid-Atlantic Ridge
411. Tristan da Cunha region
412. Bouvet Island region
413. Southwest of Africa
414. Southeastern Atlantic Ocean
738. Reykjanes Ridge
739. Azores-Cape St. Vincent Ridge

Seismic Region 33
Indian Ocean

415. Eastern Gulf of Aden
416. Socotra region
417. Arabian Sea
418. Lakshadweep region
419. Northeastern Somalia
420. North Indian Ocean
421. Carlsberg Ridge
422. Maldive Islands region
423. Laccadive Sea
424. Sri Lanka
425. South Indian Ocean
426. Chagos Archipelago region
427. Mauritius-Reunion region
428. Southwest Indian Ridge
429. Mid-Indian Ridge
430. South of Africa
431. Prince Edward Islands region
432. Crozet Islands region
433. Kerguelen Islands region
434. Broken Ridge
435. Southeast Indian Ridge
436. Southern Kerguelen Plateau
437. South of Australia
740. Owen Fracture Zone region
741. Indian Ocean Triple Junction
742. Western Indian-Antarctic Ridge

Seismic Region 34
Eastern North America

438. Saskatchewan
439. Manitoba
440. Hudson Bay
441. Ontario
442. Hudson Strait region
443. Northern Quebec
444. Davis Strait
445. Labrador
446. Labrador Sea
447. Southern Quebec
448. Gaspe Peninsula
449. Eastern Quebec
450. Anticosti Island
451. New Brunswick
452. Nova Scotia
453. Prince Edward Island
454. Gulf of St. Lawrence
455. Newfoundland
456. Montana
457. Eastern Idaho
458. Hebgen Lake region, Montana
459. Yellowstone region
460. Wyoming
461. North Dakota
462. South Dakota
463. Nebraska
464. Minnesota
465. Iowa
466. Wisconsin
467. Illinois
468. Michigan
469. Indiana
470. Southern Ontario
471. Ohio
472. New York
473. Pennsylvania
474. Vermont-New Hampshire region
475. Maine
476. Southern New England
477. Gulf of Maine
478. Utah
479. Colorado
480. Kansas
481. Iowa-Missouri border region
482. Missouri-Kansas border region
483. Missouri
484. Missouri-Arkansas border region
485. Missouri-Illinois border region
486. New Madrid region, Missouri
487. Cape Girardeau region, Missouri
488. Southern Illinois
489. Southern Indiana
490. Kentucky
491. West Virginia
492. Virginia
493. Chesapeake Bay region
494. New Jersey
495. Eastern Arizona
496. New Mexico
497. Northwestern Texas-Oklahoma border region
498. Western Texas
499. Oklahoma
500. Central Texas
501. Arkansas-Oklahoma border region
502. Arkansas
503. Louisiana-Texas border region
504. Louisiana
505. Mississippi
506. Tennessee
507. Alabama
508. Western Florida
509. Georgia
510. Florida-Georgia border region
511. South Carolina
512. North Carolina
513. Off east coast of United States
514. Florida Peninsula
515. Bahama Islands
516. Eastern Arizona-Sonora border region
517. New Mexico-Chihuahua border region
518. Texas-Mexico border region
519. Southern Texas
520. Near coast of Texas
521. Chihuahua
522. Northern Mexico
523. Central Mexico
524. Jalisco
525. Veracruz
526. Gulf of Mexico
527. Bay of Campeche

Seismic Region 35
Eastern South America
528. Brazil
529. Guyana
530. Suriname
531. French Guiana

Seismic Region 36
Northwestern Europe
532. Eire
533. United Kingdom
534. North Sea
535. Southern Norway
536. Sweden
537. Baltic Sea
538. France
539. Bay of Biscay
540. The Netherlands
541. Belgium
542. Denmark
543. Germany
544. Switzerland
545. Northern Italy
546. Austria
547. Czech and Slovak Republics
548. Poland
549. Hungary

Seismic Region 37
Africa
550. Northwest Africa (REGION NOT IN USE)
551. Southern Algeria
552. Libya
553. Egypt
554. Red Sea
555. Western Arabian Peninsula
556. Chad region
557. Sudan
558. Ethiopia
559. Western Gulf of Aden
560. Northwestern Somalia
561. Off south coast of northwest Africa
562. Cameroon
563. Equatorial Guinea
564. Central African Republic
565. Gabon
566. Congo
567. Zaire
568. Uganda
569. Lake Victoria region
570. Kenya
571. Southern Somalia
572. Lake Tanganyika region
573. Tanzania
574. Northwest of Madagascar
575. Angola
576. Zambia
577. Malawi
578. Namibia
579. Botswana
580. Zimbabwe
581. Mozambique
582. Mozambique Channel
583. Madagascar
584. South Africa
585. Lesotho
586. Swaziland
587. Off coast of South Africa
743. Western Sahara
744. Mauritania
745. Mali
746. Senegal-Gambia region
747. Guinea region
748. Sierra Leone
749. Liberia region
750. Cote d'Ivoire
751. Burkina Faso
752. Ghana
753. Benin-Togo region
754. Niger
755. Nigeria

Seismic Region 38
Australia
588. Northwest of Australia
589. West of Australia
590. Western Australia
591. Northern Territory
592. South Australia
593. Gulf of Carpentaria
594. Queensland
595. Coral Sea
596. Northwest of New Caledonia
597. New Caledonia region
598. Southwest of Australia
599. Off south coast of Australia
600. Near coast of South Australia
601. New South Wales
602. Victoria
603. Near southeast coast of Australia
604. Near east coast of Australia
605. East of Australia
606. Norfolk Island region
607. Northwest of New Zealand
608. Bass Strait
609. Tasmania region
610. Southeast of Australia

Seismic Region 39
Pacific Basin
611. North Pacific Ocean
612. Hawaiian Islands region
613. Hawaiian Islands
614. Eastern Caroline Islands region
615. Marshall Islands region
616. Enewetak Atoll region
617. Bikini Atoll region
618. Gilbert Islands region
619. Johnston Island region
620. Line Islands region
621. Palmyra Island region
622. Kiritimati region
623. Tuvalu region
624. Phoenix Islands region
625. Tokelau Islands region
626. Northern Cook Islands
627. Cook Islands region
628. Society Islands region
629. Tubuai Islands region
630. Marquesas Islands region
631. Tuamotu Archipelago region
632. South Pacific Ocean

Seismic Region 40
Arctic Zone
633. Lomonosov Ridge
634. Arctic Ocean
635. Near north coast of Kalaallit Nunaat
636. Eastern Kalaallit Nunaat
637. Iceland region
638. Iceland
639. Jan Mayen Island region
640. Greenland Sea
641. North of Svalbard
642. Norwegian Sea
643. Svalbard region
644. North of Franz Josef Land
645. Franz Josef Land
646. Northern Norway
647. Barents Sea
648. Novaya Zemlya
649. Kara Sea
650. Near coast of northwestern Siberia
651. North of Severnaya Zemlya
652. Severnaya Zemlya
653. Near coast of northern Siberia
654. East of Severnaya Zemlya
655. Laptev Sea

Seismic Region 41
Eastern Asia
656. Southeastern Siberia
657. Priamurye-Northeastern China border region
658. Northeastern China
659. North Korea

660. Sea of Japan
661. Primorye
662. Sakhalin Island
663. Sea of Okhotsk
664. Southeastern China
665. Yellow Sea
666. Off east coast of southeastern China

Seismic Region 42
Northeastern Asia, Northern Alaska to Greenland

667. North of New Siberian Islands
668. New Siberian Islands
669. Eastern Siberian Sea
670. Near north coast of eastern Siberia
671. Eastern Siberia
672. Chukchi Sea
673. Bering Strait
674. St. Lawrence Island region
675. Beaufort Sea
676. Northern Alaska
677. Northern Yukon Territory
678. Queen Elizabeth Islands
679. Northwest Territories
680. Western Kalaallit Nunaat
681. Baffin Bay
682. Baffin Island region

Seismic Region 43
Southeastern and Antarctic Pacific Ocean

683. Southeastcentral Pacific Ocean
684. Southern East Pacific Rise
685. Easter Island region
686. West Chile Rise
687. Juan Fernandez Islands region
688. East of North Island
689. Chatham Islands region
690. South of Chatham Islands
691. Pacific-Antarctic Ridge
692. Southern Pacific Ocean
756. Southeast of Easter Island

Seismic Region 44
Galapagos Area

693. Eastcentral Pacific Ocean
694. Central East Pacific Rise
695. West of Galapagos Islands
696. Galapagos Islands region
697. Galapagos Islands
698. Southwest of Galapagos Islands
699. Southeast of Galapagos Islands
757. Galapagos Triple Junction region

Seismic Region 45
Macquarie Loop

700. South of Tasmania
701. West of Macquarie Island
702. Balleny Islands region

Seismic Region 46
Andaman Islands to Sumatera

703. Andaman Islands region
704. Nicobar Islands region
705. Off west coast of northern Sumatera
706. Northern Sumatera
707. Malay Peninsula
708. Gulf of Thailand

Seismic Region 47
Baluchistan

709. Southeastern Afghanistan
710. Pakistan
711. Southwestern Kashmir
712. India-Pakistan border region

Seismic Region 48
Hindu Kush and Pamir

713. Central Kazakhstan
714. Southeastern Uzbekistan
715. Tajikistan
716. Kyrgyzstan
717. Afghanistan-Tajikistan border region
718. Hindu Kush region
719. Tajikistan-Xinjiang border region
720. Northwestern Kashmir

Seismic Region 49
Northern Eurasia

721. Finland
722. Norway-Murmansk border region
723. Finland-Karelia border region
724. Baltic States-Belarus-Northwestern Russia
725. Northwestern Siberia
726. Northern and central Siberia

Seismic Region 50
Antarctica

727. Victoria Land
728. Ross Sea
729. Antarctica

10.2.3 IASPEI Magnitudes

The ISC publishes a diversity of magnitude data. Although trying to be as complete and specific as possible, preference is now given to magnitudes determined according to standard procedures recommended by the Working Group on Magnitude Measurements of the IASPEI Commission on Seismological Observation and Interpretation (CoSOI). So far, such standards have been agreed upon for the local magnitude ML, the local-regional mb_Lg, and for two types each of body-wave (mb and mB_BB) and surface-wave magnitudes (Ms_20 and Ms_BB). With the exception of ML, all other standard magnitudes are measured on vertical-component records only. BB stands for direct measurement on unfiltered velocity broadband records in a wide range of periods, provided that their passband covers at least the period range within which mB_BB and Ms_BB are supposed to be measured. Otherwise, a deconvolution has to be applied prior to the amplitude and period measurement so as to assure that this specification is met. In contrast, mb_Lg, mb and Ms_20 are based on narrowband amplitude measurements around periods of 1 s and 20 s, respectively.

ML is consistent with the original definition of the local magnitude by *Richter* (1935) and mB_BB in close agreement with the original definition of medium-period body-wave magnitude mB measured in a wide range of periods between some 2 to 20 s and calibrated with the *Gutenberg and Richter* (1956) Q-function for vertical-component P waves. Similarly, Ms_BB is best tuned to the unbiased use of the IASPEI (1967) recommended standard magnitude formula for surface-wave amplitudes in a wide range of periods and distances, as proposed by its authors *Vaněk et al.* (1962). In contrast, mb and Ms_20 are chiefly based on measurement standards defined by US agencies in the 1960s in conjunction with the global deployment of the World-Wide Standard Seismograph Network (WWSSN), which did not include medium or broadband recordings. Some modifications were made in the 1970s to account for IASPEI recommendations on extended measurement time windows for mb. Although not optimal for calibrating narrow-band spectral amplitudes measured around 1 s and 20 s only, mb and Ms_20 use the same original calibrations functions as mB_BB and Ms_BB. But mb and Ms_20 data constitute by far the largest available magnitude data sets. Therefore they continue to be used, with appreciation for their advantages (e.g., mb is by far the most frequently measured teleseismic magnitude and often the only available and reasonably good magnitude estimator for small earthquakes) and their shortcomings (see section 3.2.5.2 of Chapter 3 in NMSOP-2).

Abbreviated descriptions of the standard procedures for ML, mb_Lg, mb, mB_BB and Ms_BB are summarised below. For more details, including also the transfer functions of the simulation filters to be used, see www.iaspei.org/commissions/CSOI/Summary_WG-Recommendations_20130327.pdf.

All amplitudes used in the magnitude formulas below are in most circumstances to be measured as one-half the maximum deflection of the seismogram trace, peak-to-adjacent-trough or trough-to-adjacent-peak, where the peak and trough are separated by one crossing of the zero-line: this measurement is sometimes described as "one-half peak-to-peak amplitude." The periods are to be measured as twice the time-intervals separating the peak and adjacent-trough from which the amplitudes are measured. The amplitude-phase arrival-times are to be measured and reported too as the time of the zero-crossing between the peak and adjacent-trough from which the amplitudes are measured. The issue of amplitude and period measuring procedures, and circumstances under which alternative procedures are acceptable or preferable, is discussed further in Section 5 of IS 3.3 and in section 3.2.3.3 of Chapter 3 of NMSOP-2.

Amplitudes measured according to recommended IASPEI standard procedures should be reported with the following ISF amplitude "phase names": IAML, IAmb_Lg, IAmb, IAMs_20, IVmB_BB and IVMs_BB. "I" stands for "International" or "IASPEI", "A" for displacement amplitude, measured in nm, and "V" for velocity amplitude, measured in nm/s. Although the ISC will calculate standard surface-wave magnitudes only for earthquakes shallower than 60 km, contributing agencies or stations are encouraged to report standard amplitude measurements of IAMs_20 and IVMs_BB for deeper earthquakes as well.

Note that the commonly known classical calibration relationships have been modified in the following to be consistent with displacements measured in nm, and velocities in nm/s, which is now common with high-resolution digital data and analysis tools. With these general definitions of the measurement parameters, where R is hypocentral distance in km (typically less than 1000 km), Δ is epicentral distance in degrees and h is hypocentre depth in km, the standard formulas and procedures read as follows:

ML:

$$ML = \log_{10}(A) + 1.11\log_{10}R + 0.00189R - 2.09 \tag{10.14}$$

for crustal earthquakes in regions with attenuative properties similar to those of southern California, and with A being the maximum trace amplitude in nm that is measured on output from a horizontal-component instrument that is filtered so that the response of the seismograph/filter system replicates that of a Wood-Anderson standard seismograph (but with a static magnification of 1). For the normalised simulated response curve and related poles and zeros see Figure 1 and Table 1 in IS 3.3 of NMSOP-2.

Equation (10.14) is an expansion of that of *Hutton and Boore* (1987). The constant term in equation (10.14), −2.09, is based on an experimentally determined static magnification of the Wood-Anderson of 2080 (see *Uhrhammer and Collins* (1990)), rather than the theoretical magnification of 2800 that was specified by the seismograph´s manufacturer. The formulation of equation (10.14) assures that reported ML amplitude data are not affected by uncertainty in the static magnification of the Wood-Anderson seismograph.

For seismographic stations containing two horizontal components, amplitudes are measured independently from each horizontal component and each amplitude is treated as a single datum. There is no effort to measure the two observations at the same time, and there is no attempt to compute a vector average. For crustal earthquakes in regions with attenuative properties that are different from those of coastal California and for measuring magnitudes with vertical-component seismographs the constants in the above equation have to be re-determined to adjust for the different regional attenuation and travel paths as well as for systematic differences between amplitudes measured on horizontal and vertical seismographs.

mb_Lg:

$$mb\_Lg = \log_{10}(A) + 0.833\log_{10}R + 0.434\gamma(R-10) - 0.87 \tag{10.15}$$

where A = "sustained ground-motion amplitude" in nm, defined as the third largest amplitude in the time window corresponding to group velocities of 3.6 to 3.2 km/s, in the period (T) range 0.7 s to 1.3

s; R = epicentral distance in km, γ = coefficient of attenuation in km^{-1}. γ is related to the quality factor Q through the equation $\gamma = \pi/(QUT)$, where U is group velocity and T is the wave period of the L_g wave. γ is a strong function of crustal structure and should be determined specifically for the region in which the mb_Lg is to be used. A and T are measured on output from a vertical-component instrument that is filtered so that the frequency response of the seismograph/filter system replicates that of a WWSSN short-period seismograph (see Figure 1 and Table 1 in IS 3.3 of NMSOP-2). Arrival times with respect to the origin of the seismic disturbance are used, along with epicentral distance, to compute group velocity U.

mb:

$$mb = \log_{10}(A/T) + Q(\Delta, h) - 3.0 \tag{10.16}$$

where A = vertical component P-wave ground amplitude in nm measured at distances $20° \le \Delta \le 100°$ and calculated from the maximum trace-amplitude with $T < 3$ s in the entire P-phase train (time spanned by P, pP, sP, and possibly PcP and their codas, and ending preferably before PP). A and T are measured on output from an instrument that is filtered so that the frequency response of the seismograph/filter system replicates that of a WWSSN short-period seismograph (see Figure 1 and Table 1 in IS 3.3 of NMSOP-2). A is determined by dividing the maximum trace amplitude by the magnification of the simulated WWSSN-SP response at period T.

$Q(\Delta, h)$ = attenuation function for PZ (P-waves recorded on vertical component seismographs) established by *Gutenberg and Richter* (1956) in the tabulated or algorithmic form as used by the U.S. Geological Survey/National Earthquake Information Center (USGS/NEIC) (see Table 2 in IS 3.3 and program description PD 3.1 in NMSOP-2);

mB_BB:

$$mB\_BB = \log_{10}(Vmax/2\pi) + Q(\Delta, h) - 3.0 \tag{10.17}$$

where $Vmax$ = vertical component ground velocity in nm/s at periods between 0.2 s $< T <$ 30 s, measured in the range $20° \le \Delta \le 100°$. $Vmax$ is calculated from the maximum trace-amplitude in the entire P-phase train (see mb), as recorded on a seismogram that is proportional to velocity at least in the period range of measurements. $Q(\Delta, h)$ = attenuation function for PZ established by *Gutenberg and Richter* (1956) (see 10.16). Equation (10.16) differs from the equation for mB of *Gutenberg and Richter* (1956) by virtue of the $log_{10}(Vmax/2\pi)$ term, which replaces the classical $\log_{10}(A/T)_{max}$ term. Contributors should continue to send observations of A and T to ISC.

Ms_20:

$$Ms\_20 = \log_{10}(A/T) + 1.66\log_{10}\Delta + 0.3 \tag{10.18}$$

where A = vertical-component ground displacement in nm at $20° \le \Delta \le 160°$ epicentral distance measured from the maximum trace amplitude of a surface-wave phase having a period T between 18 s and 22 s on a waveform that has been filtered so that the frequency response of the seismograph/filter replicates that of a WWSSN long-period seismograph (see Figure 1 and Table 1 in IS 3.3 of NMSOP-2). A is determined by dividing the maximum trace amplitude by the magnification of the simulated WWSSN-LP response at period T. Equation (10.18) is formally equivalent to the Ms equation proposed by *Vaněk et al.* (1962) but is here applied to vertical motion measurements in a narrow range of periods.

Ms_BB:

$$Ms\_BB = \log_{10}(Vmax/2\pi) + 1.66\log_{10}\Delta + 0.3 \tag{10.19}$$

where $Vmax$ = vertical-component ground velocity in nm/s associated with the maximum trace-amplitude in the surface-wave train at periods between 3 s $< T <$ 60 s as recorded at distances $2° \leq \Delta \leq 160°$ on a seismogram that is proportional to velocity in that range of considered periods. Equation (10.19) is based on the Ms equation proposed by *Vaněk et al.* (1962), but is here applied to vertical motion measurements and is used with the $\log_{10}(Vmax/2\pi)$ term replacing the $\log_{10}(A/T)_{max}$ term of the original. As for mB_BB, observations of A and T should be reported to ISC.

Mw:

$$Mw = (\log_{10} M_0 - 9.1)/1.5 \tag{10.20}$$

Moment magnitude Mw is calculated from data of the scalar seismic moment M_0 (when given in Nm), or

$$Mw = (\log_{10} M_0 - 16.1)/1.5 \tag{10.21}$$

its CGS equivalent when M_0 is in dyne·cm.

Please note that the magnitude nomenclature used in this Section uses the IASPEI standards as the reference. However, the magnitude type is typically written in plain text in most typical data reports and so it is in this document. Moreover, writing magnitude types in plain text allows us to reproduce the magnitude type as stored in the database and provides a more direct identification of the magnitude type reported by different agencies. A short description of the common magnitude types available in this Summary is given in table 7.6.

10.2.4 The IASPEI Seismic Format (ISF)

The ISF is the IASPEI approved standard format for the exchange of parametric seismological data (hypocentres, magnitudes, phase arrivals, moment tensors etc.) and is one of the formats used by the ISC. It was adopted as standard in August 2001 and is an extension of the International Monitoring System 1.0 (IMS1.0) standard, which was developed for exchanging data used to monitor the Comprehensive Nuclear-Test-Ban Treaty. An example of the ISF is shown in Listing 10.1.

Bulletins which use the ISF are comprised of origin and arrival information, provided in a series of data blocks. These include: a bulletin title block; an event title block; an origin block; a magnitude sub-block; an effect block; a reference block; and a phase block.

Within these blocks an important extension of the IMS1.0 standard is the ability to add additional comments and thus provide further parametric information. The ISF comments are distinguishable within the open parentheses required for IMS1.0 comments by beginning with a hash mark (#) followed by a keyword identifying the type of formatted comment. Each additional line required in the ISF comment begins with the hash (within the comment parentheses) followed by blank spaces at least as long as the keyword. Optional lines within the comment are signified with a plus sign (+) instead of a hash mark. The keywords include `PRIME` (to designate a prime origin of a hypocentre); `CENTROID` (to indicate the centroid origin); `MOMTENS` (moment tensor solution); `FAULT_PLANE` (fault plane solution); `PRINAX` (principal axes); `PARAM` (an origin parameter e.g. hypocentre depth given by a depth phase).

The full documentation for the ISF is maintained at the ISC and can be downloaded from:
www.isc.ac.uk/doc/code/isf/isf.pdf

The documentation for the IMS1.0 standard can be downloaded from:
www.isc.ac.uk/doc/code/isf/ims1_0.pdf

Listing 10.1: *Example of an ISF formatted event*

```
Event 15146084 Near east coast of eastern Honshu
   Date       Time        Err   RMS Latitude Longitude  Smaj  Smin  Az Depth   Err Ndef Nsta Gap  mdist  Mdist Qual   Author      OrigID
2010/09/01 07:32:00                37.9000  141.9000f                   44.0                                             NIED       17047453
 (#MOMTENS sc    M0 fCLVD    MRR    MTT    MPP    MRT    MTP    MPR NST1 NST2 Author   )
 (#             eM0 eCLVD    eRR    eTT    ePP    eRT    eTP    ePR NCO1 NCO2 Duration )
 (#       16 5.760                                                  NIED       )
 (#                                                                            )
 (#FAULT_PLANE Typ Strike   Dip    Rake  NP  NS Plane Author    )
 (#            BDC 199.00 19.00   86.00                NIED     )
 (+                23.00 71.00   91.00                          )
 (Epicenter information from JMA Focal Mechanism Solution Determined Manually Variance reduction = 96.98%)
2010/09/01 07:32:47.50         1.470  37.8300  142.2400                 37.0         71       281  11.00  51.10     uk BJI       15275482
2010/09/01 07:32:52.20   0.92         38.0320  141.8090   6.7   4.5 110  44.0        114                                 MOS       16741494
2010/09/01 07:32:52.53   0.35 0.889  37.9202  141.8229 4.090 2.740 145  49.7  2.76  490  478 122   0.65  92.01 m i fe ISCJB     01631732
 (#PARAM pP_DEPTH=41.11021)
2010/09/01 07:32:52.60   0.10         37.9100  141.8700   1.1   0.9  -1  43.0   1.0                                   fe JMA       16271222
 (Felt I=III-III J1)
2010/09/01 07:32:53.66   0.42 0.770  37.9250  141.7880   5.1   3.4 140  44.4   3.9  102       127   3.17 127.67     fe NEIC      01134459
 (#MOMTENS sc    M0 fCLVD    MRR    MTT    MPP    MRT    MTP    MPR NST1 NST2 Author   )
 (#             eM0 eCLVD    eRR    eTT    ePP    eRT    eTP    ePR NCO1 NCO2 Duration )
 (#       16 5.800         3.600 -0.550 -3.040  1.850 -1.140  4.150           NIED       )
 (#                                                                            )
 (#FAULT_PLANE Typ Strike   Dip    Rake  NP  NS Plane Author    )
 (#            BDC 199.00 19.00   86.00                NIED     )
 (+                23.00 71.00   91.00                          )
 (Recorded [3 JMA] in Miyagi; [2 JMA] in Fukushima and Iwate; [1 JMA] in Akita, Aomori, Ibaraki, Tochigi and Yamagata.)
2010/09/01 07:32:53.70   0.20         37.9300  142.0600 2.224 1.112  -1  50.3   1.0  262   89                            GCMT      00124877
 (#CENTROID)
 (#MOMTENS sc    M0 fCLVD    MRR    MTT    MPP    MRT    MTP    MPR NST1 NST2 Author   )
 (#             eM0 eCLVD    eRR    eTT    ePP    eRT    eTP    ePR NCO1 NCO2 Duration )
 (#       16 6.891         5.430 -0.440 -4.990  1.500 -2.070  3.710   64   89 GCMT       )
 (#                        0.173  0.118  0.120  0.100  0.094  0.110  102  160      0.90 )
 (#FAULT_PLANE Typ Strike   Dip    Rake  NP  NS Plane Author    )
 (#            BDC  22.00 63.00   91.00                GCMT     )
 (+               201.00 27.00   89.00                          )
 (#PRINAX sc  T_val T_azim  T_pl  B_val B_azim  B_pl  P_val P_azim  P_pl Author    )
 (#       16  6.711 293.00 72.00  0.360 201.00  0.00 -7.072 111.00 18.00 GCMT      )
 (nsta1 refers to body waves, cutoff=40s. nsta2 refers to surface waves, cutoff=50s.)
2010/09/01 07:32:55.05   1.77 1.070  37.8692  141.9450  12.9  10.4 100  63.6  16.8   36       127   3.24 117.04     uk IDC       16680924
2010/09/01 07:32:52.23   0.30 1.333  37.8836  141.9148 5.558 4.001 142  38.9  2.33  542  478  61   0.72 141.68 m i se ISC       01237353
 (#PRIME)
 (#PARAM pP_DEPTH=39.00000)

Magnitude  Err Nsta Author      OrigID
Mw      5.1          NIED       17047453
Ms      4.8       61 BJI        15275482
Ms7     4.6       58 BJI        15275482
mB      5.1       48 BJI        15275482
mb      5.0       63 BJI        15275482
MS      4.7       19 MOS        16741494
mb      5.2       49 MOS        16741494
MS      4.6       43 ISCJB      01631732
mb      4.9      138 ISCJB      01631732
        5.0          JMA        16271222
mb      5.0       55 NEIC       01134459
MW      5.1          NIED       01134459
MW      5.2       89 GCMT       00124877
MS      4.4 0.1   28 IDC        16680924
Ms1     4.4 0.1   28 IDC        16680924
mb      4.4 0.1   27 IDC        16680924
mb1     4.5 0.0   33 IDC        16680924
mb1mx   4.4 0.0   37 IDC        16680924
mbtmp   4.7 0.1   33 IDC        16680924
ms1mx   4.3 0.1   31 IDC        16680924
MS      4.7 0.2   43 ISC        01237353
mb      4.9 0.2  145 ISC        01237353

Sta      Dist  EvAz Phase        Time       TRes  Azim AzRes   Slow   SRes Def   SNR       Amp   Per Qual Magnitude     ArrID
JIO      0.72 322.1 Pn        07:33:05.9   -0.06                           T__                     d_                49540510
JIO      0.72 322.1 Sn        07:33:15.0   -0.82                           T__                     __                49540511
JMM      0.89 269.2 Pn        07:33:08.4     0.2                           T__                     d_                49540512
JMM      0.89 269.2 Sn        07:33:19.2   -0.68                           T__                     __                49540513
JFK      0.97 238.3 Pn        07:33:09.5     0.1                           T__                     d_                49540514
JFK      0.97 238.3 Sn        07:33:21.5   -0.54                           T__                     __                49540515
JOU      1.10 296.4 Pn        07:33:11.5     0.4                           T__                     d_                49540516
JOU      1.10 296.4 Sn        07:33:25.4     0.3                           T__                     _e                49540517
ONAJ     1.18 229.0 Pn        07:33:12.4     0.1                           T__                     d_                49540530
JMK      1.20 333.1 Pn        07:33:12.5     0.0                           T__                     d_                49540518
JMK      1.20 333.1 Sn        07:33:27.1   -0.39                           T__                     _e                49540519
OFUJ     1.21 350.9 Pn        07:33:12.3   -0.34                           T__                     d_                49540531
.
.
.
532A    91.05  49.8 P         07:45:52.799 -0.00  90.9                     T__                     __                05504129
334A    91.18  47.9 P         07:45:54.012   0.7  91.0                     T__                     __                05504128
H06N1   91.36  64.9 T         09:27:33.559                                 ___   6.0               __                58438458
MIAR    91.43  42.9 P         07:45:54.85    0.5  91.2                     T__                     __                05504179
Y39A    91.60  43.6 P         07:45:55.543   0.4  91.4                     T__                     __                05504214
534A    91.98  49.0 P         07:45:57.308   0.2  91.8                     T__                     __                05504130
KEST    94.59 323.1 LR        08:33:52.432       320.5         38.70       ___          466.5 18.65 __                58438480
ESDC    96.70 334.2 LR        08:34:40.011       345.0         38.30       ___          375.8 20.18 __                58438449
TORD   117.01 315.6 PKPdf     07:51:32.55  -0.82  17.7          2.30       T__   5.1      0.4  0.70 __                58438504
TORD   117.01 315.6 PP        07:52:39.3   -2.90  31.2          6.30       T__   6.5      1.3  0.68 __                58438505
QSPA   127.62 180.0 PKPdf     07:51:52.02  -0.16                           T__                     _e                23535420
SNAA   141.68 197.1 PKPdf     07:52:13.751 -4.52                           T__                     __                20375340
VNA2   143.24 196.3 PKPbc     07:52:18.562   0.4 122.0          2.31       ___                     __                20375338
VNA1   143.64 196.2 PKPbc     07:52:19.77    0.6                           ___                     __                20375339
```

10.2.5 Ground Truth (GT) Events

Accurate locations are crucial in testing Earth models derived from body and surface wave tomography as well as in location calibration studies. 'Ground Truth' (GT) events are well-established source locations and origin times. A database of IASPEI reference events (GT earthquakes and explosions) is hosted at the ISC (www.isc.ac.uk). A full description of GT selection criteria can be found in *Bondár and McLaughlin* (2009a).

The events are coded by category GT0, GT1, GT2 or GT5, where the epicentre of a GTX event is known to within X km to a 95% confidence level. A map of all IASPEI reference events is shown in Figure 10.13 and the types of event are categorised in Figure 10.14. GT0 are explosions with announced locations and origin times. GT1 and GT2 are typically explosions, mine blasts or rock bursts either associated to explosion phenomenology located upon overhead imagery with seismically determined origin times, or precisely located by in-mine seismic networks. GT1-2 events are assumed to be shallow, but depth is unknown.

The database consists of nuclear explosions of GT0–5 quality, adopted from the Nuclear Explosion Database (*Bennett et al.*, 2010); GT0–5 chemical explosions, rock bursts, mine-induced events, as well as a few earthquakes, inherited from the reference event set by *Bondár et al.* (2004); GT5 events (typically earthquakes with crustal depths) which have been identified using either the method of *Bondár et al.* (2008) (2,275 events) or *Bondár and McLaughlin* (2009a) (updated regularly from the EHB catalogue (*Engdahl et al.*, 1998)), which uses the following criteria:

- 10 or more stations within 150 km from the epicentre
- one or more stations within 10 km
- $\Delta U \leq 0.35$
- a secondary azimuthal gap $\leq 160°$

where ΔU is the network quality metric defined as the mean absolute deviation between the best-fitting uniformly distributed network of stations and the actual network:

$$\Delta U = \frac{4\sum|esaz_i - (unif_i + b)|}{360N}, 0 \leq \Delta U \leq 1 \qquad (10.22)$$

where N is the number of stations, $esaz_i$ is the ith event-to-station azimuth, $unif_i = 360i/N$ for $i = 0$, ..., $N-1$, and $b = avg\,(esaz_i) - avg\,(unif_i)$. ΔU is normalised so that it is 0 when the stations are uniformly distributed in azimuth and 1 when all the stations are at the same azimuth.

The seismological community is invited to participate in this project by nominating seismic events for the reference event database. Submitters may be contacted for further confirmation and for arrival time data. The IASPEI Reference Event List will be periodically published both in written and electronic form with proper acknowledgement of all submitters.

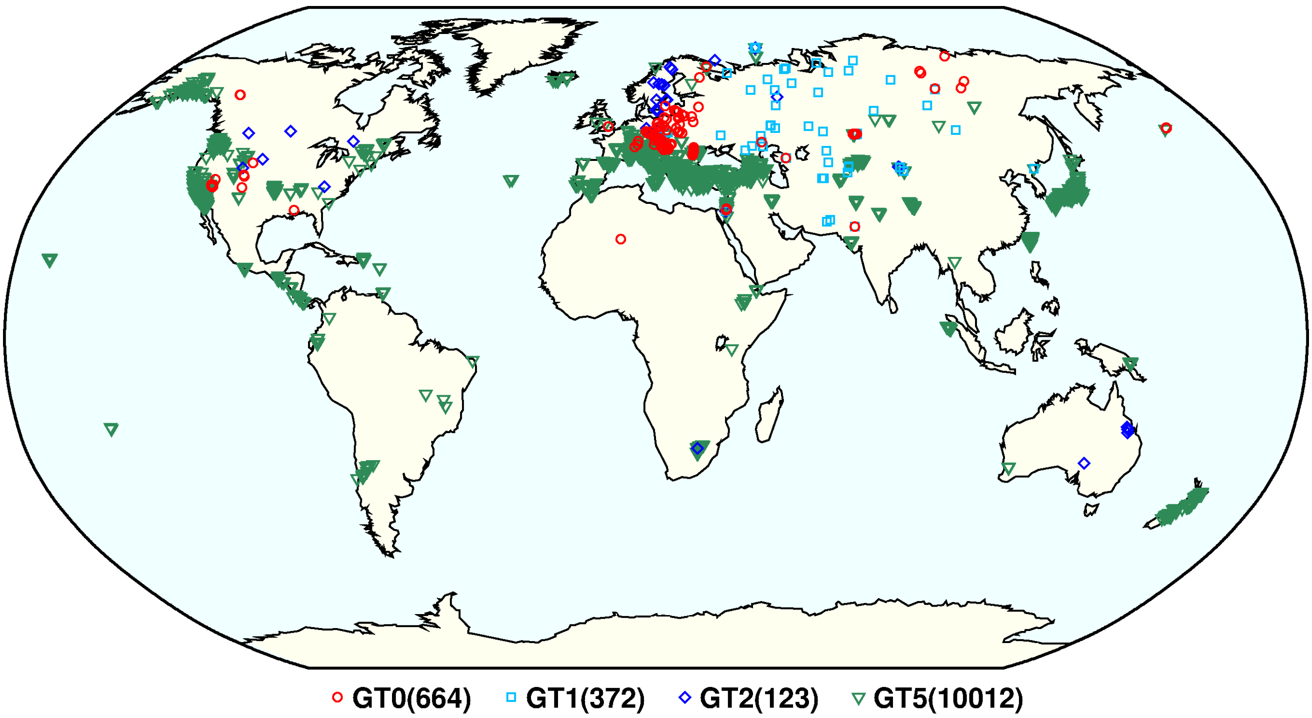

Figure 10.13: *Map of all IASPEI Reference Events as of July 2020.*

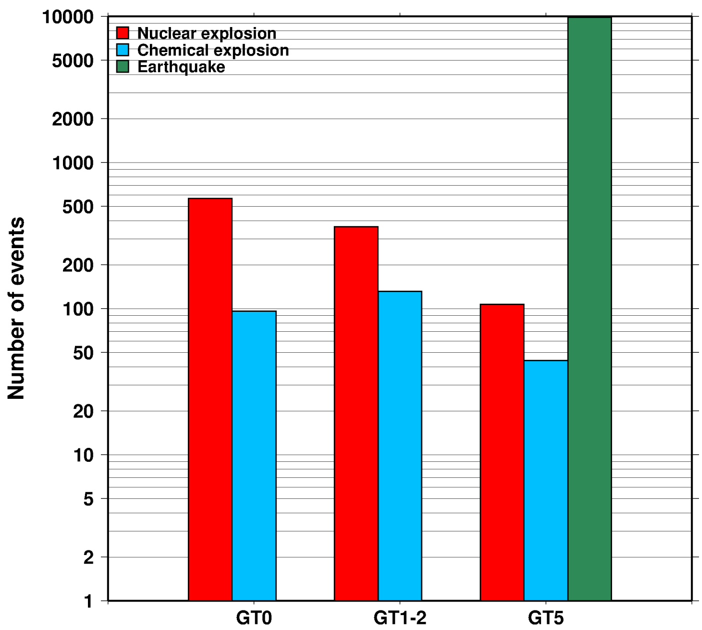

Figure 10.14: *Histogram showing the event types within the IASPEI Reference Event list as of July 2020.*

10.2.6 Nomenclature of Event Types

The nomenclature of event types currently used in the ISC Bulletin takes its origin from the IASPEI International Seismic Format (ISF).

Event type codes are composed of a leading character that generally indicates the confidence with which the type of the event is asserted and a trailing character that generally gives the type of the event. The leading and trailing characters may be used in any combination.

The **leading** characters are:

- s = suspected
- k = known
- f = felt (implies known)
- d = damaging (implies felt and known)

The **trailing** characters are:

- c = meteoritic event
- e = earthquake
- h = chemical explosion
- i = induced event
- l = landslide
- m = mining explosion
- n = nuclear explosion
- r = rock burst
- x = experimental explosion

A chemical explosion might be for mining or experimental purposes, and it is conceivable that other types of event might be assigned two or more different event type codes. This is deliberate, and matches the ambiguous identification of events in existing databases.

In addition, the code `uk` is used for events of unknown type and `ls` is used for known landslides.

The frequency of the different event types designated in the ISC Bulletin since 1964 is indicated in Figure 10.15.

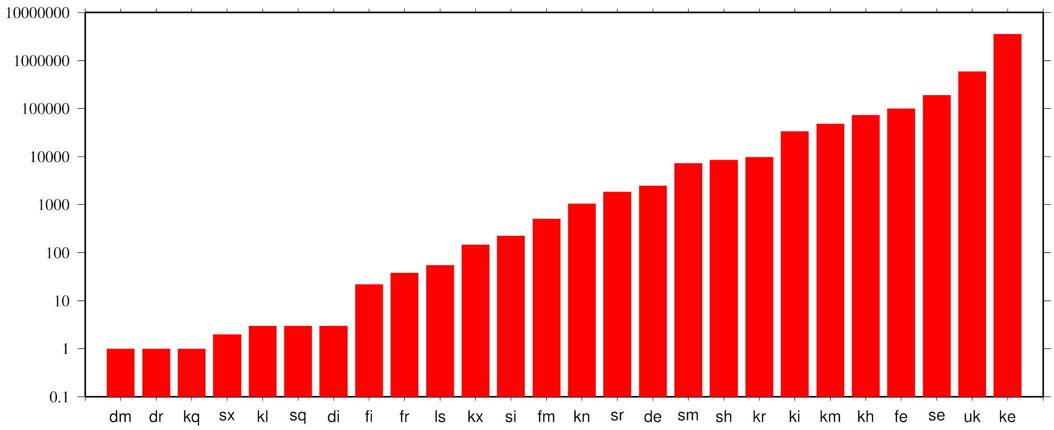

Figure 10.15: *Event types in the ISC Bulletin*

There are currently plans to revise this nomenclature as part of the coordination process between the National Earthquake Information Center (NEIC/USGS), European-Mediterranean Seismological Centre (CSEM) and the ISC.

10.3 Tables

Table 10.2: *Listing of all 389 agencies that have directly reported to the ISC. The 149 agencies highlighted in bold have reported data to the ISC Bulletin for the period of this Bulletin Summary.*

Agency Code	Agency Name
AAA	Alma-ata, Kazakhstan
AAE	University of Addis Ababa, Ethiopia
AAM	University of Michigan, USA
ADE	Primary Industries and Resources SA, Australia
ADH	Observatorio Afonso Chaves, Portugal
AEIC	Alaska Earthquake Information Center, USA
AFAD	**Disaster and Emergency Management Presidency, Turkey**
AFAR	The Afar Depression: Interpretation of the 1960-2000 Earthquakes, Israel
AFUA	University of Alabama, USA
ALG	Algiers University, Algeria
ANDRE	USSR
ANF	USArray Array Network Facility, USA
ANT	Antofagasta, Chile
ARE	Instituto Geofisico del Peru, Peru
ARO	Observatoire Géophysique d'Arta, Djibouti
ASIES	**Institute of Earth Sciences, Academia Sinica, Chinese Taipei**
ASL	Albuquerque Seismological Laboratory, USA
ASM	University of Asmara, Eritrea
ASRS	**Altai-Sayan Seismological Centre, GS SB RAS, Russia**
ATA	The Earthquake Research Center Ataturk University, Turkey
ATH	**National Observatory of Athens, Greece**
AUST	**Geoscience Australia, Australia**
AVETI	USSR
AWI	**Alfred Wegener Institute for Polar and Marine Research, Germany**

Table 10.2: *Continued.*

Agency Code	Agency Name
AZER	**Republican Seismic Survey Center of Azerbaijan National Academy of Sciences, Azerbaijan**
BCIS	Bureau Central International de Sismologie, France
BDF	Observatório Sismológico da Universidade de Brasília, Brazil
BELR	**Centre of Geophysical Monitoring of the National Academy of Sciences of Belarus, Republic of Belarus**
BEO	**Seismological Survey of Serbia, Serbia**
BER	**University of Bergen, Norway**
BERK	Berkheimer H, Germany
BGR	**Bundesanstalt für Geowissenschaften und Rohstoffe, Germany**
BGS	**British Geological Survey, United Kingdom**
BGSI	**Botswana Geoscience Institute, Botswana**
BHUJ2	Study of Aftershocks of the Bhuj Earthquake by Japanese Research Team, Japan
BIAK	Biak earthquake aftershocks (17-Feb-1996), USA
BJI	**China Earthquake Networks Center, China**
BKK	**Thai Meteorological Department, Thailand**
BNS	Erdbebenstation, Geologisches Institut der Universität, Köl, Germany
BOG	Universidad Javeriana, Colombia
BRA	**Geophysical Institute, Slovak Academy of Sciences, Slovakia**
BRG	**Seismological Observatory Berggießhübel, TU Bergakademie Freiberg, Germany**
BRK	Berkeley Seismological Laboratory, USA
BRS	Brisbane Seismograph Station, Australia
BUC	**National Institute for Earth Physics, Romania**
BUD	Geodetic and Geophysical Research Institute, Hungary
BUEE	Earth & Environment, USA
BUG	Institute of Geology, Mineralogy & Geophysics, Germany
BUL	**Goetz Observatory, Zimbabwe**
BUT	Montana Bureau of Mines and Geology, USA
BYKL	**Baykal Regional Seismological Centre, GS SB RAS, Russia**
CADCG	Central America Data Centre, Costa Rica
CAN	Australian National University, Australia
CANSK	Canadian and Scandinavian Networks, Sweden
CAR	Instituto Sismologico de Caracas, Venezuela
CASC	Central American Seismic Center, Costa Rica
CATAC	**Central American Tsunami Advisory Center, Nicaragua**
CENT	Centennial Earthquake Catalog, USA
CERI	Center for Earthquake Research and Information, USA
CFUSG	**Inst. of Seismology and Geodynamics, V.I. Vernadsky Crimean Federal University, Republic of Crimea**
CLL	**Geophysikalisches Observatorium Collm, Germany**
CMWS	Laboratory of Seismic Monitoring of Caucasus Mineral Water Region, GSRAS, Russia
CNG	Seismographic Station Changalane, Mozambique
CNRM	**Centre National de Recherche, Morocco**
COSMOS	Consortium of Organizations for Strong Motion Observations, USA
CRAAG	**Centre de Recherche en Astronomie, Astrophysique et Géophysique, Algeria**

Table 10.2: Continued.

Agency Code	Agency Name
CSC	University of South Carolina, USA
CSEM	Centre Sismologique Euro-Méditerranéen (CSEM/EMSC), France
CUPWA	**Curtin University, Australia**
DASA	Defense Atomic Support Agency, USA
DBN	Koninklijk Nederlands Meteorologisch Instituut, Netherlands
DDA	General Directorate of Disaster Affairs, Turkey
DHMR	Yemen National Seismological Center, Yemen
DIAS	**Dublin Institute for Advanced Studies, Ireland**
DJA	**Badan Meteorologi, Klimatologi dan Geofisika, Indonesia**
DMN	**National Seismological Centre, Nepal, Nepal**
DNAG	USA
DNK	**Geological Survey of Denmark and Greenland, Denmark**
DRS	Dagestan Branch, Geophysical Survey, Russian Academy of Sciences, Russia
DSN	**Dubai Seismic Network, United Arab Emirates**
DUSS	Damascus University, Syria, Syria
EAF	East African Network, Unknown
EAGLE	Ethiopia-Afar Geoscientific Lithospheric Experiment, Unknown
EBR	Observatori de l'Ebre, Spain
EBSE	Ethiopian Broadband Seismic Experiment, Unknown
ECGS	European Center for Geodynamics and Seismology, Luxembourg
ECX	**Centro de Investigación Científica y de Educación Superior de Ensenada, Mexico**
EFATE	OBS Experiment near Efate, Vanuatu, USA
EHB	Engdahl, van der Hilst and Buland, USA
EIDC	Experimental (GSETT3) International Data Center, USA
EKA	Eskdalemuir Array Station, United Kingdom
ENT	Geological Survey and Mines Department, Uganda
EPSI	Reference events computed by the ISC for EPSI project, United Kingdom
ERDA	Energy Research and Development Administration, USA
EST	Geological Survey of Estonia, Estonia
EUROP	Unknown
EVBIB	Data from publications listed in the ISC Event Bibliography, Unknown
FBR	Fabra Observatory, Spain
FCIAR	**Federal Center for Integrated Arctic Research, Russia**
FDF	Fort de France, Martinique
FIA0	Finessa Array, Finland
FOR	Unknown Historical Agency, Unknown - historical agency
FUBES	Earth Science Dept., Geophysics Section, Germany
FUNV	**Fundación Venezolana de Investigaciones Sismológicas, Venezuela**
FUR	Geophysikalisches Observatorium der Universität München, Germany
GBZT	Marmara Research Center, Turkey
GCG	**INSIVUMEH, Guatemala**
GCMT	**The Global CMT Project, USA**
GDNRW	Geologischer Dienst Nordrhein-Westfalen, Germany
GEN	**Dipartimento per lo Studio del Territorio e delle sue Risorse (RSNI), Italy**
GEOAZ	UMR Géoazur, France

Table 10.2: *Continued.*

Agency Code	Agency Name
GEOMR	GEOMAR, Germany
GFZ	Helmholtz Centre Potsdam GFZ German Research Centre For Geosciences, Germany
GII	**The Geophysical Institute of Israel, Israel**
GOM	Observatoire Volcanologique de Goma, Democratic Republic of the Congo
GRAL	**National Council for Scientific Research, Lebanon**
GSDM	**Geological Survey Department Malawi, Malawi**
GSET2	Group of Scientific Experts Second Technical Test 1991, April 22 - June 2, Unknown
GTFE	German Task Force for Earthquakes, Germany
GUC	**Centro Sismológico Nacional, Universidad de Chile, Chile**
HAN	Hannover, Germany
HDC	Observatorio Vulcanológico y Sismológico de Costa Rica, Costa Rica
HEL	**Institute of Seismology, University of Helsinki, Finland**
HFS	Hagfors Observatory, Sweden
HFS1	Hagfors Observatory, Sweden
HFS2	Hagfors Observatory, Sweden
HIMNT	Himalayan Nepal Tibet Experiment, USA
HKC	**Hong Kong Observatory, Hong Kong**
HLUG	Hessisches Landesamt für Umwelt und Geologie, Germany
HLW	**National Research Institute of Astronomy and Geophysics, Egypt**
HNR	Ministry of Mines, Energy and Rural Electrification, Solomon Islands
HON	Pacific Tsunami Warning Center - NOAA, USA
HRVD	Harvard University, USA
HRVD_LR	Department of Geological Sciences, Harvard University, USA
HVO	Hawaiian Volcano Observatory, USA
HYB	**National Geophysical Research Institute, India**
HYD	National Geophysical Research Institute, India
IAG	Instituto Andaluz de Geofisica, Spain
IASBS	Institute for Advanced Studies in Basic Sciences, Iran
IASPEI	IASPEI Working Group on Reference Events, USA
ICE	Instituto Costarricense de Electricidad, Costa Rica
IDC	**International Data Centre, CTBTO, Austria**
IDG	Institute of Dynamics of Geosphere, Russian Academy of Sciences, Russia
IEC	Institute of the Earth Crust, SB RAS, Russia
IEPN	Institute of Environmental Problems of the North, Russian Academy of Sciences, Russia
IFREE	Institute For Research on Earth Evolution, Japan
IGGSL	Seismology Lab, Institute of Geology & Geophysics, Chinese Academy of Sciences, China
IGIL	**Instituto Dom Luiz, University of Lisbon, Portugal**
IGQ	**Servicio Nacional de Sismología y Vulcanología, Ecuador**
IGS	Institute of Geological Sciences, United Kingdom
INAM	Instituto Nacional de Meteorologia e Geofisica - INAMET, Angola
INDEPTH3	International Deep Profiling of Tibet and the Himalayas, USA
INET	Instituto Nicaraguense de Estudios Territoriales - INETER, Nicaragua

Table 10.2: Continued.

Agency Code	Agency Name
INMG	**Instituto Português do Mar e da Atmosfera, I.P., Portugal**
INMGC	Instituto Nacional de Meteorologia e Geofísica, Cape Verde
IPEC	**The Institute of Physics of the Earth (IPEC), Czech Republic**
IPER	Institute of Physics of the Earth, Academy of Sciences, Moscow, Russia
IPGP	**Institut de Physique du Globe de Paris, France**
IPRG	Institute for Petroleum Research and Geophysics, Israel
IRIS	**IRIS Data Management Center, USA**
IRSM	Institute of Rock Structure and Mechanics, Czech Republic
ISC	**International Seismological Centre, United Kingdom**
ISC-PPSM	**International Seismological Centre Probabilistic Point Source Model, United Kingdom**
ISK	**Kandilli Observatory and Research Institute, Turkey**
ISN	**Iraqi Meteorological and Seismology Organisation, Iraq**
ISS	International Seismological Summary, United Kingdom
IST	Institute of Physics of the Earth, Technical University of Istanbul, Turkey
ISU	**Institute of Seismology, Academy of Sciences, Republic of Uzbekistan, Uzbekistan**
ITU	Faculty of Mines, Department of Geophysical Engineering, Turkey
JEN	Geodynamisches Observatorium Moxa, Germany
JMA	**Japan Meteorological Agency, Japan**
JOH	Bernard Price Institute of Geophysics, South Africa
JSN	**Jamaica Seismic Network, Jamaica**
JSO	**Jordan Seismological Observatory, Jordan**
KBC	Institut de Recherches Géologiques et Minières, Cameroon
KEA	**Korea Earthquake Administration, Democratic People's Republic of Korea**
KEW	Kew Observatory, United Kingdom
KHC	Institute of Geophysics, Czech Academy of Sciences, Czech Republic
KISR	Kuwait Institute for Scientific Research, Kuwait
KLM	Malaysian Meteorological Service, Malaysia
KMA	**Korea Meteorological Administration, Republic of Korea**
KNET	**Kyrgyz Seismic Network, Kyrgyzstan**
KOLA	**Kola Regional Seismic Centre, GS RAS, Russia**
KRAR	Krasnoyarsk Scientific Research Inst. of Geology and Mineral Resources, Russia, Russia
KRL	Geodätisches Institut der Universität Karlsruhe, Germany
KRNET	**Institute of Seismology, Academy of Sciences of Kyrgyz Republic, Kyrgyzstan**
KRSC	**Kamchatka Branch of the Geophyiscal Survey of the RAS, Russia**
KRSZO	**Geodetic and Geophysical Reasearch Institute, Hungarian Academy of Sciences, Hungary**
KSA	Observatoire de Ksara, Lebanon
KUK	Geological Survey Department of Ghana, Ghana
LAO	Large Aperture Seismic Array, USA
LDG	**Laboratoire de Détection et de Géophysique/CEA, France**
LDN	University of Western Ontario, Canada
LDO	Lamont-Doherty Earth Observatory, USA
LED	Landeserdbebendienst Baden-Württemberg, Germany

Table 10.2: Continued.

Agency Code	Agency Name
LEDBW	Landeserdbebendienst Baden-Württemberg, Germany
LER	Besucherbergwerk Binweide Station, Germany
LIB	Tripoli, Libya
LIC	Station Géophysique de Lamto, Ivory Coast
LIM	Lima, Peru
LIS	Instituto de Meteorologia, Portugal
LIT	**Geological Survey of Lithuania**, **Lithuania**
LJU	**Slovenian Environment Agency**, **Slovenia**
LPA	**Universidad Nacional de La Plata**, **Argentina**
LPZ	Observatorio San Calixto, Bolivia
LRSM	Long Range Seismic Measurements Project, Unknown
LSZ	Geological Survey Department of Zambia, Zambia
LVSN	**Latvian Seismic Network**, **Latvia**
MAN	**Philippine Institute of Volcanology and Seismology**, **Philippines**
MAT	The Matsushiro Seismological Observatory, Japan
MATSS	USSR
MCO	**Macao Meteorological and Geophysical Bureau**, **Macao, China**
MCSM	**Main Centre for Special Monitoring**, **Ukraine**
MDD	**Instituto Geográfico Nacional**, **Spain**
MED_RCMT	**MedNet Regional Centroid - Moment Tensors**, **Italy**
MERI	Maharashta Engineering Research Institute, India
MES	Messina Seismological Observatory, Italy
MEX	**Instituto de Geofísica de la UNAM**, **Mexico**
MIRAS	**Mining Institute of the Ural Branch of the Russian Academy of Sciences**, **Russia**
MNH	Institut für Angewandte Geophysik der Universitat Munchen, Germany
MOLD	**Institute of Geophysics and Geology**, **Moldova**
MOS	**Geophysical Survey of Russian Academy of Sciences**, **Russia**
MOZ	Direccao Nacional de Geologia, Mozambique
MOZAR	Mozambique
MRB	**Institut Cartogràfic i Geològic de Catalunya**, **Spain**
MSI	Messina Seismological Observatory, Italy
MSSP	Micro Seismic Studies Programme, PINSTECH, Pakistan
MSUGS	Michigan State University, Department of Geological Sciences, USA
MUN	Mundaring Observatory, Australia
NAI	University of Nairobi, Kenya
NAM	**The Geological Survey of Namibia**, **Namibia**
NAO	**Stiftelsen NORSAR**, **Norway**
NCEDC	Northern California Earthquake Data Center, USA
NDI	**National Centre for Seismology of the Ministry of Earth Sciences of India**, **India**
NEIC	**National Earthquake Information Center**, **USA**
NEIS	National Earthquake Information Service, USA
NERS	**North Eastern Regional Seismological Centre, GS RAS**, **Russia**
NIC	**Cyprus Geological Survey Department**, **Cyprus**
NIED	**National Research Institute for Earth Science and Disaster Resilience**, **Japan**
NKSZ	USSR
NNC	**National Nuclear Center**, **Kazakhstan**

Table 10.2: *Continued.*

Agency Code	Agency Name
NORS	North Ossetia (Alania) Branch, Geophysical Survey, Russian Academy of Sciences, Russia
NOU	**IRD Centre de Nouméa**, **New Caledonia**
NSSC	National Syrian Seismological Center, Syria
NSSP	**National Survey of Seismic Protection**, **Armenia**
OBM	Research Centre of Astronomy and Geophysics, Mongolia
OGAUC	Centro de Investigação da Terra e do Espaço da Universidade de Coimbra, Portugal
OGSO	Ohio Geological Survey, USA
OMAN	**Sultan Qaboos University**, **Oman**
ORF	Orfeus Data Center, Netherlands
OSPL	**Observatorio Sismologico Politecnico Loyola**, **Dominican Republic**
OSUB	Osservatorio Sismologico Universita di Bari, Italy
OSUNB	**Observatory Seismological of the University of Brasilia**, **Brazil**
OTT	**Canadian Hazards Information Service, Natural Resources Canada**, **Canada**
PAL	Palisades, USA
PAS	California Institute of Technology, USA
PDA	Universidade dos Açores, Portugal
PDG	**Seismological Institute of Montenegro**, **Montenegro**
PEK	Peking, China
PGC	Pacific Geoscience Centre, Canada
PJWWP	**Private Observatory of Pawel Jacek Wiejacz, D.Sc.**, **Poland**
PLV	**Institute of Geophysics, Viet Nam Academy of Science and Technology**, **Viet Nam**
PMEL	Pacific seismicity from hydrophones, USA
PMR	Alaska Tsunami Warning Center,, USA
PNNL	Pacific Northwest National Laboratory, USA
PNSN	**Pacific Northwest Seismic Network**, **USA**
PPT	**Laboratoire de Géophysique/CEA**, **French Polynesia**
PRE	**Council for Geoscience**, **South Africa**
PRU	**Institute of Geophysics, Czech Academy of Sciences**, **Czech Republic**
PTO	Instituto Geofísico da Universidade do Porto, Portugal
PTWC	Pacific Tsunami Warning Center, USA
QCP	**Manila Observatory**, **Philippines**
QUE	Pakistan Meteorological Department, Pakistan
QUI	Escuela Politécnica Nacional, Ecuador
RAB	Rabaul Volcanological Observatory, Papua New Guinea
RBA	Université Mohammed V, Morocco
REN	MacKay School of Mines, USA
REY	**Icelandic Meteorological Office**, **Iceland**
RHSSO	**Republic Hydrometeorological Service, Seismological Observatory, Banja Luka**, **Bosnia and Herzegovina**
RISSC	**Laboratory of Research on Experimental and Computational Seimology**, **Italy**
RMIT	Royal Melbourne Institute of Technology, Australia
ROC	Odenbach Seismic Observatory, USA

Table 10.2: Continued.

Agency Code	Agency Name
ROM	**Istituto Nazionale di Geofisica e Vulcanologia**, **Italy**
RRLJ	Regional Research Laboratory Jorhat, India
RSMAC	Red Sísmica Mexicana de Apertura Continental, Mexico
RSNC	**Red Sismológica Nacional de Colombia**, **Colombia**
RSPR	**Red Sísmica de Puerto Rico**, **USA**
RYD	King Saud University, Saudi Arabia
SAPSE	Southern Alps Passive Seismic Experiment, New Zealand
SAR	Sarajevo Seismological Station, Bosnia and Herzegovina
SBDV	USSR
SCB	**Observatorio San Calixto**, **Bolivia**
SCEDC	Southern California Earthquake Data Center, USA
SCSIO	Key Laboratory of Ocean and Marginal Sea Geology, South China Sea, China
SDD	**Universidad Autonoma de Santo Domingo**, **Dominican Republic**
SEA	Geophysics Program AK-50, USA
SET	Setif Observatory, Algeria
SFS	**Real Instituto y Observatorio de la Armada**, **Spain**
SGS	**Saudi Geological Survey**, **Saudi Arabia**
SHL	Central Seismological Observatory, India
SIGU	**Subbotin Institute of Geophysics, National Academy of Sciences**, **Ukraine**
SIK	Seismic Institute of Kosovo, Unknown
SIO	Scripps Institution of Oceanography, USA
SJA	**Instituto Nacional de Prevención Sísmica**, **Argentina**
SJS	Instituto Costarricense de Electricidad, Costa Rica
SKHL	**Sakhalin Experimental and Methodological Seismological Expedition, GS RAS**, **Russia**
SKL	Sakhalin Complex Scientific Research Institute, Russia
SKO	**Seismological Observatory Skopje**, **North Macedonia**
SLC	Salt Lake City, USA
SLM	Saint Louis University, USA
SNET	**Servicio Nacional de Estudios Territoriales**, **El Salvador**
SNM	New Mexico Institute of Mining and Technology, USA
SNSN	Saudi National Seismic Network, Saudi Arabia
SOF	**National Institute of Geophysics, Geology and Geography**, **Bulgaria**
SOMC	Seismological Observatory of Mount Cameroon, Cameroon
SOME	**Seismological Experimental Methodological Expedition**, **Kazakhstan**
SPA	USGS - South Pole, Antarctica
SPGM	Service de Physique du Globe, Morocco
SPITAK	Armenia
SRI	Stanford Research Institute, USA
SSN	Sudan Seismic Network, Sudan
SSNC	**Servicio Sismológico Nacional Cubano**, **Cuba**
SSS	Centro de Estudios y Investigaciones Geotecnicas del San Salvador, El Salvador
STK	Stockholm Seismological Station, Sweden

Table 10.2: *Continued.*

Agency Code	Agency Name
STR	**EOST / RéNaSS, France**
STU	Stuttgart Seismological Station, Germany
SVSA	**Sistema de Vigilância Sismológica dos Açores, Portugal**
SYO	**National Institute of Polar Research, Japan**
SZGRF	Seismologisches Zentralobservatorium Gräfenberg, Germany
TAC	Estación Central de Tacubaya, Mexico
TAN	**Antananarivo, Madagascar**
TANZANIA	Tanzania Broadband Seismic Experiment, USA
TAP	**Central Weather Bureau (CWB), Chinese Taipei**
TAU	University of Tasmania, Australia
TEH	**Tehran University, Iran**
TEIC	Center for Earthquake Research and Information, USA
THE	**Department of Geophysics, Aristotle University of Thessaloniki, Greece**
THR	**International Institute of Earthquake Engineering and Seismology (IIEES), Iran**
TIF	**Institute of Earth Sciences/ National Seismic Monitoring Center, Georgia**
TIR	**The Institute of Seismology, Academy of Sciences of Albania, Albania**
TRI	**Istituto Nazionale di Oceanografia e di Geofisica Sperimentale (OGS), Italy**
TRN	**The Seismic Research Centre, Trinidad and Tobago**
TTG	Titograd Seismological Station, Montenegro
TUL	Oklahoma Geological Survey, USA
TUN	**Institut National de la Météorologie, Tunisia**
TVA	Tennessee Valley Authority, USA
TXNET	**Texas Seismological Network, University of Texas at Austin, USA**
TZN	University of Dar Es Salaam, Tanzania
UAF	Department of Geosciences, USA
UATDG	The University of Arizona, Department of Geosciences, USA
UAV	Red Sismológica de Los Andes Venezolanos, Venezuela
UCB	University of Colorado, Boulder, USA
UCC	**Royal Observatory of Belgium, Belgium**
UCDES	Department of Earth Sciences, United Kingdom
UCR	**Sección de Sismología, Vulcanología y Exploración Geofísica, Costa Rica**
UCSC	Earth & Planetary Sciences, USA
UESG	School of Geosciences, United Kingdom
UGN	Institute of Geonics AS CR, Czech Republic
ULE	University of Leeds, United Kingdom
UNAH	Universidad Nacional Autonoma de Honduras, Honduras
UPA	**Universidad de Panama, Panama**
UPIES	Institute of Earth- and Environmental Science, Germany
UPP	**University of Uppsala, Sweden**
UPSL	**University of Patras, Department of Geology, Greece**
UREES	Department of Earth and Environmental Science, USA
USAEC	United States Atomic Energy Commission, USA

Table 10.2: Continued.

Agency Code	Agency Name
USCGS	United States Coast and Geodetic Survey, USA
USGS	United States Geological Survey, USA
UTEP	Department of Geological Sciences, USA
UUSS	The University of Utah Seismograph Stations, USA
UVC	Universidad del Valle, Colombia
UWMDG	University of Wisconsin-Madison, Department of Geoscience, USA
VAO	**Instituto Astronomico e Geofísico, Brazil**
VIE	**Zentralanstalt für Meteorologie und Geodynamik (ZAMG), Austria**
VKMS	Lab. of Seismic Monitoring, Voronezh region, GSRAS & Voronezh State University, Russia
VLA	Vladivostok Seismological Station, Russia
VSI	University of Athens, Greece
VUW	Victoria University of Wellington, New Zealand
WAR	**Institute of Geophysics, Polish Academy of Sciences, Poland**
WASN	USA
WBNET	**Institute of Geophysics, Czech Academy of Sciences, Czech Republic**
WEL	**Institute of Geological and Nuclear Sciences, New Zealand**
WES	Weston Observatory, USA
WUSTL	Washington University Earth and Planentary Sciences, USA
YARS	**Yakutiya Regional Seismological Center, GS SB RAS, Russia**
ZAG	**Seismological Survey of the Republic of Croatia, Croatia**
ZEMSU	USSR
ZUR	**Swiss Seismological Service (SED), Switzerland**
ZUR_RMT	Zurich Moment Tensors, Switzerland

Table 10.3: *Phases reported to the ISC. These include phases that could not be matched to an appropriate* ak135 *phases. Those agencies that reported at least 10% of a particular phase are also shown.*

Reported Phase	Total	Agencies reporting
P	4185671	
S	2024307	TAP (18%), JMA (15%)
AML	621962	ROM (73%), AFAD (16%)
NULL	499620	IDC (35%), NEIC (33%), AEIC (14%)
IAmb	456935	NEIC (98%)
IAML	438466	NEIC (61%)
Pg	298799	ISK (21%), STR (17%)
Pn	271957	NEIC (36%), ISK (21%)
Sg	207720	STR (21%), ISK (13%)
LR	146537	IDC (64%), BJI (17%), INMG (14%)
pmax	126920	MOS (67%), BJI (21%), INMG (12%)
IAMs_20	107238	NEIC (98%)
Sn	70982	IDC (16%)
SG	69432	HEL (63%), PRU (18%)
PG	63889	HEL (65%), PRU (13%)
PKP	41197	IDC (39%), VIE (14%)
Lg	36895	NNC (67%), IDC (19%)
MSG	36015	HEL (100%)
PN	32347	MOS (43%), HEL (36%)
T	25784	IDC (99%)
SN	23657	HEL (82%), OTT (11%)
pP	18707	BJI (20%), INMG (17%), IDC (17%), ISC1 (14%)
PKPbc	18161	IDC (64%), NEIC (14%)
PKIKP	16544	MOS (99%)
PcP	14983	IDC (60%)
IAmb_Lg	14782	NEIC (100%)
Vmb_Lg	14771	MDD (100%)
MLR	14737	MOS (100%)
PP	14381	IDC (19%), INMG (18%), BELR (15%), BJI (13%)
A	14184	SKHL (50%), JMA (50%)
SB	13892	HEL (100%)
PKPdf	11846	NEIC (48%), INMG (14%)
PB	10811	HEL (100%)
SS	10734	MOS (31%), BELR (21%), BJI (12%), INMG (12%)
sP	7388	BJI (40%), INMG (28%), ISC1 (13%)
smax	6863	MOS (77%), BJI (17%)
PKPab	6289	IDC (44%), INMG (17%), NEIC (14%), BGR (13%)
AMS	5304	PRU (73%), CLL (16%)
PKiKP	5156	IDC (35%), VIE (26%), BELR (12%)
Sb	4976	IRIS (99%)
SPECP	4710	AFAD (100%)
AMB	4648	SKHL (84%)
x	4527	BRG (44%), CLL (28%), PRU (13%)
LRM	4524	BELR (91%)
IVmb_Lg	4312	MDD (100%)
ScP	4274	IDC (71%)
Trac	4110	OTT (100%)
PPP	4047	BELR (47%), MOS (47%)
Amp	3613	BRG (100%)
Pdiff	3547	IRIS (55%), IDC (19%), VIE (14%)
SSS	3386	BELR (59%), MOS (34%)
PKP2	3122	MOS (99%)
Amb	2943	INMG (94%)
PKKPbc	2656	IDC (97%)
*PP	2640	MOS (100%)
I	2603	IDC (100%)
LQ	2423	BELR (67%), PPT (23%)
LG	2229	BRA (78%), OTT (22%)
sS	2126	BJI (39%), INMG (36%), BELR (16%)
Pb	2067	IRIS (93%)
PKhKP	1980	IDC (100%)
SKS	1975	BELR (30%), BJI (25%), INMG (13%), PRU (12%)
pPKP	1957	VIE (36%), IDC (31%)
AMd	1636	TIR (100%)
IVMs_BB	1542	BER (91%)
L	1334	BGR (46%), MOLD (28%), WAR (25%)
IVmB_BB	1283	BER (89%)
SKPbc	1221	IDC (93%)
PS	1145	MOS (43%), BELR (18%), CLL (13%)
ScS	1098	BJI (35%), INMG (29%), IDC (16%), BELR (12%)

Table 10.3: *(continued)*

Reported Phase	Total	Agencies reporting
PKKP	1059	VIE (42%), IDC (42%)
Smax	1049	BYKL (99%)
X	982	JMA (88%)
SKSac	966	BER (62%), AWI (13%)
PKPPKP	927	IDC (96%)
Sm	885	CFUSG (87%), SIGU (13%)
Vmb_V	877	MDD (100%)
Pdif	865	NEIC (24%), BER (17%), UCC (12%), BJI (12%)
AMs_20	864	INMG (99%)
Pmax	845	BYKL (94%)
END	821	ROM (100%)
PKHKP	766	MOS (99%)
AMP	761	UPA (94%)
SP	756	BER (41%), MOS (22%)
SKP	724	IDC (41%), INMG (21%), BELR (14%), VIE (12%)
SKKS	621	BELR (42%), BJI (25%), INMG (20%)
tx	614	INMG (89%)
pPKPbc	592	IDC (62%), BGR (28%)
AMs_VX	560	NEIC (100%)
PDIFF	535	BRA (51%), PRU (29%), IPEC (19%)
PKPAB	513	PRU (100%)
Pm	504	CFUSG (78%), SIGU (22%)
Sgmax	482	NERS (100%)
*SP	458	MOS (100%)
PnA	452	THR (100%)
PKPDF	435	PRU (100%)
*SS	431	MOS (100%)
sPKP	426	BJI (50%), INMG (27%), BELR (12%)
pPKiKP	335	VIE (61%), BELR (21%)
SKKPbc	319	IDC (97%)
pPKPdf	290	BGR (28%), NEIC (25%), CLL (11%), BER (11%)
max	280	BYKL (100%)
PKKPab	279	IDC (96%)
PKP2bc	238	IDC (100%)
PPS	235	CLL (62%), MOS (21%)
PcS	233	INMG (52%), BJI (42%)
AmB	227	KEA (100%)
pPKPab	196	BGR (38%), IDC (31%), CLL (23%)
SKPdf	191	BER (47%), INMG (19%), CLL (19%)
P3KPbc	179	IDC (100%)
Pgmax	177	NERS (99%)
PKS	173	BELR (47%), BJI (28%), INMG (16%)
IVmBBB	172	BER (98%)
SKKP	169	VIE (49%), BELR (24%), IDC (20%)
IVmb_VC	167	MDD (100%)
p	160	ROM (100%)
P4KPbc	158	IDC (100%)
SSSS	151	CLL (100%)
P'P'	125	VIE (86%)
pPdiff	106	SYO (56%), VIE (39%)
PKPpre	106	NEIC (81%)
sPKiKP	86	BELR (41%), VIE (35%), HYB (15%)
LQM	82	MOLD (100%)
rx	79	SKHL (89%)
Rg	78	IDC (72%), NNC (15%), UCC (12%)
SKKSac	77	CLL (66%), HYB (29%)
Snm	76	CFUSG (100%)
SmS	75	BGR (73%), ZUR (27%)
PmP	72	BGR (60%), ZUR (40%)
PKPdif	71	DIAS (48%), CLL (38%)
PKP2ab	67	IDC (100%)
Sdif	64	CLL (86%), BELR (14%)
H	63	IDC (100%)
pPP	61	CLL (49%), LPA (36%)
PKP1	60	PPT (63%), LDG (37%)
SKPab	60	IDC (78%), BGR (13%)
sPP	52	CLL (96%)
PCP	50	LPA (36%), PRU (32%), MOS (14%)
Sgm	49	CFUSG (100%)
AMl	48	NIC (100%)
PPPP	47	CLL (100%)

Table 10.3: *(continued)*

Reported Phase	Total	Agencies reporting
pPcP	46	IDC (91%)
m	45	SIGU (100%)
P3KP	45	IDC (98%)
Px	45	CLL (100%)
PA	44	GCG (100%)
SKSdf	44	HYB (52%), BER (27%), CLL (14%)
r	43	BRG (100%)
P*	42	BGR (83%), MOS (12%)
MSN	41	HEL (80%), BER (20%)
Pif	41	BRG (100%)
dur	40	MOLD (100%)
PKPf	39	BRG (100%)
PKKPdf	37	AWI (76%), CLL (19%)
PKSdf	37	BER (68%), CLL (30%)
MPN	36	HEL (58%), BER (42%)
Sdiff	35	BGR (74%), VIE (11%), IDC (11%)
PSKS	32	CLL (100%)
E	31	YARS (74%), ZAG (26%)
Pn_3	30	ATH (100%)
PgA	29	THR (100%)
PgPg	29	BYKL (100%)
Pgm	28	CFUSG (100%)
PKKS	26	BELR (77%)
SKIKS	26	LPA (100%)
sPKPdf	25	CLL (44%), SYO (32%), INMG (16%)
IAmL	25	NDI (100%)
Pnm	24	CFUSG (100%)
SKIKP	23	LPA (100%)
PKIKS	23	LPA (100%)
sPKPab	23	INMG (78%), CLL (13%)
sSKS	23	BELR (96%)
IAMb	23	NDI (100%)
SgSg	22	BYKL (100%)
ASSG	21	OSPL (100%)
(sP)	21	CLL (100%)
ATPG	21	OSPL (100%)
ASPG	21	OSPL (100%)
sSS	20	CLL (100%)
P'P'df	20	AWI (60%), LJU (40%)
ATSG	20	OSPL (100%)
SPP	19	CLL (53%), BELR (26%), MOS (21%)
Pg_3	19	ATH (100%)
SKiKP	19	IDC (100%)
sPdiff	19	SYO (100%)
Pn_2	18	ATH (100%)
pPdif	17	BELR (47%), CLL (47%)
Lq	17	MOLD (100%)
SKSp	17	BRA (88%), WAR (12%)
PKPlp	16	CLL (100%)
(PP)	16	CLL (100%)
SDIF	16	PRU (100%)
Sif	15	BRG (100%)
PKPPKPdf	15	CLL (100%)
(PKiKP)	15	CLL (100%)
R2	15	CLL (100%)
(PKPab)	14	CLL (100%)
SDIFF	14	BRA (50%), LPA (36%), IPEC (14%)
SCS	14	LPA (100%)
S*	14	BGR (86%), BJI (14%)
PKPmax	14	CLL (100%)
Sx	13	CLL (100%)
PPPrev	13	CLL (100%)
(SSS)	13	CLL (100%)
sPdif	13	CLL (54%), BELR (46%)
M	12	MOLD (67%), ISC (25%)
sPS	12	CLL (100%)
AP	12	MOS (100%)
SKSP	11	CLL (73%), MOLD (27%)
sPPP	11	CLL (100%)
Plp	11	CLL (100%)
LqM	11	MOLD (100%)

Table 10.3: (continued)

Reported Phase	Total	Agencies reporting
(SSSS)	10	CLL (100%)
PSP	10	LPA (100%)
LH	10	CLL (100%)
SKKPdf	10	CLL (80%), AWI (20%)
(pP)	10	CLL (100%)
pS	9	WAR (44%), CLL (44%), BRG (11%)
(PKPbc)	9	CLL (100%)
sSdif	9	CLL (56%), BELR (44%)
sPPS	9	CLL (100%)
(sPP)	9	CLL (100%)
(Pg)	9	CLL (89%), RHSSO (11%)
(SS)	9	CLL (100%)
AS	8	PRU (100%)
IVMsBB	8	BER (100%)
Pg_4	8	ATH (100%)
sSSS	7	CLL (100%)
PPlp	7	CLL (100%)
del	7	KNET (100%)
sSKSac	7	CLL (100%)
(PcP)	7	CLL (100%)
Li	7	MOLD (100%)
(PKPdf)	7	CLL (100%)
sPKKPbc	7	CLL (100%)
XP	6	MOS (100%)
PPmax	6	CLL (100%)
(pPKPdf)	6	CLL (100%)
PKPc	6	PJWWP (100%)
PKPM	6	MOLD (100%)
SKKSa	6	BRG (100%)
RG	5	HEL (100%)
PnPn	5	SYO (40%), KRSZO (40%), HYB (20%)
(SP)	5	CLL (100%)
(PKPdif)	5	CLL (100%)
pPKKPbc	5	CLL (100%)
PSPS	5	CLL (100%)
DIFF	5	BRA (100%)
pPS	5	CLL (100%)
(Pdif)	4	CLL (100%)
1	4	DNK (100%)
sPKPbc	4	CLL (50%), IDC (25%), INMG (25%)
sSSSS	4	CLL (100%)
pPif	4	BRG (100%)
SKPd	4	BER (100%)
Sglp	4	CLL (100%)
SKPPKPdf	4	CLL (100%)
Pn_1	4	ATH (100%)
SSmax	4	CLL (100%)
AMSN	4	SJA (100%)
SKKSdf	4	CLL (100%)
SH	4	SYO (100%)
(Sb)	3	CLL (100%)
pPKKPab	3	CLL (100%)
SKSacmax	3	CLL (100%)
Pg_2	3	ATH (100%)
PPlmax	3	CLL (100%)
Sg_2	3	ATH (100%)
(pPKPab)	3	CLL (100%)
XSKS	3	PRU (100%)
PKKSbc	3	CLL (67%), HYB (33%)
PM	3	MOLD (100%)
pPPP	3	CLL (100%)
PKPPKP'	3	BRG (100%)
(PPP)	3	CLL (100%)
P4KP	3	IDC (100%)
PSS	3	CLL (100%)
sSKSac	3	CLL (100%)
(PPPP)	3	CLL (100%)
sPn	3	SYO (100%)
pSP	3	CLL (100%)
pwP	3	ISC1 (100%)
SA	3	SJA (100%)

Table 10.3: (continued)

Reported Phase	Total	Agencies reporting
SN4	2	LVSN (100%)
(Pn)	2	CLL (100%)
Sg_3	2	ATH (100%)
SKSSKSac	2	CLL (100%)
sPif	2	BRG (100%)
sSKPdf	2	CLL (100%)
Pn_0	2	ATH (100%)
P(2)	2	CLL (100%)
APKP	2	MOS (100%)
IVmBB	2	HYB (50%), BER (50%)
pPKKPdf	2	CLL (100%)
pPKP2	2	INMG (100%)
sSn	2	LJU (100%)
R3	2	CLL (100%)
PKiK	2	NAO (50%), BER (50%)
AMPN	2	SJA (100%)
pSKSac	2	CLL (100%)
3PKPbc	2	CLL (100%)
SnSn	2	KRSZO (100%)
(sSdif)	2	CLL (100%)
P5KP	2	NAO (100%)
(PPS)	2	CLL (100%)
LV	2	CLL (100%)
(PKP)	2	CLL (100%)
P9	2	MEX (50%), BER (50%)
IAML4	2	DNK (100%)
2	2	DNK (100%)
(sPdif)	2	CLL (100%)
SKPa	2	NAO (100%)
pSKKPbc	2	CLL (100%)
(SKPdf)	2	CLL (100%)
l	2	MOLD (100%)
SCP	2	NAO (100%)
SKPf	2	BRG (100%)
(pPKiKP)	2	CLL (100%)
pPn	2	INMG (50%), LJU (50%)
PKPdfmax	2	CLL (100%)
PKSab	2	CLL (100%)
PKKSdf	2	HYB (100%)
4	2	DNK (100%)
XS	2	PRU (100%)
sPPPP	2	CLL (100%)
3PKPab	2	CLL (100%)
SKSf	1	BRG (100%)
sPPlp	1	CLL (100%)
Pg_0	1	ATH (100%)
PPPPmax	1	CLL (100%)
pSKPbc	1	CLL (100%)
sPSSrev	1	CLL (100%)
SPn	1	HYB (100%)
sSP	1	CLL (100%)
(PSPS)	1	CLL (100%)
pp	1	SYO (100%)
PPk	1	CLL (100%)
(SKPbc)	1	CLL (100%)
(sPPP)	1	CLL (100%)
PKPbcmax	1	CLL (100%)
Siff	1	BRG (100%)
(sPSS)	1	CLL (100%)
SKKPf	1	BRG (100%)
LgM	1	MOLD (100%)
PKKPmax	1	CLL (100%)
SSKKS	1	MOLD (100%)
sPcP	1	CLL (100%)
PNc	1	PJWWP (100%)
Pp	1	BELR (100%)
PN4	1	LVSN (100%)
ePPS	1	CLL (100%)
pPKSab	1	CLL (100%)
PdfZ	1	SYO (100%)
(SKKPdf)	1	CLL (100%)

Table 10.3: (continued)

Reported Phase	Total	Agencies reporting
sScS	1	BJI (100%)
pSKKSac	1	CLL (100%)
PPM	1	MOLD (100%)
SKPPKPbc	1	CLL (100%)
sSSP	1	CLL (100%)
PKM	1	MOLD (100%)
SKSM	1	MOLD (100%)
sP(2)	1	CLL (100%)
(Sg)	1	CLL (100%)
DMd	1	NEIC (100%)
sSKSP	1	CLL (100%)
RM	1	MOLD (100%)
Pdifmax	1	CLL (100%)
S5KP	1	CLL (100%)
sPSS	1	CLL (100%)
eSP	1	CLL (100%)
PSKP	1	LPA (100%)
PKPg	1	NAO (100%)
pPPPP	1	CLL (100%)
PSKSrev	1	CLL (100%)
pPKPdif	1	CLL (100%)
RPP	1	CLL (100%)
MPKiK	1	MOLD (100%)
pPPlp	1	CLL (100%)
(pPdif)	1	CLL (100%)
pSKSdf	1	CLL (100%)
(sSSS)	1	CLL (100%)
(SKKSac)	1	CLL (100%)
p3PKPbc	1	CLL (100%)
sScP	1	CLL (100%)
(sPKPbc)	1	CLL (100%)
(SSP)	1	CLL (100%)
S5KP(2)	1	CLL (100%)
sp	1	CLL (100%)
pPIkP	1	SYO (100%)
PiKP	1	BELR (100%)
sPSKS	1	CLL (100%)
PKPab(2)	1	CLL (100%)
pPKSdf	1	CLL (100%)
PKPdfc	1	PJWWP (100%)
PKPabc	1	PJWWP (100%)
(sPKPdf)	1	CLL (100%)
sPKKPab	1	CLL (100%)
(PSSrev)	1	CLL (100%)
pSPP	1	CLL (100%)
(SKSac)	1	CLL (100%)
sSKKPbc	1	CLL (100%)
SKPb	1	BRG (100%)
3PKPdf	1	CLL (100%)
Pdifflp	1	CLL (100%)
PSSrev	1	CLL (100%)
sPKP2	1	INMG (100%)
BAZ	1	DNK (100%)
XM	1	MOLD (100%)
pPmax	1	CLL (100%)
SKPdfmax	1	CLL (100%)
PKPdfd	1	PJWWP (100%)
pn	1	ISN (100%)
PKPbc(2)	1	CLL (100%)
IAML_BB	1	THR (100%)
PKPdf(2)	1	CLL (100%)
(sSKPbc)	1	CLL (100%)
(pS)	1	CLL (100%)
S5	1	INMG (100%)
(SKKSdf)	1	CLL (100%)
PKPdif2	1	CLL (100%)
(SPP)	1	CLL (100%)
(sPKPab)	1	CLL (100%)
(PKSdf)	1	CLL (100%)
SKSac(2)	1	CLL (100%)
e	1	CLL (100%)

Table 10.3: (continued)

Reported Phase	Total	Agencies reporting
sPKi	1	HYB (100%)
SSP	1	CLL (100%)
PKPPKPbc	1	CLL (100%)

Table 10.4: Reporters of amplitude data

Agency	Number of reported amplitudes	Number of amplitudes in ISC located events	Number used for ISC mb	Number used for ISC MS
NEIC	835416	300968	200786	50217
IDC	546251	514354	136430	68609
ROM	452253	10122	0	0
WEL	309222	42739	0	0
MOS	110690	104958	52682	10377
AFAD	108871	7779	0	0
ATH	103656	11658	0	0
DJA	95375	52563	8180	0
BJI	88734	85656	24613	27494
ISK	86807	15000	0	0
NNC	82389	28093	48	0
AUST	57955	12295	9015	0
VIE	45249	27202	9716	0
SOME	43078	14177	2938	0
INMG	39751	11677	72	0
TXNET	39592	923	0	0
HEL	36227	2036	0	0
RSNC	32055	12267	727	0
THE	29884	8674	0	0
GUC	29290	7615	0	0
SVSA	29240	1664	65	0
SJA	26836	10599	0	0
MDD	20127	3249	0	0
MCSM	14955	9019	5664	0
PRE	14925	972	0	0
LDG	14311	1867	0	0
JMA	14095	13941	0	0
BER	13920	6710	1536	257
MRB	12434	289	0	0
SKHL	11253	5044	0	0
SDD	10997	3682	0	0
PPT	10598	9898	607	0
AWI	8735	5084	1897	0
BELR	8529	2655	392	595
NDI	8327	7414	1971	294
DNK	8275	4625	3650	63
PRU	8270	4687	0	2818
ZUR	8245	377	0	0
SSNC	7963	1282	0	0
LJU	7709	222	0	0
WBNET	6939	22	0	0
BGR	5815	5161	2589	0
PDG	4715	2740	0	0
NIC	4501	1941	0	0
TIR	4445	1686	0	0
GCG	4404	1975	0	0

Table 10.4: *Continued.*

Agency	Number of reported amplitudes	Number of amplitudes in ISC located events	Number used for ISC mb	Number used for ISC MS
OTT	4110	228	0	0
ECX	4099	588	0	0
BRG	3613	1550	0	0
YARS	3558	134	1	0
KRSZO	3372	0	0	0
OSPL	3366	1520	0	0
NOU	3346	3235	2031	0
BGS	3291	2037	1113	431
BUC	3175	853	0	0
CLL	2941	1957	329	369
KNET	2744	1225	0	0
SNET	2572	984	0	0
NAO	2286	2260	1522	0
UCC	2216	2044	1775	0
BYKL	2147	739	0	0
BKK	1990	1035	13	0
LVSN	1673	136	0	0
SCB	1631	259	0	0
SKO	1578	474	0	0
CFUSG	1513	1289	0	0
IPEC	1395	330	0	0
IGIL	1164	639	133	185
ISN	1130	1008	0	0
ASRS	1109	555	0	0
BGSI	1043	418	0	0
DMN	973	684	0	0
MOLD	963	652	107	0
KEA	859	559	0	136
THR	848	738	0	0
UPA	719	109	0	0
NERS	671	95	0	0
FCIAR	488	241	10	0
MIRAS	446	68	0	0
SIGU	355	209	0	0
WAR	342	323	0	250
PLV	244	56	0	0
HYB	211	211	2	1
JSO	32	28	0	0
NAM	23	1	0	0
PJWWP	17	16	0	0
ISC	15	15	0	0
BUD	7	0	0	0

International Seismological Centre

11

Glossary of ISC Terminology

- Agency/ISC data contributor

  An academic or government institute, seismological organisation or company, geological/meteorological survey, station operator or author that reports or contributed data in the past to the ISC or one of its predecessors. Agencies may contribute data to the ISC directly, or indirectly through other ISC data contributors.

- Agency code

  A unique, maximum eight-character code for a data reporting agency (e.g. NEIC, GFZ, BUD) or author (e.g. ISC, ISC-EHB, IASPEI). Often the agency code is the commonly used acronym of the reporting institute.

- Arrival

  A phase pick at a station is characterised by a phase name and an arrival time.

- Associated phase

  Associated phase arrival or amplitude measurements represent a collection of observations belonging to (i.e. generated by) an event. The complete set of observations are associated to the prime hypocentre.

- Azimuthal gap/Secondary azimuthal gap

  The azimuthal gap for an event is defined as the largest angle between two stations with defining phases when the stations are ordered by their event-to-station azimuths. The secondary azimuthal gap is the largest azimuthal gap a single station closes.

- BAAS

  Seismological bulletins published by the British Association for the Advancement of Science (1913-1917) under the leadership of H.H. Turner. These bulletins are the predecessors of the ISS Bulletins and include reports from stations distributed worldwide.

- Bulletin

  An ordered list of event hypocentres, uncertainties, focal mechanisms, network magnitudes, as well as phase arrival and amplitude observations associated to each event. An event bulletin may list all the reported hypocentres for an event. The convention in the ISC Bulletin is that the preferred (prime) hypocentre appears last in the list of reported hypocentres for an event.

- Catalogue

  An ordered list of event hypocentres, uncertainties and magnitudes. An event catalogue typically lists only the preferred (prime) hypocentres and network magnitudes.

- CoSOI/IASPEI

  Commission on Seismological Observation and Interpretation, a commission of IASPEI that prepares and discusses international standards and procedures in seismological observation and interpretation.

- Defining/Non-defining phase

  A defining phase is used in the location of the event (time-defining) or in the calculation of the network magnitude (magnitude-defining). Non-defining phases are not used in the calculations because they suffer from large residuals or could not be identified.

- Direct/Indirect report

  A data report sent (e-mailed) directly to the ISC, or indirectly through another ISC data contributor.

- Duplicates

  Nearly identical phase arrival time data reported by one or more agencies for the same station. Duplicates may be created by agencies reporting observations from other agencies, or several agencies independently analysing the waveforms from the same station.

- Event

  A natural (e.g. earthquake, landslide, asteroid impact) or anthropogenic (e.g. explosion) phenomenon that generates seismic waves and its source can be identified by an event location algorithm.

- Grouping

  The ISC algorithm that organises reported hypocentres into groups of events. Phases associated to any of the reported hypocentres will also be associated to the preferred (prime) hypocentre. The grouping algorithm also attempts to associate phases that were reported without an accompanying hypocentre to events.

- Ground Truth

  An event with a hypocentre known to certain accuracy at a high confidence level. For instance, GT0 stands for events with exactly known location, depth and origin time (typically explosions); GT5 stands for events with their epicentre known to 5 km accuracy at the 95% confidence level, while their depth and origin time may be known with less accuracy.

- Ground Truth database

  On behalf of IASPEI, the ISC hosts and maintains the IASPEI Reference Event List, a bulletin of ground truth events.

- IASPEI

  International Association of Seismology and Physics of the Earth Interior, www.iaspei.org.

- International Registry of Seismograph Stations (IR)

  Registry of seismographic stations, jointly run by the ISC and the World Data Center for Seismology, Denver (NEIC). The registry provides and maintains unique five-letter codes for stations participating in the international parametric and waveform data exchange.

- ISC Bulletin

  The comprehensive bulletin of the seismicity of the Earth stored in the ISC database and accessible through the ISC website. The bulletin contains both natural and anthropogenic events. Currently the ISC Bulletin spans more than 50 years (1960-to date) and it is constantly extended by adding both recent and past data. Eventually the ISC Bulletin will contain all instrumentally recorded events since 1900.

- ISC Governing Council

  According to the ISC Working Statutes the Governing Council is the governing body of the ISC, comprising one representative for each ISC Member.

- ISC-located events

  A subset of the events selected for ISC review are located by the ISC. The rules for selecting an event for location are described in Section 10.1.3; ISC-located events are denoted by the author ISC.

- ISC Member

  An academic or government institute, seismological organisation or company, geological/meteorological survey, station operator, national/international scientific organisation that contribute to the ISC budget by paying membership fees. ISC members have voting rights in the ISC Governing Council.

- ISC-reviewed events

  A subset of the events reported to the ISC are selected for ISC analyst review. These events may or may not be located by the ISC. The rules for selecting an event for review are described in Section 10.1.3. Non-reviewed events are explicitly marked in the ISC Bulletin by the comment following the prime hypocentre "Event not reviewed by the ISC".

- ISF

  International Seismic Format (www.isc.ac.uk/standards/isf). A standard bulletin format approved by IASPEI. The ISC Bulletin is presented in this format at the ISC website.

- ISS

  International Seismological Summary (1918-1963). These bulletins are the predecessors of the ISC Bulletin and represent the major source of instrumental seismological data before the digital era. The ISS contains regionally and teleseismically recorded events from several hundreds of globally distributed stations.

- Network magnitude

The event magnitude reported by an agency or computed by the ISC locator. An agency can report several network magnitudes for the same event and also several values for the same magnitude type. The network magnitude obtained with the ISC locator is defined as the median of station magnitudes of the same magnitude type.

- Phase

  A maximum eight-character code for a seismic, infrasonic, or hydroacoustic phase. During the ISC processing, reported phases are mapped to standard IASPEI phase names. Amplitude measurements are identified by specific phase names to facilitate the computation of body-wave and surface-wave magnitudes.

- Prime hypocentre

  The preferred hypocentre solution for an event from a list of hypocentres reported by various agencies or calculated by the ISC.

- Reading

  Parametric data that are associated to a single event and reported by a single agency from a single station. A reading typically includes one or more phase names, arrival time and/or amplitude/period measurements.

- Report/Data report

  All data that are reported to the ISC are parsed and stored in the ISC database. These may include event bulletins, focal mechanisms, moment tensor solutions, macroseismic descriptions and other event comments, as well as phase arrival data that are not associated to events. Every single report sent to the ISC can be traced back in the ISC database via its unique report identifier.

- Shide Circulars

  Collections of station reports for large earthquakes occurring in the period 1899-1912. These reports were compiled through the efforts of J. Milne. The reports are mainly for stations of the British Empire equipped with Milne seismographs. After Milne's death, the Shide Circulars were replaced by the Seismological Bulletins of the BAAS.

- Station code

  A unique, maximum six-character code for a station. The ISC Bulletin contains data exclusively from stations registered in the International Registry of Seismograph Stations.

12

Acknowledgements

We thank our colleagues at the University of Bergen for kindly accepting our invitation and preparing an article for this issue of the Summary with assistance from ISC staff.

We are also grateful to the developers of the Generic Mapping Tools (GMT) suite of software (Wessel et al., 2019) that was used extensively for producing the figures.

Finally, we thank the ISC Member Institutions, Data Contributors, Funding Agencies (including NSF Award EAR-1811737, USGS Awards G19AS00033 and G20AP00060) and Sponsors for supporting the long-term operation of the ISC.

References

Adamaki, A. (2017), Seismicity Analysis Using Dense Network Data : Catalogue Statistics and Possible Foreshocks Investigated Using Empirical and Synthetic Data, Ph.D. thesis, Uppsala University, urn:nbn:se:uu:diva-328057.

Adams, R. D., A. A. Hughes, and D. M. McGregor (1982), Analysis procedures at the International Seismological Centre, *Physics of the Earth and Planetary Interiors*, *30*, 85–93.

Amante, C., and B. W. Eakins (2009), ETOPO1 1 arc-minute global relief model: procedures, data sources and analysis, *NOAA Technical Memorandum NESDIS NGDC-24*, NOAA.

Balfour, N., R. Baldwin, and A. Bird (2008), Magnitude calculations in Antelope 4.10, *Analysis Group Note of Geological Survey of Canada*, pp. 1–13.

Bennett, T. J., V. Oancea, B. W. Barker, Y.-L. Kung, M. Bahavar, B. C. Kohl, J. . Murphy, and I. K. Bondár (2010), The nuclear explosion database NEDB: a new database and web site for accessing nuclear explosion source information and waveforms, *Seismological Research Letters*, *81*, https://doi.org/10.1785/gssrl.81.1.12.

Bisztricsany, E. A. (1958), A new method for the determination of the magnitude of earthquakes, *Geofiz. Kozl*, pp. 69–76.

Bolt, B. A. (1960), The revision of earthquake epicentres, focal depths and origin time using a high-speed computer, *Geophysical Journal of the Royal Astronomical Society*, *3*, 434–440.

Bondár, I., and K. McLaughlin (2009a), A new ground truth data set for seismic studies, *Seismological Research Letters*, *80*, 465–472.

Bondár, I., and K. McLaughlin (2009b), Seismic location bias and uncertainty in the presence of correlated and non-Gaussian travel-time errors, *Bulletin of the Seismological Society of America*, *99*, 172–193.

Bondár, I., and D. Storchak (2011), Improved location procedures at the International Seismological Centre, *Geophysical Journal International*, *186*, 1220–1244.

Bondár, I., E. R. Engdahl, X. Yang, H. A. A. Ghalib, A. Hofstetter, V. Kirchenko, R. Wagner, I. Gupta, G. Ekström, E. Bergman, H. Israelsson, and K. McLaughlin (2004), Collection of a reference event set for regional and teleseismic location calibration, *Bulletin of the Seismological Society of America*, *94*, 1528–1545.

Bondár, I., E. Bergman, E. R. Engdahl, B. Kohl, Y.-L. Kung, and K. McLaughlin (2008), A hybrid multiple event location technique to obtain ground truth event locations, *Geophysical Journal International*, *175*, https://doi.org/10.1111/j.1365246X.2008.03867x.

Bormann, P., and J. W. Dewey (2012), The new IASPEI standards for determining magnitudes from digital data and their relation to classical magnitudes, IS 3.3, *New Manual of Seismological Observatory Practice 2 (NMSOP-2), P. Bormann (Ed.)*, pp. 1–44, https://doi.org/10.2312/GFZ.NMSOP-2_IS_3.3,10.2312/GFZ.NMSOP-2.

Bormann, P., and J. Saul (2008), The new IASPEI standard broadband magnitude mB, *Seism. Res. Lett*, *79*(5), 698–705.

Bormann, P., R. Liu, X. Ren, R. Gutdeutsch, D. Kaiser, and S. Castellaro (2007), Chinese national network magnitudes, their Relation to NEIC magnitudes and recommendations for new IASPEI magnitude standards, *Bulletin of the Seismological Society of America*, *97*(1B), 114–127, https://doi.org/10.1785/012006007835.

Bormann, P., R. Liu, Z. Xu, R. Ren, and S. Wendt (2009), First application of the new IASPEI teleseismic magnitude standards to data of the China National Seismographic Network, *Bulletin of the Seismological Society of America*, *99*, 1868–1891, https://doi.org/10.1785/0120080010.

Chang, A. C., R. H. Shumway, R. R. Blandford, and B. W. Barker (1983), Two methods to improve location estimates - preliminary results, *Bulletin of the Seismological Society of America*, *73*, 281–295.

Choy, G. L., and J. L. Boatwright (1995), Global patterns of readiated seismic energy and apparent stress, *J. Geophys. Res.*, *100*(B9), 18,205–18,228.

Dziewonski, A. M., and F. Gilbert (1976), The effect of small, aspherical perturbations on travel times and a re-examination of the correction for ellipticity, *Geophysical Journal of the Royal Astronomical Society*, *44*, 7–17.

Dziewonski, A. M., T.-A. Chou, and J. H. Woodhouse (1981), Determination of earthquake source parameters from waveform data for studies of global and regional seismicity, *J. Geophys. Res.*, *86*, 2825–2852.

Engdahl, E. R., and R. H. Gunst (1966), Use of a high speed computer for the preliminary determination of earthquake hypocentres, *Bulletin of the Seismological Society of America*, *56*, 325–336.

Engdahl, E. R., R. van der Hilst, and R. Buland (1998), Global teleseismic earthquake relocation with improved travel times and procedures for depth determination, *Bulletin of the Seismological Society of America*, *88*, 722–743.

Flinn, E. A., and E. R. Engdahl (1965), Proposed basis for geographical and seismic regionalization, *Reviews of Geophysics*, *3*(1), 123–149.

Flinn, E. A., E. R. Engdahl, and A. R. Hill (1974), Seismic and geographical regionalization, *Bulletin of the Seismological Society of America*, *64*, 771–993.

Gutenberg, B. (1945a), Amplitudes of P, PP and S and magnitude of shallow earthquakes, *Bulletin of the Seismological Society of America*, *35*, 57–69.

Gutenberg, B. (1945b), Magnitude determination of deep-focus earthquakes, *Bulletin of the Seismological Society of America*, *35*, 117–130.

Gutenberg, B. (1945c), Amplitudes of surface waves and magnitudes of shallow earthquakes, *Bulletin of the Seismological Society of America*, *35*, 3–12.

Gutenberg, B., and C. F. Richter (1956), Magnitude and Energy of earthquakes, *Ann. Geof.*, *9*, 1–5.

Hutton, L. K., and D. M. Boore (1987), The ML scale in southern California, *Bulletin of the Seismological Society of America*, *77*, 2074–2094.

IASPEI (2005), Summary of Magnitude Working group recommendations on standard procedures for determining earthquake magnitudes from digital data, http://www.iaspei.org/commissions/CSOI.html#wgmm,http://www.iaspei.org/commissions/CSOI/summary_of_WG_recommendations_2005.pdf.

IASPEI (2013), Summary of magnitude working group recommendations on standard procedures for determining earthquake magnitudes from digital data, http://www.iaspei.org/commissions/CSOI/Summary_of_WG_recommendations_20130327.pdf.

IDC (1999), IDC processing of seismic, hydroacoustic and infrasonic data, *IDC Documentation*.

Jeffreys, H., and K. E. Bullen (1940), *Seismological Tables*, British Association for the Advancement of Science.

Kanamori, H. (1977), The energy release in great earthquakes, *J. Geophys. Res.*, *82*, 2981–2987.

Kennett, B. L. N. (2006), Non-linear methods for event location in a global context, *Physics of the Earth and Planetary Interiors*, *158*, 45–64.

Kennett, B. L. N., E. R. Engdahl, and R. Buland (1995), Constraints on seismic velocities in the Earth from traveltimes, *Geophysical Journal International*, *122*, 108–124.

Kennett, B. L. N., E. R. Engdahl, and R. Buland (1996), Ellipticity corrections for seismic phases, *Geophysical Journal International*, *127*, 40–48.

Lee, W. H. K., R. Bennet, and K. Meagher (1972), A method of estimating magnitude of local earthquakes from signal duration, *U.S. Geol. Surv.*, Open-File Rep.

Lentas, K., D. D. Giacomo, J. Harris, and D. A. Storchak (2019), The ISC Bulletin as a comprehensive source of earthquake source mechanisms, *Earth System Science Data*, *11*(2), 565–578, `https://doi.org/10.5194/essd-11-565-2019`.

Leptokaropoulos, K. M., A. K. Adamaki, R. G. Roberts, C. G. Gkarlaouni, and P. M. Paradisopoulou (2018), Impact of magnitude uncertainties on seismic catalogue properties, *Geophysical Journal International*, *213*(2), 940–951, `https://doi.org/10.1093/gji/ggy023`.

Murphy, J. R., and B. W. Barker (2006), Improved focal-depth determination through automated identication of the seismic depth phases pP and sP, *Bulletin of the Seismological Society of America*, *96*, 1213–1229.

NMSOP-2 (2012), *New Manual of Seismological Observatory Practice (NMSOP-2)*, IASPEI, GFZ, German Research Centre for Geosciences, Potsdam, `https://doi.org/10.2312/GFZ.NMSOP-2`.

Nuttli, O. W. (1973), Seismic wave attenuation and magnitude relations for eastern North America, *J. Geophys. Res.*, *78*, 876–885.

Richter, C. F. (1935), An instrumental earthquake magnitude scale, *Bulletin of the Seismological Society of America*, *25*, 1–32.

Ringdal, F. (1976), Maximum-likelihood estimation of seismic magnitude, *Bulletin of the Seismological Society of America*, *66*(3), 789–802.

Sambridge, M. (1999), Geophysical inversion with a neighbourhood algorithm, *Geophysical Journal International*, *138*, 479–494.

Sambridge, M., and B. L. N. Kennett (2001), Seismic event location: non-linear inversion using a neighbourhood algorithm, *Pure and Applied Geophysics*, *158*, 241–257.

Storchak, D. A., J. Schweitzer, and P. Bormann (2003), The IASPEI standard seismic phases list, *Seismological Research Letters*, *74*(6), 761–772.

Storchak, D. A., J. Schweitzer, and P. Bormann (2011), Seismic phase names: IASPEI Standard, in *Encyclopedia of Solid Earth Geophysics*, edited by H.K. Gupta, pp. 1162–1173, Springer.

Storchak, D. A., J. Harris, L. Brown, K. Lieser, B. Shumba, R. Verney, D. Di Giacomo, and E. I. M. Korger (2017), Rebuild of the Bulletin of the International Seismological Centre (ISC), part 1: 1964–1979, *Geoscience Letters*, *4*(32), `https://doi.org/10.1186/s40562-017-0098-z`.

Storchak, D. A., J. Harris, L. Brown, K. Lieser, B. Shumba, and D. Di Giacomo (2020), Rebuild of the Bulletin of the International Seismological Centre (ISC)-part 2: 1980–2010, *Geoscience Letters*, *7*(18), `https://doi.org/10.1186/s40562-020-00164-6`.

Stähler, S., and K. Sigloch (2014), Fully probabilistic seismic source inversion–Part 1: Efficient parameterisation, *Solid Earth*, *5*(2), 1055–1069, `https://doi.org/10.5194/se-5-1055-2014`.

Stähler, S., and K. Sigloch (2016), Fully probabilistic seismic source inversion–Part 2: Modelling errors and station covariances, *Solid Earth*, *7*(6), 1521–1536, `https://doi.org/10.5194/se-7-1521-2016`.

Tsuboi, C. (1954), Determination of the Gutenberg-Richter's magnitude of earthquakes occurring in and near Japan, *Zisin (J. Seism. Soc. Japan)*, *Ser. II*(7), 185–193.

Tsuboi, S., K. Abe, K. Takano, and Y. Yamanaka (1995), Rapid determination of Mw from broadband P waveforms, *Bulletin of the Seismological Society of America*, *85*(2), 606–613.

Uhrhammer, R. A., and E. R. Collins (1990), Synthesis of Wood-Anderson Seismograms from Broadband Digital Records, *Bulletin of the Seismological Society of America*, *80*(3), 702–716.

Vaněk, J., A. Zapotek, V. Karnik, N. V. Kondorskaya, Y. V. Riznichenko, E. F. Savarensky, S. L. Solov'yov, and N. V. Shebalin (1962), Standardization of magnitude scales, *Izvestiya Akad. SSSR., Ser. Geofiz.*(2), 153–158, Pages 108–111 in the English translation.

Villaseñor, A., and E. R. Engdahl (2005), A digital hypocenter catalog for the International Seismological Summary, *Seismological Research Letters*, *76*, 554–559.

Villaseñor, A., and E. R. Engdahl (2007), Systematic relocation of early instrumental seismicity: Earthquakes in the International Seismological Summary for 1960–1963, *Bulletin of the Seismological Society of America*, *97*, 1820–1832.

Woessner, J., and S. Wiemer (2005), Assessing the quality of earthquake catalogues: estimating the magnitude of completeness and its uncertainty, *Bulletin of the Seismological Society of America*, *95*(2), https://doi.org/10/1785/012040007.

Young, J. B., B. W. Presgrave, H. Aichele, D. A. Wiens, and E. A. Flinn (1996), The Flinn-Engdahl regionalisation scheme: the 1995 revision, *Physics of the Earth and Planetary Interiors*, *96*, 223–297.

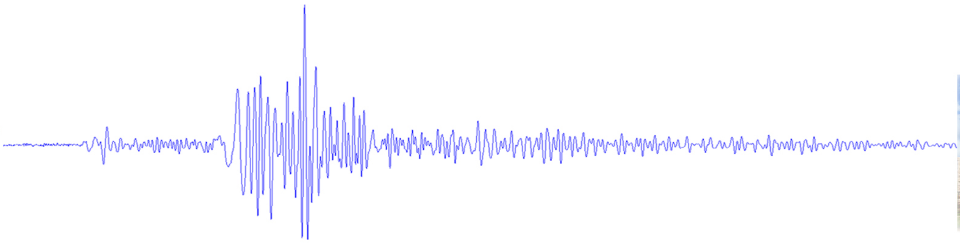

TDE-324CI/FI Digitizer

Key Features:

- True 26-bit, exceptionally low noise, up to 1000sps, high dynamic range > 145dB@100sps
- High precision time Service: better than 0.05ppm
- Records in MiniSEED, standard storages 32GB, max 256GB supports Liss, Seedlink, JOPENS data streaming protocols
- Compatible with any seismometers & accelerometers
- Humanized Interface, include pushbuttons and large LCD, setup & display real-time wave and running status
- Built-in seismic station performance and data quality analysis, include PSD/PDF, sine/pulse calibration, sensor response, waveform, run rate, environmental status monitoring etc.
- Installation checking & setup available for both android and IOS devices
- Remote control multiple seismometers calibration, mass center, mass lock/unlock

TDE-324CI Digitizer

TDE-324FI Digitizer

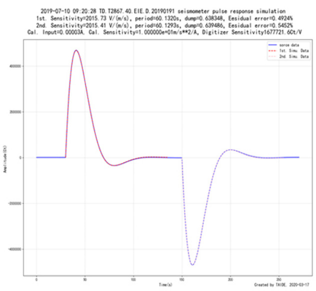

Built in auto pulse cal. signal analysis

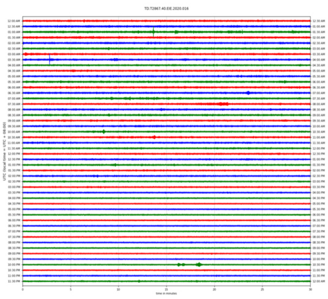

Built-in 1 day's seismic wave display

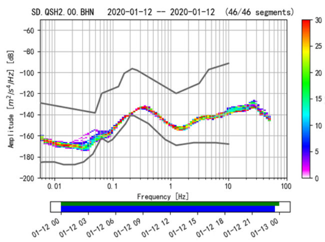

Built-in 1 day's PDF analysis

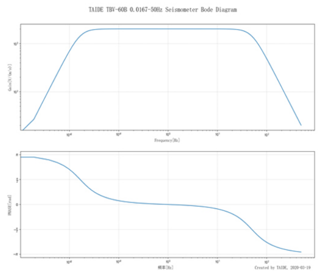

Built-in seismometer response analysis

Technical Specifications:

Channels	TDE-324CI: 3 channels TDE-324FI: 6 channels	Main channel resolution	True 26 bits, ≥145dB@100sps Support 24 bits output
Input noise	<1.0μVrms(input ±20Vpp)	Interface	Standard 10/100M RJ45/LAN
Time Service	Support Beidou,GPS Satellites Support NTP Time Service Time error: better than 0.01ms Timing accuracy:better than 0.05ppm	Signal input	Differential Input, ±20Vpp Full Scale, Program Gain 1/2/4
Sample rate	1sps、10sps、20sps、50sps、100sps、200sps、500sps、1000sps	Environment	Temperature: -40℃～70℃, Humidity: 0～100%(RH),IP67

0756-2521081 519085 zhtaide@163.com http://www.tai-de.com
TAIDE ENTERPRISE CO,. LTD. No.60 4th Jinding Chuangxin Road, Xiangzhou, Zhuhai, China


REF TEK
SYSTEMS INC.
REFTEK
WRANGLER
3031B
RELIABLE, HIGH QUALITY & ROBUST
Renewed commitment to customer service and product development.
QUESTIONS?
sales@reftek.com
support@reftek.com
www.reftek.com
HIGH RESOLUTION SEISMIC RECORDERS, SENSORS & SOFTWARE


WRANGLER
3031B

sara

www.sara.pg.it

contact us at: info@sara.pg.it
or by telephone: +39 075 5051014

Weak motion sensor and
microtremor (HVSR)
Nodal systems - Terrabot

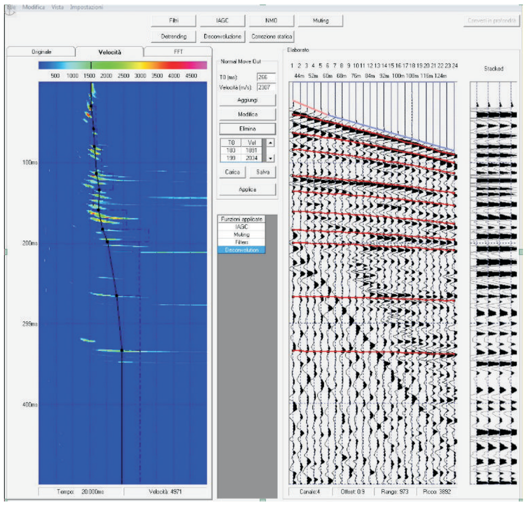

Geophysical exploration software